NASA CONTRACTOR
REPORT

NASA CR-1269

C. 1

NASA CR-1269

LOSS FACTOR AND RESONANT FREQUENCY OF VISCOELASTIC SHEAR-DAMPED STRUCTURAL COMPOSITES

by Thomas F. Derby and Jerome E. Ruzicka

NASA CR-1269

LOSS FACTOR AND RESONANT FREQUENCY OF

VISCOELASTIC SHEAR-DAMPED STRUCTURAL COMPOSITES

By Thomas F. Derby and Jerome E. Ruzicka

LOSS FACTOR AND RESONANT FREQUENCY OF
VISCOELASTIC SHEAR-DAMPED STRUCTURAL COMPOSITES

by Thomas F. Derby and Jerome E. Ruzicka

ABSTRACT

An investigation is conducted to evaluate the loss factor, resonant frequency and thermal conductivity characteristics of structural composites with viscoelastic shear-damping mechanisms. Theoretical solutions and graphical design data for damping and resonant frequency are developed for four types of viscoelastic shear-damped structural composites: two-elastic-element, symmetrical three-elastic-element, unsymmetrical three-elastic-element and N identical-elastic-laminate configurations. The equations and design procedures for predicting loss factor and resonant frequency are verified by the results of experimental measurements made on laboratory beam specimens. Thermal conductivity characteristics of laminated visco-elastic shear-damped plates are investigated theoretically and experimentally, with consideration given to methods for increasing thermal conductivity and the subsequent effect on structural damping.

CONTENTS

LOSS FACTOR AND RESONANT FREQUENCY OF
VISCOELASTIC SHEAR-DAMPED STRUCTURAL COMPOSITES

by Thomas F. Derby and Jerome E. Ruzicka

Barry Controls
Division of Barry Wright Corporation
Watertown, Massachusetts

SUMMARY

An analysis of the loss factor and resonant frequency characteristics of viscoelastic shear-damped structural composites has been conducted. The structural composites considered included two-elastic-element, symmetrical three-elastic-element, unsymmetrical three-elastic-element and N identical-elastic-laminate configurations.

The mathematical relations for loss factor are typically dependent upon three parameters: the geometrical parameter, the uncoupled shear parameter and the viscoelastic material loss factor. The resonant frequency analyses demonstrate the validity of assuming the effective flexural rigidity of the composite structure equals the real part of the complex flexural rigidity.

Extensive design graphs for the prediction of structure loss factor and resonant frequency have been developed for wide parametric variations of the viscoelastic damping material loss factor and the geometrical and uncoupled shear parameters. The design procedures presented allow rapid determination of damping and resonant frequency characteristics without the necessity of an iteration process. Discussion of a design example demonstrates the application of the design procedure.

Laboratory experiments have been performed to verify the theoretical predictions of loss factor and resonant frequency for a set of 44 different beam specimens that employed aluminum and/or fibre-glass structural materials. A total of 226 loss factor and 164 resonant frequency measurements were made at various free-free bending modes of the beam specimens. A statistical analysis of this data compared to the theoretical values of loss factor and resonant frequency indicated that the loss factor difference had a mean value of 1.5 percent and a standard deviation of approximately 25 percent, whereas the resonant frequency difference had a mean value of 0.7 percent and a standard deviation of approximately 9 percent. It is concluded that the theory and design procedures for loss factor and resonant frequency is satisfactory within accepted engineering practice.

Methods for increasing the thermal conductivity of viscoelastic shear-damped laminated plates have been evaluated. Addition of a high thermal conductivity material to the viscoelastic material increases the thermal conductivity of the structural composite; however, it appears that this can be done only at the expense of structural damping and the peel strength of the laminated plate.

SECTION 1: INTRODUCTION

Design procedures and graphs have previously been developed to predict the damping properties of structural composites comprised of two elastic elements separated by a viscoelastic layer. The results of that study are reported in NASA Contract Report CR-742, "Damping of Structural Composites with Viscoelastic Shear-Damping Mechanisms" [Ref. 1]. The study reported herein results in design procedures and graphs to determine the damping properties and resonant frequencies of structural composites comprised of two elastic elements, three elastic elements and any number of identical elastic laminates separated by thin layers of viscoelastic material. The analyses for these structures, mainly contained in the appendices, are based on, and are an extension of, existing theoretical analyses [Ref. 2-8]. The measure of damping used in this report, as well as in the previous report, is the structure loss factor, which may be related to other measures of damping such as the logarithmic decrement and the fraction of critical damping [Ref. 2 and 9].

The design procedures developed herein are easier to use than those developed in Reference 1 in that the structure loss factor can be read directly from the design graphs and there is no iteration process required. The major difficulty in predicting structure loss factor has been in determining one of the parameters in the expression for the loss factor; namely, the shear parameter X. For the present study, it has been determined that, in the functional relationship for the structure loss factor η, the shear parameter X may be replaced by the uncoupled shear parameter X_o, as follows:

$$\eta = \eta(\beta, X_o, Y) \tag{1}$$

where β is the loss factor of the viscoelastic shear-damping material, X_o is defined as the uncoupled shear parameter, and Y is defined as the geometrical parameter.

The damping material loss factor β is the ratio of the imaginary and real components of the complex shear modulus $G^* = G' + iG''$, as follows

$$\beta = G''/G' \tag{2}$$

where G'' and G' are the loss modulus and storage modulus of the viscoelastic material, respectively. The uncoupled shear parameter X_0 is similar to the shear parameter X used previously [Ref. 1]; however, its dependence on the properties of the viscoelastic material and the frequency of vibration is considerably simpler. The uncoupled shear parameter X_0 can be expressed as follows

$$X_0 = C\left(G'/f\right) \tag{3}$$

where C is defined as the shear parameter coefficient which depends on the cross-section geometry of the structure and the modulus of elasticity of the elastic elements, but is independent of the properties of the viscoelastic material and the frequency of vibration f. The geometrical parameter Y is also only a function of the cross-section geometry of the structure and modulus of elasticity, and may be expressed as follows [Ref. 1]

$$Y = \frac{(EI)_\infty}{(EI)_0} - 1 \tag{4}$$

where $(EI)_0$ is the flexural rigidity of the structural composite when its elastic members are uncoupled and $(EI)_\infty$ is the flexural rigidity of the structural composite when its elastic members are completely coupled. The geometrical parameter has been determined and graphically displayed for a wide variety of cross-sections of the type of structural composites considered in this report [Ref. 1].

The present investigation is concerned with the development of procedures and graphical data useful in the design of viscoelastic shear-damped composite structural beams and the experimental verification of theorteical predictions of structure loss factor, resonant frequency, and steady-state frequency response. Analyses and experiments have been limited to structural

3

composite designs which incorporate thin layers of relatively soft viscoelastic damping material; consequently, the results of the studies are particularly applicable to structural composites that incorporate thin self-bonding adhesive damping layers. The investigation encompasses the following studies:

(1) Theoretical analysis of structure loss factor.

(2) Theoretical analysis of structure resonant frequency.

(3) Development of design procedures and graphs for predicting the structure loss factors and resonant frequencies.

(4) Comparison of theoretical to experimental results pertaining to structure loss factor, resonant frequency, and transmissibility of various structural composites.

(5) Thermal conductivity of laminated elastic and viscoelastic plates.

These five studies are discussed, respectively, in the following sections of the report.

SECTION 2: THEORETICAL LOSS FACTOR ANALYSES

With one exception, the method of calculating theoretical structure
loss factors employed herein follows fairly closely the analysis presented in
Reference 2(pp. 55-61). The one exception is for structures having visco-
elastic layers not parallel to the neutral plane of bending, and is discussed in
the last subsection of this section. For composite structural beams comprised
of elastic elements separated by layers of viscoelastic material parallel to the
neutral plane of bending, the following general discussion is applicable.

General Loss Factor Equations

The structure loss factor η is defined as the ratio of the imaginary
part of the complex flexural rigidity to the real part, as follows

$$\eta = \frac{\text{Im}[(EI)^*]}{\text{Re}[(EI)^*]} \tag{5}$$

where $(EI)^*$ denotes the complex flexural rigidity of the structural composite.
The complex flexural rigidity is obtained by considering the structural composite
to be in pure bending so that

$$M = (EI)^* \frac{\partial \varphi}{\partial x} \tag{6}$$

where M is the applied moment and $\frac{\partial \varphi}{\partial x}$ is the resulting curvature of the
beam. The steady-state response of $\frac{\partial \varphi}{\partial x}$ to the input $M = M_0 e^{i\omega t}$ is

$$\frac{\partial \varphi}{\partial x} = \left(\frac{\partial \varphi}{\partial x}\right)_0 e^{i(\omega t - \theta)} \tag{7}$$

where the phase angle θ indicates the presence of damping.

Evaluation of the structure loss factor η by use of Equation (5)
requires the determination of the complex flexural rigidity $(EI)^*$. The method
of determining $(EI)^*$ is to first assume it is a real number by considering the
shear modulus of the viscoelastic material to be a real number (i. e., being

5

purely elastic). When the expression for flexural rigidity is obtained, the shear modulus of the viscoelastic material G is replaced by

$$G^* = G'(1 + i\beta) \tag{8}$$

where G' is the storage modulus (real part) of the shear modulus and β is the loss factor of the viscoelastic material.

Consider an element of a beam in pure bending as shown in Figures 1 and 2. Two assumptions are made. The first is that all of the elastic elements undergo the same curvature $\frac{\partial \varphi}{\partial x}$. The second is that the moments and extensional forces acting on the viscoelastic layers are negligible compared to those acting on the elastic elements; i. e., the elastic elements are considerably stiffer in extension than the viscoelastic material. The strain in each element is also shown in Figure 1.

The total bending moment can be considered as the sums of the bending moments on each elastic element. The bending moment on each elastic element is composed of the moment required to bend the element about its own neutral plane plus the net extensional force on the element times the distance from the element's neutral plane to the reference composite neutral plane, as follows

$$M = (EI)^* \; \frac{\partial \varphi}{\partial x} = \Sigma M_{ii} + \Sigma F_i h_i \; . \tag{9}$$

where M_{ii} is the moment exerted by the forces on the ith element about its own neutral plane, F_i is the net extensional force on the ith element, and h_i is the distance from the neutral plane of the ith element to the neutral plane of the composite beam at which the extensional strain is zero.

Since all elastic elements are assumed to undergo the same curvature $\frac{\partial \varphi}{\partial x}$, the sum of the individual moments is

$$\Sigma M_{ii} = [\Sigma (EI)_i] \frac{\partial \varphi}{\partial x} = (EI)_o \frac{\partial \varphi}{\partial x} \tag{10}$$

where $(EI)_o$ is the sum of the individual elastic element flexural rigidities and is defined as the uncoupled flexural rigidity of the structural composite.

It is shown in Appendix A that

$$\Sigma F_i h_i = (\Sigma K_i \delta_i{}^2) Z^* \left(\frac{\partial \varphi}{\partial x}\right) \tag{11}$$

where

$K_i = E_i A_i$ = extensional stiffness of the ith element

δ_i = distance from the ith element to the composite neutral plane for the case where $G = \infty$ (i.e., there is no shearing)

Z^* = complex coupling parameter, defined by Equation (A-16).

The geometrical parameter Y may be defined as follows (Reference 1, p. 8)

$$Y = \frac{(EI)_\infty}{(EI)_0} - 1 = \frac{(EI)_T}{(EI)_0} \tag{12}$$

where $(EI)_0$, $(EI)_\infty$ and $(EI)_T$ represent the uncoupled, coupled and transfer flexural rigidities of the composite structure, respectively. Since the transfer flexural rigidity $(EI)_T$ is given by

$$(EI)_T = \Sigma K_i \delta_i{}^2 \tag{13}$$

Equations (9) through (13) may be combined to give

$$(EI)^* = (EI)_0 [1 + Z^* Y] \tag{14}$$

It should be noted that when the shear modulus of the viscoelastic material G^* is a complex number, the coupling parameter Z^* and the flexural rigidity $(EI)^*$ are also complex numbers. From Equations (5) and (14), the following equation for structure loss factor is obtained

$$\eta = \frac{Im(Z^*)Y}{1 + Re(Z^*)Y} \tag{15}$$

7

Specific Equations for Four Types of Structural Composites

The following is a more detailed discussion pertaining to the loss factors of structural composites comprised of: (1) two elastic elements; (2) a *symmetrical* arrangement of three elastic elements; (3) an *unsymmetrical* arrangement of three elastic elements; and (4) any number N of identical elastic laminates. These four types of structural composites are illustrated in general in Figure 3 and particular examples are shown in Figures 4 to 7.

Using Equation (15), the only two quantities required to calculate the structure loss factor η are the geometrical parameter Y and the complex coupling parameter $Z*$. The equations and graphical displays of the geometrical parameter Y for a wide variety of cross sections of the four types of structural composites indicated above can be found in Reference 1. The equations for the complex coupling parameter $Z*$ are derived in Appendix A for the first three types and in Appendix B for the fourth type of structural composites indicated above.

Two-Elastic-Element Structural Composites. – The complex coupling parameter for two-elastic-element structural composites is given by Equation (A-41) as

$$Z* = \frac{X*}{1 + X*} \tag{16}$$

where $X*$ is defined as the complex shear parameter and is given by Equation (A-38) as

$$X* = \frac{K_1 + K_2}{K_1 K_2} \frac{b \; G*}{H_v p^2} \tag{17}$$

where $K_i = E_i A_i$ = extensional stiffness of the ith element [see Figure 3(a)]; b and H_v are the width and thickness, respectively, of the viscoelastic layer; $G*$ is the complex shear modulus of the viscoelastic material [see Equation (8)]; and p is the wave number ($p = 2\pi/\lambda$, where λ is the wave length) of the particular flexural vibration being considered. A shear parameter X is defined as the real part of $X*$; that is $X = \text{Re}(X*)$. Combining

Equations (8) and (17) gives

$$X^* = X(1 + i\beta) \qquad (18)$$

Combining Equations (16) and (18), the complex coupling parameter can be written as

$$Z^* = \frac{1 + \frac{1}{X} + \beta^2}{(1 + \frac{1}{X})^2 + \beta^2} + i \frac{\frac{1}{X}\beta}{(1 + \frac{1}{X})^2 + \beta^2} \qquad (19)$$

The real part of Z^* is the coupling parameter Z, as given in Equation (32) of Reference 1. Using Equation (19) with the definition of the structure loss factor as given by Equation (15) results in the following relation

$$\eta = \frac{\beta XY}{1 + X(Y+2) + (1 + \beta^2) X^2 (Y+1)} \qquad (20)$$

which is identical to the expression given by Ungar in Equation (4.2) of Reference 3 and also to the expression given in Reference 1 as Equation (27).

Symmetrical Three-Elastic-Element Structural Composites. – For the case of a symmetrical three-elastic-element composite structure, the equation for the complex coupling parameter Z^* as a function of the complex shear parameter X^* is identical to the expression given by Equation (16) for the two-elastic-element case. However, the complex shear parameter has a slightly different definition, given by Equation (A-46) as

$$X^* = \frac{bG^*}{K_1 H_v p^2} \qquad (21)$$

where $K_1 = E_1 A_1$ = extensional stiffness of element 1 [see Figure 3(b)] and the other terms have the same definition as for the two-elastic-element case. With this slight change in the definition of the shear parameter all of the discussion in Reference 1 is applicable to the symmetrical three-elastic-element structures. Of course, the definitions for other parameters such as Y and $(EI)_o$ will have to be those applicable to the symmetrical three-elastic-element structure.

9

Unsymmetrical Three-Elastic-Element Structural Composites. - For the case of an unsymmetrical arrangement of a three-elastic-element structure, the expression for the structural loss factor cannot be cast in the form of the two-elastic-element structure. Appendix A provides an analysis of an unsymmetrical three-elastic-element structure having two of the elements identical. For this case, the expression for Z^* given by Equation (A-55) is a function of three parameters, as follows

$$Z^* = f(d_{12}, K_{12}, X^*) \tag{22}$$

where $d_{12} = d_1/d_2$, $K_{12} = K_1/K_2 = E_1 A_1/E_2 A_2$ [see Figure 3(c)], and X^* is the same shear parameter as was defined for the symmetrical three-elastic-element structure, as given by Equation (21). The only difference in calculating Z^* for the unsymmetrical case is a slightly more complicated expression and two additional parameters. Because of the additional two parameters, the design procedures for the two-elastic-element and the symmetrical three-elastic-element cases are not applicable for the unsymmetrical three-elastic-element case. Appendix C presents an analysis comparing the loss factor of the symmetrical and the unsymmetrical three-elastic-element structural components.

N Identical-Elastic-Laminate Structural Composites. - For the case of N identical elastic laminates, the solution for the loss factor η is more complicated in that it requires the solution of N-1 (for N odd) or N (for N even) linear simultaneous equations. The equations to be solved are developed in Appendix B.

Definition of the Uncoupled Shear Parameter

As stated previously, the uncoupled shear parameter X_0 is one of three parameters $(\beta, Y$ and $X_0)$ that completely define the structure loss factor η. The following analysis defines the uncoupled shear parameter X_0 and relates it to the shear parameter X.

For all of the structures considered in this investigation, there is defined a complex shear parameter of the form

$$X^* = X(1 + i\beta) \tag{23}$$

where β is the loss factor of the viscoelastic material and X is defined as a shear parameter and has the general form

$$X = \frac{bG'}{K H_v p^2} \tag{24}$$

where b is the cross-sectional length of the viscoelastic layer, G' is the real part of the complex shear modulus of the viscoelastic material, K is an extensional stiffness or a modified extensional stiffness of an elastic element, H_v is the thickness of the viscoelastic layer(s) and p is the wave number for the flexural wave shape of the composite structural beam. If the wavelength of the flexural vibration wave λ is known, the wave number p is simply determined from $p = 2\pi/\lambda$. However, the structural designer is frequently interested in predicting the variation of the structure loss factor η as a function of the frequency of vibration f so that the degree of damping at the various structural resonances can be established.

For a purely elastic structure the wave number p is related to the frequency of vibration f as follows

$$p^2 = 2\pi f \sqrt{\frac{w}{g(EI)}} \tag{25}$$

where w is the weight per unit length, g is the gravitational acceleration constant and (EI) is the flexural rigidity of the structure. As an extension of the above equation to apply to viscoelastic shear-damped structures, (EI) is redefined as an effective flexural rigidity $(EI)_r$ of the composite structure. If it is assumed that the effective flexural rigidity $(EI)_r$ is equal to the real part of the complex flexural rigidity as written in Equation (14)

$$(EI)_r = Re[(EI)^*] = (EI)_0 [1 + Re(Z^*)Y] \tag{26}$$

then the loss factor expression of Ungar [Ref. 3] is equivalent to that obtained by DiTaranto [Ref. 4]. This equivalence is shown in Appendix D. This assumption is also supported by the analyses to determine resonant frequencies (see Section 3) and subsequent experimental confirmation of the design procedures developed based on this assumption.

11

The effective flexural rigidity $(EI)_r$ has a value between the completely uncoupled flexural rigidity $(EI)_o$ and the completely coupled flexural rigidity $(EI)_\infty$. as follows

$$(EI)_o \leq (EI)_r \leq (EI)_\infty \tag{27}$$

where, from Equation (12) $(EI)_\infty$ is given by

$$(EI)_\infty = (EI)_o \; (Y+1) \tag{28}$$

The degree of coupling is indicated by the value of $Re(Z^*)$ so that $Z = Re(Z^*)$ is defined as the coupling parameter which has values bounded between zero and unity, as follows

$$0 \leq Re(Z^*) \leq 1 \tag{29}$$

Using the definition $Z = Re(Z^*)$, and Equations (24), (25), and (26), the following relation may be written

$$X = \left[\frac{\sqrt{g}}{2\pi} \; \frac{b}{K\,H_V} \sqrt{\frac{(EI)_o}{w}} \right] \left(\frac{G'}{f} \right) \sqrt{1 + ZY} \tag{30}$$

The quantity in brackets is defined as a shear parameter coefficient C. An uncoupled shear parameter X_0 is defined as the value of X when $Z = 0$. Now the shear parameter X is defined as

$$X = X_0 \sqrt{1 + ZY} \tag{31a}$$

$$X_0 = C \left(\frac{G'}{f} \right) \tag{31b}$$

$$C = \frac{\sqrt{g}}{2\pi} \; \frac{b}{K\,H_V} \sqrt{\frac{(EI)_o}{w}} \tag{31c}$$

These equations are basic in the development of the design procedures and graphs as discussed in Section 4.

12

Symmetrical Three-Elastic-Element Structural Composites
Having Viscoelastic Layers not Parallel to the Neutral Plane of Bending

For the general case of a symmetrical arrangement of a three-elastic-element structure for which the outside elements are not separated from the inside element by a layer of viscoelastic material parallel to the neutral plane of bending but have other geometries (structural composites illustrated in Figure 5(f)-(h) and in Figure 6), the preceding analyses do not apply. Ungar used a strain energy approach to solve for the loss factors of more general structural composites (Ref. 3). Starting with Ungar's Equation (1.8) in Reference 3, Appendix E derives the loss factor expression for the general case of symmetrical three-elastic-element structural composites. This analysis shows that the only difference between this case and the three-elastic-element structure incorporating viscoelastic layers parallel to the neutral plane of bending is in the definition of the length b. This is not an unexpected result since Ungar found the same to be true for the two-elastic-element structure [Ref. 3]. When the elastic elements are separated by viscoelastic layers. parallel to the neutral plane of bending, the length b is the width of the layers. A more general definition of the length b is the cross-sectional length of one of the two symmetrical viscoelastic layers experiencing shear deformation. This definition of b is more clearly illustrated in the table on the following page which gives the value of b for each of the structural composite cross-sections shown in Figures 5 and 6.

STRUCTURAL CONFIGURATION	VALUES OF LENGTH b
Fig. 5(a)-(e)	B
Fig. 5(f)	perimeter of area A_1
Fig. 5(g)	2 (perimeter of area A_1)
Fig. 5(h)	$4(A + H_1)$
Fig. 6(a)-(c)	$4B$
Fig. 6(d)	$B + 2H$
Fig. 6(e)	$A + 2H$
Fig. 6(f)	$\sqrt{2}\ B$
Fig. 6(g)	$(1 + \frac{\pi}{2})B$
Fig. 6(h)	A
Fig. 6(i)	$2A$

SECTION 3: THEORETICAL RESONANT FREQUENCY ANALYSES

An expression for the resonant frequencies of two-elastic-element structural composites was given by Equation (34) of Reference 1 as

$$f_r/f_o = \sqrt{1 + ZY} \qquad (32)$$

where

f_r = resonant frequency

f_o = a reference frequency which is determined by the beam or plate natural frequency equation using $(EI)_o$ as the flexural rigidity

Z = $Re(Z*)$ = coupling parameter

Y = geometrical parameter

This equation was derived by assuming that the damped resonant frequencies could be determined by the appropriate undamped natural frequency formula using the real part of the complex flexural rigidity as an effective flexural rigidity.

For all of the types of structural composites considered in this report, the real part of the complex flexural rigidity, and hence, the effective flexural rigidity is given by Equation (26) as

$$(EI)_r = (EI)_o (1 + ZY) \qquad (33)$$

For flexural vibrations of beams and plates, the natural frequency varies as the square root of the flexural rigidity so that Equation (32) is obtained from Equation (33) and is, therefore, applicable to all of the structural composites considered herein. Of course, the appropriate values of $(EI)_o$, Y, and Z must be used for the particular structure being considered. Specific equations for the uncoupled flexural rigidity $(EI)_o$ and geometrical parameter Y for many structural composites are given in Reference 1. The general definition of Z* from which Z (the real part of Z*) can be obtained is given in Appendix A as

Equation (A-16). Also specific equations for Z are given in Section 4 for two-elastic-element, symmetrical three-elastic-element, unsymmetrical three-elastic element, and N identical-elastic-laminate structures.

Natural Frequency Expression of DiTaranto

DiTaranto [Ref. 5] has obtained an expression for the natural frequencies of laminated beams (two-elastic-element structures comprised of solid structural sheets) which he claims to be exact for simply supported beams and postulates that it is a good approximation for other end conditions. The expression for natural frequencies is given as

$$\omega_1{}^2 = \lambda_0{}^2 \frac{B_1 + B_3 + K_1 \delta^2 \alpha}{\rho} \qquad \text{(Ref. 5, Eq. III-4)} \qquad (34)$$

where

$$\alpha = \frac{R_1 [\lambda_0 + R_1 S(1 + \beta^2)]}{\lambda_0{}^2 + 2 \lambda_0 S R_1 + S^2 R_1{}^2 (1 + \beta^2)} \qquad \text{(Ref. 5, Eq. III-5)} \qquad (35)$$

and it is assumed that*

$$\lambda_0 = \frac{a_n}{L^2} \qquad (36)$$

which is the square of the wave number p. Changing from DiTaranto's notation to our notation

$$\rho = \frac{w}{g} \qquad\qquad \lambda_0 = p^2$$

$$R_1 = \frac{bG'}{K_1 H_v} \qquad\qquad B_1 + B_3 = (EI)_0 \qquad (37)$$

$$S = \frac{K_1 + K_2}{K_2} \qquad\qquad \delta^2 = d^2$$

---

* For simply supported beams this relation was found to be exact.

16

where $(EI)_0$ is the uncoupled flexural rigidity, d is the distance between the centers of the two elastic laminates, w is the weight per unit length of the beam, g is the acceleration of gravity, b is the width of the viscoelastic layer, G' is the real part of the viscoelastic shear modulus, H_v is the thickness of the viscoelastic layer, and K_1 and K_2 are the extensional stiffnesses ($K_i = E_i A_i$ where E_i is the elastic modulus and A_i is the cross sectional area of the ith element) of the top and bottom elastic elements, respectively.

Noting that

$$\frac{K_1 \delta^2}{S(B_1 + B_3)} = \frac{K_1 K_2 d^2}{(K_1 + K_2)(EI)_0} \equiv Y$$

$$\frac{\lambda_0}{2\pi} \sqrt{\frac{B_1 + B_3}{\rho}} = p^2 \frac{\sqrt{g}}{2\pi} \sqrt{\frac{(EI)_0}{w}} \equiv f_0 \tag{38}$$

$$\frac{R_1 S}{\lambda_0} = \frac{K_1 + K_2}{K_1 K_2} \frac{bG'}{H_v p^2} \equiv X$$

Equations III-4 and III-5 of Reference 5 can be rewritten as

$$f_1 = f_0 \sqrt{1 + (S \alpha) Y} \tag{39}$$

where

$$S \alpha = \frac{X[1 + X(1 + \beta^2)]}{1 + 2X + X^2(1 + \beta^2)} \equiv Z \tag{40}$$

which is recognized as the coupling parameter for two-elastic-element structures. Making this substitution in Equation (39) results in Equation (32).

17

Theoretical Results of Snowdon

Snowdon [Ref. 6] has studied the response of internally damped beams by replacing Young's Modulus by a complex Young's Modulus in the equations of motion for elastic beams. The theoretical analysis of composite elastic and viscoelastic structures assumes that the composite structure acts essentially as a solid structure having a complex flexural rigidity obtained from an analysis of the composite structure. Under this assumption, the results of Snowdon are applicable to the composite structures under study. Snowdon has shown that for beams with the same real part of the complex flexural rigidity but with loss factors of 0.01 and 0.1, the resonant frequencies are practically the same. A loss factor of 0.01 is representative of the internal damping possessed by a metal beam. A loss factor of 0.1 is representative of viscoelastic shear-damped composite structures. Snowdon also obtained results for a loss factor of 1.0 and the resonant frequencies were, in general, not the same as for the lower loss factors, especially in the higher modes. However, this value of loss factor is considered to be outside the range of practical interest. These results support the assumption that the resonant frequencies of viscoelastic shear-damped structures can be obtained from the undamped frequency equations by replacing the flexural rigidity by the real part of the complex flexural rigidity.

Lumped Parameter Model Studies

As part of the resonant frequency analyses, single-degree-of-freedom lumped parameter systems were studied since exact theoretical results are known for these systems. The single-degree-of-freedom system is represented by a lumped mass m and a complex stiffness K* as shown by the sketch on the following page. Vibration excitation of the system is the harmonic motion a of the foundation and the response is the harmonic motion x of the mass.
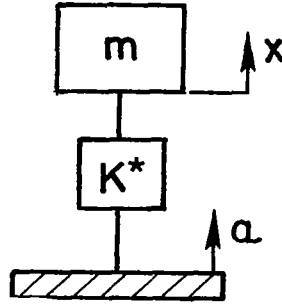
The equation of motion is

$$m\ddot{x} = - K^* (x-a) \tag{41}$$

For the excitation $a = a_0 e^{i\omega t}$, the response is $x = x_0 e^{i(\omega t-\varphi)t}$, so that

$$\frac{x_0}{a_0} e^{-i\varphi} = \frac{K^*}{K^*-m \omega^2} \tag{42}$$

Writing K^* as a complex quantity

$$K^* = \text{Re} \, (K^*) (1 + i\epsilon) \tag{43}$$

and defining a reference frequency ω_R in terms of the real part of the complex stiffness K^*, as follows

$$\omega_R^2 = \frac{\text{Re}(K^*)}{m} \tag{44}$$

Equation (42) becomes

$$\frac{x_0}{a_0} e^{-i\varphi} = \frac{1 + i\epsilon}{1 - (\frac{\omega}{\omega_R})^2 + i\epsilon} \cdot \tag{45}$$

19

and therefore

$$\frac{x_0}{a_0} = \left[\frac{1 + \epsilon^2}{\{1 - (\frac{\omega}{\omega_R})^2\}^2 + \epsilon^2}\right]^{\frac{1}{2}} \tag{46}$$

$$\varphi = \tan^{-1}\left[\frac{-\epsilon(\frac{\omega}{\omega_R})^2}{1 - (\frac{\omega}{\omega_R})^2 + \epsilon^2}\right] \tag{47}$$

To solve for the resonant frequency, take the derivative of $\frac{x_0}{a_0}$ with respect to ω and set the result to zero. Defining

$$\Omega \equiv \frac{d\omega_R}{d\omega} \tag{48}$$

and

$$E \equiv \frac{d\epsilon}{d\omega} \tag{49}$$

The resonant frequency equation can be written as

$$-\frac{2(1 + \epsilon^2)\,\Omega + \epsilon\,\omega_R E}{2(1 + \epsilon^2)\,\omega_R}\,\omega^3 + \omega^2 + \frac{\omega_R\,[(1 + \epsilon^2)\,\Omega + \epsilon\,\omega_R E]}{1 + \epsilon^2}\,\omega - \omega_R^2 = 0 \tag{50}$$

In general the quantities ω_R, Ω, ϵ, and E are all functions of frequency ω so that the solution of Equation (50) can be quite difficult. It is interesting to note, however, that if ϵ is not a function of frequency (i.e., $E = 0$), then $\omega = \omega_R$ satisfies the resonant frequency equation. In other words, if the ratio of the imaginary part to the real part of the complex stiffness is constant with respect to frequency, then the resonant frequency can be obtained from the undamped frequency equation by replacing the stiffness by the real part of the complex stiffness.

The case of relaxation type damping (elastically coupled viscous damping) was studied in some detail since this lumped parameter model has certain similarities with viscoelastic shear-damped beams [Ref. 7]. A sketch of this system is shown below where N is a dimensionless stiffness ratio (which is comparable to the geometrical parameter Y for viscoelastic shear-damped structural composites).
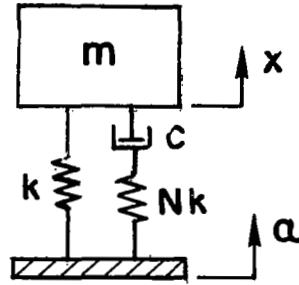
The undamped natural frequency ω_0 is defined as

$$\omega_0{}^2 = k/m \tag{51}$$

and the fraction of critical damping ζ is

$$\zeta = \frac{C}{2\omega_0 m} \tag{52}$$

For this system, use of Equation (44) gives

$$\omega_R{}^2 = \frac{1 + (N+1)\left(\frac{2\zeta}{N}\right)^2 \left(\frac{\omega}{\omega_0}\right)^2}{1 + \left(\frac{2\zeta}{N}\right)^2 \left(\frac{\omega}{\omega_0}\right)^2} \, \omega_0{}^2 \tag{53}$$

and

$$\epsilon = \frac{2\zeta \frac{\omega}{\omega_0}}{1 + (N+1)\left(\frac{2\zeta}{N}\right)^2 \left(\frac{\omega}{\omega_0}\right)^2} \tag{54}$$

21

For this system, ϵ is a function of frequency so that it cannot be expected that ω_R will be the exact resonant frequency. However, it can be seen that as ζ approaches zero, ω_R approaches ω_0 and, as ζ approaches infinity, ω_R approaches $\sqrt{N+1}\,\omega_0$, which are the correct values for the resonant frequency for this system [Ref. 8]. Also, for one intermediate value of ζ, the slope of ϵ is equal to zero (i.e., $E = 0$) so that, at this value of ζ, ω_R is the correct value for the resonant frequency. Therefore ω_R approaches the correct asymptotes as ζ approaches zero or infinity, and has one correct value between the asymptotes. The exact resonant frequency is calculated by substituting the expression for ω_R given by Equation (53) into Equation (50) and solving for $\dfrac{\omega}{\omega_0}$. The approximate resonant frequency is calculated by setting $\omega = \omega_R$ in Equation (53) and solving for $\dfrac{\omega_R}{\omega_0}$.

The above discussion of resonant frequency was applicable to absolute transmissibility T_A (i.e., the excitation is the motion of the foundation and the response is the motion of the mass). However, other resonant responses can be defined. Some of these are: 1) relative transmissibility T_R (i.e., the excitation is the motion of the foundation and the response is the relative motion between the mass and the foundation); 2) acceleration amplification factor H_a (i.e., the excitation is a force on the mass and the response is the acceleration of the mass); 3) driving point mobility M (i.e., the excitation is a force on the mass and the response is the velocity of the mass). Another frequency of interest is the damped free vibration natural frequency ω_d. Of all the above resonant or natural frequencies, only the ones for relative transmissibility and acceleration amplification factor are the same.

Another approximate resonant or natural frequency can be defined as the square root of the ratio of the modulus of the complex stiffness K^* to the mass m, as follows

$$\omega_M^2 = \frac{\mathrm{Re}(K^*)\sqrt{1+\epsilon^2}}{m} \tag{55}$$

All of the above defined resonant frequencies, as well as the damped natural frequency and the two approximate frequencies, are shown graphically in

Figure 8 as a resonant or natural frequency ratio $\frac{\omega}{\omega_0}$ versus the fraction of critical damping ζ for a value of N = 3. The frequency ratio $\frac{\omega}{\omega_0}$ is the ratio of the resonant or damped natural frequency to the undamped natural frequency ω_0. The resonant frequencies for absolute transmissibility and driving point mobility and the damped natural frequency are fairly close. For these frequencies, the approximation using Re(K*) is better for low values of ζ, whereas the approximation using the modulus of K*(i.e., Re(K*)$\sqrt{1 + \epsilon^2}$), is better for high values of ζ. The approximation using the modulus of K* is better at all values of ζ for the resonant frequencies of relative transmissibility and acceleration amplification factor. A case could be made for using the modulus approximation. However, these results represent rather large values of ϵ, which is comparable to the loss factor of damped beams. For low values of ϵ, there is very little difference between the modulus approximation and the Re(K*) approximation. Another consideration is that the Re(K*) approximation is much easier to calculate.

The conclusions that are drawn from the lumped parameter model studies are: 1) using the Re(K*) in the undamped natural frequency equation did not give the exact answer for any of the resonant frequencies or for the damped natural frequency; 2) the frequency calculated by using the Re(K*) will give a fairly good approximation to the resonant frequencies and the damped natural frequency, especially when the damping is small; 3) the various resonant frequencies and the damped natural frequency are in general not the same and determination of the exact frequencies requires a separate analysis for each of these frequencies.

Summary of the Resonant Frequency Analyses

The relation for calculating resonant frequencies of viscoelastic shear-damped structural composites, as given by Equation (32), was derived based on the assumption that there is an effective flexural rigidity of these structural composites equal to the real part of the complex flexural rigidity. As was the case when considering structural loss factors, this assumption is again supported by the theoretical work of DiTaranto [Ref. 5], and also by the theoretical results of Snowdon [Ref. 6]. Lumped parameter model studies have also indicated that there is some justification for this postulate and

subsequent experimental results have shown good agreement with theoretical results based on this postulate (see Section 5).

SECTION 4: DESIGN PROCEDURES

This section of the report presents design procedures and design graphs pertaining to the structure loss factors and resonant frequencies of the four types of structural composites illustrated in Figure 3. In all of these illustrations, the elastic and viscoelastic elements are shown as laminates; however, this restriction is applicable only to the N identical-elastic-laminate structure shown in Figure 3(d).

Six cross-sections of two-elastic-element structures are shown in Figure 4. The angle design shown in Figure 4(f) can be considered as a two-elastic-element structure since the two plates will act as one element [Ref. 1]. Typical cross-sections of symmetrical three-elastic-element structural composite designs are shown in Figures 5 and 6. In some cases, there are actually more than three elastic elements employed in the design; however, because of the physical orientation and identical flexural bending properties of the identical elastic elements located on either side of the central elastic element, the structural composites may be considered to be in the symmetrical three-elastic-element design category. Figure 7 shows six representative cross-sections of the unsymmetrical three-elastic-element type of structure.

Numerical iterative design procedures are presented below for obtaining the structure loss factor η for a given resonant frequency f_r and for obtaining the structure resonant frequency f_r for a given reference frequency f_o. These procedures may be employed (either manually or with digital computer facilities) to achieve virtually any desired degree of accuracy.

A graphical design procedure (requiring no iteration process) is then presented for obtaining structure loss factor as a function of frequency and the structure resonant frequencies. This procedure involves the use of a set of design graphs that provide the structure loss factor η and the resonant frequency ratio f_o/f_r as a function of the uncoupled shear parameter X_o. Since this design procedure is relatively simple to use, it provides a rapid means of assessing the suitability of a proposed composite structural design with regard to the structure loss factor. The accuracy of this procedure, however, is limited to that associated with reading the design graphs.

Definition of Design Parameters

Use of Equation (15) for structure loss factor η and Equation (32) for resonant frequency ratio f_r/f_0 require the determination of the geometrical parameter Y and the complex coupling parameter Z*. The geometrical parameters for a wide variety of cross-sections of the four types of structural composites considered are given in Reference 1. The real and imaginary parts of the complex coupling parameter Re(Z*) and Im(Z*), respectively, are defined below for each of the four types of structures, as a function of the parameter X, the viscoelastic material loss factor β and other parameters when necessary. The shear parameter for all of these structures is given by Equation (31). The extensional stiffness K in Equation (31c) is the only quantity whose definition will be different for the four types of structures and is given below, along with Re(Z*) and Im(Z*).

Two-Elastic-Element Structures

$$K = \frac{K_1 K_2}{K_1 + K_2} \tag{56}$$

$$Re(Z^*) = \frac{X(1+X) + X^2 \beta^2}{(1+X)^2 + X^2 \beta^2} \, . \tag{57}$$

$$Im(Z^*) = \frac{X\beta}{(1+X)^2 + X^2 \beta^2} \tag{58}$$

Symmetrical Three-Elastic-Element Structures

$$K = K_1 \tag{59}$$

$$Re(Z^*) = \frac{X(1+X) + X^2 \beta^2}{(1+X)^2 + X^2 \beta^2} \tag{60}$$

26

$$Im(Z^*) = \frac{X\beta}{(1+X)^2 + X^2\beta^2} \tag{61}$$

Unsymmetrical Three-Elastic Element Structures

$$K = K_1 \tag{62}$$

$$Re(Z^*) = \frac{(C_4/C_1)\{C_2 + [C_2 C_3 (1+\beta^2) + C_1(1-\beta^2)]X + (C_1 C_3 + C_2 C_4)(1+\beta^2)X^2 + C_1 C_4(1+\beta^2)^2 X^3\}X}{[1+C_3 X + C_4(1-\beta^2)X^2]^2 + [C_3 + 2C_4 X]^2 \beta^2 X^2} \tag{63}$$

$$Im(Z^*) = \frac{(C_4/C_1)\{C_2 + 2C_1 X + (C_1 C_3 - C_2 C_4)(1+\beta^2)X^2\}\beta X}{[1+C_3 X + C_4(1-\beta^2)X^2]^2 + [C_3 + 2C_4 X]^2 \beta^2 X^2} \tag{64}$$

where

$$C_1 = 1 + (d_1/d_2)^2 + (d_1/d_2 - 1)^2 K_1/K_2$$

$$C_2 = 1 + (d_1/d_2 - 1)^2$$

$$C_3 = 3 + K_1/K_2$$

$$C_4 = 1 + 2K_1/K_2$$

N Identical-Elastic-Laminate Structures

$$K = EBH \tag{65}$$

For N odd, define $n = (N-1)/2$

$$Re(Z^*) = \frac{6X}{n(n+1)(2n+1)}[n - Re(Q_n) + \beta.Im(Q_n)] \tag{66a}$$

27

$$\text{Im}(Z^*) = \frac{6X}{n(n+1)(2n+1)}[\beta n - \beta \text{Re}(Q_n) - \text{Im}(Q_n)] \tag{67a}$$

where $\text{Re}(Q_n)$ and $\text{Im}(Q_n)$ are obtained by solving the 2n simultaneous equations with $i = 1, 2, \ldots, n$.

$$\sum_{j=1}^{i-1} j\text{Re}(Q_j) + (i+X)\text{Re}(Q_i) + i\sum_{j=i+1}^{n} \text{Re}(Q_j) - X\beta \text{Im}(Q_i) = iX$$

$$\tag{68a}$$

$$\sum_{j=1}^{i-1} j\text{Im}(Q_j) + (i+X)\text{Im}(Q_i) + i\sum_{j=i+1}^{n} \text{Im}(Q_j) + X\beta \text{Re}(Q_i) = iX\beta$$

For N even, define $n = N/2$

$$\text{Re}(Z^*) = \frac{12X}{n(4n^2-1)}[n-1/2 - \text{Re}(Q_n) + \beta \text{Im}(Q_n)] \tag{66b}$$

$$\text{Im}(Z^*) = \frac{12X}{n(4n^2-1)}[\beta(n-1/2) - \beta \text{Re}(Q_n) - \text{Im}(Q_n)] \tag{67b}$$

where $\text{Re}(Q_n)$ and $\text{Im}(Q_n)$ are obtained by solving the 2n simultaneous equations with $i = 1, 2, \ldots, n$.

$$\sum_{j=1}^{i-1} (j-1/2)\text{Re}(Q_j) + (i-1/2+X)\text{Re}(Q_i) + (i-1/2)\sum_{j=i+1}^{n} \text{Re}(Q_j) - X\beta \text{Im}(Q_i) = (i-1/2)X$$

$$\tag{68b}$$

$$\sum_{j=1}^{i-1} (j-1/2)\text{Im}(Q_j) + (i-1/2+X)\text{Im}(Q_i) + (i-1/2)\sum_{j=i+1}^{n} \text{Im}(Q_j) + X\beta \text{Re}(Q_i) = (i-1/2)X\beta$$

28

Resonant Frequencies and Loss Factors for a Given
Beam and Viscoelastic Material

The following iterative design procedure can be employed to calculate the structural resonances and the structure loss factor at these resonances for a given beam configuration. For the particular beam cross-section, calculate the geometrical parameter Y and, using Equation (31c) with the proper definition of extensional stiffness K for the four types of structures, calculate the shear parameter coefficient C. For a given length of beam and end conditions, calculate the various modes of interest of the reference frequency f_o using $(EI)_o$ as the flexural rigidity in the undamped natural frequency equation. For each reference frequency f_o, the following iteration procedure is required to calculate the corresponding structure resonant frequency f_r. Initially set $Z = 0$ and hence $f_r = f_o$. With this value of f_r, obtain G' and β for the viscoelastic material used. With these values of Z, f, and G', calculate X from Equation (31). With these values of β and X calculate Z from the appropriate equation for the type of structure being considered. Substitute this value of Z into Equation (32) to obtain an improved value of f_r. This procedure is then repeated using the improved value of f_r so obtained. Four or five iterations are required using the criteria that the last two values of f_r calculated differ by less than 1/10 of one percent. To obtain the loss factor at this frequency, use the last values calculated for β and X and calculate $Im(Z^*)$ from the appropriate equation for the type of structure being considered. Using this value of $Im(Z^*)$ and using the last value of Z calculated above for $Re(Z^*)$, calculate the structure loss factor η from Equation (15). For digital computer computations, the values of G' and β as a function of frequency have to be entered into the computer in either tabular or equation form.

Development of Design Graphs

For the four types of structural composites considered, relationships have been found expressing the coupling parameter $Z = RE(Z^*)$ as a function of the shear parameter $X = Re(X^*)$, as given by Equations (57), (60), (63), and (66). These relationships, which will always contain the parameter β and may contain other parameters depending on the particular type of structural composite, can be expressed in general as

$$Z = Z(X) \qquad\qquad (69)$$

An iteration procedure is now used to determine Z and X. First, assume some value of X_0. To begin this iteration let $X = X_0$. Insert this value of X into the particular form of Equation (69) that is applicable for the type of structure being considered and obtain a value of Z. This value of Z is used with Equation (31a) to obtain an improved value of X. Repeat the procedure to any desired degree of accuracy. In this iteration process, it is not necessary to give particular values to G', f, or any of the values used to calculate C in Equation (31c). It is necessary only to give values to X_0, Y, β, and any other parameters necessary in the particular form of Equation (69) being used.

The imaginary part of the complex coupling parameter $Im(Z^*)$ is a function of the same parameters as is Z so that, after Z and X are determined, $Im(Z^*)$ can be calculated. With the real and imaginary parts of Z^* and a value of the geometrical parameter Y, the structure loss factor η is calculated by using Equation (15) and the frequency ratio f_0/f_r is calculated using Equation (32). The above calculations are repeated for other values of X_0 and design graphs can be constructed providing η and f_0/f_r as a function of X_0 (defined by Equation (31b) for a particular type of structure) and given values of β, Y, and any other parameters necessary in the particular form of Equation (69).

For some particular cases, β and Y are the only parameters necessary. In these cases a series of graphs can be drawn, each with a different value of Y. On each of these graphs there can be a series of curves, each with a different value of β. Alternatively the graphs can be drawn, each with a different value of β, having a series of curves, each with a different value of Y. Such a group of design graphs represents a complete graphical description of the structural loss factor and resonant frequency ratio for the particular type of structural composite considered. For the particular type of structural composite that the design graphs apply to, the parameters C and Y are calculated and, for a particular frequency of interest, β and G' are obtained from data for the particular viscoelastic shear-damping material being used.

30

In the definition for C given by Equation (31c), K is the only quantity whose basic definition will be different for different types of structural composites. The definition of K for the four types of structures are given by Equations (56), (59), (62), and (65).

Two-Elastic-Element and Symmetrical Three-Elastic-Element Structures.
For two-elastic-element and symmetrical three-elastic element structures, the only parameters required to prepare the design graphs of η and f_o/f_r versus X_o are the geometrical parameter Y and loss factor β. A set of design graphs developed for these two types of structural composites are presented in Figures 9 through 19, where β varies on each graph for a given value of Y. For the design graphs presented in Figures 20 through 37, Y varies on each graph for a given value of β. The values of η plotted were generally between 0.01 and 1.0. Values of η below 0.01 would indicate a poor structural composite design since this is comparable to a resonance amplification factor of 100. Values of η above 1.0 represent poor designs from the static stiffness and weight points of view [Ref. 1].

All of the η versus X_o curves have a slope (on log paper) of +1 for low values of X_o and -1 for high values of X_o. The sharpness of the peaks increases and the value of X_o at the peaks decreases as β and/or Y increases. It is interesting to note that for high values of X_o (low values of frequency), the $\beta = 1$ curve in Figures 9 through 19 and the $Y = 2$ curve in Figures 20 through 37 represent the maximum obtainable structure loss factors. These general characteristics are illustrated in Figure 38. Referring to Figures 9 through 19, for a given value of X_o and Y, there is a finite value of β between 1 and ∞ that will give the maximum value of the structure loss factor η. Referring to Figures 20 through 37, for a given value of X_o and β, there is a finite value of Y between 2 and ∞ that will give the maximum value of the structure loss factor η. The physical significance of an optimum value of Y is somewhat nebulous since the same physical properties of the structure's cross-section are used in calculating both Y and the shear parameter coefficient C, to which X_o is proportional. The physical

31

significance of an optimum value of β is that, as the viscoelastic material becomes more viscous (higher value of β), the elastic elements become more coupled together and, therefore, there is less shearing action. Since the structure loss factor depends on the viscosity of the viscoelastic material and the amount of shearing, it seems reasonable that there would be some value of β that would give the optimum combination of viscosity and the amount of shearing.

The frequency ratio f_o/f_r approaches a value of unity as the uncoupled shear parameter X_o approaches zero; furthermore, f_o/f_r approaches a value of $1/\sqrt{1+Y}$ as X_o approaches infinity. This dependence can be seen from Equation (32) and the fact that, as X_o approaches zero, the coupling parameter Z approaches zero, and as X_o approaches infinity Z approaches unity. The relationship between the uncoupled shear parameter X_o and the shear parameter X can be seen by considering Equations (31a) and (32), so that X_o/X is equal to the frequency ratio f_o/f_r.

In Figures 9 through 37, for any curve (i.e., for any given values of β and Y), there is one peak value of structure loss factor. This is defined as the maximum structure loss factor η_{max} and is presented graphically as a function of the geometrical parameter Y for various values of the viscoelastic material loss factor β in Figure 39 [Ref. 1]. Also, the value of the uncoupled shear parameter X_o at which $\eta = \eta_{max}$, which is defined as the optimum uncoupled shear parameter $(X_o)_{op}$, is presented graphically as a function of the geometrical parameter Y for various values of β in Figure 40.

Approximation for Unsymmetrical Three-Elastic-Element Structures. - Using the appropriate definitions for the geometrical parameter Y and the uncoupled shear parameter X_o, the loss factor design curves presented in Figures 9 through 37 apply for the two-elastic-element and the symmetrical three-elastic-element type structures. They can also be used as an approximation for the unsymmetrical three-elastic-element type structural composite by using the method developed in Appendix D. This method indicates that the X_o scale should be multiplied by some number depending on the parameters d_1/d_2 and $K_1/K_2 = E_1 A_1/E_2 A_2$ (see Figure 3c for the definitions of d_1, d_2, E_1, E_2, A_1 and A_2). However, it is probably easier to determine a

corrective multiplier for X_o, rather than actually changing the X_o scale. The corrective multiplier is just the reciprocal of the scale multiplier. The corrective multiplier has been plotted versus the parameter K_1/K_2 for various values of d_1/d_2 in Figure 41. Loss factors and resonant frequencies for the unsymmetrical three-elastic-element structural composite can be obtained by multiplying X_o by the value obtained from Figure 41 before entering the curves presented in Figures 9 through 37.

Shear Parameter Coefficient for Two- and Three-Elastic-Laminate Plates.- The design graphs of structure loss factor η versus the uncoupled shear parameter X_o presented in Figures 9 through 37 can be used to predict the variation of structure loss factor with frequency. For any given frequency f, the uncoupled shear parameter can be calculated by using Equations (31b) and (31c). To facilitate this calculation, the shear parameter coefficient C times the thickness of the viscoelastic layer(s) H_v has been calculated and plotted for some common cross-sections. The cross-sections are of two-elastic-element and three-elastic element composite structural plates comprised of various combinations of fibre-glass, magnesium, aluminum, titanium and steel sheets. The properties of these five materials used in the calculations are listed in the table below. Graphs of the quantity CH_v versus the thickness ratio H_1/H_2 [see Figures 4(a), 5(a), and 7(a)] are presented in Figures

MATERIAL	ELASTIC MODULUS (psi)	DENSITY (lb/in^3)
FIBRE-GLASS	2.5×10^6	0.064
MAGNESIUM	6.5×10^6	0.064
ALUMINUM	10×10^6	0.098
TITANIUM	14.8×10^6	0.175
STEEL	28×10^6	0.29

42 and 43. Figure 42 is for two-elastic-element composite structural plates, and Figure 43 is for three-elastic-element composite structural plates (either symmetrical or unsymmetrical). For these particular structural composites, the graphs of CH_v versus H_1/H_2 can be used as a design guide for determining the value of the thickness of the viscoelastic layer H_v and the thickness ratio H_1/H_2.

Comparison of the Symmetrical and Unsymmetrical Three-Elastic-Element Structures. - From the analysis in Appendix C, it is seen that changing a three-elastic-element structure from a symmetrical arrangement to an unsymmetrical arrangement essentially shifts the η versus X_0 curve to the right for most practical structures. Since X_0 is proportional to G'/f, which decreases with increasing frequency for most viscoelastic materials [Ref. 2, p. 73], a plot of η versus frequency will be shifted to the left (see Figure 44). Neglecting the effects of the geometrical parameter, the unsymmetrical arrangement will have higher loss factors in the low frequency region which is usually the more important since the frequency where $\eta = \eta_{max}$ is usually quite high.

For the special case where the elastic elements are structural sheets and $E_1/E_2 \geq 1$, the geometrical parameter for the unsymmetrical arrangement is greater than or equal to the geometrical parameter for the symmetrical arrangement [Ref. 1, p. 85]. Therefore, for this case the unsymmetrical arrangement is better for the low frequency range. This comparison is based on the two structures having the same weight, static stiffness and shear parameter coefficient C since the only difference assumed was in changing the arrangement of the elements.

For the most common case of structural composites composed of a lamination of structural sheets, a comparison of the symmetrical and unsymmetrical three-elastic-element type structures has been made. This is shown graphically in Figures 45 and 46. It is assumed that the thickness of the viscoelastic layers H_v is small compared to $H_1 + H_2$ so that its value is taken as zero in the calculation of the distance d for the symmetrical case, and of the distances d_1 and d_2 for the unsymmetrical case. The only other parameters necessary for these calculations are the ratios H_1/H_2 and E_1/E_2.

34

<u>N Identical-Elastic-Laminates</u>. - For the case of N identical elastic laminates, the analytical solution is considerably more complicated than for the two and three-elastic element cases. As was shown in Appendix A, the solution for a general N elastic element structure requires the solution of N - 1 complex simultaneous equations or 2(N-1) real simultaneous equations. The reason for this is that there is one complex equation for each viscoelastic layer. For N identical elastic laminates the solution is somewhat simplified. There are two reasons for this: (1) Since all the elements are identical, the extensional stiffness terms K_i can be taken outside of the summations, thereby simplifying the equations; and (2) due to symmetry, the number of complex equations reduces to (N-1)/2 when the composite neutral axis passes through an elastic element (i.e., N is odd) or N/2 when the composite neutral axis passes through a viscoelastic element (i.e., N is even). The equations to be solved are Equations (68a) when N is odd and Equations (68b) when N is even. The only parameters necessary to solve these equations are X_o, Y, β, and N.

The geometrical parameter $Y = (N^2 - 1)(1 + 2V)^2$, where $V = H_v/2H$, H_v is the thickness of the viscoelastic damping layers, and H is the thickness of the elastic laminates. Therefore, for given values of N, V, and β, a design graph of the structure loss factor η versus the uncoupled shear parameter X_o can be obtained. This was accomplished for the five values of N equal to 2, 3, 4, 6, and 8. For each value of N, four values of the viscoelastic layer thickness parameter V were selected equal to 0, 0.05, 0.1, and 0.15, and values of the viscoelastic material loss factor β ranging between 0.05 and 5 were selected. The results are displayed graphically in Figures 47 to 56.

The shape of these curves is quite similar to those for the two- and three-elastic-element structures. Here again, for high values of X_o (low values of frequency), the $\beta = 1$ curve represents the highest obtainable structure loss factors. Of course, for N = 2 and N = 3, these results are just special cases of the two- and three-elastic-element structures, respectively.

For the purpose of illustrating the effect of increasing the number of laminates, the maximum structure loss factor η_{max} and the optimum uncoupled shear parameter $(X_o)_{op}$ have been plotted versus the viscoelastic material

loss factor β for values of N equal to 2, 3, 4, 5, 6 and 8 in Figures 57 and 58. For these curves, it was assumed that $H_V << H$, so that $V = 0$. At first there is a large increase in η_{max} as N is increased, but the rate of increase in η_{max} decreases for further increase in N. This is necessarily so since, as N approaches infinity, η_{max} approaches β.

Due to the fact that all elastic elements are assumed to be identical structural sheets, the uncoupled shear parameter X_0 for this case takes a particularly simple form. From Equation (31c)

$$C = \frac{0.903}{H_V \sqrt{E\gamma}} \tag{70}$$

where H_V is the thickness of the viscoelastic damping layer (in), E is the modulus of elasticity (lbs/in^2) and γ is the weight density (lbs/in^3) of the elastic elements. From Equation (31b)

$$X_0 = \frac{0.903}{H_V \sqrt{E\gamma}} \left(\frac{G'}{f} \right) \tag{71}$$

where G' is the real part of the complex shear modulus (lbs/in^2) of the viscoelastic material, and f is the resonant frequency (Hz).

Design Example

As an example of the use of the design graphs for predicting resonant frequencies and associated loss factors, one of the beams from the experimental tests (see Figure 67) was chosen. This is a two-elastic element beam comprised of aluminum plates. The pertinent cross-section dimensions of the beams are: thickness of the top aluminum laminate $H_1 = 0.0309$ inches; thickness of the bottom aluminum laminate $H_2 = 0.0899$ inches; and thickness of the viscoelastic layer $H_V = 0.0048$ inches. The viscoelastic material is 3M No. 466 adhesive transfer tape.

The thickness ratio $H_1/H_2 = 0.344$ so that, using Figure 2.11(B) of NASA CR-742 [Ref. 1], the uncorrected geometrical parameter Y_0 is 1.33. The viscoelastic thickness parameter $V = H_V/(H_1 + H_2) = 0.0397$ so that,

using the graph on page 15 of NASA CR-742, the geometrical parameter ratio is 1.165 and, therefore, the geometrical parameter $Y = 1.55$. To calculate the shear parameter coefficient C, use of Figure 42 with $H_1/H_2 = 0.344$ gives $CH_v = 3.1 \times 10^{-3}$ and, therefore, $C = 0.646$. Using Figure 63, values of the uncoupled shear parameter $X_0 = C(G'/f)$ were obtained for frequencies in the range of 10 to 1000 Hz and an assumed temperature of $75°$ F. With these values and using Figure 14, values of the structure loss factor η and the frequency ratio f_0/f_r are obtained. (The value of 1.55 for the geometrical parameter is considered close enough to 1.5 so that interpolation between graphs with different values of Y was not necessary). For every frequency $f = f_r$, the frequency ratio f_0/f_r is multiplied by f_r to obtain f_0. These results are tabulated below, from which the graphs of f_r versus f_0 and η versus f_r shown in Figure 59 were obtained.

f	$\dfrac{G'}{f}$	$X_0 = C\left(\dfrac{G'}{f}\right)$	β	η	f_0/f_r	f_0
10	4.65	3.00	1.40	0.055	0.648	6.48
15	3.90	2.52	1.40	0.065	0.652	9.78
20	3.40	2.20	1.40	0.074	0.655	13.1
30	2.80	1.81	1.40	0.088	0.658	19.7
40	2.45	1.58	1.41	0.10	0.664	26.6
50	2.23	1.44	1.41	0.11	0.67	33.5
70	1.90	1.23	1.41	0.125	0.675	47.2
100	1.62	1.05	1.42	0.135	0.683	68.3
150	1.33	0.859	1.42	0.16	0.692	104
200	1.17	0.756	1.42	0.17	0.70	140
300	0.97	0.627	1.43	0.19	0.715	215
400	0.85	0.549	1.43	0.205	0.73	292
500	0.77	0.497	1.43	0.21	0.74	370
700	0.66	0.426	1.43	0.225	0.763	534
1000	0.56	0.362	1.43	0.235	0.78	780

Up to this point, the length, width, or end conditions of the beam have not influenced the design process. For the particular beam under consideration, the length ℓ = 36 inches and the width b = 3 inches. The beam was used as a free-free beam in the experimental test. In this test the resonant frequencies and the corresponding loss factors were measured for seven modes. To determine these quantities from Figure 59, it is first necessary to calculate the reference frequency f_o for these seven modes of this free-free beam. The equation for reference frequency is

$$f_o = \frac{\sqrt{g}}{2\pi} \frac{\alpha_m}{\ell^2} \sqrt{\frac{(EI)_o}{w}} \tag{72}$$

where α_m is a number associated with mode m. The table below gives α_m for the first ten modes of a free-free beam.

m	1	2	3	4	5	6	7	8	9	10
α_m	22.2	61.6	121	200	299	417	555	713	891	1088

The weight per unit length for this beam was measured and is w = 0.0355 pounds per inch. The uncoupled flexural rigidity was calculated to be $(EI)_o$ = 1895 lb-in^2. The reference frequencies f_o for the first ten modes were calculated from the above equation and with these values, the corresponding resonant frequencies f_r and structure loss factor η were obtained from Figure 59. The results are tabulated below.

Mode	f_o	f_r	η
1	12.4	19	0.073
2	34.3	51	0.11
3	67.5	100	0.14
4	111	160	0.163
5	167	235	0.18
6	232	320	0.195
7	309	420	0.207
8	397	530	0.217
9	497	660	0.225
10	607	785	0.23

The values of f_r and η from this table are plotted in Figure 60. Also on this graph are the values of f_r and η obtained experimentally. It can be seen that modes five, seven, and either nine or ten in the experimental data are missing. This is due to the particular location of the point of excitation for this experiment.

SECTION 5: EXPERIMENTAL VERIFICATION OF THE THEORETICAL CALCULATIONS

This section of the report presents a comparison of the theoretical predictions and experimental measurements of the structure loss factor and resonant frequencies of two-elastic-element, symmetrical three-elastic-element, unsymmetrical three-elastic-element and N identical-elastic-laminate viscoelastic shear-damped structural composite beams. Cross-sections of the experimental structural specimens, which included laminated beams comprised of solid sheets, solid and honeycomb sheets, solid sheet with channel section, and various bars and tubes, are presented in Figures 61 and 62. Aluminum and fibre-glass structural materials were employed, and the viscoelastic damping material was 3M No. 466 adhesive transfer tape. The dynamic elastic properties of the damping material are presented in Figure 63. The experiments were performed at temperatures ranging between 70° and 80° F.

Measurement of Structure Loss Factor

The decay rate method was selected to measure the loss factor of the viscoelastic shear-damped beam specimens since the measurements can be made with considerable speed and the method is generally accepted by researchers in the field of structural damping [Ref. 9-10]. Repeated measurements of vibration decay can be made on a structural member under the same conditions in rapid sequence thereby providing an accurate measurement of damping through averaging of data. If the rate of decay is measured in terms of the reverberation time T_{60}, the structure loss factor η is given by

$$\eta = \frac{2.2}{f_r \, T_{60}} = \frac{2.2\tau_r}{T_{60}} \tag{73}$$

where T_{60} is the time required for the amplitude of free vibration to be attenuated by 60 db (corresponding to a factor of 1000), f_r is the resonant frequency of the decaying vibration for the particular mode of vibration being

evaluated, and $\tau_r = 1/f_r$ is the period of the vibration at each particular resonance.

The experimental system for measuring the loss factor of the visco-elastic shear-damped beam specimens is shown in Figure 64; the instrumentation for the experimental system is identified in the chart presented below.

INSTRUMENTATION FOR MEASUREMENT OF STRUCTURE LOSS FACTOR		
Instrumentation	Manufacturer	Model Number
Electrodynamic Exciter (Magnetic Housing and Driver Coil)	Acoustic Research, Inc.	AR-10 Driver Coil and Magnet Assembly
Accelerometer	B&K	4336
Cathode Follower Amplifier	Columbia Research Lab.	6003
High-Pass Filter	Krohn-Hite	330-M
Decay Rate Meter	Spencer-Kennedy Lab.	507
Power Amplifier	Dynaco	Mark III
Oscilloscope	Tektronix	564/2867/3A3
Harmonic Oscillator	Exact Electronics	502

The structural specimen is supported vertically by a string suspension. A small driver coil is cemented to the specimen in a manner which will add a minimum amount of stiffness or weight and allow centering of the driver coil within the magnetic housing of the electrodynamic exciter, which provides a linear magnetic field for the driver coil. The electrodynamic exciter, which is driven by the harmonic oscillator through a power amplifier, is capable of delivering 25 watts of power to a beam specimen for an extended period of time at a maximum linear peak-to-peak displacement of one-half inch.

The response of the beam specimen is detected by the accelerometer which is mounted near the end of the beam with a counter weight of equal magnitude (2 grams) mounted on the opposite end of the beam for purpose of balance. The high-pass filter is used to reject all frequencies less than the particular

resonant frequency at which the loss factor is being measured. The decay rate meter provides electronic switching between two alternating functions: (1) processing the signal from the high-pass filter through a logarithmic amplifier, and (2) generating a calibrated logarithmic decay signal. The oscilloscope provides alternate displays of the logarithmic decay signal representing the beam vibration and the calibrated logarithmic decay signal.

The experimental procedure for the measurement of the structure loss factor is as follows. The structural specimen is excited by harmonic vibration at each of its resonant frequencies so as to attain a steady-state vibration condition. The cutoff frequency of the high-pass filter is set approximately at the resonant frequency. As part of the electronic switching function performed by the decay rate meter, the excitation vibration is abruptly removed from the structure and the ensuing vibration decay is sensed by the accelerometer. The accelerometer signal is processed through the cathode follower amplifier, high-pass filter and decay rate meter. The decay rate meter processes the signal through a logarithmic amplifier and generates a separate calibrated logarithmic decay signal. The structure vibration decay signal and the calibrated decay signal are alternately displayed on the oscilloscope on a repetitive basis thereby allowing adjustment of the calibrated decay signal to match the vibration decay signal. When the calibrated decay signal is adjusted to match the structure vibration decay signal, the value of the reverberation time T_{60} is read from the decay rate meter and the structure loss factor is calculated from Equation (73).

Loss factor measurements are made at the various resonances of the structure and, therefore, data is obtained at discrete frequencies. However, a curve may be passed through the discrete loss factor data points to generate a description of loss factor as a continuous function of frequency. The connotation is that if the structure were to resonate at an intermediate frequency, the continuous curve of loss factor versus frequency indicates the loss factor which exists for that particular mode of vibration.

The filter in the experimental system places a limitation on the maximum value of structure loss factor which can be measured accurately. Because of its "ringing" characteristic, the filter itself exhibits a decay

rate characteristic and, hence, the experimental system may be employed
only to measure vibration decay rates which are less than that of the filter.
The active high-pass filter was selected because of its high rejection
rate (24 db/octave) below the cutoff frequency and its favorable ringing
characteristic. Based on the fact that the effective loss factor of the
filter was generally greater than 0.5 over the frequency range of interest
(10 Hz to 1000 Hz), data can be obtained for structure loss factor measure-
ments as high as 0.5. Actually, even if the range of loss factor measurement
was not limited by the filter ringing characteristic, there would be another
limitation imposed by the physical difficulty encountered in interpreting the
decay of a signal having a few cycles of oscillation, which would be the
case for values of loss factor greater than 0.5 (see Figure 65). It is concluded
that the experimental system is capable of measuring maximum values of
structure loss factor equal to 0.5.

Another limitation on the measurement of structure loss factor is due
to the limitation of the reverberation time T_{60} of the decay rate meter. This
limitation is

$$0.01 \leq T_{60} \leq 10 \tag{74}$$

so that, from Equation (73)

$$\frac{0.22}{f_r} \leq \eta \leq \frac{220}{f_r} \tag{75}$$

This limitation as well as $\eta \leq 0.5$ are depicted graphically in Figure 66.
If a theoretically calculated value of the loss factor fell within the shaded
area, then the corresponding experimentally determined value was rejected
from the statistical analysis of the experimental data.

Measurement of Resonant Frequency

The resonant frequencies are found by slowly varying the frequency of
the harmonic oscillator until the output from the accelerometer goes through
a peak value. Since the sharpness of the peak depends upon the positioning

43

of the accelerometer and the driver coil, the mode of vibration, and the loss factor, some modes were easier to determine than others and some modes did not show up at all. In general, the higher modes were more difficult to determine and are also very closely spaced when plotted on log paper. For this reason any mode greater than the fifth was rejected from the statistical analysis of resonant frequency.

Presentation of Experimental Data

The experimentally determined values of structure loss factors and resonant frequencies for 44 different beam specimens are plotted in Figures 67 through 110. Also the theoretical structure loss factor curve has been drawn on these graphs. The relevant modulus and dimension data are presented with each graph as well as the value of the geometrical parameter Y and the shear parameter coefficient C. There are 16 two-elastic-element beams shown in Figures 67 through 82. The effect of varying the thickness of the viscoelastic layer H_v is illustrated in Figures 71, 72 and 73 where H_v is 0.0045 inches, 0.0146 inches, and 0.025 inches, respectively, and all other dimensions are the same for the three beams. There are 21 symmetrical three-elastic-element beams shown in Figures 83 through 103 and 4 unsymmetrical three-elastic element beams shown in Figures 104 through 107. Only three N identical-elastic laminate beams are included and those are shown in Figures 108 through 110. The value of N for these beams is 2, 3, and 4 respectively. Four other N identical-elastic-laminate beams having N = 5, 6, 7 and 8 were tested but the loss factors for these beams were greater than 0.5 and therefore, could not be measured accurately based on the aforementioned limitations on loss factor measurements.

Sources of Errors. - The discrepancies between the experimental and theoretical data indicated in Figures 67 through 110 indicate the degree of accuracy that can be expected when predicting structure loss factors. While there can be many sources of errors, it is felt that the most significant are the following: (1) the loss factor β and the storage modulus G' of the viscoelastic damping material are not easily determined and vary considerably with the frequency of vibration and temperature; (2) the thickness of the

44

viscoelastic layer(s) H_v is difficult to measure and in many cases causes an error in the structure loss factor proportional to the error in measuring H_v; (3) the viscoelastic material may not have perfect contact at the interfaces with the elastic elements and/or may have entrapped air bubbles. Of course, the experimentally measured values can also be in error and this will add to the discrepancies between theory and experiment.

Statistical Analysis of Experimental Data

The experimentally determined values of structure loss factor η_e and resonant frequency $(f_r)_e$ are plotted versus their theoretically predicted values η_t and $(f_r)_t$, respectively, in Figures 111 and 112. The data point symbols used in these figures are identified in the chart below.

SYMBOLS USED IN FIGURES 111 and 112	
TYPE OF STRUCTURAL COMPOSITE	SYMBOL
Two-elastic-element	*
Symmetrical three-elastic-element	●
Unsymmetrical three-elastic-element	○
N identical-elastic-laminate	✗

A linear regression of $\ln \eta_e$ on $\ln \eta_t$, representing a least squares fit for η_e on log paper, was obtained for 226 data points for which the equation is

$$\ln \eta_e = 0.017575 + 1.00126 \ln \eta_t \tag{76}$$

or

$$\eta_e = 1.0177 \, \eta_t^{1.00126} \tag{77}$$

This result indicates excellent agreement between experiment and theory; however, the correlation coefficient squared (a measure of the goodness of fit) is 0.92, which is only fairly good.

Also, a linear regression of $\ln (f_r)_e$ on $\ln (f_r)_t$, representing a least squares fit for $(f_r)_e$ on log paper, was obtained for 164 data points for which the equation is

$$\ln (f_r)_e = 0.1769 + 0.962 \ln (f_r)_t \tag{78}$$

or

$$(f_r)_e = 1.19 (f_r)_t^{0.962} \tag{79}$$

This result indicates fair agreement between experiment and theory; however, the correlation coefficient squared is 0.997, which is excellent.

Statistical analyses were made of the 226 values of $\ln \eta_e - \ln \eta_t$, which is the same as $\ln (\eta_e/\eta_t)$, and of the 164 values of $\ln(f_r)_e - \ln(f_r)_t$, which is the same as $\ln[(f_r)_e/(f_r)_t]$. The calculated means were 0.0148 and 0.00735, respectively. Since the logarithm of the geometric mean is the arithmetic mean of the logarithms of the values being analyzed, the geometric mean of η_e/η_t is 1.015 and the geometric mean of $(f_r)_e/(f_r)_t$ is 0.993. These values for the geometric means show excellent agreement between experiment and theory.

The standardized probability densities of $\ln (\eta_e/\eta_t)$ and of $\ln [(f_r)_e/(f_r)_t]$ are shown compared to the standardized normal distribution in Figures 113 and 114, respectively. It was expected that these distributions would be approximately normal since it seems that the errors are caused by many factors, none of which represents a predominant influence [Ref. 1 and 11]. The hypothesis that $\ln (\eta_e/\eta_t)$ is normally distributed is well justified (in comparing this distribution with the normal, χ^2 with six degrees of freedom = 5.44). The hypothesis that $\ln [(f_r)_e/(f_r)_t]$ is normally distributed is not so well justified (in comparing this distribution with the normal, χ^2 with six degrees of freedom = 13.6). However, the following discussion will assume that both $\ln(\eta_e/\eta_t)$ and $\ln[(f_r)_e/(f_r)_t]$ are normally distributed with a zero mean value.

The standard deviation of $\ln (\eta_e/\eta_t)$ is 0.253 so that it can be expected that 68 percent of the values of η_e/η_t will be between 0.78 and 1.29 and

95 percent will be between 0.6 and 1.66. The standard deviation of $\ln[(f_r)_e/(f_r)_t]$ is 0.0846 so that it can be expected that 68 percent of the values of $(f_r)_e/(f_r)_t$ will be between 0.92 and 1.09 and 95 percent will be between 0.844 and 1.18. Alternatively, it could be stated that the percent errors of η_e with respect to η_t corresponding to plus and minus one standard deviation of $\ln(\eta_e/\eta_t)$ are +29 and -22, and that the percent errors of $(f_r)_e$ with respect to $(f_r)_t$ corresponding to plus and minus one standard deviation of $\ln[(f_r)_e/(f_r)_t]$ are +9 and -8.

Based on the results of the statistical analyses of the experimental data compared to the theoretical predictions, it is concluded that the theory and design procedures for calculating the loss factor and resonant frequencies of two-elastic-element, symmetrical three-elastic-element, unsymmetrical three-elastic-element, and N identical-elastic-laminate viscoelastic shear-damped structural composites is satisfactory within accepted engineering accuracy.

Transmissibility of Viscoelastic Shear-Damped Beams

Transmissibility tests were run on two of the beams that were used in the loss factor and resonant frequency analysis (see Figures 67 and 85 for the cross section dimensions of these beams). The experimental setup was as illustrated in Figure 115. The original beam was clamped at its center, making two equal cantilever beams. This was done to avoid applying unbalanced moments to the shaker armature. In both cases the beam length ℓ was 17.5 inches. The input vibration was measured at the clamp and the output was measured at the end of the beam using a small (2-gram weight) accelerometer. The transmissibility is defined as the ratio of the amplitude of the output to the amplitude of the input.

The theoretical transmissibility for a damped beam is obtained by using the transmissibility expression for an undamped beam, replacing the flexural rigidity by the complex flexural rigidity, and taking the square root of the sum of the squares of the real and imaginary parts. The expression for the undamped transmissibility is given as [Ref. 7]

$$T(\ell, f) = \frac{\cosh \beta\ell + \cos \beta\ell}{\cosh \beta\ell \cos \beta\ell + 1} \; ; \beta^4 = \frac{m_B (2\pi f)^2}{\ell (EI)} \qquad (80)$$

where m_B = mass of the beam

f = frequency of vibration

ℓ = beam length

EI = flexural rigidity

The complex flexural rigidity for these beams is given as

$$(EI)^* = (EI)_0 [1 + Z^*Y] = (EI)_0 [1 + Re(Z^*)Y + i \, Im(Z^*)Y] \qquad (81)$$

The uncoupled flexural rigidity $(EI)_0$, complex coupling parameter Z^* and geometrical parameter Y have been defined previously. In Equation (80) (EI) is replaced by $(EI)^*$ so that $T(\ell, f)$ becomes a complex number, $T^*(\ell, f)$. For any particular beam, $(EI)_0$ and Y are calculated and, for every frequency f of interest, $Re(Z^*)$ and $Im(Z^*)$ are calculated as described previously. Substituting these values into Equation (80), $Re[T^*(\ell, f)]$ and $Im[T^*(\ell, f)]$ are calculated. The damped transmissibility is

$$T_d(\ell, f) = \sqrt{\{Re[T^*(\ell, f)]\}^2 + \{Im[T^*(\ell, f)]\}^2} \qquad (82)$$

The experimental and theoretical transmissibility curves for these two beams are shown in Figures 116 and 117, respectively. For both beams, the experimental and theoretical curves agree quite well for the first two resonant modes. At higher frequencies, however, the agreement is not as good. The reason for this is not clear, but it can be at least partially explained by the facts that the test fixture had structural resonances in the frequency range above 200 Hz and that the clamping device was not a perfect clamp.

Disregarding the results in the higher frequencies, the curves in Figures 116 and 117 demonstrate that the dynamic response of viscoelastic shear-damped structural composites can be obtained by replacing the flexural rigidity in the undamped dynamic response equations by the complex flexural rigidity and calculating the damped dynamic response as indicated above.

SECTION 6: THERMAL CONDUCTIVITY DESIGN STUDIES

The thermal conduction properties of viscoelastic shear-damped laminated plates is an important design consideration in space vehicle applications such as solar panels, since a specific minimum value of thermal conductivity is generally required to limit the thermal gradient across the panel. A thermal conductivity study was conducted to: (1) determine the thermal conductivity properties of laminated elastic and viscoelastic plates as compared to solid elastic plates; and (2) investigate the possibilities of increasing the thermal conductivity of laminated elastic and viscoelastic plates without seriously deteriorating their damping properties. We shall consider the steady-state heat flow through a laminated plate as shown in Figure 118. For the purpose of this discussion, it will be assumed that the temperature T_1 at Surface 1 is a given constant and that Surface 2 is in a vacuum and radiating to a black body at zero absolute temperature. It is further assumed that the laminates have perfect contact at their interfaces so that no temperature gradient occurs across the interfaces.

The rate of heat conducted per unit area q can be expressed as [Ref. 12]

$$q = \frac{\Delta t}{\Sigma H_i / k_i} \tag{83}$$

where Δt is the temperature gradient across the laminated plate, H_i is the thickness of the ith laminate and k_i is the thermal conductivity of the ith laminate. In the steady-state, the heat conducted through the laminate must be radiated from Surface 2. The equation for the heat radiated is [Ref. 12]

$$q = \epsilon \sigma T_2^4 \tag{84}$$

where ϵ is the emissivity of Surface 2, σ is the Steffan-Boltzman constant $(0.173 \times 10^{-8} \text{ BTU/hr-ft}^2 - {}^\circ R^4)$, and T_2 is the absolute temperature at Surface 2. Writing Δt as $T_1 - T_2$ and combining Equations (83) and (84) gives

$$[\Sigma H_i / k_i] \epsilon \sigma T_2^4 + T_2 - T_1 = 0 \tag{85}$$

Given T_1, ϵ, and $\Sigma H_i / k_i$, Equation (85) is solved for T_2. From this solution, Δt is calculated and, using Equation (84), q is calculated. For small temperature gradients Δt, q is approximately proportional to the emissivity

$$q \approx \epsilon \left(\sigma T_1^4 \right) \tag{86}$$

so that to have high values of q, ϵ should be high. Using Equation (86) with Equation (83), it can be seen that the temperature gradient across the laminated plate is approximately proportional to $\Sigma H_i / k_i$

$$\Delta t \approx \left[\Sigma H_i / k_i \right] \left(\epsilon \sigma T_1^4 \right) \tag{87}$$

so that to have small values of Δt, $\Sigma H_i / k_i$ should be small. This implies that the thicknesses of the laminates H_i should be small and the thermal conductivities of the laminates k_i should be high. Thermal conductivities of viscoelastic damping materials are typically much lower than thermal conductivities of metals. Thermal conductivities for many viscoelastic materials would fall within the range of 0.02 to 0.2 BTU/hr-ft-$^\circ$F whereas, for most metals, the value will be in the range of 5 to 150 BTU/hr-ft-$^\circ$ F.

As an example of thermal conductivity considerations, assume that the temperature T_1 at Surface 1 is 257° F(125° C) and that Surface 2 is coated so that its emissivity is 0.9. It is desired to determine the temperature drop across the laminated plate. The laminated plate to be investigated is comprised of two 0.063 inch (0.00525 ft) thick 3003-H14 aluminum sheets separated by a 0.030 inch (0.0025 ft) layer of a polyurethane based adhesive known commercially as CYBOND$^\circledR$ 4000 adhesive. This plate (designated as the basic specimen) as well as four others, which are essentially the same except that the viscoelastic layer has additives for improved thermal conductivity, were provided by American Cyanamid Company. The thermal conductivity of the aluminum at 70° F is 101.7 BTU/hr-ft-$^\circ$ F[Ref. 13], and the thermal conductivity of CYBOND 4000 adhesive is 0.11 BTU/hr-ft-$^\circ$ F at 200° F. For the aluminum alone $\Sigma H_i / k_i = 2(0.00525)/101.7 = 0.000103$ hr-ft^2-$^\circ$ F/BTU and for the viscoelastic material alone $\Sigma H_i / k_i = 0.0025/0.11 = 0.0227$ hr-ft^2-$^\circ$ F/BTU.

The total $\Sigma H_i/k_i = 0.000103 + 0.0227 = 0.0228$ hr-ft^2-$^\circ$F/BTU. Using this value of $\Sigma H_i/k_i$, $\epsilon = 0.9$ and $T_1 = 257^\circ$ F $= 717^\circ$ R, Δt is determined from Equation (85) to be 8.9° F. In a similar manner the temperature gradient across the aluminum alone is 0.042° F.

If the temperature gradient is considered to be too high, $\Sigma H_i/k_i$ for the viscoelastic material alone could be lowered by either making the H_i smaller or the k_i larger (see below for methods of increasing k_i). Either of these changes could affect the damping properties of the structure. The uncoupled shear parameter X_0 is inversely proportional to the viscoelastic layer thickness H_v so that making H_v smaller makes X_0 larger which may or may not increase the structure loss factor depending on whether the original value of X_0 was lower or higher than the optimum value $(X_0)_{op}$. Decreasing H_v will decrease the geometrical parameter Y which, depending on the value of X_0, may or may not decrease the structure loss factor.

The thermal conductivity of the viscoelastic material can be increased by adding to it other material having a high thermal conductivity. This can be considered as changing the properties of the viscoelastic material and not as a change in the structural configuration. Therefore, all of the existing theory would still be applicable and it would be necessary only to determine the thermal conductivity and damping properties of the new material.

The four specimens with improved thermal conductivity had the following additives to the basic viscoelastic layer which was CYBOND 4000 adhesive: Specimen 1 had a standard aluminum screen (268 openings per inch with 0.010 inch diameter wire) imbedded in the viscoelastic layer; Specimen 2 had 39 percent (by weight) graphite powder, superconductive grade, twenty micron mesh size, manufactured by Consolidated-Astronautics Inc., Long Island City, New York; Specimen 3 was the same as Specimen 2 but with the metal screen of Specimen 1 added also; Specimen 4 was the same as Specimen 2 but with a fibrous metal product (Felt Metal type FM-127 manufactured by Huyck Metals Company, Milford, Connecticut) imbedded within the viscoelastic layer. Thermal conductivity tests were performed by the Stamford Research Laboratories of the American Cyanamid Company on these specimens. The thermal conducticity values were obtained using a COLORA thermo-conductometer. The test

samples were disks of laminate, machined to a diameter of 0.7 inches. The measurements were made at a mean temperature of 200°F. Peel strengths of these samples were measured at room temperature.

Using the thermal conductivity values of the specimens, the thicknesses of the individual laminates, and the thermal conductivity of the aluminum, the thermal conductivity of the damping material was calculated for each of the specimens. These four specimens, as well as the specimen with no additives (basic specimen), were tested to determine their structure loss factors in the same manner as described in Section 5.

All of the specimens were 3 inches wide and 47 inches long except Specimen 4 which was 30 inches long. For all of the specimens, the thickness of the viscoelastic layer H_v was maintained at approximately 0.030 inches. However, since they were not exactly 0.030 inches, a corrected structure loss factor was calculated assuming $H_v = 0.03$. The frequency range over which the specimens were tested was approximately 10 - 1000 Hz. In this frequency range the structure loss factor for these specimens is approximately proportional to the viscoelastic thickness H_v and this is the basis for the corrected structure loss factor.

The results of all of the measurements and calculations described above are summarized in the table below; however, the structure loss factor data has been normalized to the basic specimen's loss factor since it is not the loss factors of these particular specimens that is significant, but the effect of the additives to the viscoelastic material on the change in loss factor. Also, for this frequency range (10 - 1000 Hz) the ratios of the loss factors are approximately constant so that one number (taken at 100 Hz) is representative of the whole frequency range.

From this table it can be seen that there is a general trend that, as the structure thermal conductivity is increased, the structure loss factor and the peel strength are decreased. For these particular specimens, this same trend regarding structure loss factor would hold true if the viscoelastic thickness H_v were decreased while holding constant the thermal conductivity of the visco-elastic material k_v. For purposes of comparing the effects of changing H_v to the effects of changing k_v, consider the basic specimen having values of H_v such that the structure thermal conductivity has values equal to Specimens 1

52

SPECIMEN PROPERTY	BASIC SPECIMEN	SPECIMENS WITH IMPROVED THERMAL CONDUCTIVITY			
		1	2	3	4
STRUCTURE THERMAL CONDUCTIVITY (BTU/hr-ft-$^\circ$ F)	0.608	0.90	2.50	3.25	5.0
DAMPING LAYER THERMAL CONDUCTIVITY (BTU/hr-ft-$^\circ$ F)	0.12	0.16	0.41	0.60	1.22
PEEL STRENGTH (lbs/in)	200	40	90	80	20
STRUCTURE LOSS FACTOR NORMALIZED TO BASIC SPECIMEN	1	0.94	0.45	0.33	0.07
THICKNESS OF DAMPING LAYER (in)	0.030	0.027	0.024	0.028	0.039
CORRECTED STRUCTURE LOSS FACTOR NORMALIZED TO BASIC SPECIMEN	1	1.04	0.56	0.35	0.054

to 4 respectively, and a constant value of $k_V = 0.12$ BTU/hr-ft-$^\circ$ F. The values of H_V can be calculated from the relation

$$\frac{H_V}{k_V} + \frac{H_A}{k_A} = \frac{H_V + H_A}{k_s} \tag{88}$$

where H_A is the total thickness of the aluminum, k_A is the thermal conductivity of the aluminum, and k_s is the structure thermal conductivity as given in the table above. Again it will be assumed that the structure loss factor for these specimens in the frequency range 10 to 1000 Hz is proportional to the thickness of the viscoelastic layer H_V. The results of the H_V and structure loss factor calculations are presented in the following table.

THEORETICAL SPECIMEN	1	2	3	4
STRUCTURE THERMAL CONDUCTIVITY (BTU/hr-ft-$^\circ$F)	0.90	2.50	3.25	5.0
THICKNESS OF DAMPING LAYER (in)	0.19	0.0062	0.0047	0.003
STRUCTURE LOSS FACTOR NORMALIZED TO BASIC SPECIMEN	0.63	0.21	0.16	0.10

Comparing these results with those obtained for Specimens 1 to 4 above, it can be seen that except for Specimen 4, it is better from the structural loss factor point of view to change k_v rather than H_v in order to get improved thermal conductivity.

Returning to the design example given above (i.e., determine Δt, given that $T_1 = 717^\circ R$ and $\epsilon = 0.9$), the quantity $\Sigma H_i/k_i$ for the four specimens with improved thermal conductivity is equal to 0.016, 0.0063, 0.0043 and 0.0022 hr-ft^2-$^\circ$F/BTU, respectively. Using these values with Equation (85), the temperature gradient across the laminated plate is calculated to be 5.3, 2.5, 1.7 and 0.88°F, respectively, for Specimens 1 through 4.

In summary, the thermal conductivity of viscoelastic shear-damped laminated plates can be increased by adding material of high thermal conductivity to the viscoelastic material or by reducing the thickness of the viscoelastic material. Judging from the results described above, however, it appears that the preferred approach is to add material of high thermal conductivity to the viscoelastic material since this causes less of a deterioration of the structure loss factor.

SECTION 7: RESULTS AND CONCLUSIONS

The results of the research investigation are:

(1) A general expression for structural loss factor and resonant frequency for any number of elastic elements separated by layers of viscoelastic material.

(2) Specific equations for structure loss factor and resonant frequency for two-elastic-element, symmetrical three-elastic-element, unsymmetrical three-elastic-element, and any number N identical-elastic-laminate structural composites with viscoelastic shear-damping mechanisms.

(3) Design graphs for the four types of structural composites defined in (2) above, from which the structure loss factor and resonant frequency ratio can be read directly without an iteration procedure.

(4) Experimental verification of the theory and design procedures developed to predict structure loss factor, resonant frequency, and transmissibility of viscoelastic shear-damped structural composites.

(5) Evaluation of various methods for increasing the thermal conductivity of viscoelastic shear-damped laminated plates.

Specific conclusions drawn are:

(1) The structure loss factor η and resonant frequency ratio f_o/f_r for two- and three-elastic-element structural composites are functions of only three parameters: (1) the viscoelastic material loss factor β; (2) the uncoupled shear parameter X_o; and (3) the geometrical parameter Y. These parameters can be calculated in terms of frequency, and the material properties and cross-section dimensions of the structural composite.

(2) For a given value of viscoelastic material loss factor β and geometrical parameter Y, there is an optimum uncoupled shear parameter $(X_o)_{op}$ that maximizes the structure loss factor. The maximum structure loss factor η_{max} is always less than the viscoelastic material loss factor β and approaches β as the geometrical parameter Y approaches infinity.

(3) The forms of the equations for structure loss factor η and resonant frequency ratio f_o/f_r for two-elastic-element and symmetrical three-elastic-

element structural composites are identical. Therefore, the same design graphs can be used for the two types of structural composites with the proper definition of the uncoupled shear parameter X_o and the geometrical parameter Y.

(4) The equations for structure loss factor η and resonant frequency ratio f_o/f_r for unsymmetrical three-elastic-element structural composites are not of the same form as those for two-elastic-element and symmetrical three-elastic-element structural composites. However, the same design graphs can be used to obtain good approximations by applying a corrective multiplier to the uncoupled shear parameter X_o.

(5) Structures incorporating either a symmetrical or unsymmetrical arrangement of three elastic elements will achieve approximately the same maximum structure loss factor η_{max}. However, the frequency at which the maximum loss factor is attained generally will be lower for the unsymmetrical arrangement of the three elastic elements.

(6) Three-elastic-element and N-identical-elastic laminate structural composites oan attain much higher values of structure loss factor η than two-elastic-element structural composites, because of the considerably higher values of the geometrical parameter Y involved. While increasing the number N of identical elastic laminates increases the structure loss factor η, the rate of change of η with N substantially decreases for values of N greater than approximately 4.

(7) For a given value of uncoupled shear parameter X_o, there is an optimum value of the viscoelastic material loss factor β that maximizes the structure loss factor. The optimum value of viscoelastic material loss factor approaches unity as X_o approaches infinity (frequency approaches zero) and is greater than unity for all other values of X_o. Consequently, for the lower modes of vibration of the structural composite, it may be undesirable for β to have a value greater than unity.

(8) With regard to predicting the structure loss factor and resonant frequency, the justification has been established for assuming there is an effective flexural rigidity equal to the real part of the complex flexural rigidity.

(9) Based on a statistical analysis of the experimentally determined values of structure loss factor and resonant frequency, the theory and design procedures for calculating these parameters for the four types of structural composites indicated in (2) above is satisfactory within accepted engineering accuracy.

(10) The thermal conductivity of viscoelastic shear-damped laminated plates can be increased by adding material of high thermal conductivity to the viscoelastic material. However, it appears that this can be done only at the expense of the structural damping and the peel strength of the laminated plate.

It is anticipated that the straightforward design procedures presented in this report will greatly simplify the analysis and design of structural composites with viscoelastic shear-damping mechanisms. Accordingly, the results of the research investigation should prove useful to structural design engineers, especially those concerned with controlling the vibration response of air-borne and aerospace structural assemblies.

APPENDIX A

GENERAL LOSS FACTOR EXPRESSION AND SPECIFIC
EQUATIONS FOR TWO-AND THREE-ELASTIC-ELEMENT
VISCOELASTIC SHEAR-DAMPED COMPOSITE STRUCTURES

APPENDIX A

GENERAL, LOSS FACTOR EXPRESSION AND SPECIFIC EQUATIONS FOR TWO- AND THREE- ELASTIC-ELEMENT VISCOELASTIC SHEAR-DAMPED COMPOSITE STRUCTURES

The moment equation for a composite beam in bending is [Ref. 2]

$$M = (EI)^* \frac{\partial \varphi}{\partial x} = (EI)_0 \frac{\partial \varphi}{\partial x} + \Sigma F_i h_i \tag{A-1}$$

where

M is the moment

$(EI)^*$ is the complex flexural rigidity

$\frac{\partial \varphi}{\partial x}$ is the curvature (assumed the same for all elastic elements)

$(EI)_0 = \Sigma(EI)_i$ = sum of the individual elastic element flexural rigidities

F_i is the net extensional force acting at the center of an individual elastic element

h_i is the distance from a reference composite neutral plane (zero extensional strain) to the center of an individual elastic element

Let d_i be the distance to the ith elastic element measured from the center of the first elastic element. Let δ_i be the distance to the ith elastic element measured from the composite neutral plane for the case where $(EI)^* = (EI)_\infty$ (i.e., where the shearing modulus is infinite so that all of the elastic elements are completely coupled). These dimensions as well as D and $\overline{\delta}$ are defined by Figure 1, which shows a beam segment and its assumed strain distribution diagram. From this diagram it can be seen that

$$\sum_1^N F_i h_i = \sum_2^N F_i d_i - D\sum_1^N F_i \tag{A-2}$$

Under the assumption of pure bending

$$\sum_1^N F_i = 0 \tag{A-3}$$

60

so that

$$\sum_{1}^{N} F_i h_i = \sum_{2}^{N} F_i d_i \tag{A-4}$$

The net extensional force on an element is obtained by multiplying the extensional stiffness by the strain at its center.

$$F_i = K_i \epsilon_i \tag{A-5}$$

In the strain diagram ψ_i is the shearing strain of the ith viscoelastic layer as shown in the Figure 2. From the strain diagram, the strain at the center of any elastic element is

$$\epsilon_i = \epsilon_1 + d_i \alpha - H_v \sum_{j=2}^{i} \theta_j \tag{A-6}$$

Using Equations (A-3) and (A-5)

$$\epsilon_1 = -\frac{1}{K_1} \sum_{2}^{N} K_i \epsilon_i$$

or, using Equation (A-6)

$$\epsilon_1 = -\frac{1}{K_T} \sum_{i=2}^{N} \left\{ K_i \left(d_i \alpha - H_v \sum_{j=2}^{i} \theta_i \right) \right\} \tag{A-7}$$

where

$$K_T = \sum_{i=1}^{N} K_i$$

Defining

$$R_j = \theta_j / \alpha \tag{A-8}$$

Equations (A-6) and (A-7) are combined to obtain

61

$$\epsilon_i = \left\{ d_i - \frac{\sum\limits_{i=2}^{N} K_i d_i}{K_T} - H_v \left[\sum\limits_{j=2}^{i} R_j - \frac{1}{K_T} \sum\limits_{j=2}^{N} \left(K_j \sum\limits_{\ell=2}^{j} R_\ell \right) \right] \right\} \alpha \qquad \text{(A-9)}$$

Using the relation

$$\sum\limits_{j=2}^{N} \left(K_j \sum\limits_{\ell=2}^{j} R_\ell \right) = \sum\limits_{j=2}^{N} \left[\left(\sum\limits_{\ell=j}^{N} K_\ell \right) R_j \right] \qquad \text{(A-10)}$$

and Equations (A-4), (A-5), and (A-9)

$$\sum\limits_{i=1}^{N} F_i h_i = \sum\limits_{i=2}^{N} \left\{ K_i d_i^2 - \frac{K_i d_i}{K_T} \sum\limits_{i=2}^{N} K_i d_i - H_v K_i d_i \left[\sum\limits_{j=2}^{i} R_j - \frac{1}{K_T} \sum\limits_{j=2}^{N} \left[\left(\sum\limits_{\ell=j}^{N} K_\ell \right) R_j \right] \right] \right\} \alpha \qquad \text{(A-11)}$$

A transfer flexural rigidity is defined as

$$(EI)_T = \sum\limits_{i=1}^{N} K_i \delta_i^2 \qquad \text{(A-12)}$$

and since

$$\delta_i = d_i - \overline{\delta}$$

$$(EI)_T = \sum\limits_{i=1}^{N} K_i d_i^2 - 2\overline{\delta} \sum\limits_{i=1}^{N} K_i d_i + \overline{\delta}^2 K_T \qquad \text{(A-13)}$$

The distance $\overline{\delta}$ is also defined as

$$\overline{\delta} = \frac{\sum\limits_{i=1}^{N} K_i d_i}{K_T} \qquad \text{(A-14)}$$

Since $d_1 = 0$, (A-13) can be written as

$$(EI)_T = \sum\limits_{i=2}^{N} K_i d_i^2 - \frac{1}{K_T} \left(\sum\limits_{i=2}^{N} K_i d_i \right)^2 \qquad \text{(A-15)}$$

62

Define

$$Z^* = 1 - \frac{H_v}{(EI)_T} \sum_{i=2}^{N} \left[K_i d_i \left\{ \sum_{j=2}^{i} R_j - \frac{1}{K_T} \sum_{j=2}^{N} \left[\left(\sum_{\ell=j}^{N} K_\ell \right) R_j \right] \right\} \right] \tag{A-16}$$

Equations (A-11), (A-15), and (A-16) can be combined to give

$$\sum_{i=1}^{N} F_i h_i = (EI)_T Z^* \alpha \tag{A-17}$$

The geometrical parameter is defined as [Ref. 1]

$$Y = \frac{(EI)_\infty}{(EI)_0} - 1 = \frac{(EI)_T}{(EI)_0} \tag{A-18}$$

So that

$$\sum_{i=1}^{N} F_i h_i = (EI)_0 Z^* Y \alpha \tag{A-19}$$

Since $\frac{\partial \varphi}{\partial x} = \alpha$, the expression for the complex flexural rigidity can be obtained from Equations (A-1) and (A-19) as

$$(EI)^* = (EI)_0 (1 + Z^* Y) \tag{A-20}$$

The structural loss factor, η, is defined as the ratio of the imaginary part to the real part of the complex flexural rigidity.

$$\eta = \frac{Im[(EI)^*]}{Re[(EI)^*]} = \frac{Im(Z^*)Y}{1 + Re(Z^*)Y} \tag{A-21}$$

It is necessary to determine the N-1 values of R_j in order to calculate Z^*. To determine the R_j it is necessary to consider the shearing relations of the viscoelastic layers. First it will be assumed that these layers are purely elastic and then when the solution is obtained for the elastic case, the

63

substitution of a complex modulus will be made for the shearing modulus of these layers.

The stress-strain relation for any layer is

$$G = \frac{S_i}{\psi_i} \qquad (A-22)$$

where

$\qquad G \;=\;$ shear modulus of elasticity

$\qquad S_i \;=\;$ shearing stress in the ith layer

$\qquad \psi_i \;=\;$ shearing strain in the ith layer

For a small section of the beam of length dx and width b, the area is

$$A = b\,dx \qquad (A-23)$$

The shearing force is obtained by considering a section of the beam as shown in the sketch below

— i^{th} element
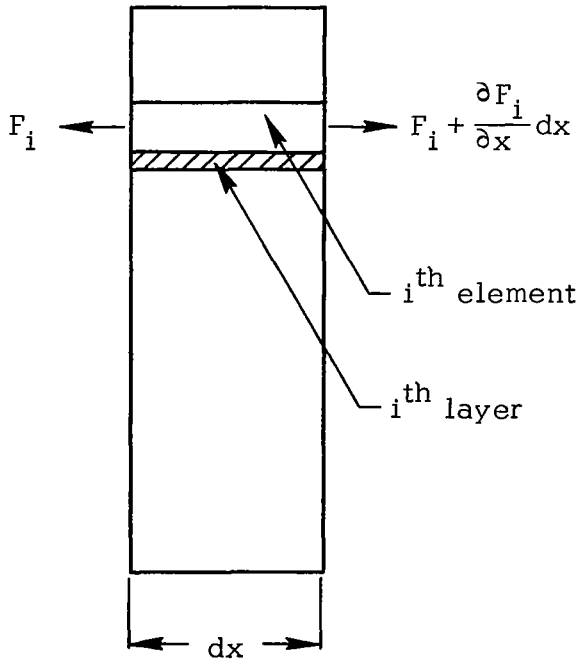
— i^{th} layer

Since $\Sigma F_i = 0$ and $\Sigma\left(F_i + \dfrac{\partial F_i}{\partial x}\,dx\right) = 0$,

$$\Sigma \frac{\partial F_i}{\partial x}\,dx = 0$$

Therefore, the sum of the forces above the ith layer must be equal but opposite in direction to those below the ith layer. This sum is the shearing force so that

$$S_i = \frac{-\displaystyle\sum_{j=i}^{N} \dfrac{\partial F_j}{\partial x}\,dx}{A} \qquad (A-24)$$

Combining (A-22), (A-23), and (A-24)

$$bG\psi_i = -\sum_{j=i}^{N} \frac{\partial F_j}{\partial x} \qquad (A-25)$$

64

Now combining Equations (A-5), (A-8), (A-9) and (A-25) and differentiating, assuming that R_i is not a function of x

$$bGR_i\alpha = -\sum_{j=i}^{N}\left\{K_jd_j - \frac{K_j}{K_T}\frac{1}{2}\sum K_id_i - H_vK_j\left[\sum_{\ell=2}^{j}R_\ell - \frac{1}{K_T}\sum_{\ell=2}^{N}\left[\left(\sum_{m=\ell}^{N}K_m\right)R_\ell\right]\right]\right\}\frac{\partial^2\alpha}{\partial x^2} \qquad (A-26)$$

Equation (A-26) implies that $\alpha = \dfrac{\partial\varphi}{\partial x}$ has a sinusoidal wave shape. Therefore, the assumption that R_i is not a function of x implies a sinusoidal wave shape. For other than sinusoidal wave shapes, R_i must be a function of x, so that this analysis is strictly applicable only for sinusoidal wave shapes. Define a wave number, p, for this differential equation and rearrange the summations so that*

$$p^2 = \cfrac{bG.R_i}{\left[\begin{array}{c}\sum\limits_{j=i}^{N}K_jd_j - \left(\frac{1}{K_T}\frac{1}{2}\sum K_id_i\right)\sum\limits_{j=i}^{N}K_j - H_v\left[\left\{\left(\sum\limits_{j=i}^{N}K_j\right)\left(\sum\limits_{j=2}^{i}R_j\right) + \sum\limits_{j=i+1}^{N}\left[\left(\sum\limits_{\ell=j}^{N}K_\ell\right)R_j\right]\right\}\right.\\ \left.+\left(\frac{1}{K_T}\sum\limits_{\ell=2}^{N}\left[\left(\sum\limits_{m=\ell}^{N}K_m\right)R_\ell\right]\right)\sum\limits_{j=i}^{N}K_j\right]\end{array}\right]} \qquad (A-27)$$

Define a shear parameter as

$$X' = \frac{bG}{H_vK_Tp^2} \qquad (A-28)$$

This shear parameter is not to be a general definition of a shear parameter. In the analyses that follow a shear parameter is defined for each type of structural composite. The purpose of defining a shear parameter is to have a convenient grouping of constants and to non-dimensionalize the equations.

The $N-1$ equations for the R_i are

65

$$\left(\frac{1}{K_T^2} \sum_{j=i}^{N} K_j\right)\left(\sum_{\ell=2}^{N}\left[\left(\sum_{m=\ell}^{N} K_m\right)R_\ell\right]\right) - \frac{1}{K_T}\left\{\left(\sum_{j=i}^{N} K_j\right)\left(\sum_{j=2}^{i} R_j\right) + \sum_{j=i+1}^{N}\left[\left(\sum_{\ell=j}^{N} K_\ell\right)R_j\right]\right\} - X R_i$$

$$= \frac{1}{K_T^2 H_v}\left(\sum_{j=i}^{N} K_j\right)\left(\sum_{i=2}^{N} K_i d_i\right) - \frac{1}{K_T H_v}\left(\sum_{j=i}^{N} K_j d_j\right) \qquad (A-29)$$

When G is made complex, there are 2(N-1) equations for the N-1 $Re(R_i)$ and the N-1 $Im(R_i)$. Also, G should be written as G* to indicate a complex quantity.

$$G* = G'(1 + i\beta) \qquad (A-30)$$

where G' is the real part and β is the ratio of the imaginary part to the real part (i.e., loss factor) of the complex shear modulus G* of the visco-elastic layers, and $i = \sqrt{-1}$. Equation (A-28) should be rewritten as

$$X' = \frac{b\, G*}{H_v K_T p^2} \qquad (A-31)$$

Now the set of equations represented by Equation (A-29) can be solved for the real and imaginary parts of the R_i's. With these, the complex number Z* can be obtained from Equation (A-16). However, the wave number p is in Equation (A-29) and it is also a function of Z*. The wave number p is related to the frequency of vibration f by

$$p^2 = 2\pi f \sqrt{\frac{w}{g(EI)_r}} \qquad (A-32)$$

where w is weight per unit length of the composite structure, g is the gravitational acceleration constant, and $(EI)_r$ is the effective flexural rigidity of the structure for the resonant mode of vibration being considered.

It is assumed that

$$(EI)_r = Re[EI)*] = (EI)_0 [1 + Re(Z*)Y] \qquad (A-33)$$

Therefore, an iteration process is required to determine $Re(Z^*)$. It is assumed that $(EI)_r$ will be bounded between $(EI)_0$ (for the completely uncoupled condition) and $(EI)_\infty$ (for the completely coupled condition) so that

$$0 \le Re(Z^*) \le 1 \tag{A-34}$$

This bounding of $Re(Z^*)$ makes the iteration process simpler which can be important when a large number of simultaneous equations must be solved during each iteration cycle.

To apply the general analysis to two-elastic-element structures, set $N = 2$ in Equation (A-16). Since there is only one d_i for this structure [see Figure 3(a)], let $d_2 = d$. Now Equation (A-16) becomes

$$Z^* = 1 - \frac{H_v}{(EI)_T}\left[K_2 d \left(1 - \frac{K_2}{K_T}\right)R_2\right] \tag{A-35}$$

From Equation (A-15)

$$(EI)_T = K_2 d^2 \left(1 - \frac{K_2}{K_T}\right) \tag{A-36}$$

and

$$K_T = K_1 + K_2 \tag{A-37}$$

The shear parameter for this case is defined as

$$X^* = \frac{K_1 + K_2}{K_1 K_2}\left(\frac{b\ G^*}{H_v p^2}\right) \tag{A-38}$$

so that Equation (A-31) becomes

$$X' = \frac{K_1 K_2}{K_T^2} X^* \tag{A-39}$$

Substituting (A-39) into (A-29) with $N = 2$ gives

$$R_2 = \frac{d}{H_v}\left(\frac{1}{1 + X^*}\right) \tag{A-40}$$

Substituting (A-36) and (A-40) into (A-35) gives

$$Z^* = \frac{X^*}{1 + X^*} \tag{A-41}$$

Equations (A-41), (A-38) and (A-30) define the complex coupling parameter Z^* for the two-elastic-element case.

To apply the general analysis to <u>three-elastic-element</u> <u>structures</u>, set $N = 3$ in Equation (A-16) to obtain

$$Z^* = 1 - \frac{H_v}{(EI)_T}\left\{\frac{K_1}{K_T}\left(K_2 d_2 + K_3 d_3\right)R_2 + \frac{K_3}{K_T}\left[K_1 d_3 + K_2\left(d_3 - d_2\right)\right]R_3\right\} \tag{A-42}$$

From Equation (A-15)

$$(EI)_T = K_2 d_2 + K_3 d_3{}^2 - \frac{1}{K_T}\left(K_2 d_2 + K_3 d_3\right)^2 \tag{A-43}$$

and

$$K_T = K_1 + K_2 + K_3 \tag{A-44}$$

Setting $N = 3$ in Equation (A-29) gives the following set of simultaneous equations for R_2 and R_3

$$\left[\left(\frac{K_2 + K_3}{K_T}\right)^2 - \left(\frac{K_2 + K_3}{K_T}\right) - X'\right]R_2 + \left[\frac{K_3\left(K_2 + K_3\right)}{K_T^2} - \frac{K_3}{K_T}\right]R_3 = -\frac{K_1}{K_T}\ \frac{K_2 d_2 + K_3 d_3}{K_T\ H_v}$$

$$\left[\frac{K_3\left(K_2 + K_3\right)}{K_T^2} - \frac{K_3}{K_T}\right]R_2 + \left[\frac{K_3{}^2}{K_T^2} - \frac{K_3}{K_T} - X'\right]R_3 = -\frac{K_3}{K_T}\ \frac{K_2\left(d_3 - d_2\right) + K_1 d_3}{K_T\ H_v} \tag{A-45}$$

For the <u>symmetrical</u> three-elastic-element case, set $K_3 = K_1$, $d_3 = 2d$, and $d_2 = d$ to agree with the definitions in Figure 3(b). Also, for this case

the shear parameter is defined as

$$X^* = \frac{bG^*}{K_1 H_v p^2} \qquad \text{(A-46)}$$

so that Equation (A-31) becomes

$$X' = \frac{K_1}{K_T} X^* \qquad \text{(A-47)}$$

with these substitutions and using Equations (A-43) and (A-44), Equation (A-42) becomes

$$Z^* = 1 - \frac{H_v}{2d}(R_2 + R_3) \qquad \text{(A-48)}$$

and the solution of Equation (A-45) is

$$R_2 = R_3 = \frac{d}{H_v}\left(\frac{1}{1 + X^*}\right) \qquad \text{(A-49)}$$

so that

$$Z^* = \frac{X^*}{1 + X^*} \qquad \text{(A-50)}$$

Equations (A-50), (A-46) and (A-30) define the complex coupling parameter Z^* for the symmetrical three-elastic-element case.

For the unsymmetrical three-elastic-element case, set $K_3 = K_1$, $K_2 = K_1$, $K_1 = K_2$, $d_3 = d_1$, and $d_2 = d_2$ to agree with the definitions in Figure 3(c). Also for this case the shear parameter is defined as

$$X^* = \frac{bG^*}{K_1 H_v p^2} \qquad \text{(A-51)}$$

So that Equation (A-31) becomes

$$X' = \frac{K_1}{K_T} X^* \qquad \text{(A-52)}$$

69

With these substitutions and using Equations (A-43) and (A-44), Equation (A-42) becomes

$$Z^* = 1 - \frac{H_v}{d_2} \left\{ \frac{(d_{12} + 1) R_2 + [d_{12} + K_{12} (d_{12} - 1)] R_3}{1 + d_{12}^2 + (d_{12} - 1)^2 K_{12}} \right\} \qquad (A-53)$$

where $d_{12} = d_1/d_2$ and $K_{12} = K_1/K_2$

and the solution of Equation (A-45) is

$$R_2 = \frac{d_2}{H_v} \left[\frac{1 + (d_{12} + 1) X^*}{1 + (3 + K_{12}) X^* + (1 + 2 K_{12})(X^*)^2} \right]$$

$$\qquad (A-54)$$

$$R_3 = \frac{d_2}{H_v} \left[\frac{d_{12} - 1 + [d_{12} + K_{12} (d_{12} - 1)] X^*}{1 + (3 + K_{12}) X^* + (1 + 2 K_{12})(X^*)^2} \right]$$

so that

$$Z^* = \frac{C_2 + C_1 X^*}{C_1 [\, 1 + C_3 X^* + C_4 (X^*)^2 \,]} \left(C_4 X^* \right) \qquad (A-55)$$

where

$$C_1 = 1 + d_{12}^2 + (d_{12} - 1)^2 K_{12}$$

$$C_2 = 1 + (d_{12} - 1)^2$$

$$C_3 = 3 + K_{12}$$

$$C_4 = 1 + 2 K_{12}$$

Equations (A-55), (A-51) and (A-30) define the complex coupling parameter Z^* for the unsymmetrical three-elastic-element case.

The equations for defining the complex coupling parameter Z^* for the N-equal-laminate case can also be developed from the general analysis, however, they have been derived independently in Appendix B.

70

APPENDIX B

LOSS FACTOR OF N IDENTICAL-ELASTIC LAMINATE
VISCOELASTIC SHEAR-DAMPED COMPOSITE STRUCTURES

APPENDIX B

LOSS FACTOR OF N IDENTICAL-ELASTIC LAMINATE VISCOELASTIC SHEAR-DAMPED COMPOSITE STRUCTURES

Shown below is a sketch of an elemental section of a beam for an odd number of laminates = N.
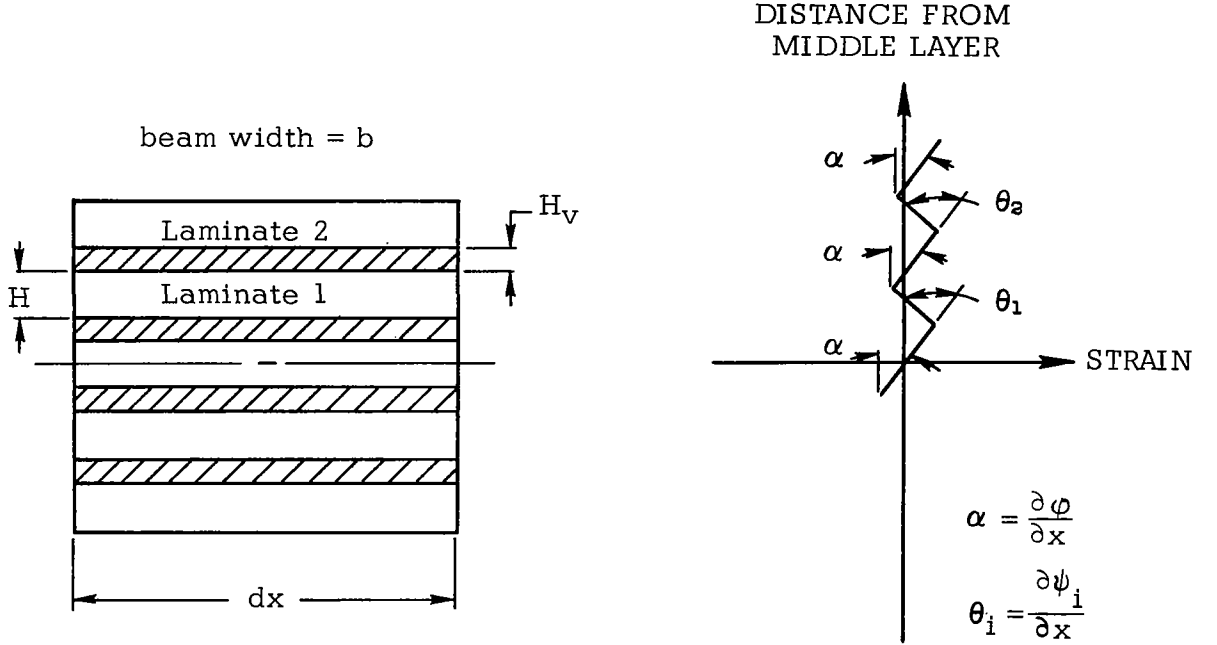
Assume that the strain distribution below the middle laminate is equal but opposite in sign to that above the middle laminate. The strain at the center of the middle laminate is zero. The strain at the center of any laminate is given by

$$\epsilon_i = i\,(H + H_v)\,\alpha - H_v \sum_{j=1}^{i} \theta_j \tag{B-1}$$

Define $R_j = \dfrac{\theta_j}{\alpha}$ and $d = H + H_v$

$$\epsilon_i = (id - H_v \sum_{j=1}^{i} R_j)\,\alpha \tag{B-2}$$

The extensional force on each laminate at its center is the extensional stiffness times the strain at the center of the laminate. The extensional stiffness K is

$$K = EbH \qquad (B-3)$$

where E is modulus of elasticity.

$$F_i = K\epsilon_i \qquad (B-4)$$

Defining $Q_i = \dfrac{F_i}{K\,d\alpha}$, and using Equations (B-2) and B-4)

$$Q_i = i - \frac{H_v}{d} \sum_{j=1}^{i} R_j \qquad (B-5)$$

The shear relation for any viscoelastic layer is

$$G = \frac{-\sum\limits_{j=i}^{n} \dfrac{\partial F_i}{\partial x} dx}{\dfrac{b\,dx}{\psi_i}} \; ; \; n = \frac{N-1}{2} \qquad (B-6)$$

where $\sum\limits_{j=i}^{n} \dfrac{\partial F_j}{\partial x} dx$ is the sum of all forces on the elements above the visco-elastic layer. It is assumed that the extensional forces in the viscoelastic layers are zero and, since the sum of all forces on any cross-sectional plane is zero, the sum of forces on all elastic layers above a viscoelastic layer must be equal but opposite in sign to the sum of forces on all elastic layers below that viscoelastic layer. This sum of forces is then the shearing force on that viscoelastic layer. The quantity "bdx" is the elemental area so that the numerator of Equation (B-6) is the shearing stress, and ψ_i is the shearing strain of the layer. The modulus of rigidity G relates shearing stress to shearing strain. Since the layer is viscoelastic, G will be a complex number.

Assuming that R_j is not a function of x, Equation (B-6) can be differentiated with respect to x to give

$$bGR_i \alpha = - Kd \sum_{j=i}^{n} Q_j \frac{\partial^2 \alpha}{\partial x^2} \qquad (B-7)$$

Define a wave number p^2 for this equation in α

$$p^2 = \frac{bGR_i}{Kd \sum_{j=i}^{n} Q_j}$$

or

$$R_i = \frac{Kd p^2}{bG} \sum_{j=i}^{n} Q_j \qquad (B-8)$$

Substituting Equation (B-8) into (B-5) gives

$$Q_i = i - \frac{1}{X^*} \sum_{j=1}^{i} \sum_{K=j}^{n} Q_K \quad ; \quad X^* = \frac{bG}{K H_v p^2} \qquad (B-9)$$

Also

$$\sum_{j=1}^{i} \sum_{K=j}^{n} Q_K = \sum_{j=1}^{i} jQ_j + i \sum_{j=i+1}^{n} Q_j \qquad (B-10)$$

so that Equation (B-9) becomes

$$Q_i = i - \frac{1}{X^*} \left[\sum_{j=1}^{i} jQ_j + i \sum_{j=i+1}^{n} Q_j \right] \qquad (B-11)$$

The flexural rigidity is implicitly defined by

$$M = (EI)^* \alpha = (EI)_o \alpha + 2 \sum_{i=1}^{n} idF_i \qquad (B-12)$$

74

where M is the total moment acting on the elemental beam section, $(EI)^*$ is the flexural rigidity of the beam, $(EI)_0$ is the sum of the individual elastic elements flexural rigidities, $2\Sigma i dF_i$ is the moment caused by the extensional forces and $(EI)_0\alpha$ is the moment caused by the moments on each elastic element. $\sum_{i=1}^{n} i dF_i$ gives the sum of moments above the middle laminate, and there is an equal moment due to the laminates below the middle laminate.

Substitute $(EI)_0$ and $F_i = kdQ_i\alpha$ into Equation (B-12)

$$(EI)^* = (EI)_0 \left[1 + \frac{2Kd^2}{(EI)_0} \sum_{i=1}^{n} Q_i \right] \tag{B-13}$$

For plates with width b, height H and modulus of elasticity E,

$$K = EbH \quad \text{and} \quad (EI)_0 = NE \frac{bH^3}{12} \tag{B-14}$$

so that

$$\frac{2Kd^2}{(EI)_0} = \frac{24}{N} (1+2V)^2 ; \quad V = \frac{H_v}{2H} \tag{B-15}$$

The geometrical parameter is

$$Y = (N^2 - 1)(1 + 2V)^2$$

so that

$$\frac{2Kd^2}{(EI)_0} = \frac{24Y}{N(N^2-1)} = \frac{6Y}{n(n+1)(2n+1)} = \frac{Y}{\sum_{i=1}^{n} i^2} \tag{B-16}$$

Substituting Equation (B-16) into (B-13)

$$(EI)^* = (EI)_0 \left[1 + \frac{\sum_{i=1}^{n} iQ_i}{\sum_{i=1}^{n} i^2} Y \right] \tag{B-17}$$

75

Define

$$Z^* = \frac{\sum\limits_{i=1}^{n} i\, Q_i}{\sum\limits_{i=1}^{n} i^2} \tag{B-18}$$

The Q_i will be complex numbers because of the dependence on X^*. Z^* is also a complex number and the structure loss factor is given by

$$\eta = \frac{\text{Im}(Z^*)Y}{1 + \text{Re}(Z^*)Y} \tag{B-19}$$

The equations for Q_i are given by Equation (B-11). When G is made complex, $2n$ linear algebraic equations must be solved simultaneously to obtain the n unknown values of $\text{Re}(Q_i)$ and $\text{Im}(Q_i)$, respectively. However, it is only necessary to obtain answers for two of these quantities. From Equation (B-11), let $i = n$

$$Q_n = n - \frac{1}{X^*}\left[\sum_{j=1}^{n} j\, Q_j + 0\right] = n - \frac{1}{X^*}\sum_{i=1}^{n} i\, Q_i \tag{B-20}$$

so that

$$\sum_{i=1}^{n} i Q_i = X^*(n - Q_n) \tag{B-21}$$

and

$$Z^* = \frac{6 X^*(n - Q_n)}{n(n+1)(2n+1)} \tag{B-22}$$

Equation (B-11) can be rewritten as

$$\sum_{j=1}^{i-1} j Q_j + (i + X^*) Q_i + i \sum_{j=i+1}^{n} Q_j = i X^* \tag{B-23}$$

When G is complex, write G as $G^* = G'(1 + i\beta)$ and

$$X^* = X(1 + i\beta) \; ; \; X = \frac{bG'}{K H_v P^2} \tag{B-24}$$

Equation (B-23) can be separated into real and imaginary parts

$$\sum_{j=1}^{i-1} j \, Re(Q_j) + (i+X) \, Re(Q_i) + i \sum_{j=i+1}^{n} Re(Q_j) - X\beta \, Im(Q_i) = iX$$

$$\tag{B-25}$$

$$\sum_{j=1}^{i-1} j \, Im(Q_j) + (i+X) \, Im(Q_i) + i \sum_{j=i+1}^{n} Im(Q_j) + X\beta \, Re(Q_i) = iX\beta$$

Equation (B-25) represents $2n$ equations. These equations must be solved for $Re(Q_n)$ and $Im(Q_n)$. From Equation (B-22)

$$Z^* = \frac{6X}{n(n+1)(2n+1)} \left[n - Re(Q_n) + \beta Im(Q_n) + i \{ \beta n - \beta Re(Q_n) - Im(Q_n) \} \right] \tag{B-26}$$

where $i = \sqrt{-1}$, G' (the real part of G^*) is the storage modulus, and β (the ratio of the imaginary to the real part of G^*) is the loss factor of the viscoelastic material.

For an even number of laminates the procedure is similar to the above. Let $n = \frac{N}{2}$. The following equations will replace Equations (B-11), (B-17), and (B-18), respectively.

$$Q_i = i - \frac{1}{2} - \frac{1}{X^*} \left[\sum_{j=1}^{i} (j - \frac{1}{2}) Q_j + (i - \frac{1}{2}) \sum_{j=i+1}^{n} Qj \right] \tag{B-27}$$

$$(EI)^* = (EI)_o \left[1 + \frac{\sum_{i=1}^{n} (i - \frac{1}{2}) Q_i}{\sum_{i=1}^{n} (i - \frac{1}{2})^2} \, Y \right] \tag{B-28}$$

$$Z^* = \frac{\sum_{i=1}^{n} (i - \frac{1}{2}) Q_i}{\sum_{i=1}^{n} (i - \frac{1}{2})^2} \tag{B-29}$$

77

Developing these equations similar to the above, Equations (B-25) and (B-26) will be replaced by the following:

$$\sum_{j=1}^{i-1} (j-\tfrac{1}{2}) \text{Re}(Q_j) + (i-\tfrac{1}{2}+X)\text{Re}(Q_i) + (i-\tfrac{1}{2}) \sum_{j=i+1}^{n} \text{Re}(Q_j) - X\beta\,\text{Im}(Q_i) = (i-\tfrac{1}{2})X$$

$$\text{(B-30)}$$

$$\sum_{j=1}^{i-1} (j-\tfrac{1}{2}) \text{Im}(Q_j) + (i-\tfrac{1}{2}+X)\text{Im}(Q_i) + (i-\tfrac{1}{2}) \sum_{j=i+1}^{n} \text{Im}(Q_j) + X\beta\,\text{Re}(Q_i) = (i-\tfrac{1}{2})X\beta$$

$$Z^* = \frac{12X}{n(4n^2-1)} \left[n-\tfrac{1}{2}-\text{Re}(Q_n)+\beta\,\text{Im}(Q_n)+i\,\{\beta(n-\tfrac{1}{2})-\beta\text{Re}(Qn)-\text{Im}(Q_n)\}\right] \qquad \text{(B-31)}$$

APPENDIX C

COMPARISON OF THE SYMMETRICAL TO THE UNSYMMETRICAL
THREE-ELASTIC-ELEMENT VISCOELASTIC SHEAR-DAMPED
COMPOSITE STRUCTURE

APPENDIX C

COMPARISON OF THE SYMMETRICAL TO THE UNSYMMETRICAL THREE-ELASTIC-ELEMENT VISCOELASTIC SHEAR-DAMPED COMPOSITE STRUCTURE

In this analysis the subscripts s and u stand for symmetrical and unsymmetrical, respectively. The complex flexural rigidity expression for both the symmetrical and unsymmetrical cases can be put in the form

$$(EI)^* = (EI)_0 \, (1 + Z^* Y) \tag{C-1}$$

where $(EI)_0$ is the sum of the individual flexural rigidities of the elastic elements,

Y is the geometrical parameter

$$Z^*_s = \frac{X^*}{1 + X^*} \quad \text{(see Equation A-50)}$$

$$Z^*_u = f(X^*, K_{12}, d_{12}) \quad \text{(see Equation A-55)}$$

$$X^* = \frac{bG'}{H_v P^2 K_1} (1 + i\beta) = X(1 + \beta)$$

From Equation (31)

$$X = X_0 \sqrt{1 + ZY} \; ; \; X_0 = C\left(\frac{G'}{f}\right) \; ; \; Z = \text{Re}(Z^*) \tag{C-2}$$

The four quantities $\text{Re}(Z^*_s)$, $\text{Im}(Z^*_s)$, $\text{Re}(Z^*_u)$, $\text{Im}(Z^*_u)$ are given by Equations (60), (61), (63) and (64), respectively. In both cases the loss factor η is

$$\eta = \frac{\text{Im}(Z^*)Y}{1 + \text{Re}(Z^*)Y} \tag{C-3}$$

First taking limits as $X \to 0$:

$$Z_s \to 0, \; \text{Im}(Z^*_s) \to \beta X$$

$$Z_u \to 0, \; \text{Im}(Z^*_u) \to \frac{C_4 C_2}{C_1} \beta X$$

Hence:

$$\underset{X_o \to 0}{\text{Lim}} \; \eta_s = \beta Y_s X_o \tag{C-4a}$$

$$\underset{X_o \to 0}{\text{Lim}} \; \eta_u = \frac{C_4 \, C_2}{C_1} \beta Y_u X_o \tag{C-4b}$$

Then taking limits as $X \to \infty$:

$$Z_s \to 1, \quad \text{Im}(Z_s^*) \to \frac{\beta}{1 + \beta^2} \frac{1}{X}$$

$$Z_u \to 1, \quad \text{Im}(Z_u^*) \to \left(\frac{C_3}{C_4} - \frac{C_2}{C_1} \right) \frac{\beta}{1 + \beta^2} \frac{1}{X}$$

Hence:

$$\underset{X_o \to \infty}{\text{Lim}} \; \eta_s = \frac{\beta Y_s}{(1 + \beta^2)(1 + Y_s) \sqrt{1 + Y_s}} X_o^{-1} \tag{C-5a}$$

$$\underset{X_o \to \infty}{\text{Lim}} \; \eta_u = \frac{\left(\dfrac{C_3}{C_4} - \dfrac{C_2}{C_1} \right) \beta Y_u}{(1 + \beta^2)(1 + Y_u) \sqrt{1 + Y_u}} \tag{C-5b}$$

Equations (C-4) and (C-5) show that when η is plotted versus X_o on log paper, there is a low shear parameter asymptote (as $X_o \to 0$) with a slope of +1 and a high shear parameter asymptote (as $X_o \to \infty$) with a slope of -1. The value of X_o at the point where these asymptotes cross each other $(X_o)_c$ is obtained by equating the value of η in Equation (C-4) to that in Equation (C-5) for both the symmetrical and unsymmetrical cases.

$$(X_o)_{cs} = \left[\frac{1}{(1 + \beta^2)(1 + Y_s) \sqrt{1 + Y_s}} \right]^{\frac{1}{2}} \tag{C-6a}$$

81

$$(X_0)_{cu} = \left[\frac{\frac{1}{C_4}\left(\frac{C_1}{C_2}\frac{C_3}{C_4} - 1\right)}{(1 + \beta^2)(1 + Y_u)\sqrt{1 + Y_u}} \right]^{\frac{1}{2}}$$

(C-6b)

Dividing Equation (C-6a) by Equation (C-6b)

$$\frac{(X_0)_{cs}}{(X_0)_{cu}} = \left[\frac{1}{\frac{1}{C_4}\left(\frac{C_1}{C_4}\frac{C_3}{C_2} - 1\right)} \right]^{\frac{1}{2}} \left[\frac{1 + Y_u}{1 + Y_s} \right]^{\frac{1}{2}}$$

(C-7)

As an approximate method of evaluating η_u, assume $\eta_u = \eta_s$ if the geometrical parameter is taken as

$$\frac{(X_0)_{cu}}{(X_0)_{cs}} = \left[\frac{1}{C_4}\left(\frac{C_1}{C_2}\frac{C_3}{C_4} - 1\right) \right]^{\frac{1}{2}}$$

(C-8)

In other words, η_s versus X_0, multiply the X_0 scale by $\left[\frac{1}{C_4}\left(\frac{C_1}{C_2}\frac{C_3}{C_4} - 1\right) \right]^{\frac{1}{2}}$ to obtain η_u versus X_0. To determine how much error is involved in this procedure, first calculate the values of the asymptotes of this approximate method and compare to the true asymptotes. Subscripting the loss factor η as η_{ij} where

> i = L for $X_0 \to 0$ asymptote
> = H for $X_0 \to \infty$ asymptote
> j = A for approximate solutions
> = E for exact solution

$$\eta_{LA} = \frac{\beta Y}{\left[\frac{1}{C_4}\left(\frac{C_1}{C_2}\frac{C_3}{C_4} - 1\right) \right]^{\frac{1}{2}}} X_0$$

(C-9a)

$$\eta_{HA} = \frac{\left[\frac{1}{C_4}\left(\frac{C_1}{C_2}\frac{C_3}{C_4} - 1\right) \right]^{\frac{1}{2}}\beta Y}{(1 + \beta^2)(1 + Y)\sqrt{1 + Y}} X_0^{-1}$$

(C-9b)

82

$$\eta_{LE} = \frac{C_4}{C_1}\frac{C_3}{} \beta Y X_0 \qquad \text{(C-9c)}$$

$$\eta_{HE} = \frac{\left(\dfrac{C_3}{C_4} - \dfrac{C_2}{C_1}\right)\beta Y}{(1 + \beta^2)(1 + Y)\sqrt{1+Y}} X_0^{-1} \qquad \text{(C-9d)}$$

For the asymptotes the per cent error $P\varepsilon$ is

$$P\varepsilon_1 = 100\left(\frac{\eta_A - \eta_E}{\eta_E}\right) = 100\left[\frac{C_1}{C_3}\sqrt{\frac{C_2}{C_1 C_3 - C_2 C_4}} - 1\right] \qquad \text{(C-10)}$$

There is no simple expression for the per cent error at intermediate values of X_0, however, for all cases tried the maximum error ε_2 was slightly less and of opposite sign than the errors on the asymptotes ε_1 as indicated on the sketch sketch below.
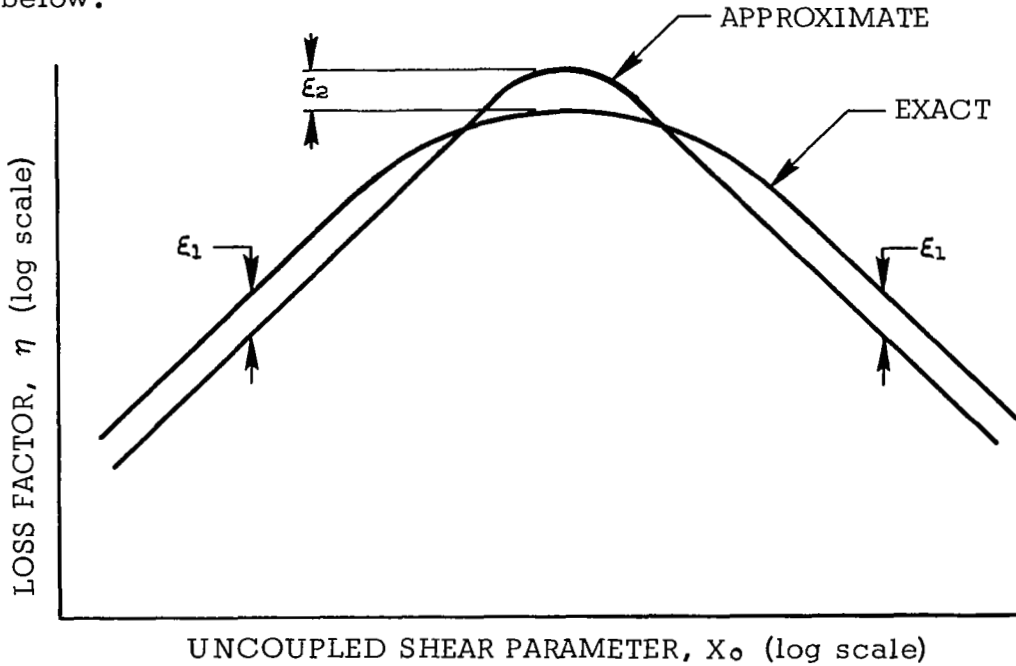
The biggest error occurs when the parameter $d_{12} = 1$, in which case ε_1 represents a 10.5 per cent error.

APPENDIX D

EQUIVALENCE OF THE LOSS FACTOR EXPRESSIONS
OF
DiTARANTO [REF. 4] AND UNGAR [REF. 3]

APPENDIX D

EQUIVALENCE OF THE LOSS FACTOR EXPRESSIONS
OF
DiTARANTO [REF. 4] AND UNGAR [3]

DiTaranto's Equation (36) can be written in the form

$$\frac{\rho \omega_1{}^2}{\lambda_0{}^2} = (B_1 + B_3) \left[1 + \frac{\frac{SR_1}{\lambda_0}\left(\frac{SR_1}{\lambda_0} + 1\right) + \left(\frac{SR_1}{\lambda_0}\beta\right)^2 K_1 \delta^2}{\left(\frac{SR_1}{\lambda_0} + 1\right)^2 + \left(\frac{SR_1}{\lambda_0}\beta\right)^2 S(B_1 + B_3)} \right] \tag{D-1}$$

and substituting $\lambda = -\lambda_0$ into DiTaranto's Equation (35) and rearranging

$$\eta = \frac{\frac{SR_1}{\lambda_0} \frac{K_1 \delta^2}{S(B_1 + B_3)} \beta}{\frac{\rho \omega_1{}^2}{\lambda_0{}^2}\left(\frac{1}{B_1 + B_3}\right)\left[\left(\frac{SR_1}{\lambda_0} + 1\right)^2 + \left(\frac{SR_1}{\lambda_0}\beta\right)^2\right]} \tag{D-2}$$

Using the definitions of Y and X in Ungar's Equation (4.7), the following substitutions can be made:

$$SR_1 = Xp^2 \tag{D-3}$$

$$\frac{K_1 \delta^2}{S(B_1 + B_3)} = Y \tag{D-4}$$

Substituting the expressions in Equations (D-1), (D-3) and (D-4) into Equation (D-2) and rearranging

$$\eta = \frac{\beta YX(p^2/\lambda_0)}{1 + (2 + Y)X(p^2/\lambda_0) + (1 + Y)(1 + \beta^2)X^2(p^4/\lambda_0{}^2)} \tag{D-5}$$

This equation for loss factor η would be identical to Ungar's Equation (4.7) if $p^2 = \lambda_0$. From Ungar's Equation (4.8), the real part of the complex

flexural rigidity B^* is

$$Re(B^*) = (B_1 + B_3) \left[1 + \frac{X(X+1) + (X\beta)^2}{(X+1)^2 + (X\beta)^2} Y \right] \qquad (D\text{-}6)$$

Assuming that for viscoelastic shear-damped structural composites, there is an effective flexural rigidity equal to the real part of the complex flexural rigidity, the wave number p is related to the circular frequency ω_1 by

$$p^4 = \frac{\rho \omega_1^2}{Re(B^*)} \qquad (D\text{-}7)$$

where ρ is the mass per unit length of the beam. Using Equation (D-6), Equation (D-7) can be solved for $\rho \omega_1^2$ as

$$\rho \omega_1^2 = p^4 (B_1 + B_3) \left[1 + \frac{X(X+1) + (X\beta)^2}{(X+1)^2 + (X\beta)^2} Y \right] \qquad (D\text{-}8)$$

Also substituting Equations (D-3) and (D-4) into (D-1) and solving for $\rho \omega_1^2$ gives

$$\rho \omega_1^2 = \lambda_0^2 (B_1 + B_3) \left[1 + \frac{X(p^2/\lambda_0)\{X(p^2/\lambda_0) + 1\} + \{X(p^2/\lambda_0)\beta\}^2}{\{X(p^2/\lambda_0) + 1\}^2 + \{X(p^2/\lambda_0)\beta\}^2} Y \right] \qquad (D\text{-}9)$$

Equating Equations (D-8) and (D-9) results in

$$p^2 = \lambda_0 \qquad (D\text{-}10)$$

and, therefore, DiTaranto's equation for loss factor is equivalent to Ungar's if the assumption is made that there is an effective flexural rigidity of shear-damped structural composites equal to the real part of the complex flexural rigidity.

APPENDIX E

GENERAL LOSS FACTOR EXPRESSION FOR THE SYMMETRICAL THREE-
ELASTIC-ELEMENT VISCOELASTIC SHEAR-DAMPED STRUCTURAL COMPOSITE

APPENDIX E

GENERAL LOSS FACTOR EXPRESSION FOR THE SYMMETRICAL THREE-ELASTIC-ELEMENT VISCOELASTIC SHEAR-DAMPED STRUCTURAL COMPOSITE.

The general expression for the loss factor of an axially uniform composite beam is given as [Ref. 3]

$$\eta = \frac{p^2 \Sigma \alpha_n (K'_n |\overline{R}_n|^2 + B'_n) + \Sigma \beta_n G'_n A_n |\overline{P}_n|^2}{p^2 \Sigma (K'_n |\overline{R}_n|^2 + B'_n) + \Sigma G'_n A_n |\overline{P}_n|^2} \tag{E-1}$$

where

p is the wave number for the assumed sinusoidal wave shape of the beam

the subscript n stands for the nth substructure of the composite structure

α_n is the extensional loss factor

K'_n is the real part of the extensional stiffness ($K'_n = E'_n A_n$, where E'_n is the real part of Young's Modulus)

B'_n is the real part of the flexural rigidity ($B'_n = E'_n I_n$, where I_n is the moment of inertia)

β_n is the shear loss factor

G'_n is the real part of the complex shear modulus

A_n is the cross-sectional area

$\overline{R}_n$ and $\overline{P}_n$ are defined by Equation (1.6) of Reference 1 as[*]

$$\overline{\delta}_n = \overline{R}_n \overline{\varphi} \ , \ \overline{\psi}_n = \overline{P}_n \overline{\varphi} \tag{E-2}$$

For a time dependent function
$$y(t) = y_0 \cos(\omega t + \theta)$$

---

[*]Quantities with bars over them are phasors.

The phasor, $\overline{y}$, is defined by

$$y(t) = \text{Re}\left[\overline{y}\, e^{i\omega t}\right]$$

The phasor $\overline{y}$ is a complex number

$$\overline{y} = \overline{y}_R + i\,\overline{y}_I$$

so that

$$\text{Re}\left[\overline{y}\, e^{i\omega t}\right] = \sqrt{\overline{y}_R^{\,2} + \overline{y}_I^{\,2}}\;\; \cos\left(\omega t + \tan^{-1}\frac{\overline{y}_I}{\overline{y}_R}\right)$$

Note that the phasor, $\overline{y}$, itself is not dependent on time but on the magnitude and phase of the time dependent function.

In Equation (E-2), φ is the angular displacement at a cross-section of the beam so that, for a beam in pure flexure, $\frac{\partial\varphi}{\partial x}$ is the curvature. It is assumed that all elastic elements undergo the same curvature $\frac{\partial\varphi}{\partial x}$. The time dependence of φ is taken care of by assuming a sinusoidal time dependence and using phasors so that

$$\frac{\partial\varphi}{\partial x} = \frac{d\overline{\varphi}}{dx} \qquad\qquad (E\text{-}3)$$

Since all elastic elements have the same curvature, there is no subscript on $\frac{d\overline{\varphi}}{dx}$. $\overline{\delta}_n$ is the phasor for translational displacement, so that the extensional strain at its neutral axis is

$$\overline{\epsilon}_n = \frac{d\overline{\delta}_n}{dx} \qquad\qquad (E\text{-}4)$$

Finally, $\overline{\psi}_n$ is the phasor for the average shear strain.

It is assumed that

$$\overline{\varphi}(x) = \overline{\varphi}_0 \cos px \qquad\qquad (E\text{-}5)$$

and, therefore

$$\overline{\delta}_n(x) = (\overline{\delta}_n)_0 \cos px$$

$$\overline{\psi}_n(x) = (\overline{\psi}_n)_0 \cos px \qquad\qquad (E\text{-}6)$$

Differentiate Equation (E-6) and use with Equations (E-4) and (E-5) in Equation (E-2)

$$\overline{R}_n = \frac{\left(\overline{\epsilon}_n\right)_0}{\left(\frac{d\overline{\varphi}}{dx}\right)_0} , \quad \overline{P}_n = \frac{\left(\frac{d\overline{\psi}_n}{dx}\right)_0}{\left(\frac{d\overline{\omega}_n}{dx}\right)_0} \qquad (E-7)$$

For the special case of the symmetrical three-elastic-element structure, only the extensional strain of one elastic element and the shear strain of the associated viscoelastic element must be considered. Consider the following sketch of the three-elastic-element beam and the associated strain diagram.

92
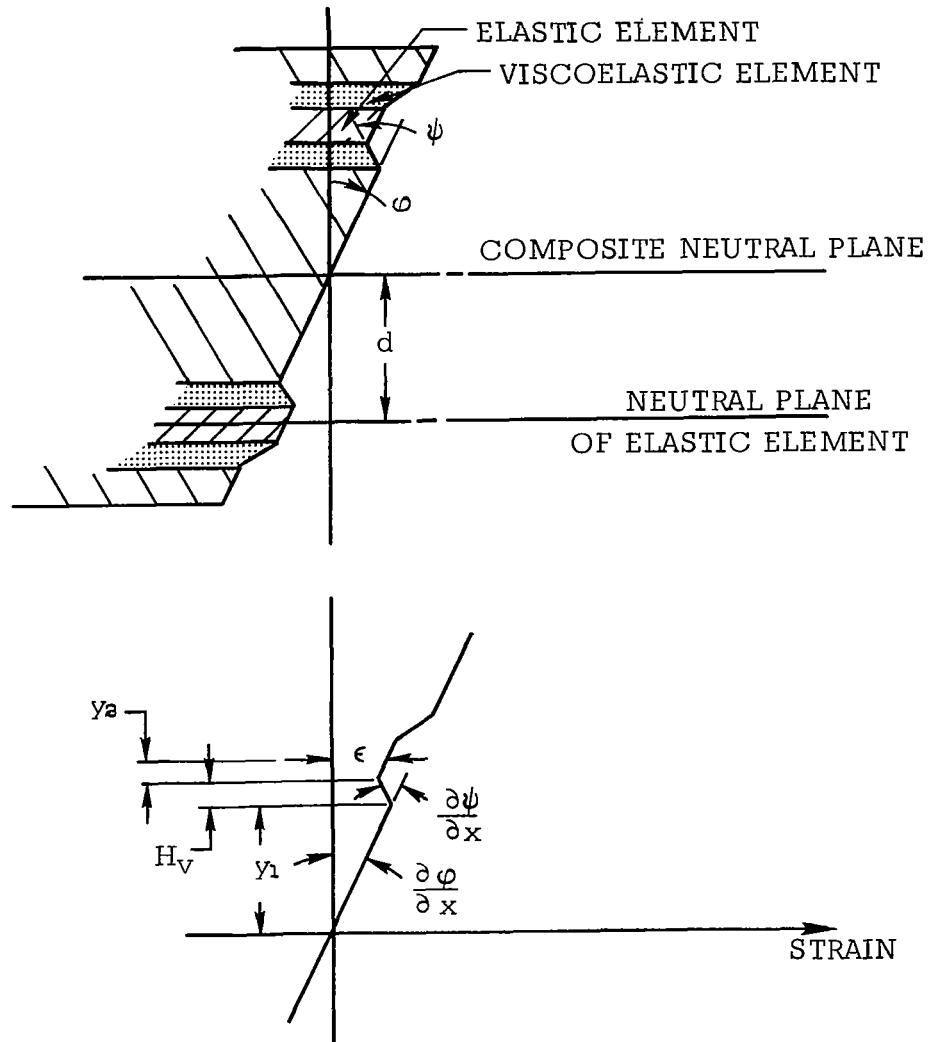
From the geometry of the strain diagram

$$\epsilon = (y_1 + y_2) \frac{\partial \varphi}{\partial x} - H_v \left(\frac{\partial \psi}{\partial x} - \frac{\partial \varphi}{\partial x} \right) \tag{E-8}$$

For small curvatures and for the thickness of the viscoelastic element approximately constant and equal to H_v, and also for $y_1 >> H_v$, the average shear strain is approximately equal to ψ as shown in the sketch.

Using phasors

$$\frac{\partial \varphi}{\partial x} = \frac{d \overline{\varphi}}{dx} \quad \text{and} \quad \frac{\partial \psi}{\partial x} = \frac{d \overline{\psi}}{dx} \tag{E-9}$$

Due to the symmetry only the $\overline{R}_n$ for one elastic element and $\overline{P}_n$ for one viscoelastic element need be considered. Therefore, dropping the subscript n and using Equations (E-7), (E-8) and (E-9)

$$\overline{R} = y_1 + y_2 - H_v (\overline{P} - 1) \tag{E-10}$$

The extensional force on the elastic element is $K\epsilon$ where K is the extensional stiffness of the elastic element. The net force on a small element of the elastic element of length, dx, is

$$\frac{\partial (K\epsilon)}{\partial x} dx = F_s \tag{E-11}$$

where F_s = shearing force.

The average shearing stress is obtained by multiplying the average value of the perimeter of the cross section b by the element, dx. The stress-strain relation is

$$\frac{F_s}{bdx} = G\psi \tag{E-12}$$

Using Equations (E-7) to (E-12)

$$K \frac{\overline{R}}{\overline{P}} \left(\frac{\partial^2 \psi}{\partial x^2} \right) + bG\psi = 0 \tag{E-13}$$

93

The wave number for this equation is p so that

$$p^2 = \frac{bG}{K \frac{\overline{R}}{\overline{P}}} \qquad (E-14)$$

Combining Equations (E-10) and (E-14)

$$\overline{R} = d \left(\frac{X^*}{1+X^*}\right)$$

$$\overline{P} = \frac{d}{H_v} \left(\frac{1}{1+X^*}\right) \qquad (E-15)$$

where $d = y_1 + y_2 + H_v$ and $X^* = \frac{bG}{H_v Kp^2}$. When G is a complex number it is written as G* which can be expressed as

$$G^* = G'(1 + i\beta) \qquad (E-16)$$

where β is the loss factor of the viscoelastic material. Now X*, defined as a complex shear parameter, can be written as

$$X^* = X(1 + i\beta) \qquad (E-17)$$

and a shear parameter X is defined as

$$X = \frac{bG'}{H_v Kp^2} \qquad (E-18)$$

Now the quantities

$$|\overline{R}|^2 = [Re(\overline{R})]^2 + [Im(\overline{R})]^2$$

and

$$|\overline{P}|^2 = [Re(\overline{P})]^2 + [Im(\overline{P})]^2 \qquad (E-19)$$

94

become

$$|\overline{R}|^2 = d^2 \frac{X^2(1+\beta^2)}{(1+X)^2 + X^2\beta^2}$$

(E-20)

$$|\overline{P}|^2 = \frac{d^2}{H_v^2} \frac{1}{(1+X)^2 + X^2\beta^2}$$

It is assumed that the loss factors of the elastic elements are zero and that the elastic elements do not shear. Also, it is assumed that the extensional stiffness and flexural rigidity of the viscoelastic elements are zero. Therefore, the first term in the numerator of Equation (E-1) is zero.

$$p^2 \sum_n \alpha_n (K_n' |\overline{R}_n|^2 + B_n') = 0$$

(E-21)

The second term in the numerator and in the denominator pertain to the two viscoelastic elements. They are

$$\sum_n \beta_n G_n' A_n |\overline{P}_n|^2 = 2\beta G' b H_v |\overline{P}|^2$$

(E-22)

and

$$\sum_n G_n' A_n |\overline{P}_n|^2 = 2G' b H_v |\overline{P}|^2$$

(E-23)

The first term in the denominator pertains to the three elastic elements. Since the extensional strain at the neutral plane of the main elastic element is zero, its value of $\overline{R}$ is zero and

$$p^2 \sum (K_n' |\overline{R}_n|^2 + B_n') = p^2 [2K|\overline{R}|^2 + (EI)_o]$$

(E-24)

where $(EI)_o = \sum B_n'$

For this structure the geometrical parameter is

$$Y = \frac{2Kd^2}{(EI)_o}$$

(E-25)

95

Combining Equations (E-17) and (E-20) to (E-25) with Equation (E-1) gives

$$\eta = \frac{\beta YX}{1 + (2+Y)X + (1+\beta^2)(1+Y)X^2}$$ (E-26)

This is the same equation as was obtained for the symmetrical three-elastic-element beam where the elastic elements are separated by layers of viscoelastic material. The only difference in the two cases is the definition of b as illustrated below.

b = 4s   b

96
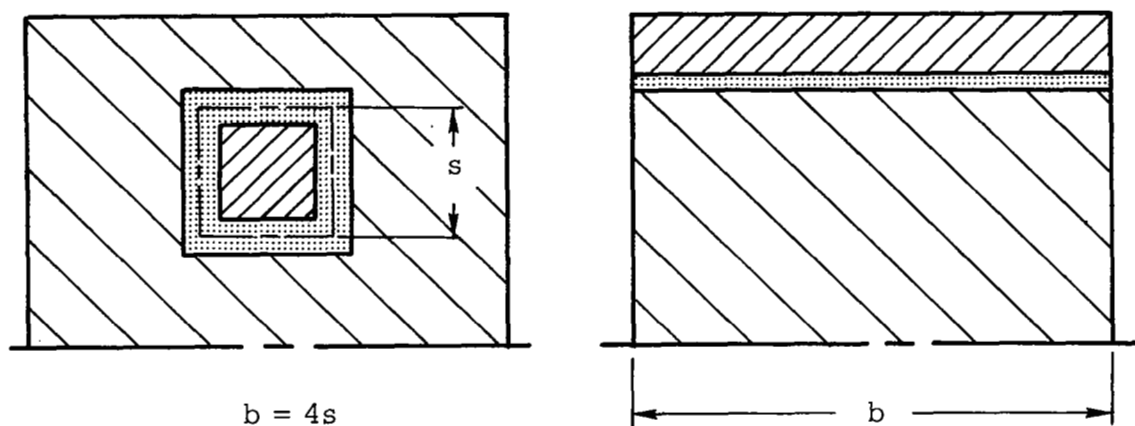
REFERENCES

1. Ruzicka, J. E.; Derby, T. F.; Schubert, D. W.; and Pepi, J. S. : Damping of Structural Composites with Viscoelastic Shear-Damping Mechanisms. NASA CR-742, March 1967.

2. Ross, R.,; Ungar, E. E.; and Kerwin, E. M., Jr.: Damping of Plate Flexural Vibrations by Means of Viscoelastic Laminae. Structural Damping, (edited by J. E. Ruzicka), ASME, New York, 1959, pp. 49-87.

3. Ungar, E. E.: Loss Factors of Viscoelastically Damped Beam Structures. J. Acoust. Soc. Am., vol. 34, no. 8, Aug. 1962, pp. 1082-1089.

4. DiTaranto, R. A.: Theory of Vibratory Bending for Elastic and Viscoelastic Layered Finite Length Beams. Journal of Applied Mechanics, vol. 32, Series E, No. 4, Dec. 1965, pp. 881-886.

5. DiTaranto, R. A.: Natural Frequencies and Damping Capabilities of Laminated Beams. U. S. Navy Marine Engineering Laboratory, Research and Development Report 295/66, June 1966.

6. Snowdon, J. C.: Vibration and Shock in Damped Mechanical Systems. John Wiley and Sons, Inc., 1968.

7. Ruzicka, J. E.: Damping Structural Resonances Using Viscoelastic Shear-Damping Mechanisms. J. Eng. Industry, Trans. ASME, Series B, vol. 83, no. 4, Nov. 1961, pp. 403-424.

8. Ruzicka, J. E.: Resonance Characteristics of Unidirectional Viscous and Coulomb-Damped Vibration Isolation Systems. J. Eng. Industry, Trans. ASME, vol. 89, Series B, no. 4, Nov. 1967, pp. 729-740.

9. Plunkett, R.: Measurement of Damping. Structural Damping, (edited by J. E. Ruzicka), ASME, New York, 1959, pp. 117-131.

10. Ungar, E. E.: Energy Dissipation of Structural Joints; Mechanisms and Magnitudes. FDL-TDR-64-98, Aug. 1964.

11. Mood, A. M.; Graybill, F. A.: Introduction to the Theory of Statistics. Second Edition, McGraw Hill, 1963, pp.156.

12. McAdams, W. H.: Heat Transmission. Third Edition, McGraw-Hill, New York, 1954.

13. Anon.: Alcoa Aluminum Handbook. Aluminum Company of America, Pittsburgh, Penn., 1959.
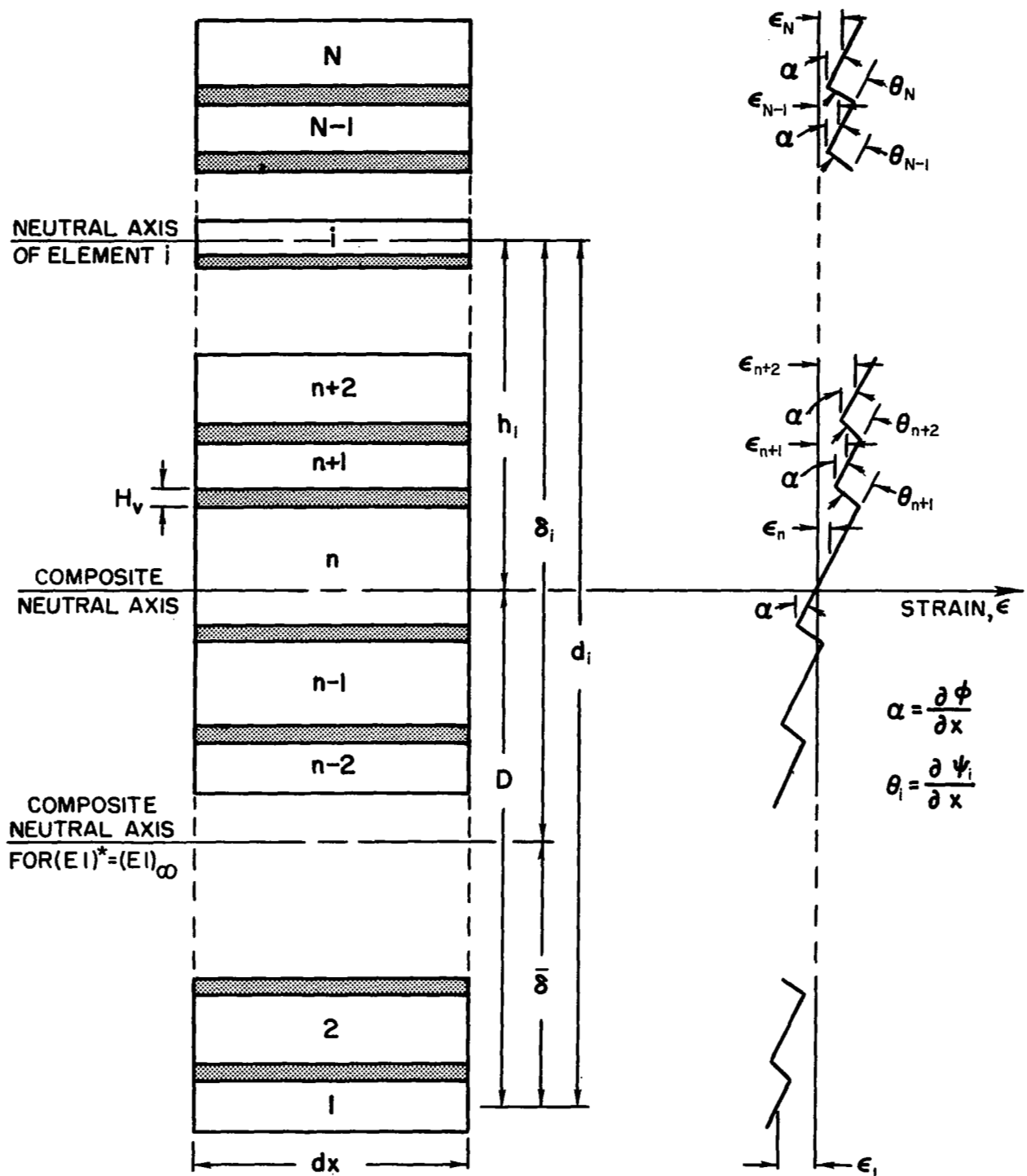
Figure 1. – Elemental section and strain diagram of a beam comprised
of N elastic elements separated by viscoelastic layers
undergoing flexural vibration
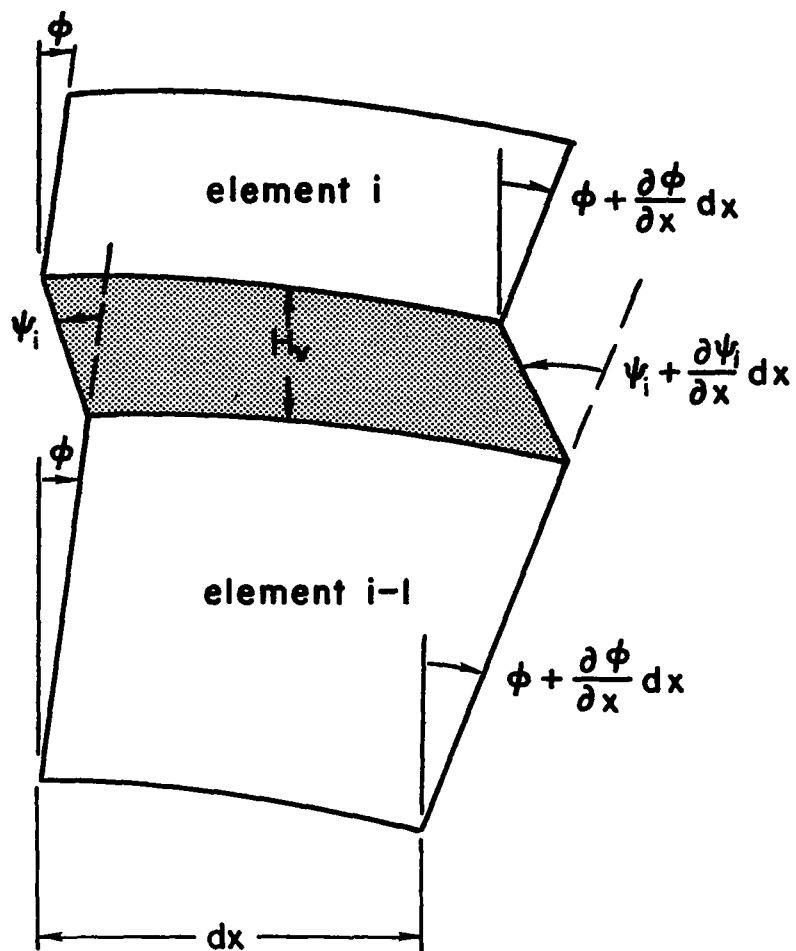
Figure 2. – Elemental section of two elastic elements separated by a viscoelastic layer undergoing flexural vibration
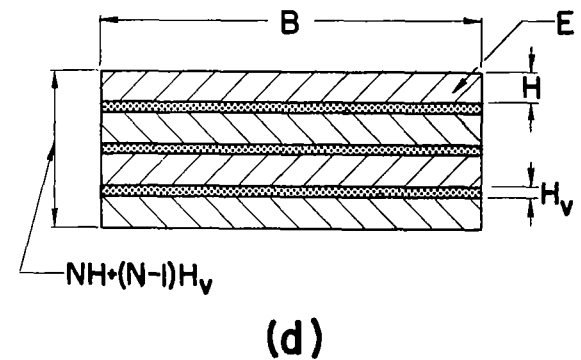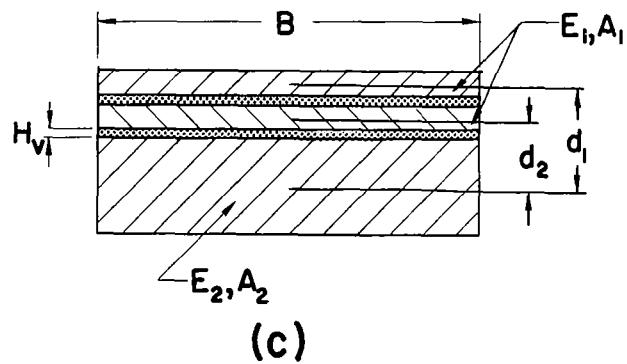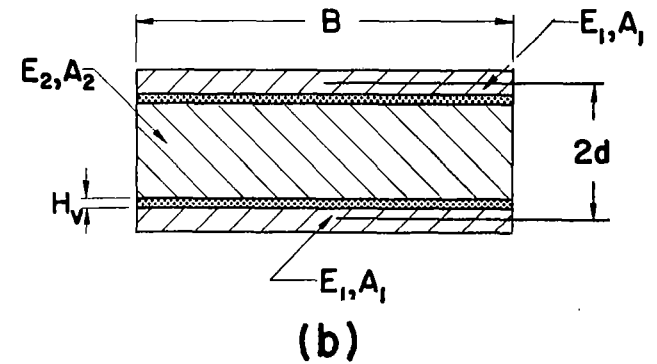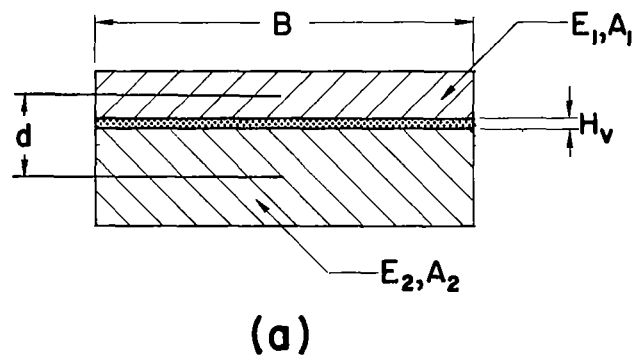
Figure 3. – Cross-sections of four types of viscoelastic shear-
damped structural composites: (a) two-elastic element;
(b) symmetrical three-elastic-element; (c) unsymmetrical
three-elastic element; and (d) N identical-elastic-
laminate
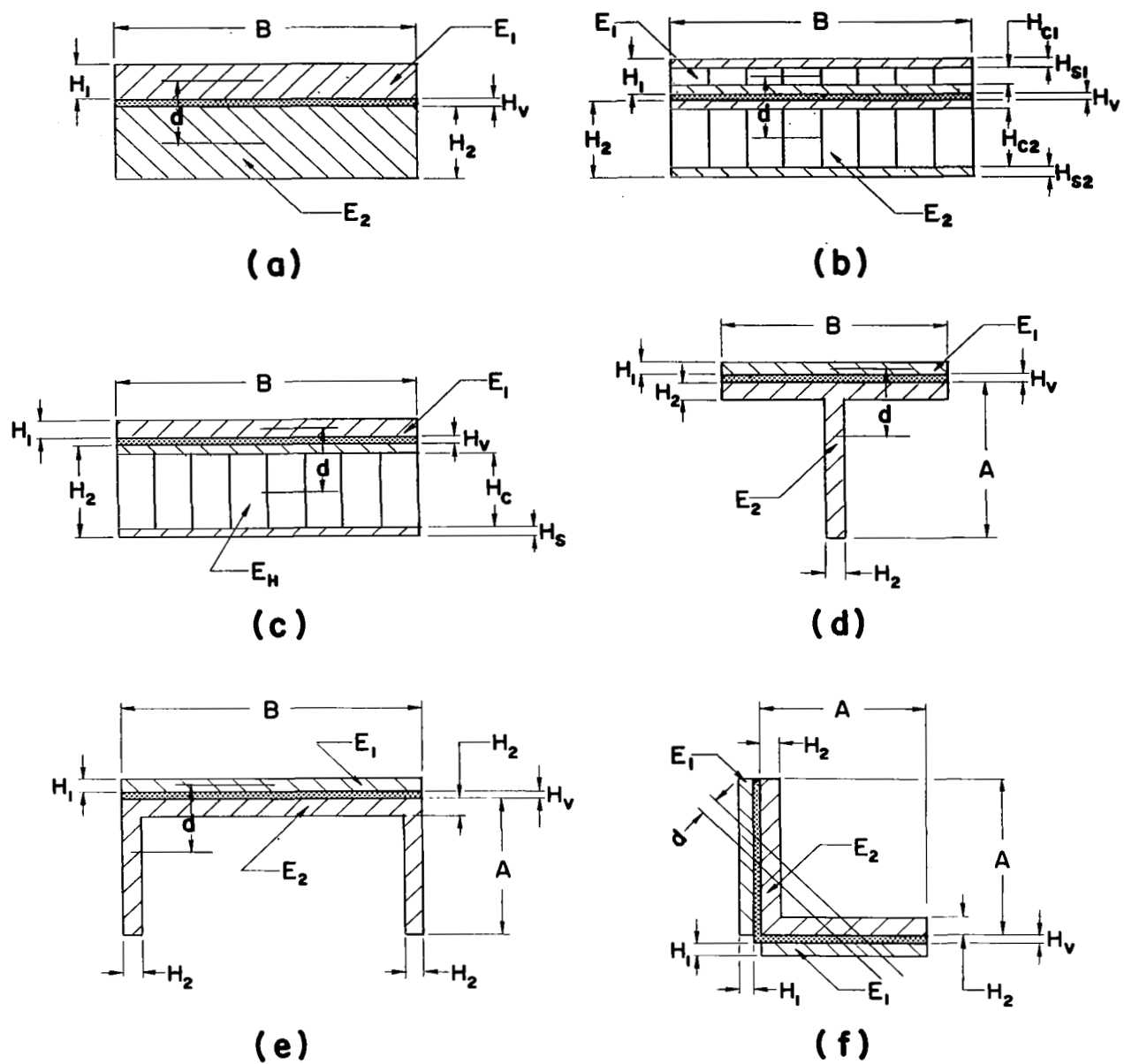
Figure 4. – Typical two-elastic-element composite structures
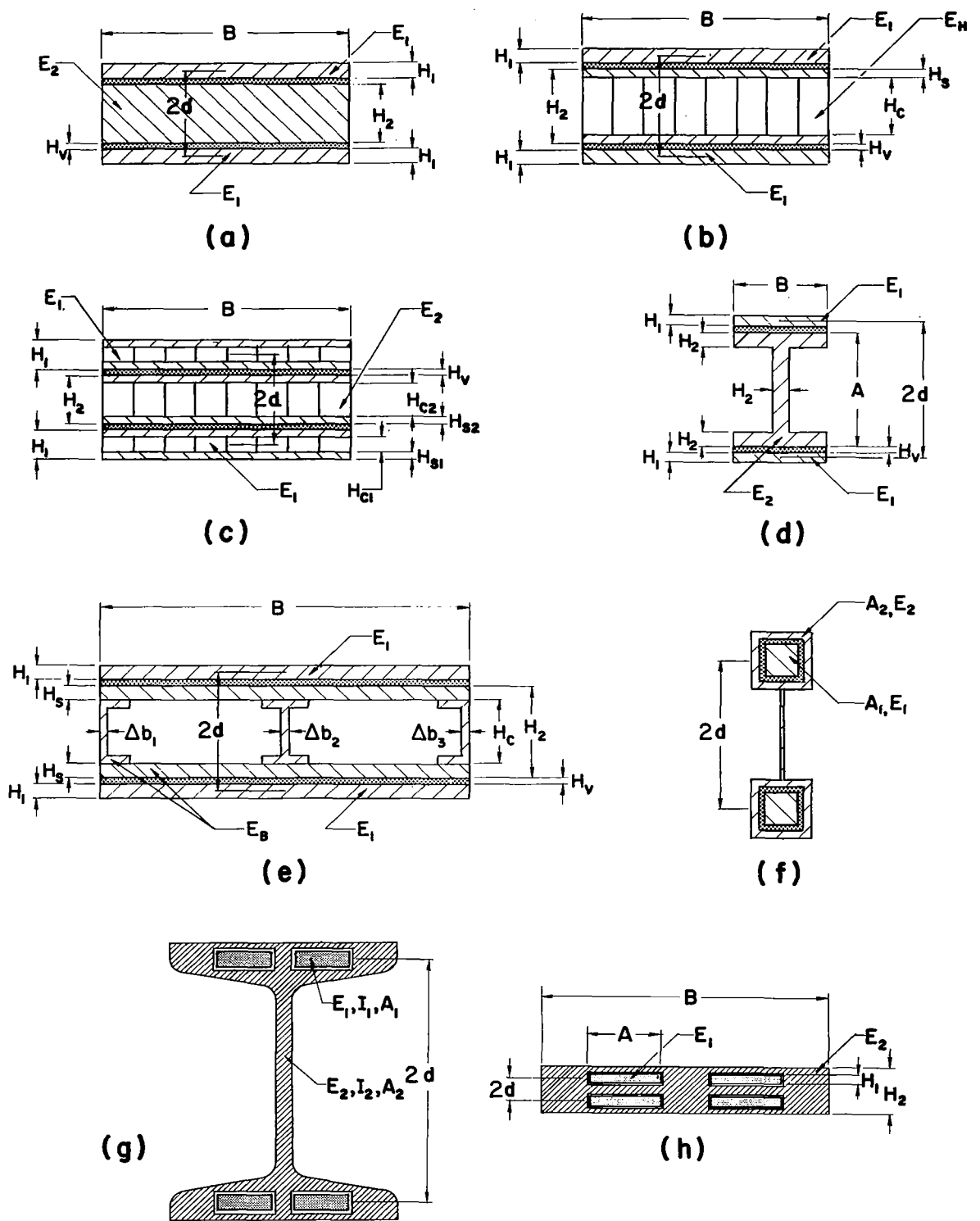
Figure 5. — Typical symmetrical three-elastic-element structural composites
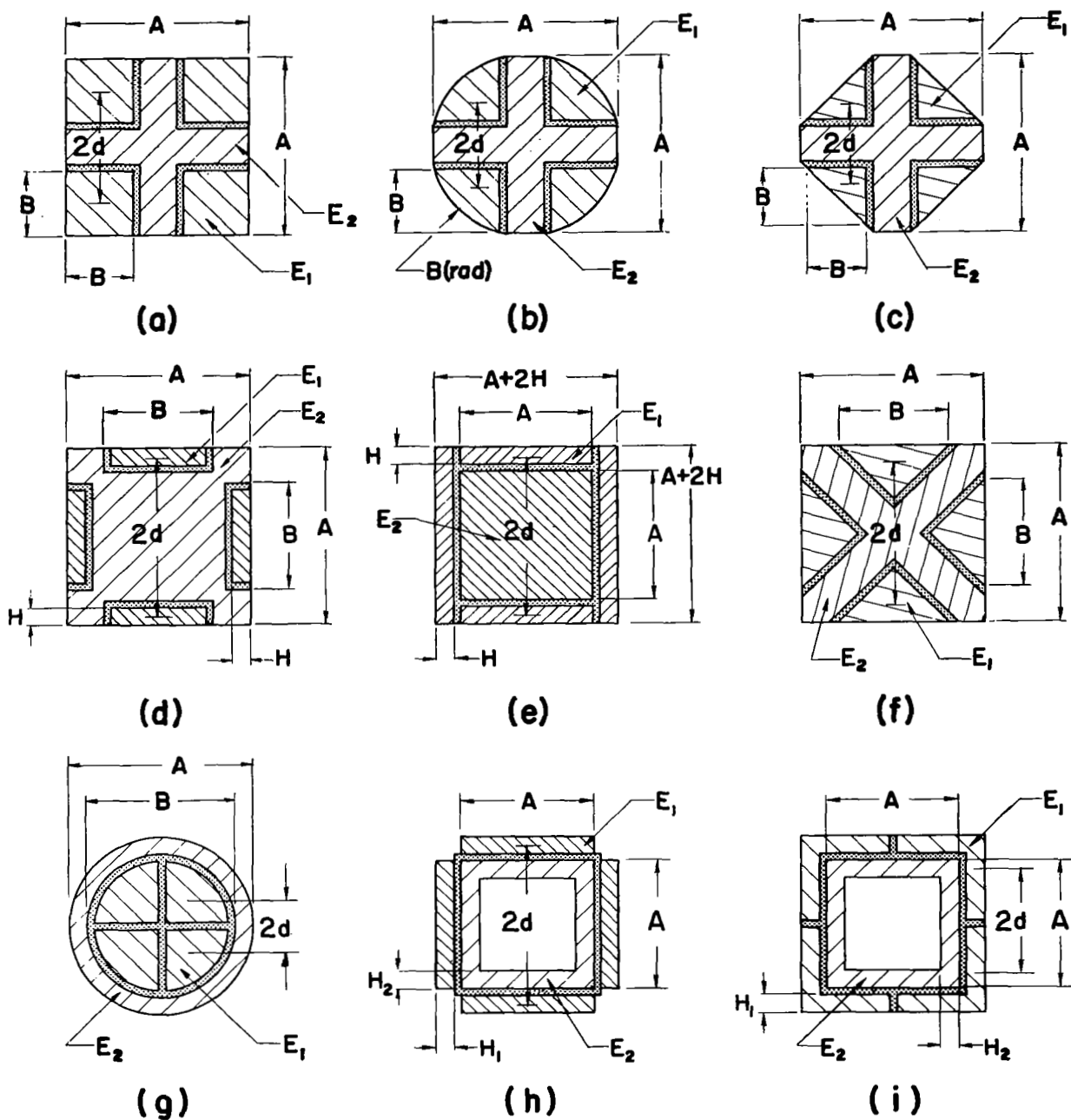
Figure 6. – Typical symmetrical three-elastic-element bar and
tube designs
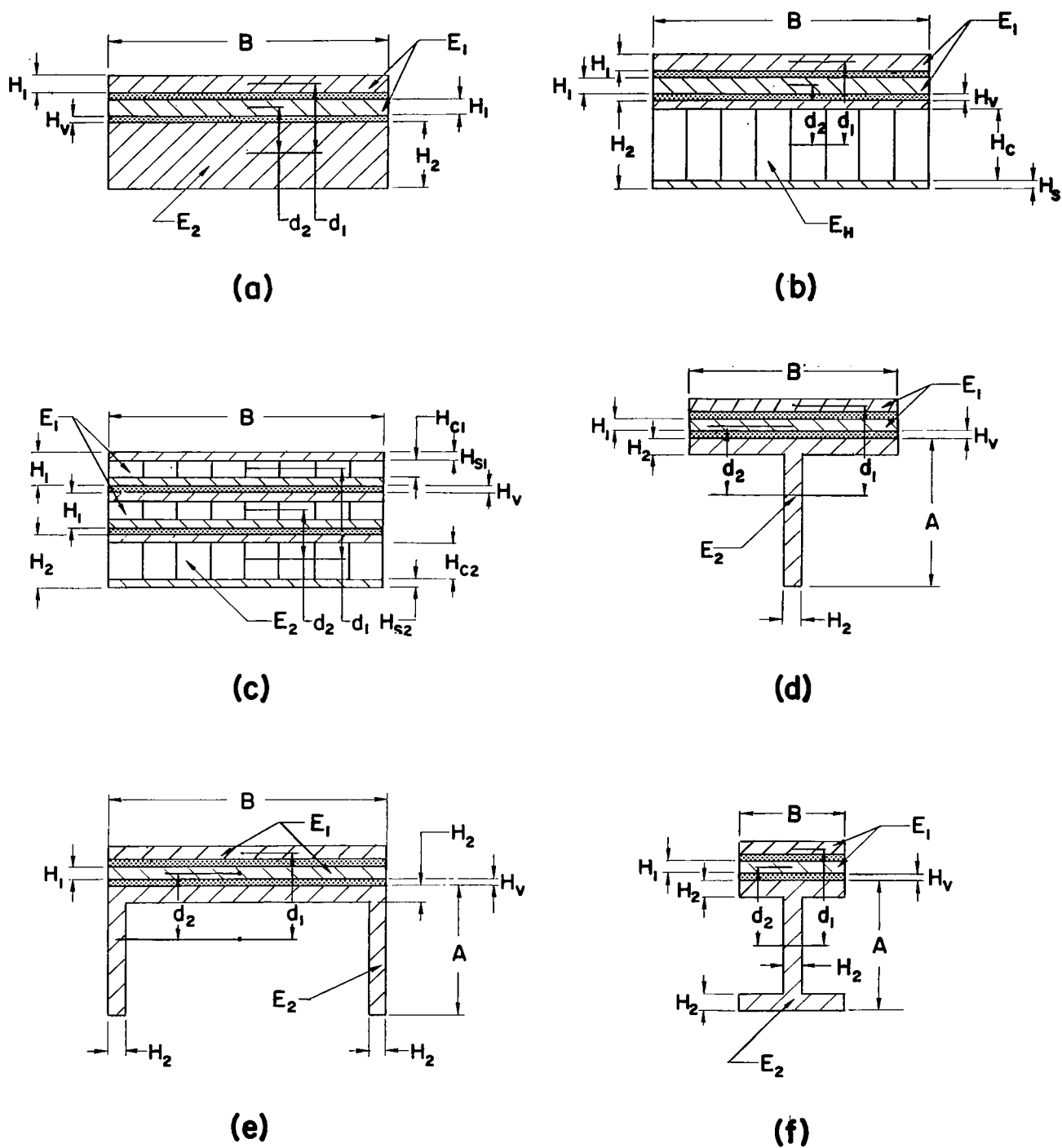
Figure 7. – Typical unsymmetrical three-elastic-element structural composites
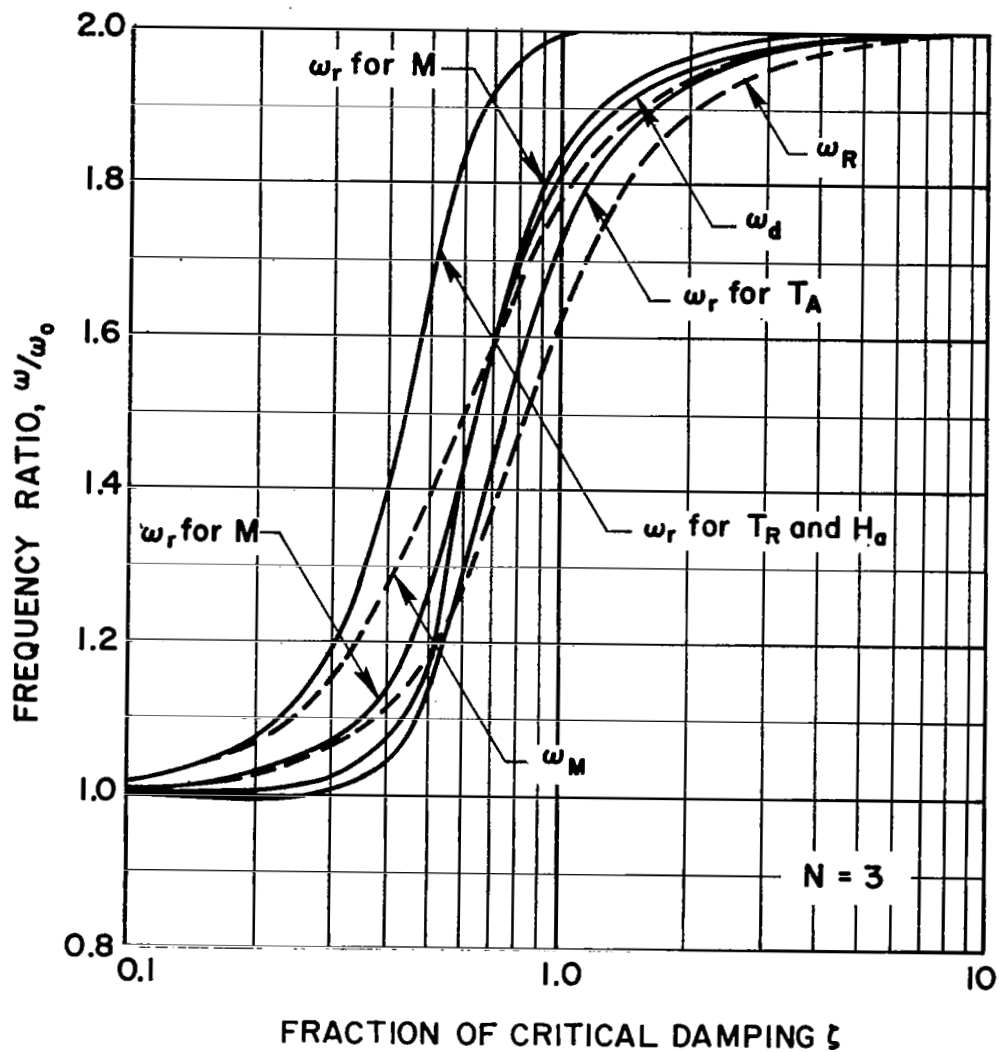
Figure 8. – Frequency ratio for the resonant frequencies ω_r for T_A, T_R, H_a, and M; for the damped free vibration natural frequency ω_d; and for the two approximations ω_R and ω_M
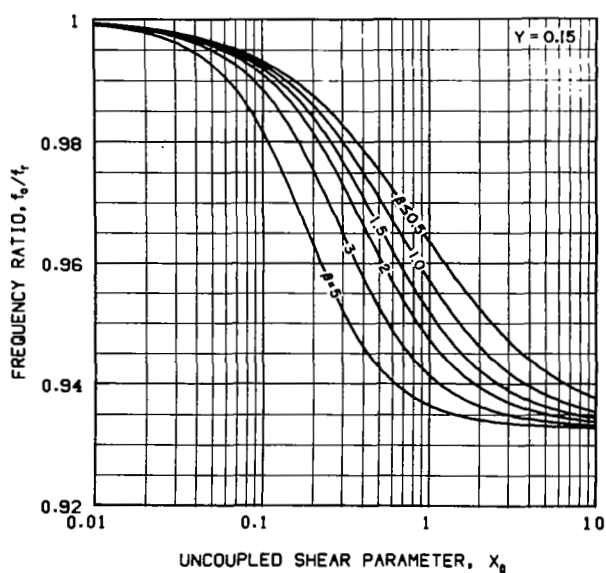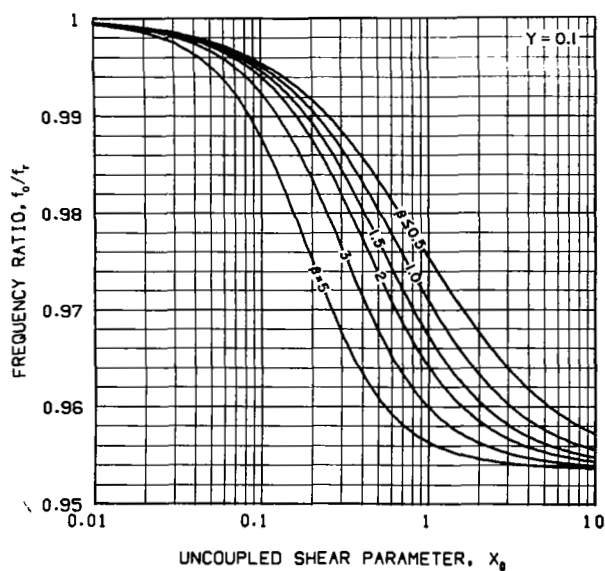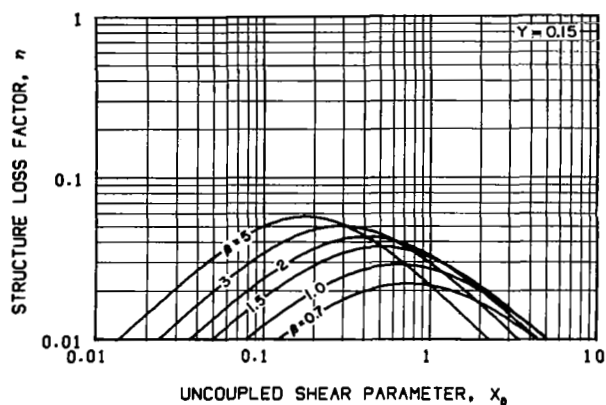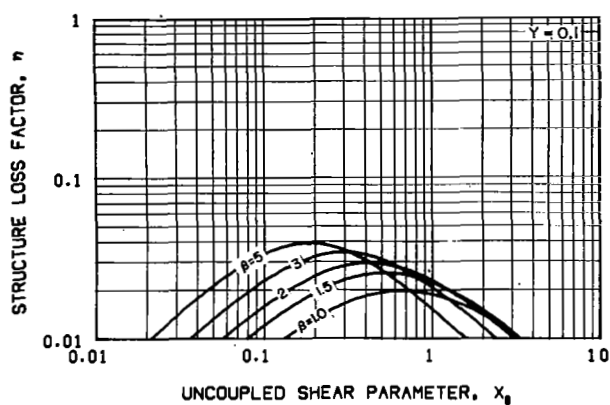
Figure 9. – Structure loss factor and frequency ratio of two- and three-elastic-element structural composites with geometric parameter Y = 0.1 and 0.15
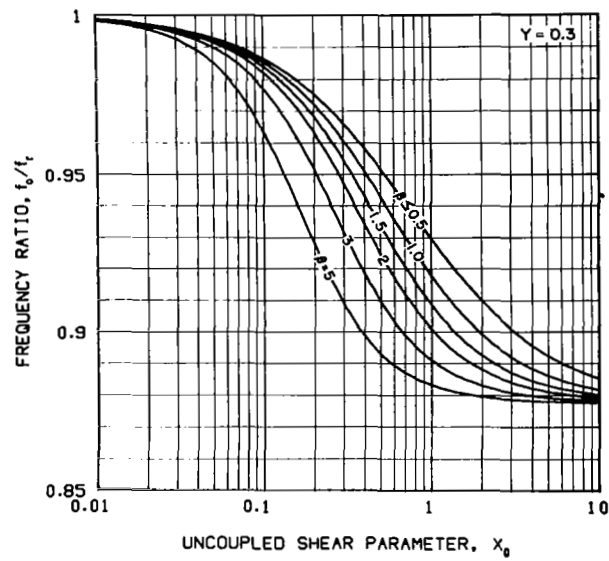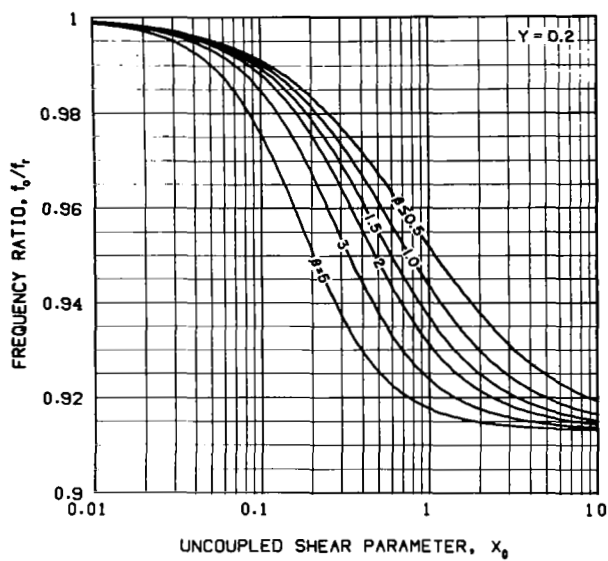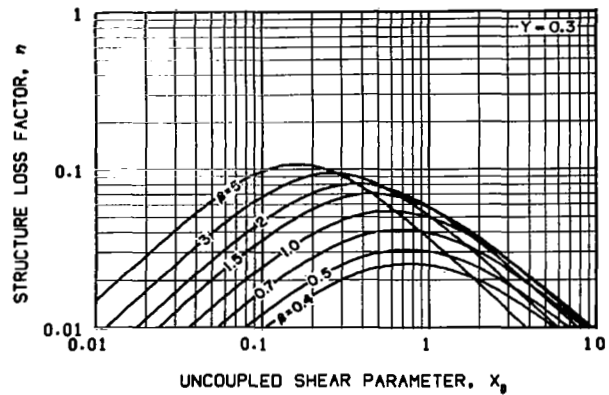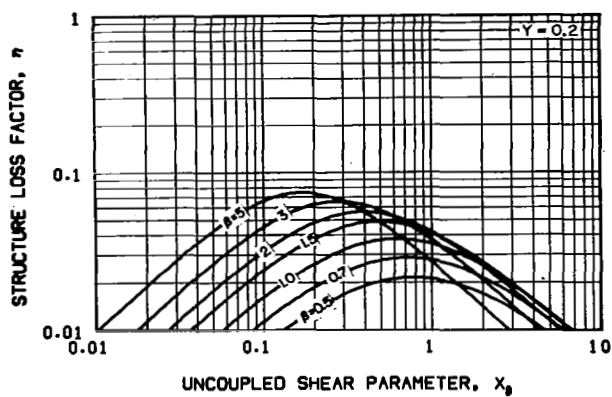
Figure 10. – Structure loss factor and frequency ratio of two- and
three-elastic-element structural composites with
geometric parameter Y = 0.2 and 0.3
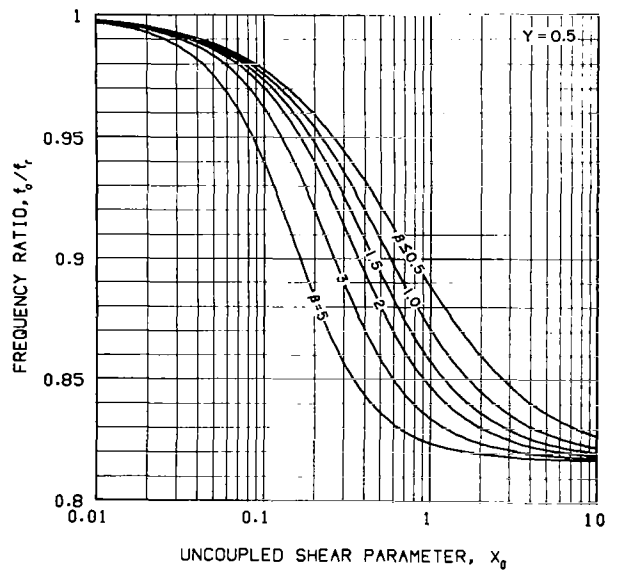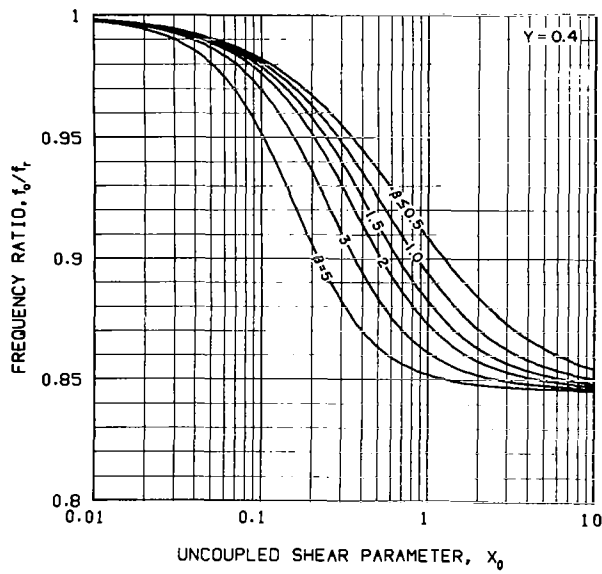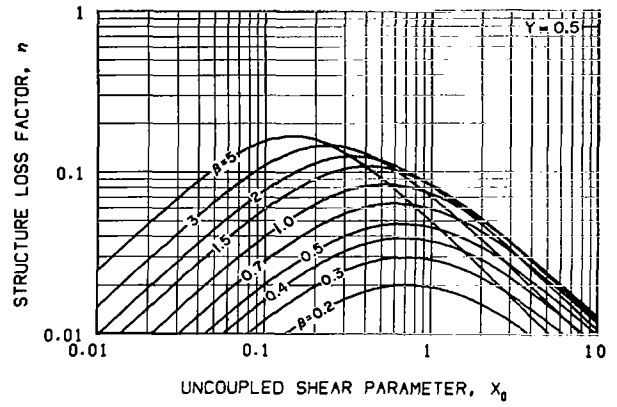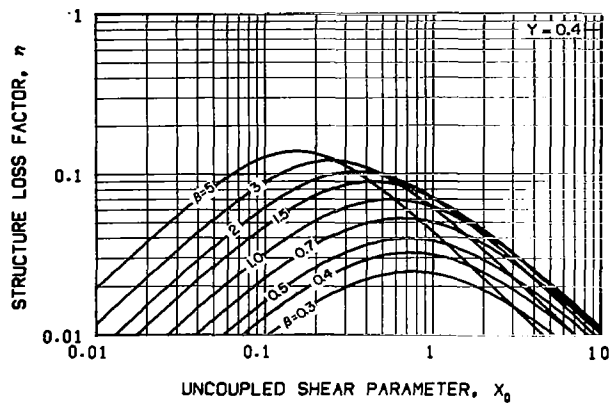
Figure 11. – Structure loss factor and frequency ratio of two- and three-elastic-element structural composites with geometric parameter Y = 0.4 and 0.5
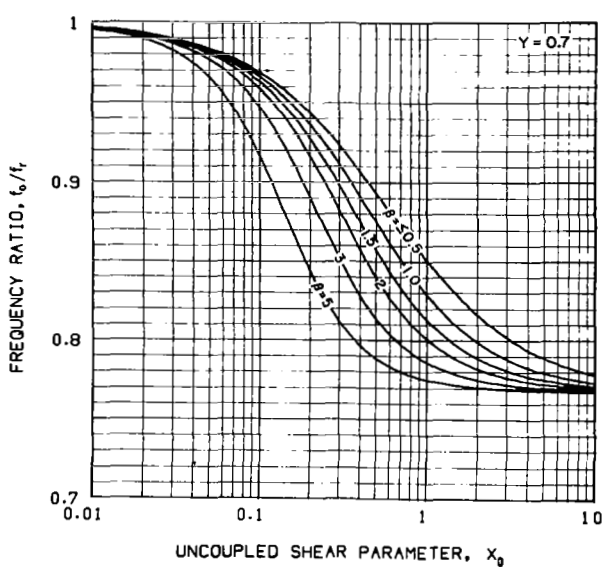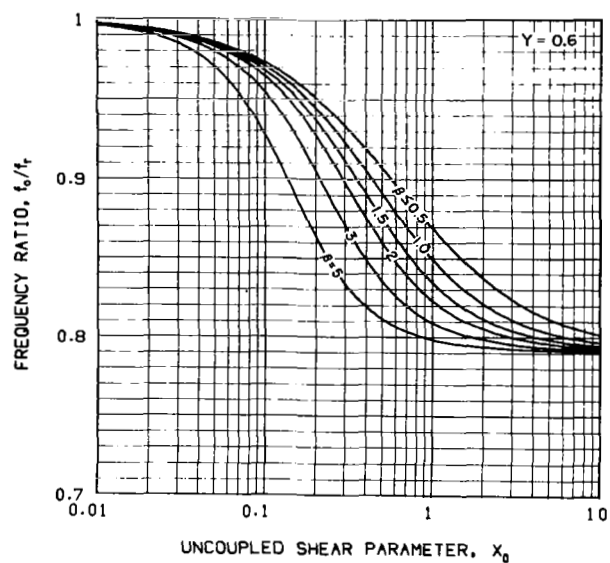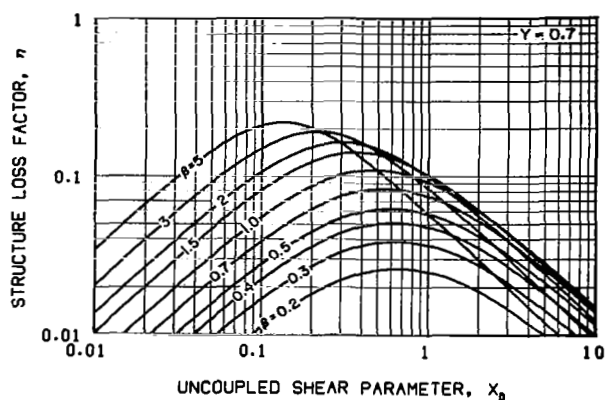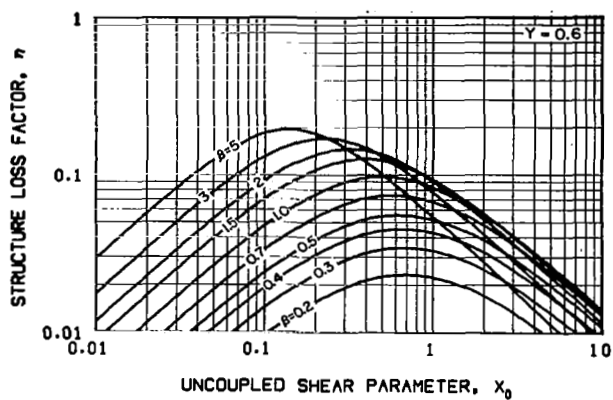
Figure 12. – Structure loss factor and frequency ratio of two- and three-elastic element structural composites with geometric parameter Y = 0.6 and 0.7
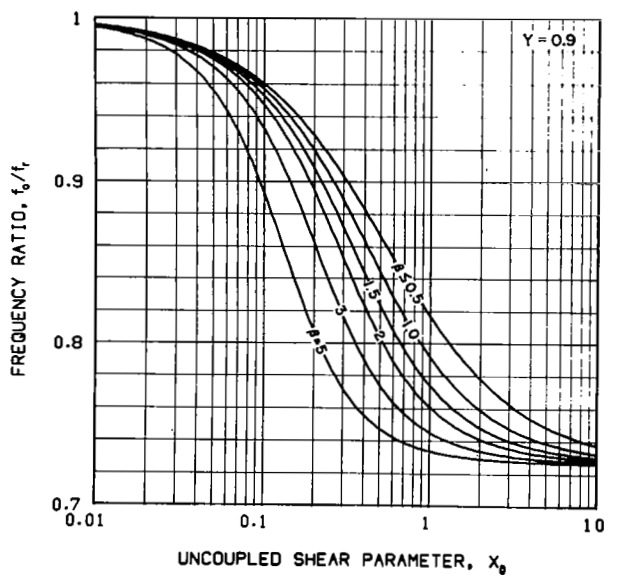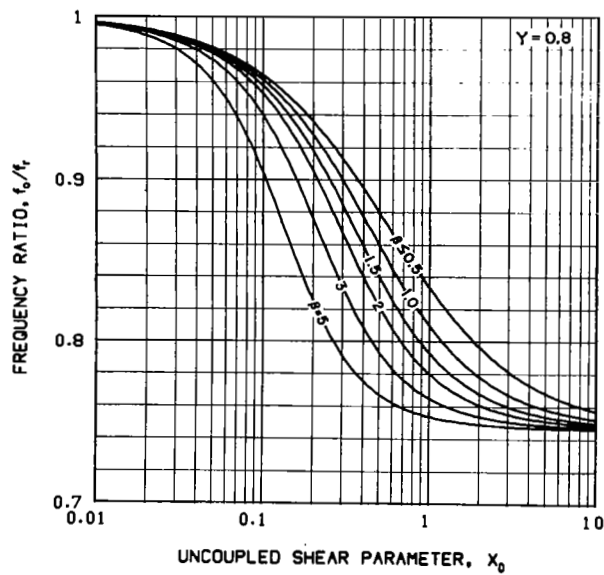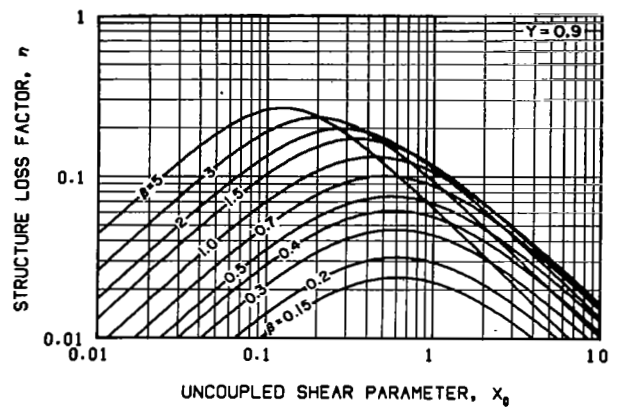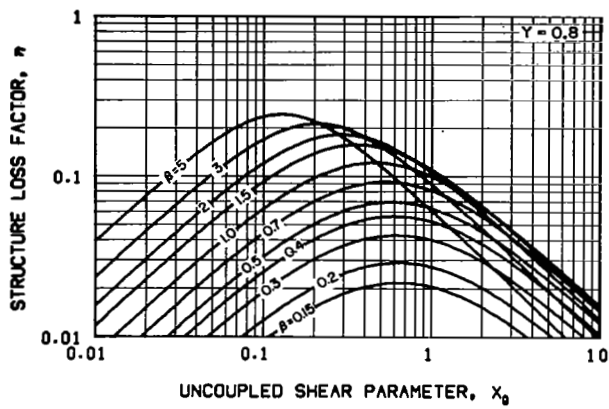
Figure 13. – Structure loss factor and frequency ratio of two- and three-elastic element structural composites with geometric parameter Y = 0.8 and 0.9
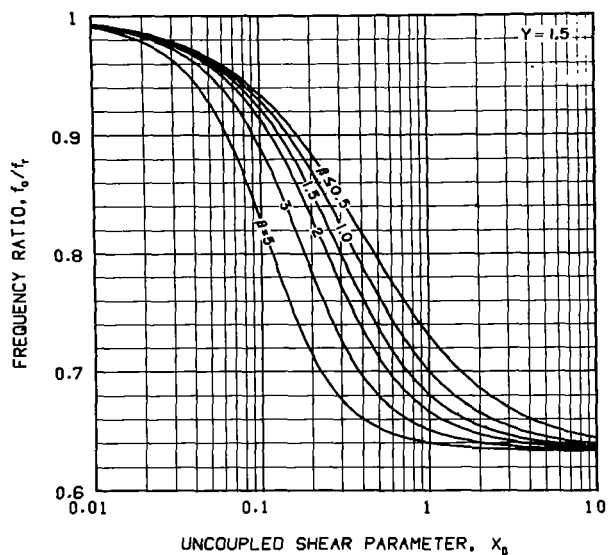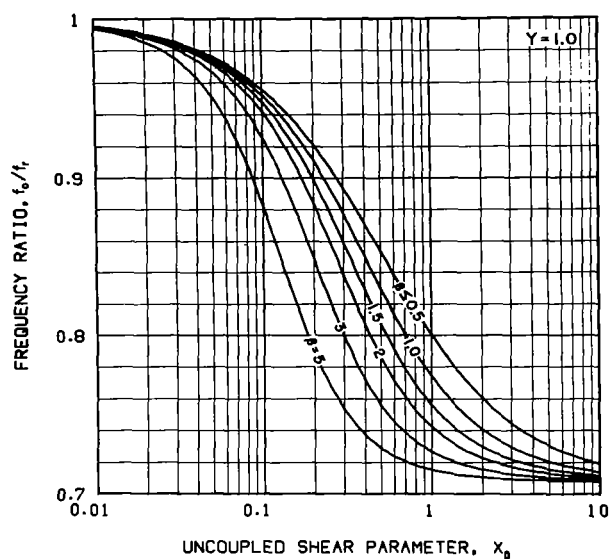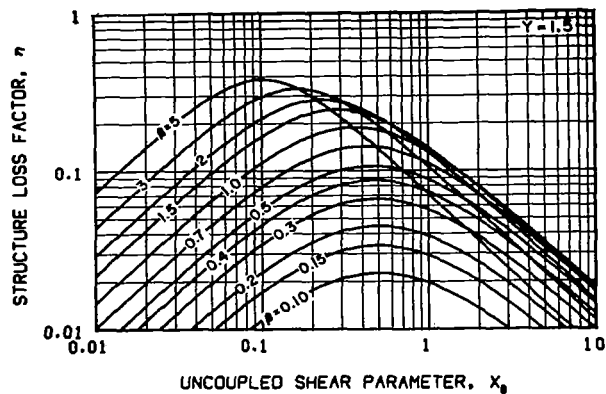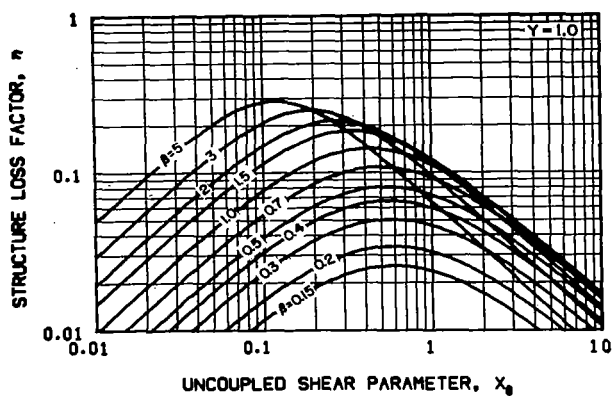
Figure 14. – Structure loss factor and frequency ratio of two- and three-elastic element structural composites with geometric parameter Y = 1.0 and 1.5
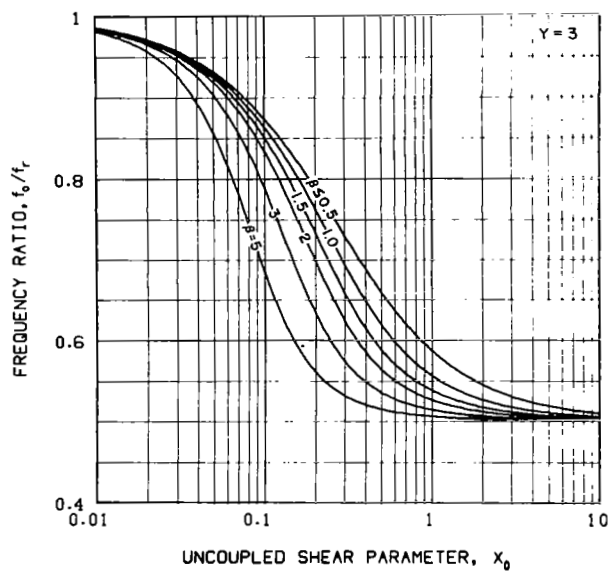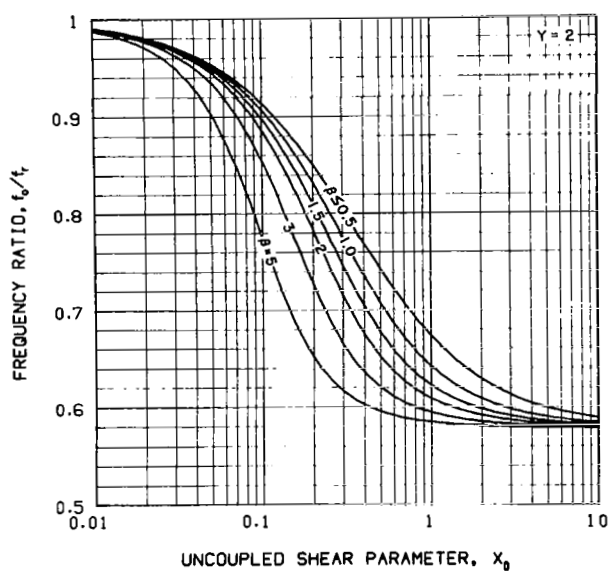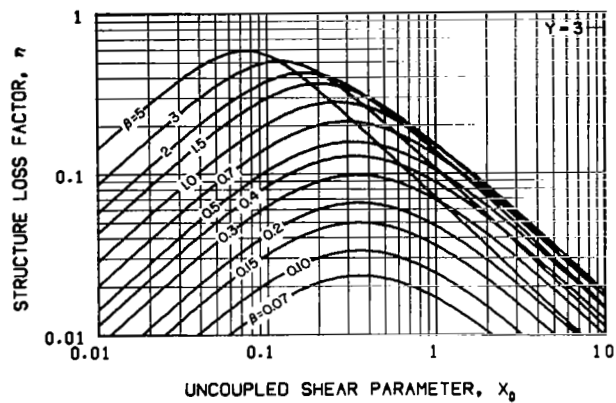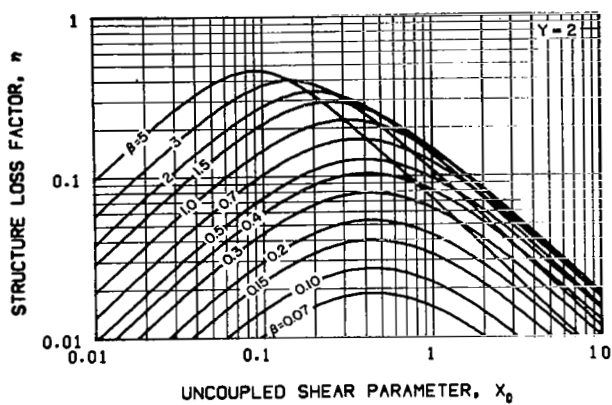
Figure 15. – Structure loss factor and frequency ratio of two- and three-elastic element structural composites with geometric parameter $Y = 2$ and 3
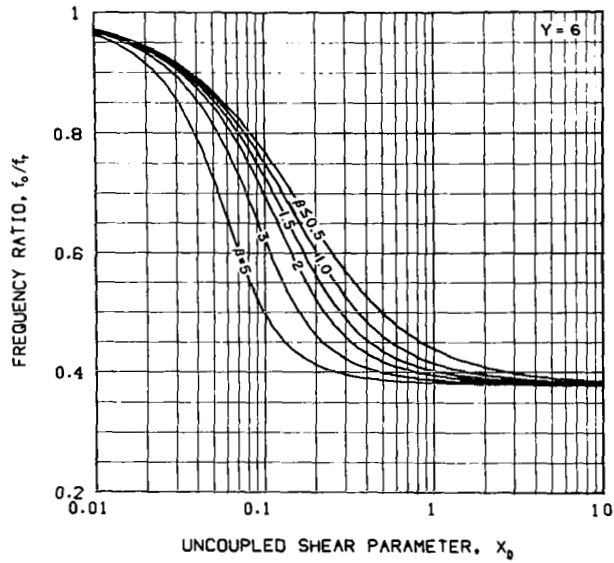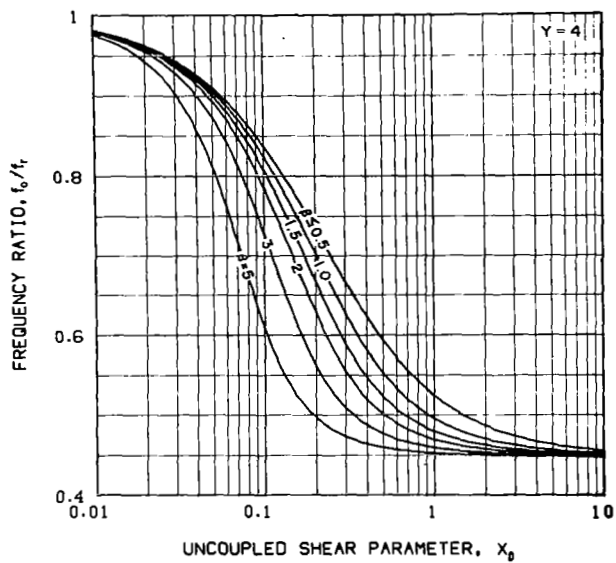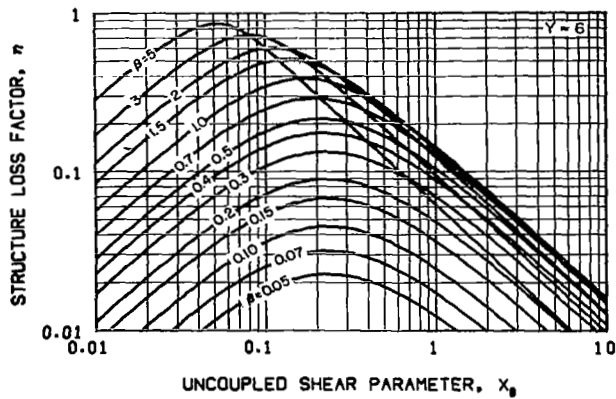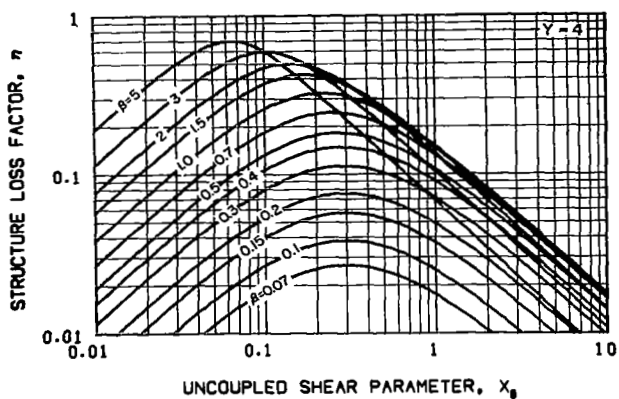
Figure 16. – Structure loss factor and frequency ratio of two- and three-elastic element structural composites with geometric parameter Y = 4 and 6

113
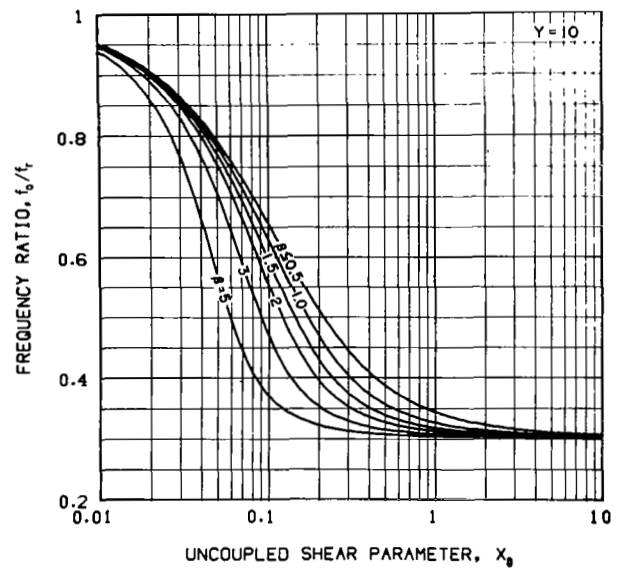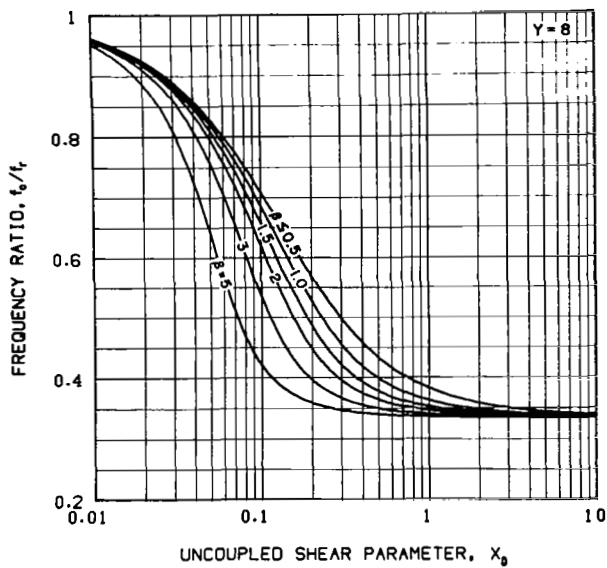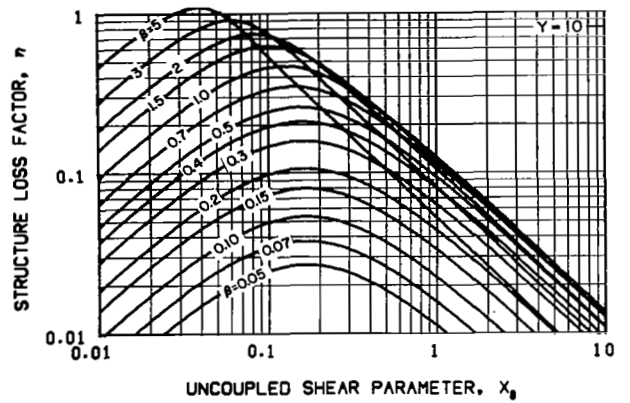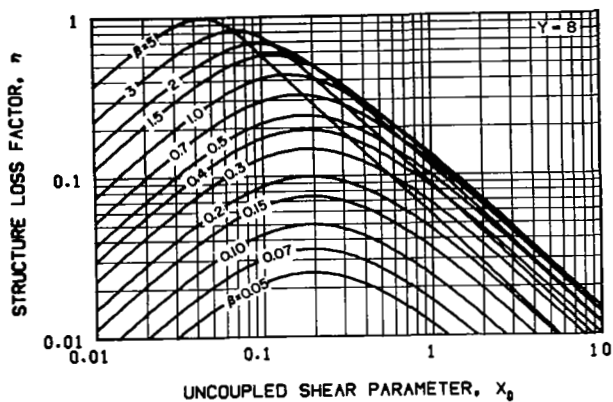
Figure 17. – Structure loss factor and frequency ratio of two- and three-elastic element structural composites with geometric parameter Y = 8 and 10

114
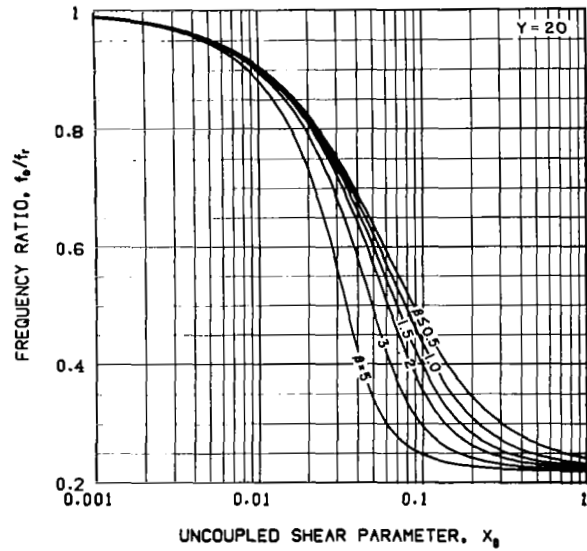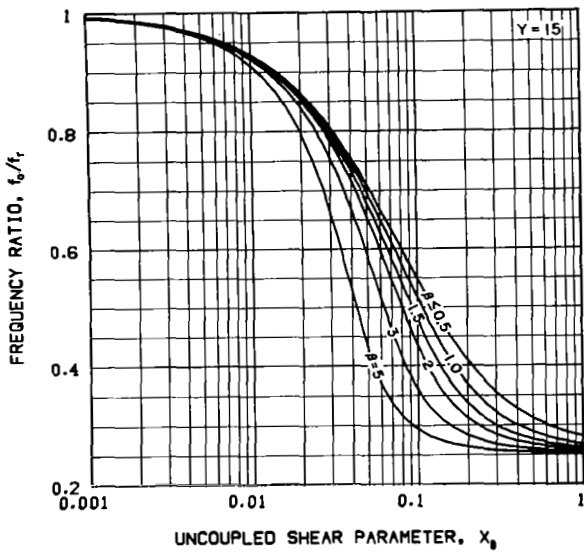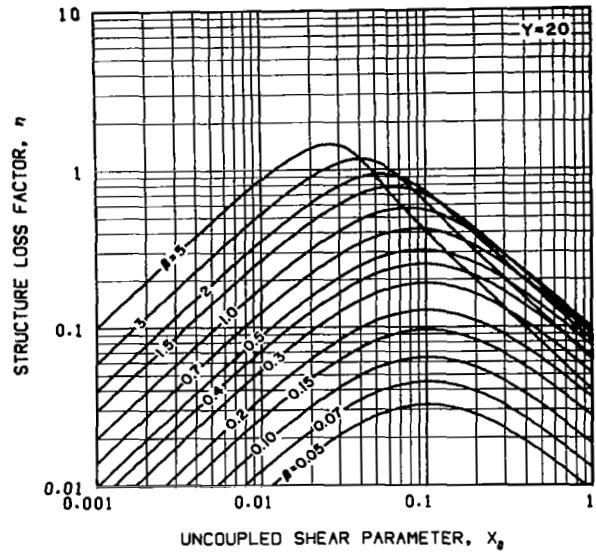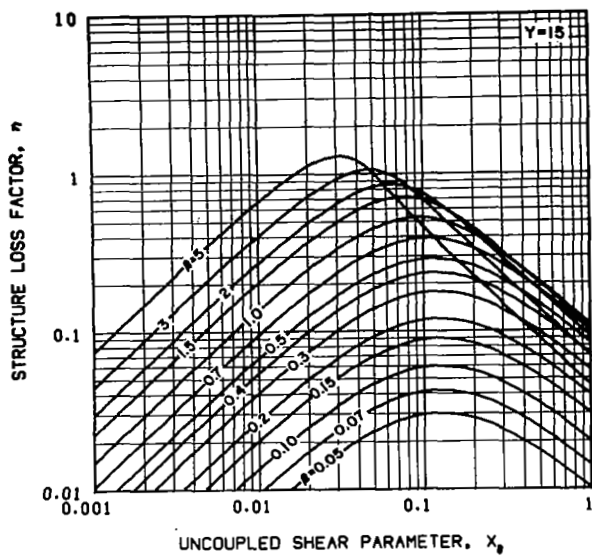
Figure 18. – Structure loss factor and frequency ratio of two- and three-elastic element structural composites with geometric parameter Y = 15 and 20.
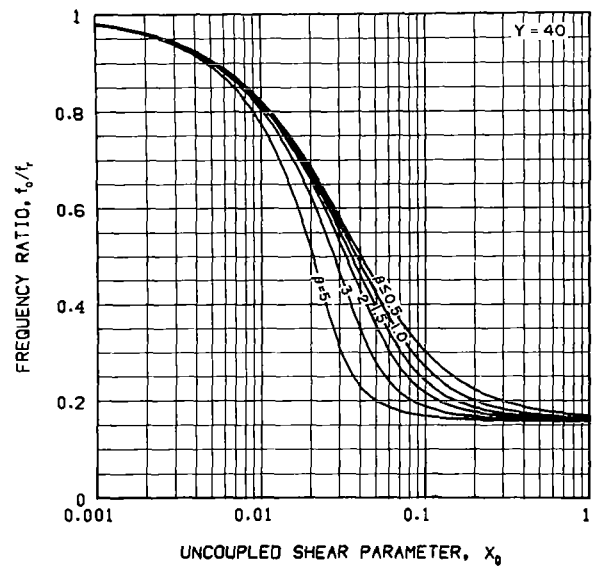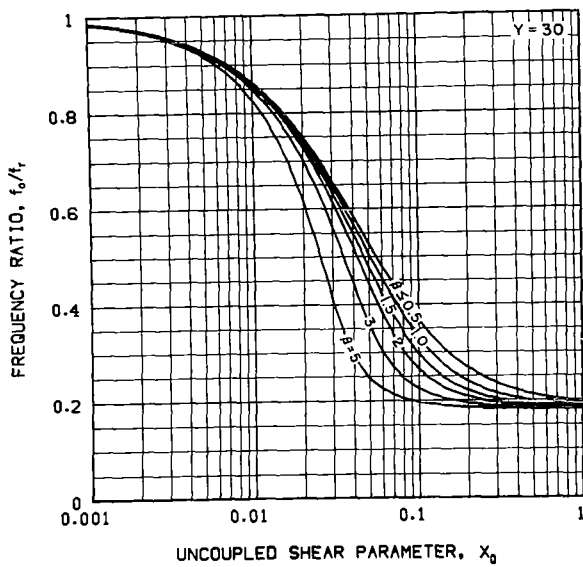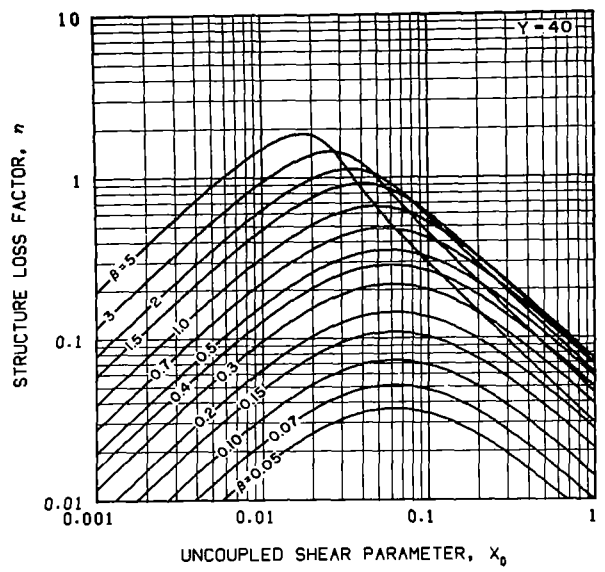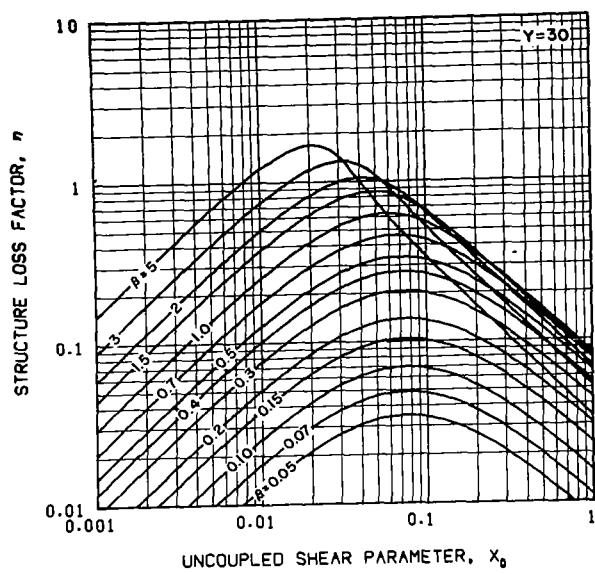
Figure 19. – Structure loss factor and frequency ratio of two- and three-elastic element structural composites with geometric parameter Y = 30 and 40

116
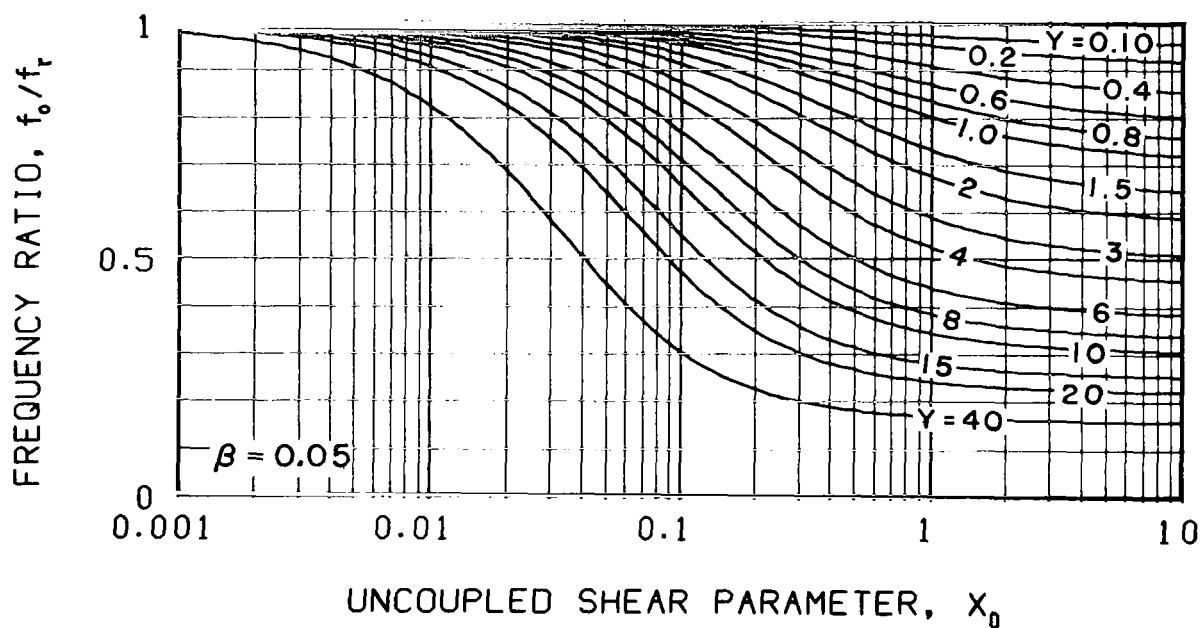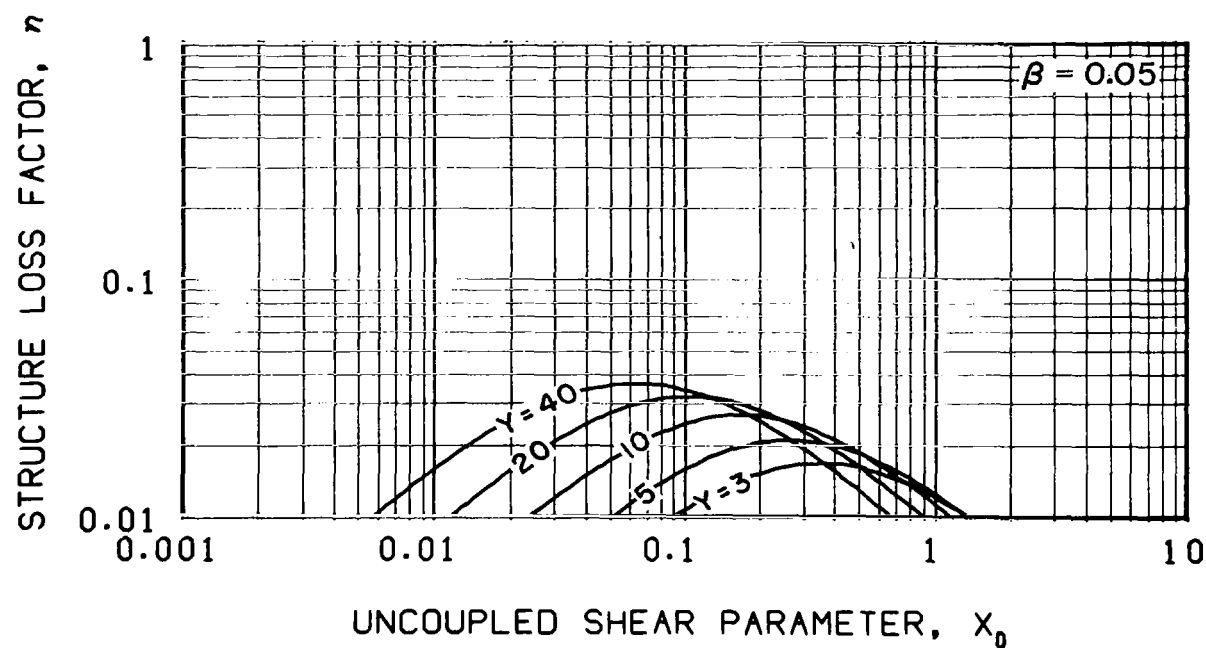
Figure 20. – Structure loss factor and frequency ratio of two- and three-elastic-element structural composites with the viscoelastic material loss factor $\beta = 0.05$

117
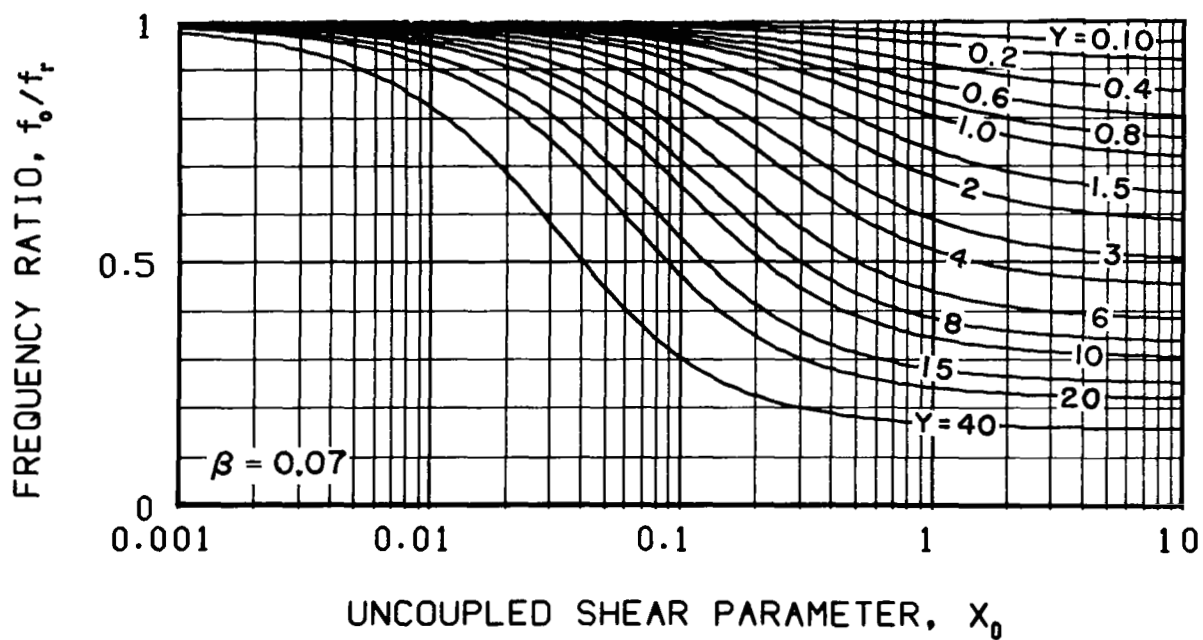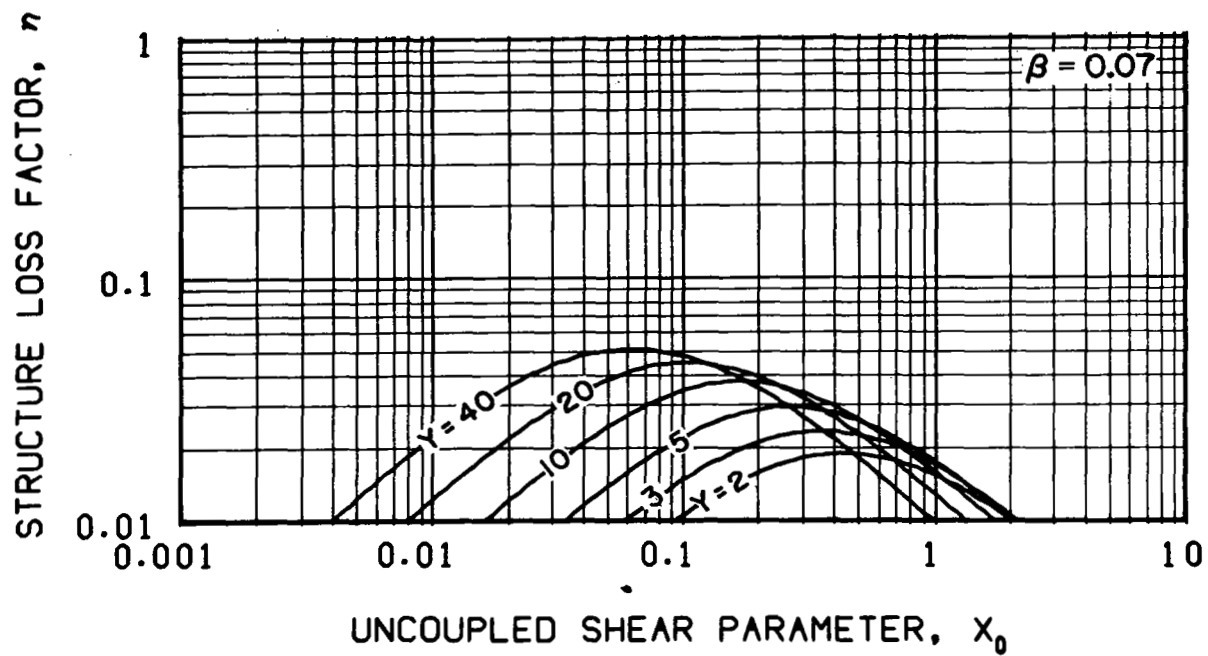
Figure 21. – Structure loss factor and frequency ratio of two- and three-elastic-element structural composites with the viscoelastic material loss factor $\beta = 0.07$
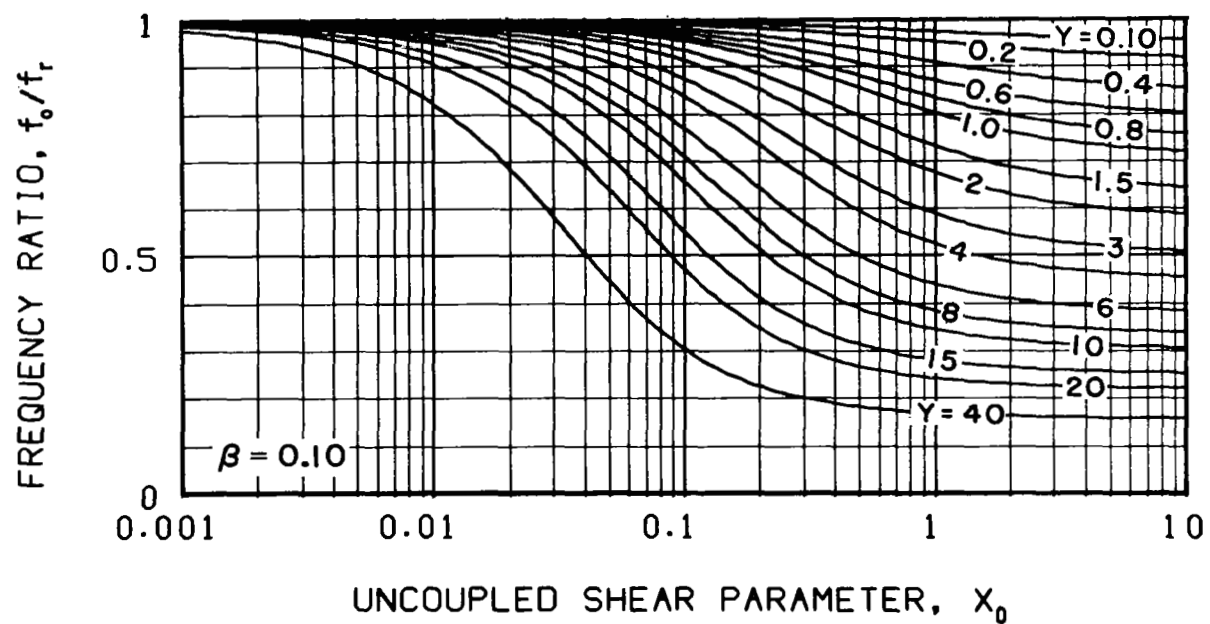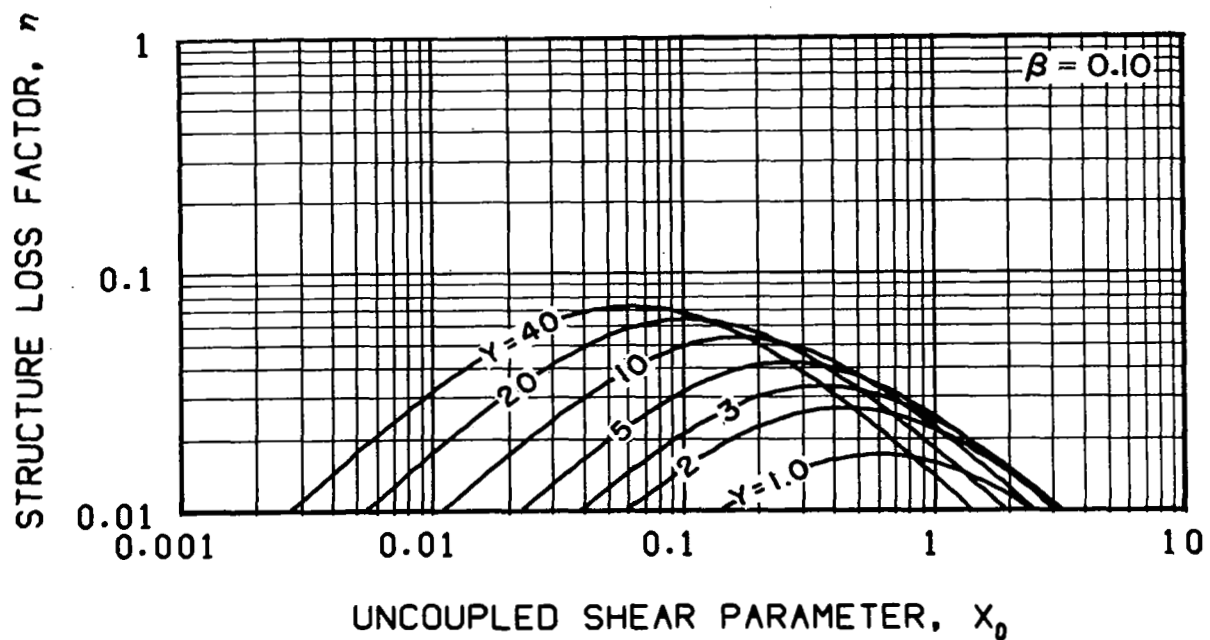
Figure 22. – Structure loss factor and frequency ratio of two- and three-elastic-element structural composites with the viscoelastic material loss factor $\beta = 0.1$

119
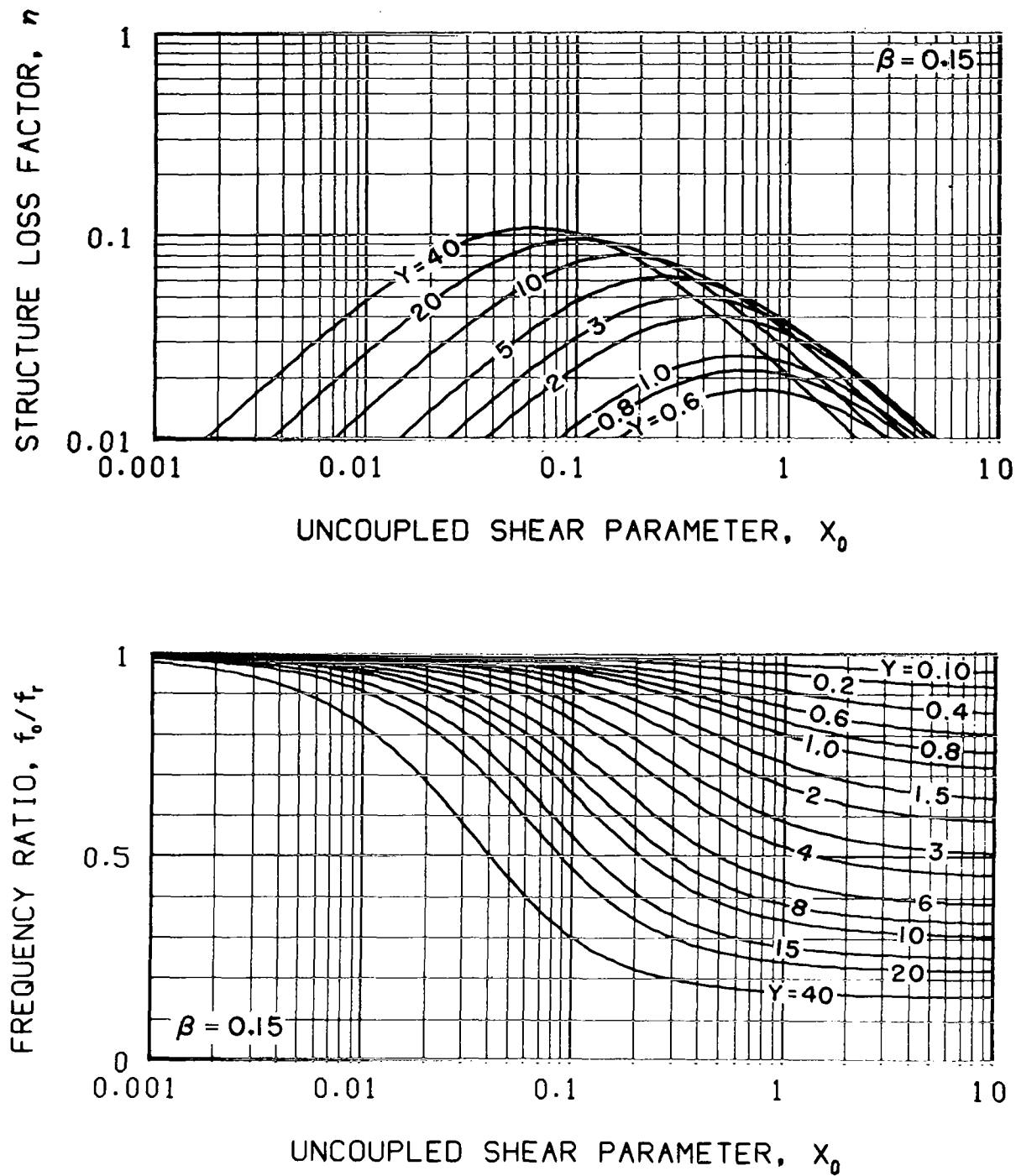
Figure 23. – Structure loss factor and frequency ratio of two- and three-elastic-element structural composites with the viscoelastic material loss factor $\beta = 0.15$

120
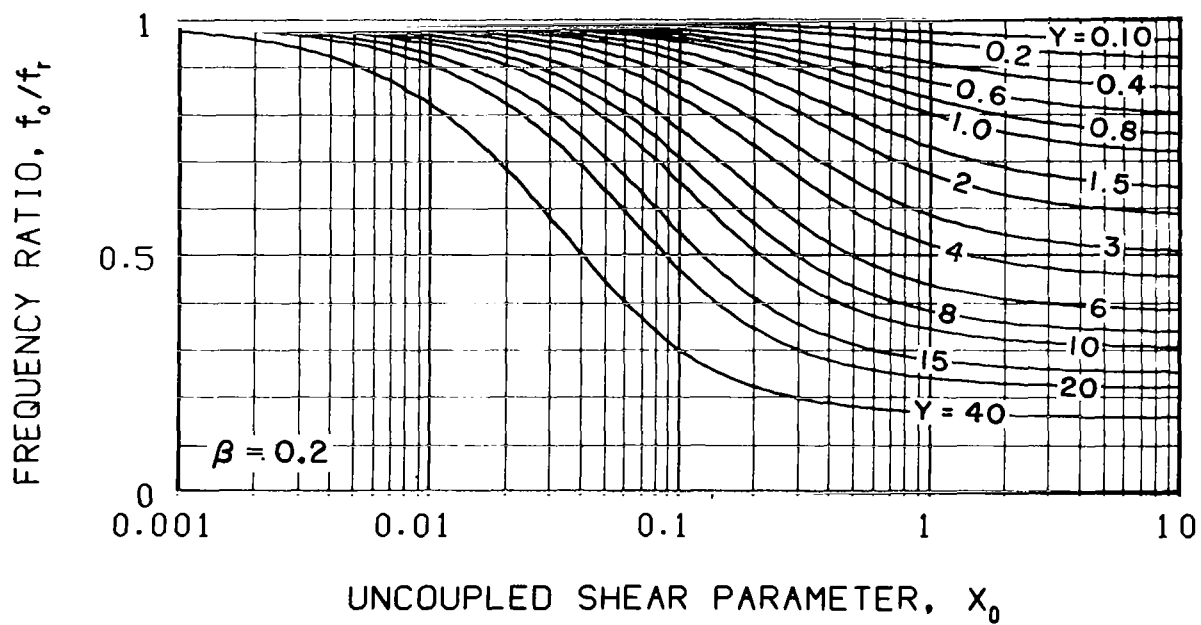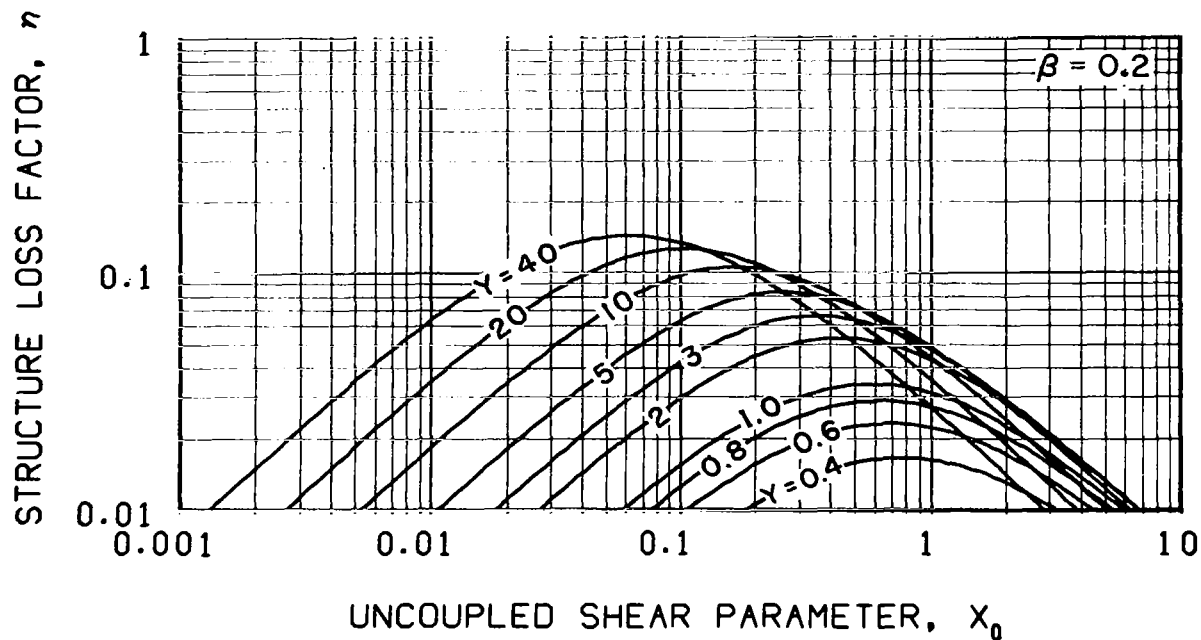
Figure 24. — Structure loss factor and frequency ratio of two- and three-elastic-element structural composites with the viscoelastic material loss factor $\beta = 0.2$

121
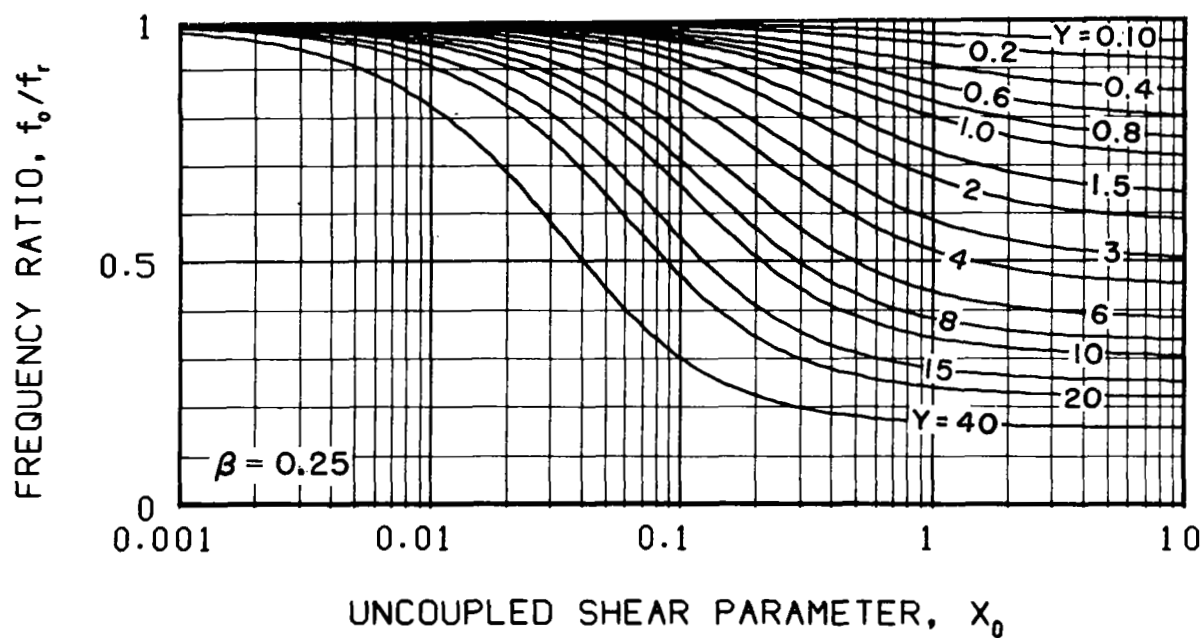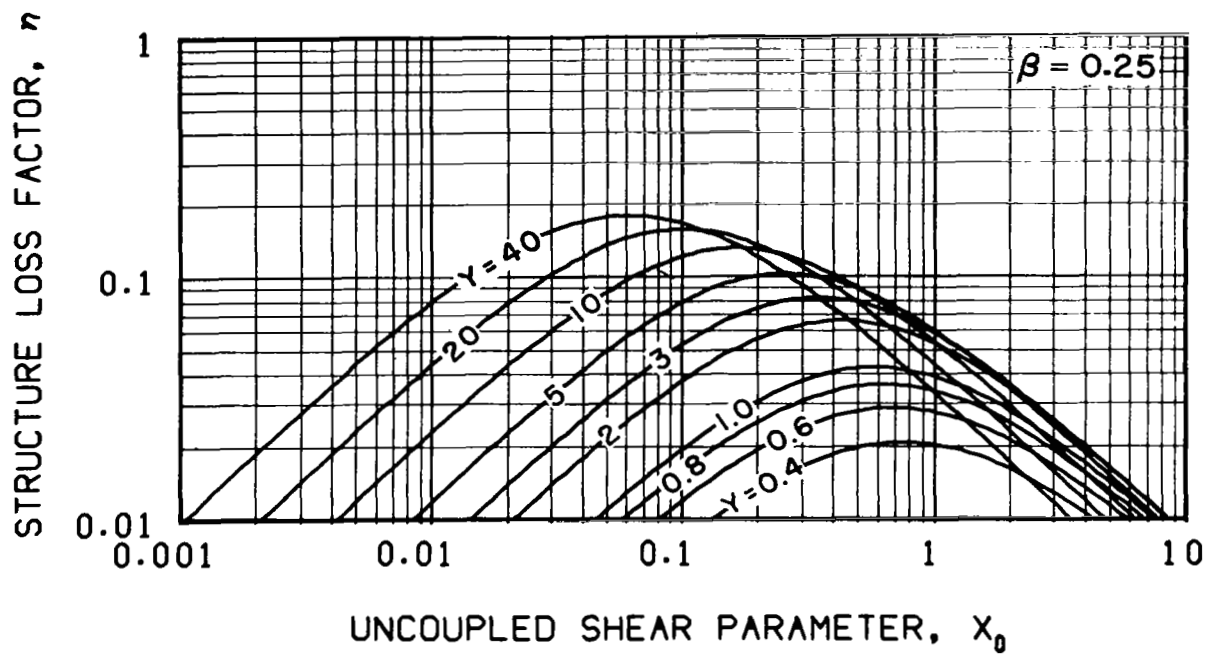
Figure 25. – Structure loss factor and frequency ratio of two- and three-elastic-element structural composites with the viscoelastic material loss factor $\beta = 0.25$

122
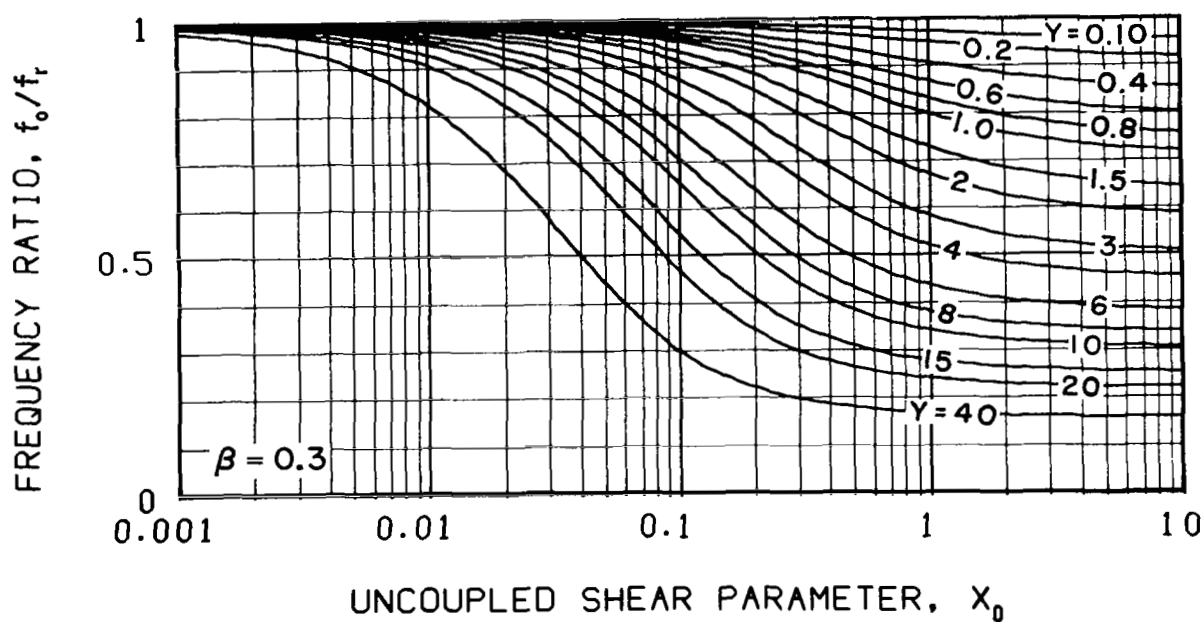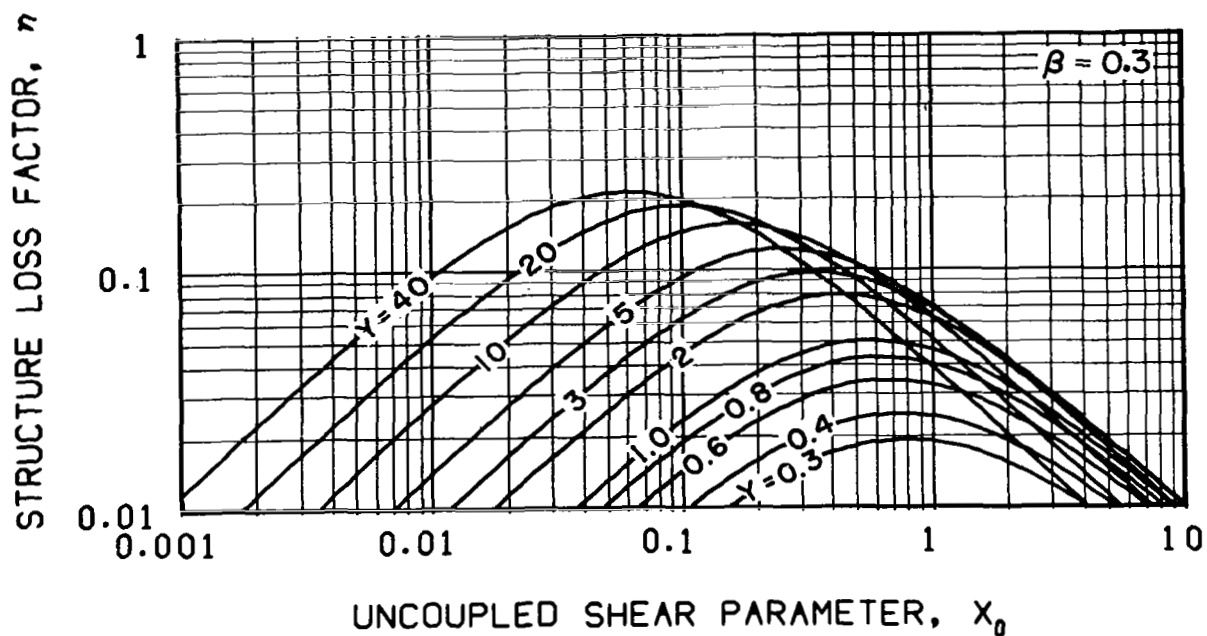
Figure 26. – Structure loss factor and frequency ratio of two- and three-elastic-element structural composites with the viscoelastic material loss factor $\beta = 0.3$

123
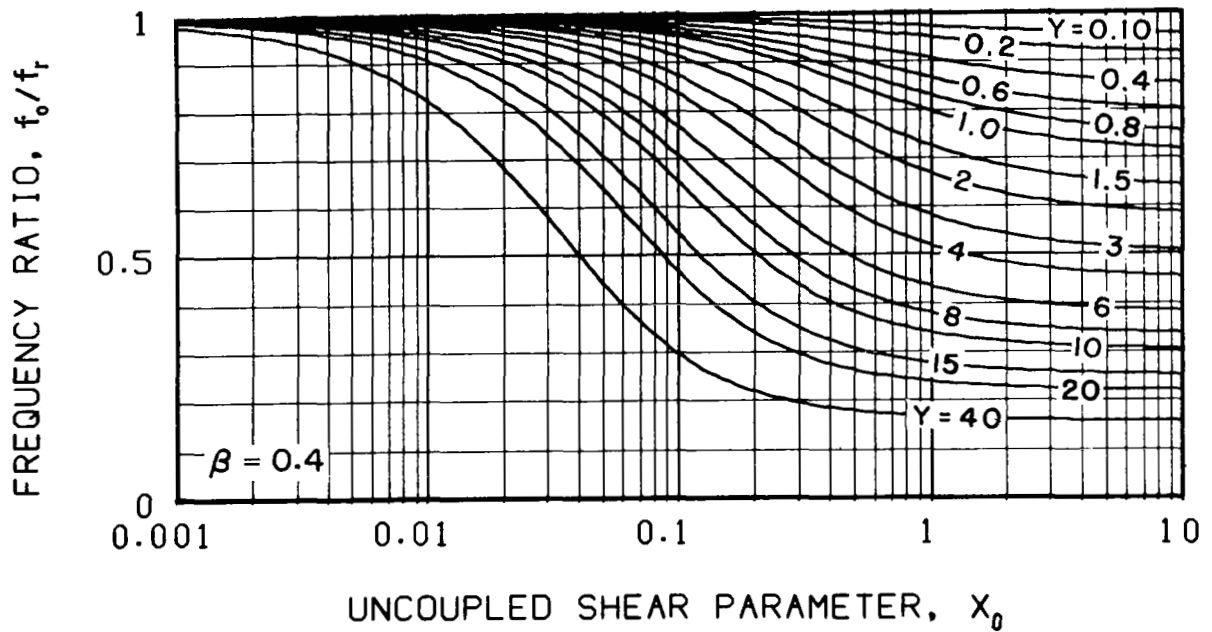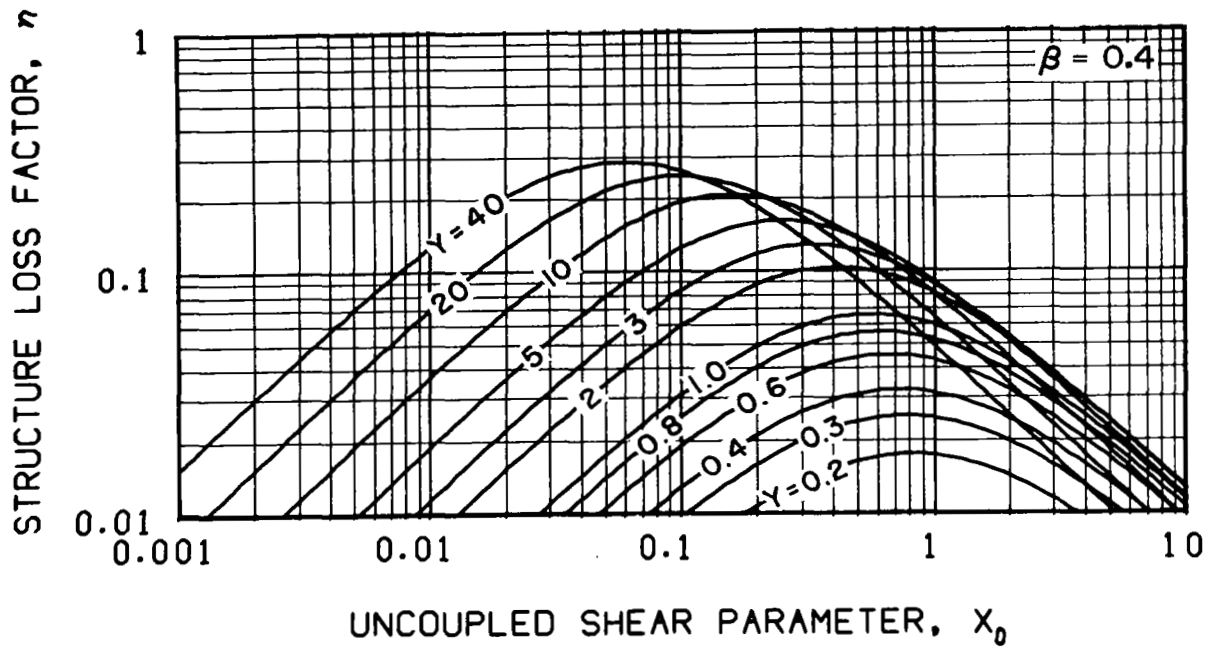
Figure 27. – Structure loss factor and frequency ratio of two- and three-elastic-element structural composites with the viscoelastic material loss factor $\beta = 0.4$

124
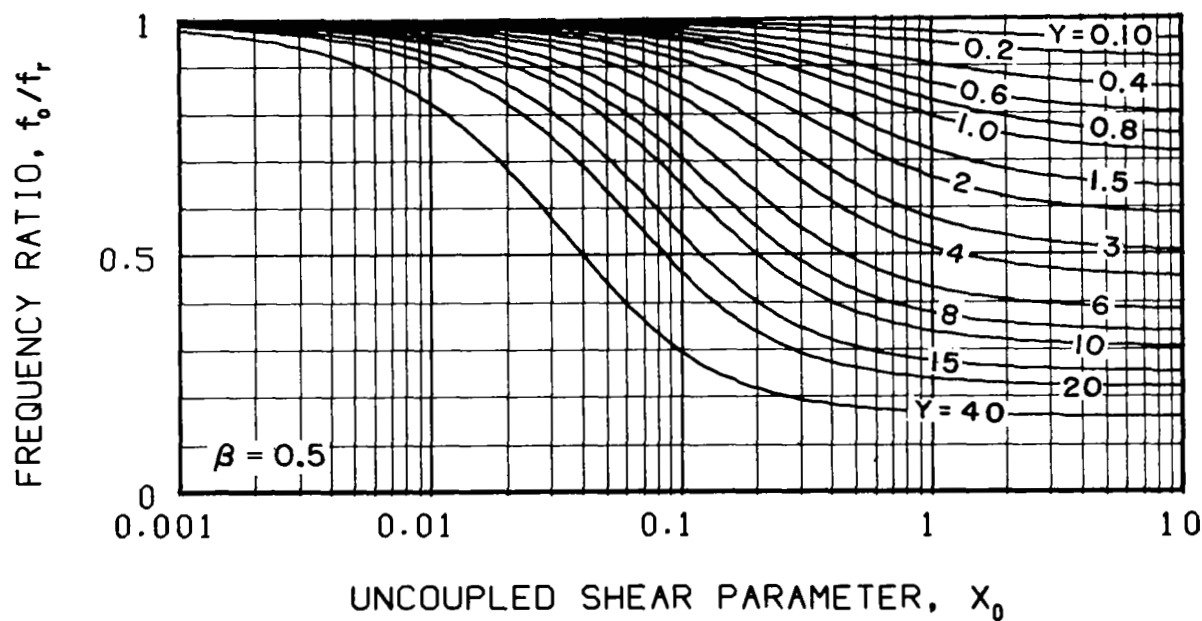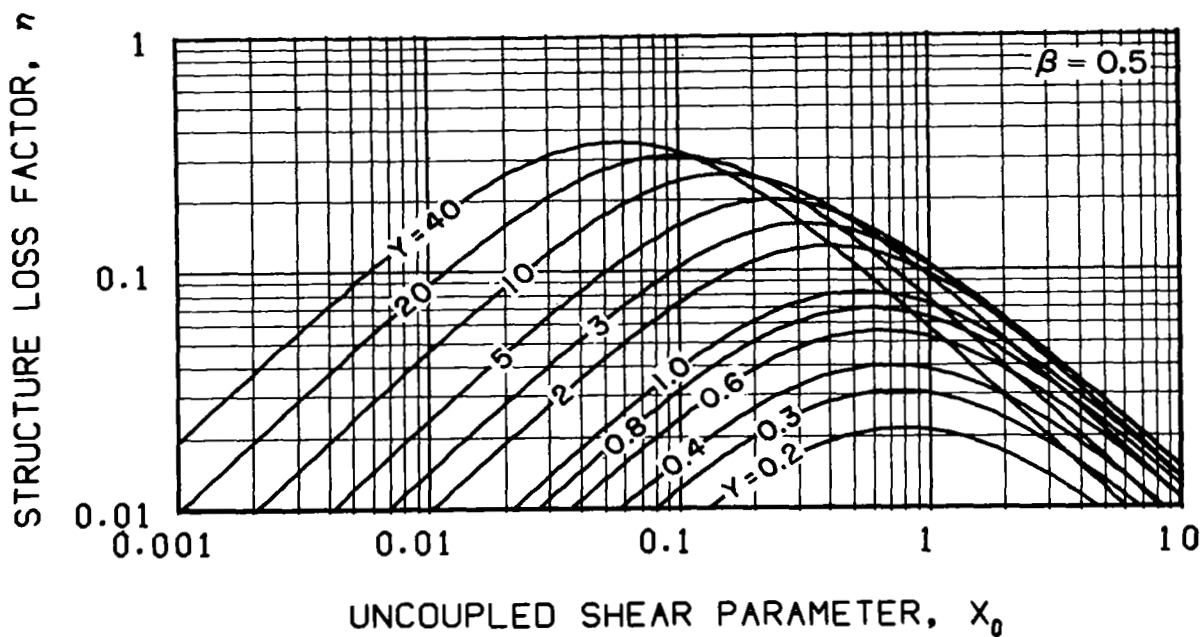
Figure 28. – Structure loss factor and frequency ratio of two- and three-elastic-element structural composites with the viscoelastic material loss factor $\beta = 0.5$
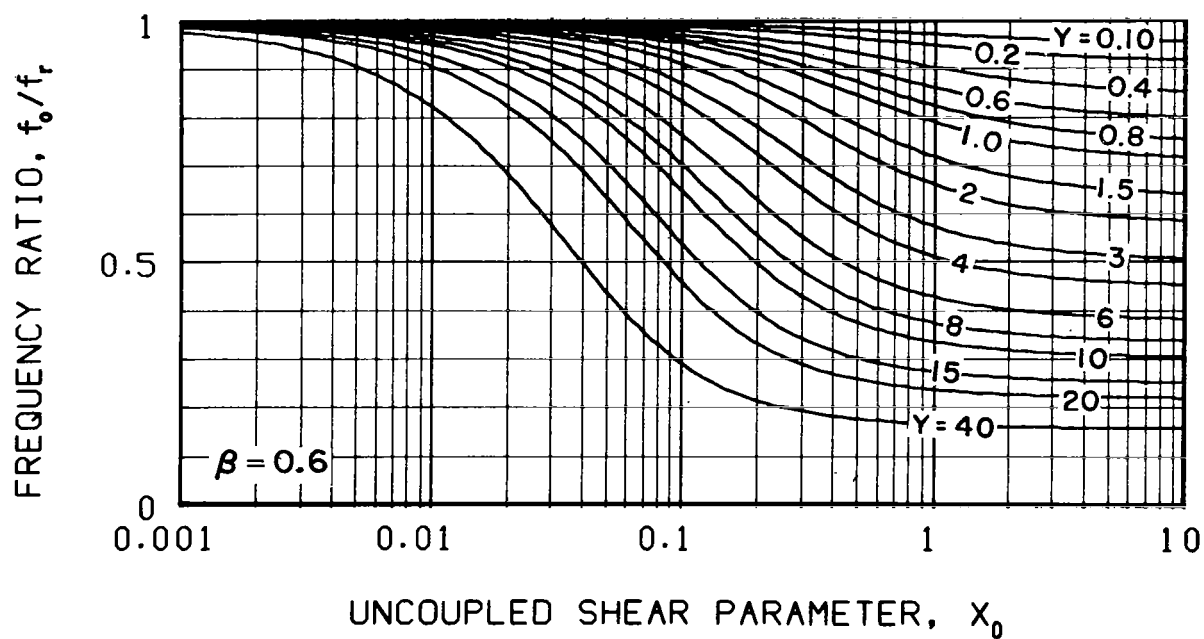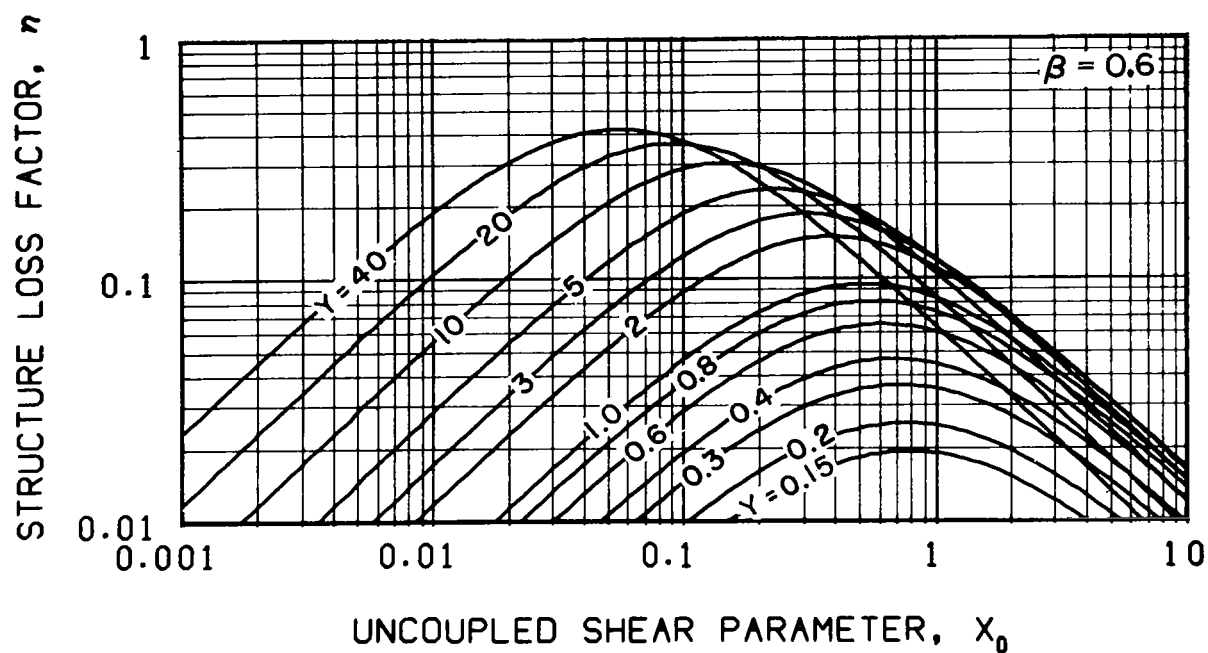
Figure 29. – Structure loss factor and frequency ratio of two- and three-elastic-element structural composites with the viscoelastic material loss factor $\beta = 0.6$
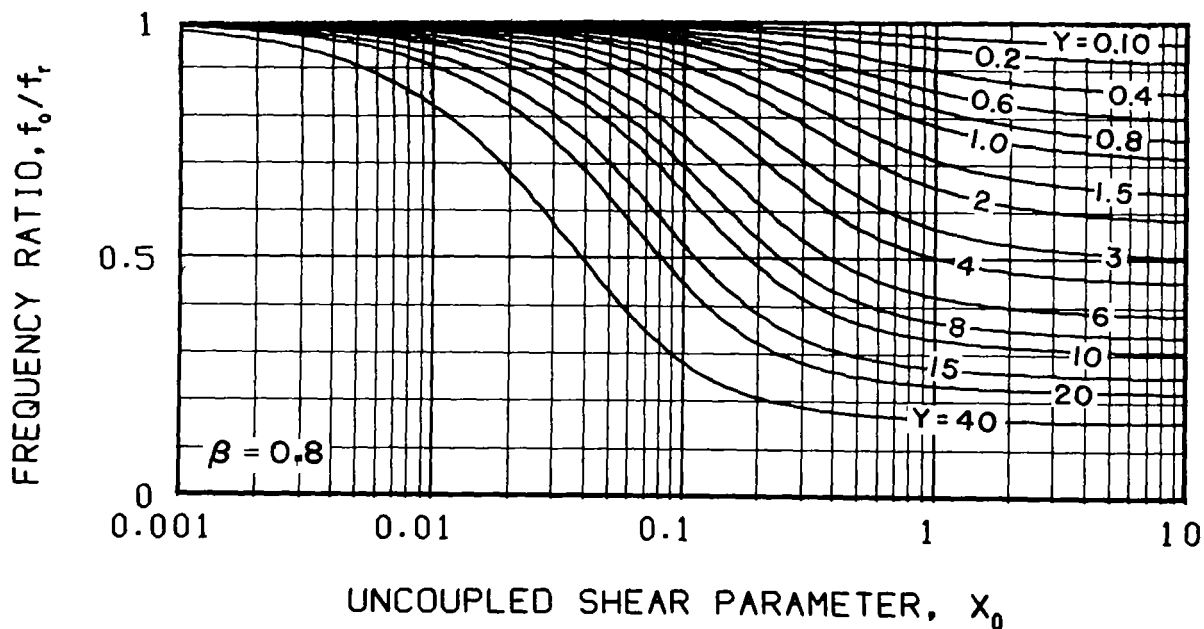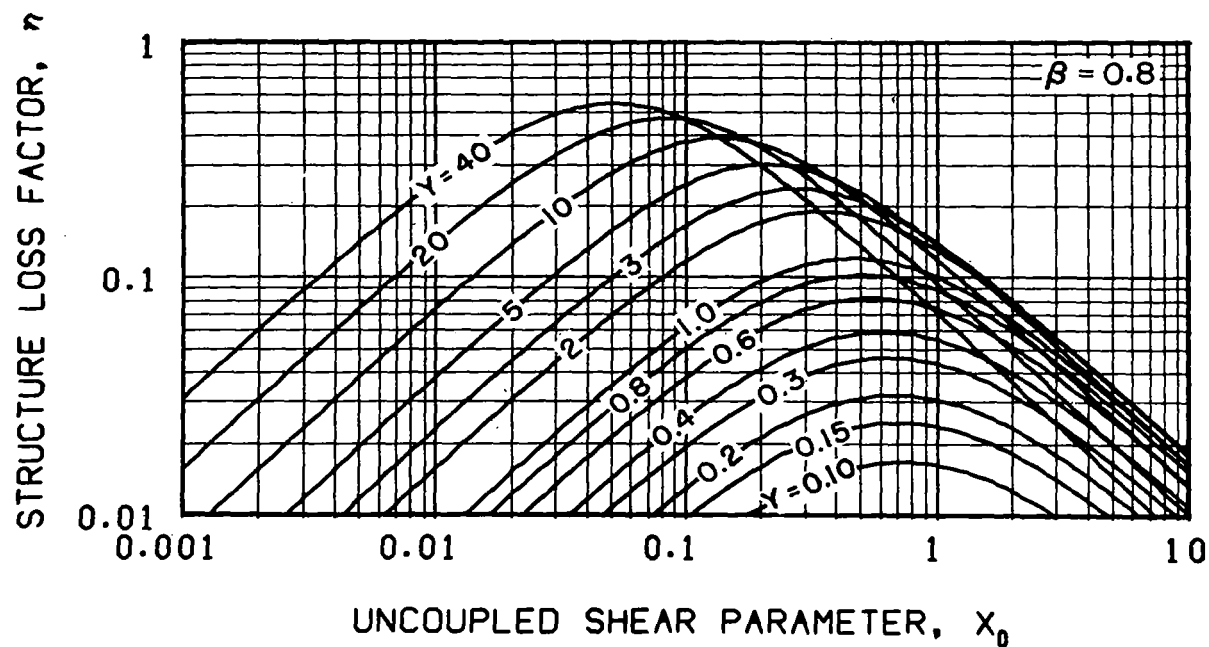
Figure 30. – Structure loss factor and frequency ratio of two- and three-elastic-element structural composites with the viscoelastic material loss factor $\beta = 0.8$

127
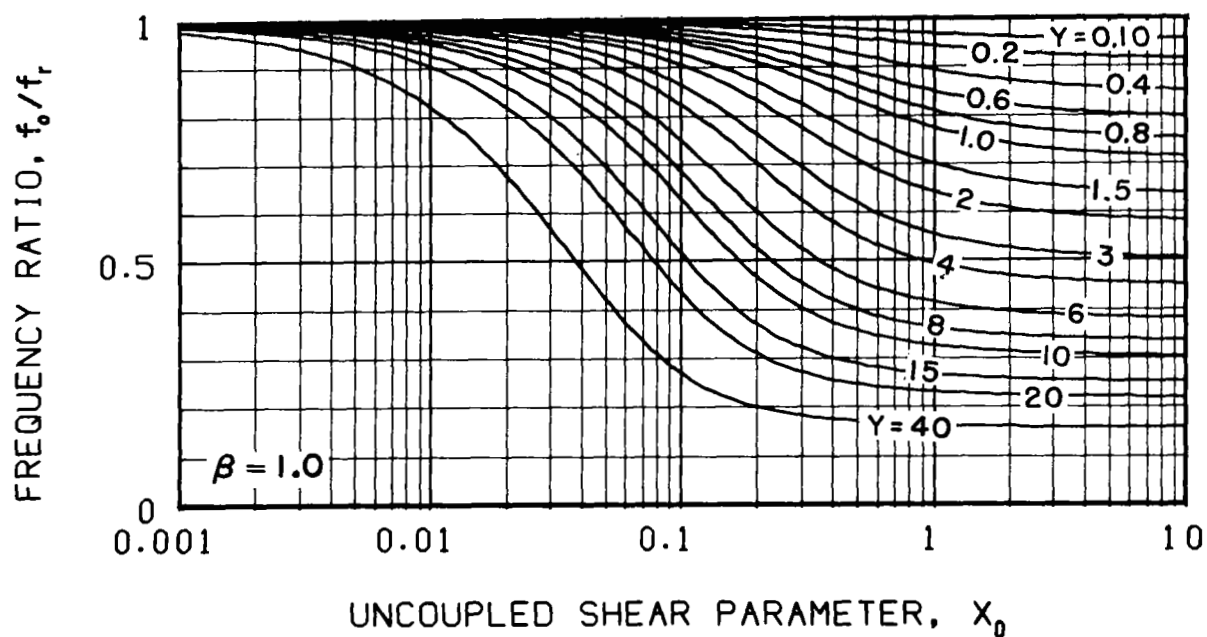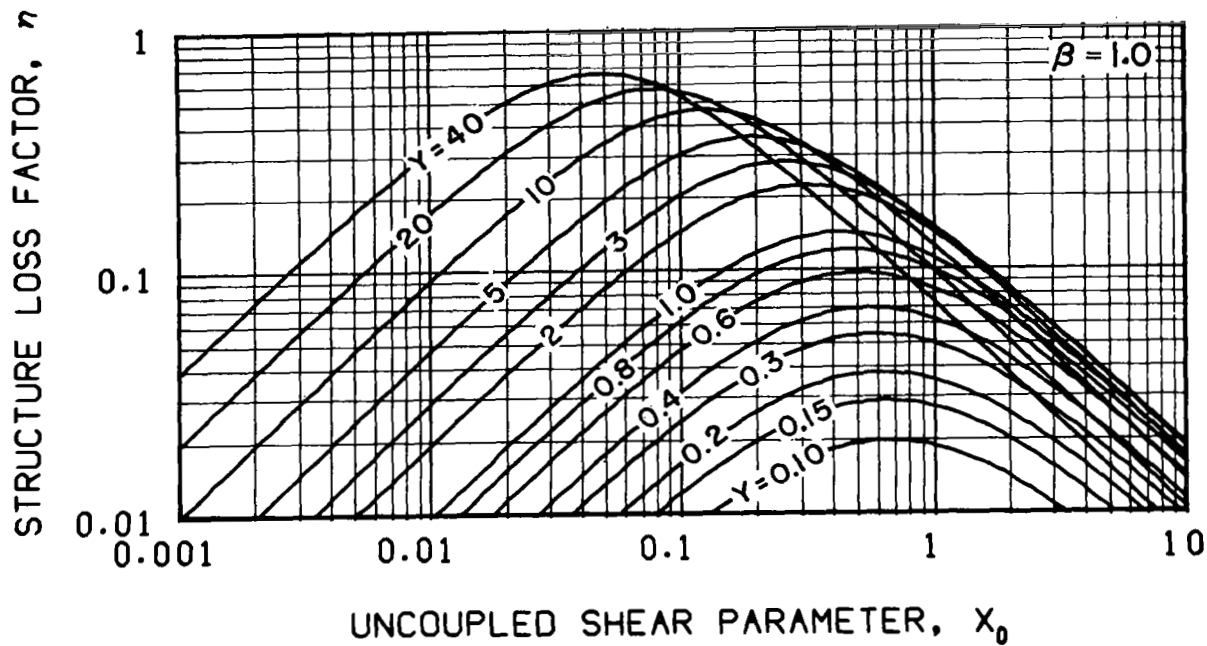
Figure 31. – Structure loss factor and frequency ratio of two- and three-elastic-element structural composites with the viscoelastic material loss factor $\beta = 1.0$
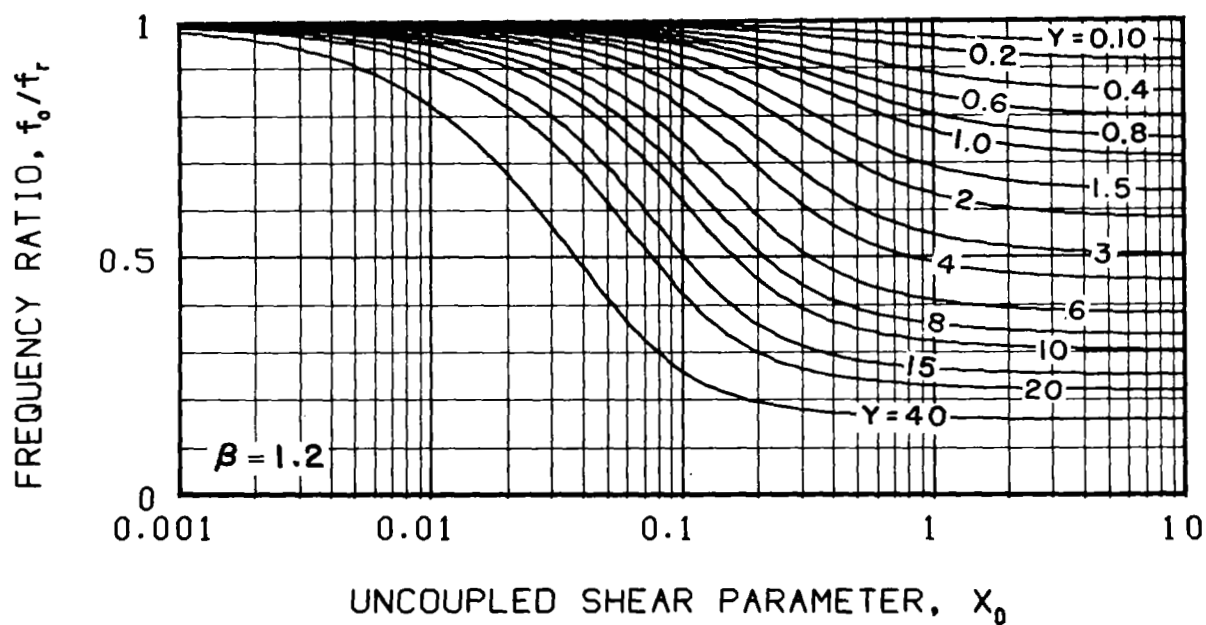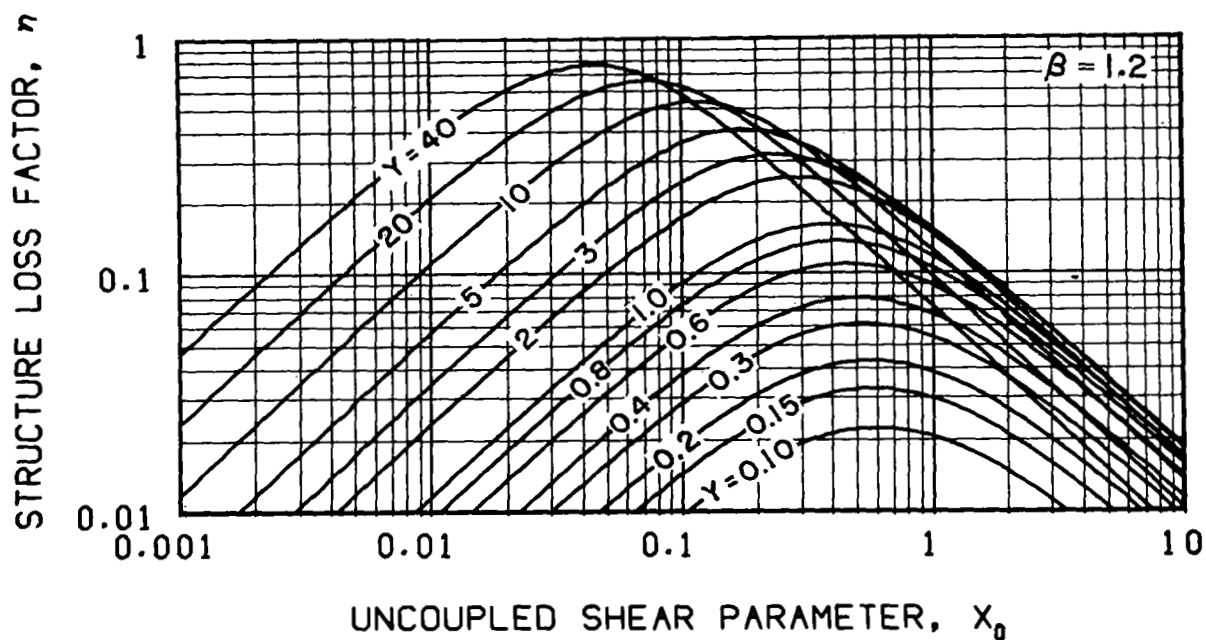
Figure 32. — Structure loss factor and frequency ratio of two- and three-elastic-element structural composites with the viscoelastic material loss factor $\beta = 1.2$

129
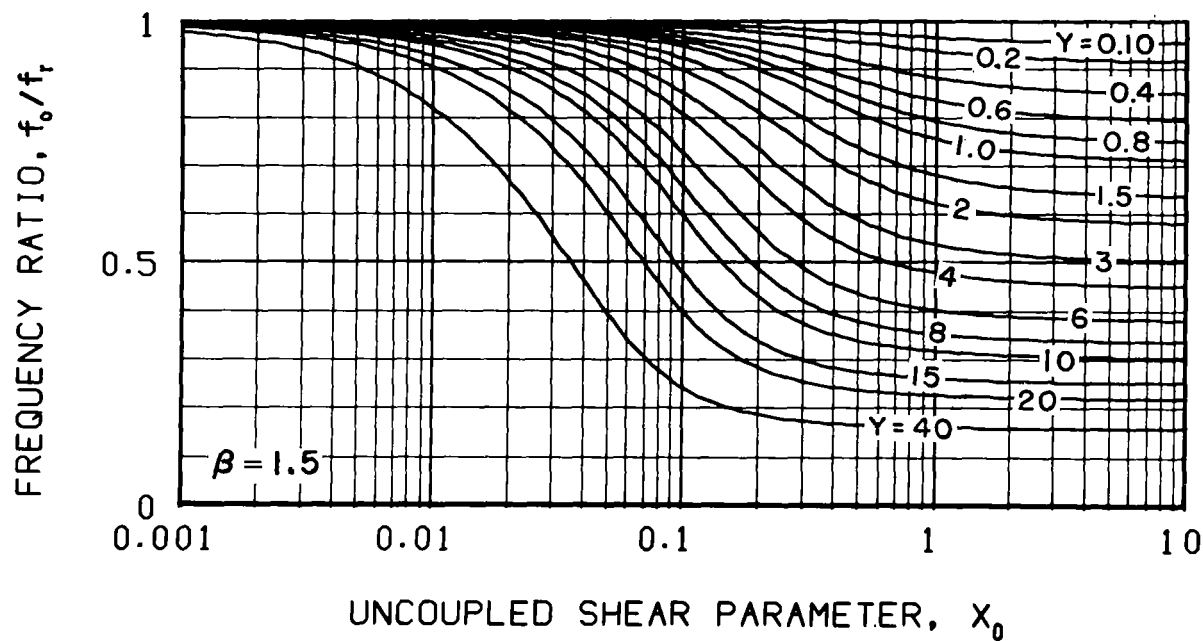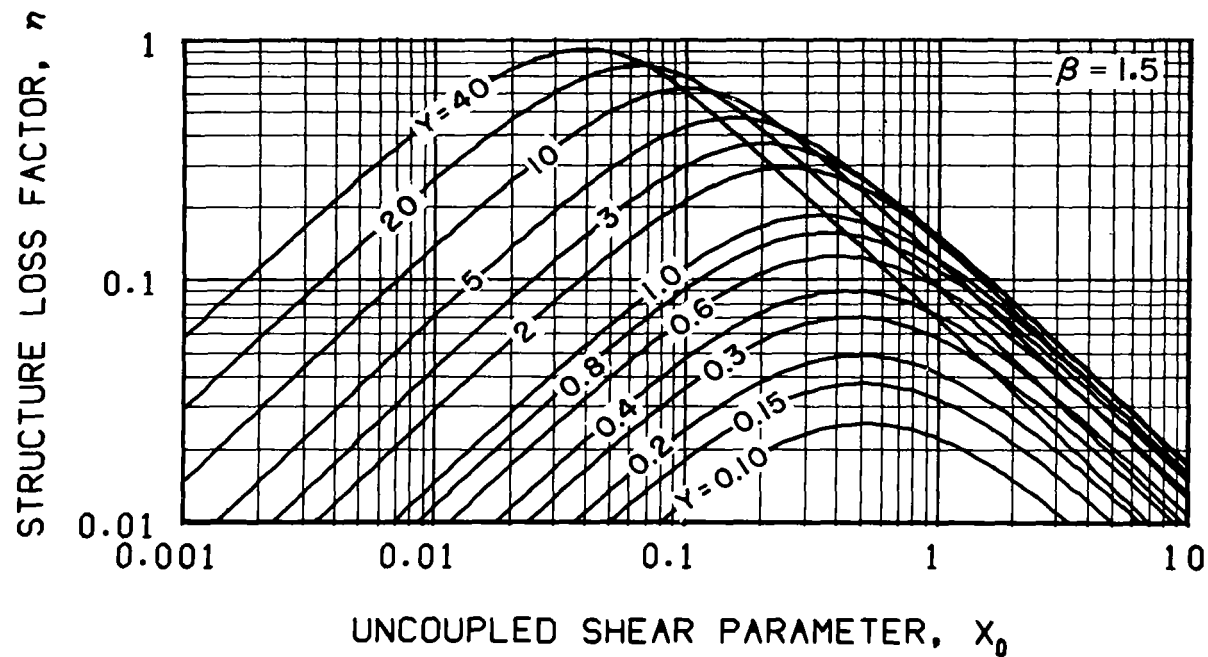
Figure 33. – Structure loss factor and frequency ratio of two- and three-elastic-element structural composites with the viscoelastic material loss factor $\beta = 1.5$

130
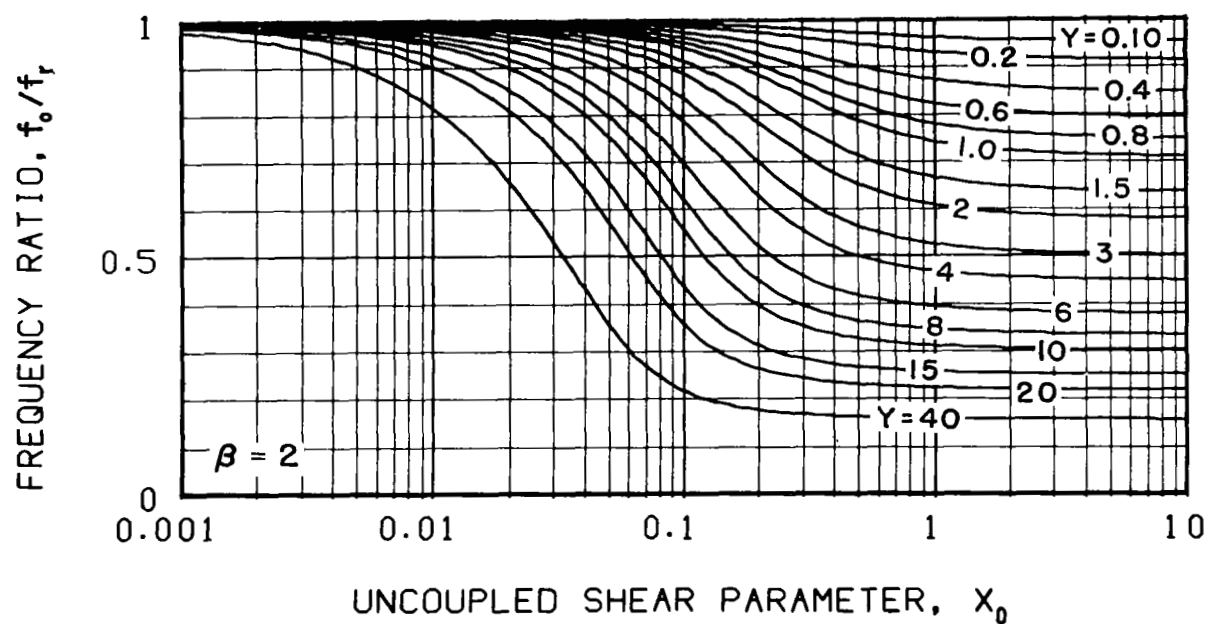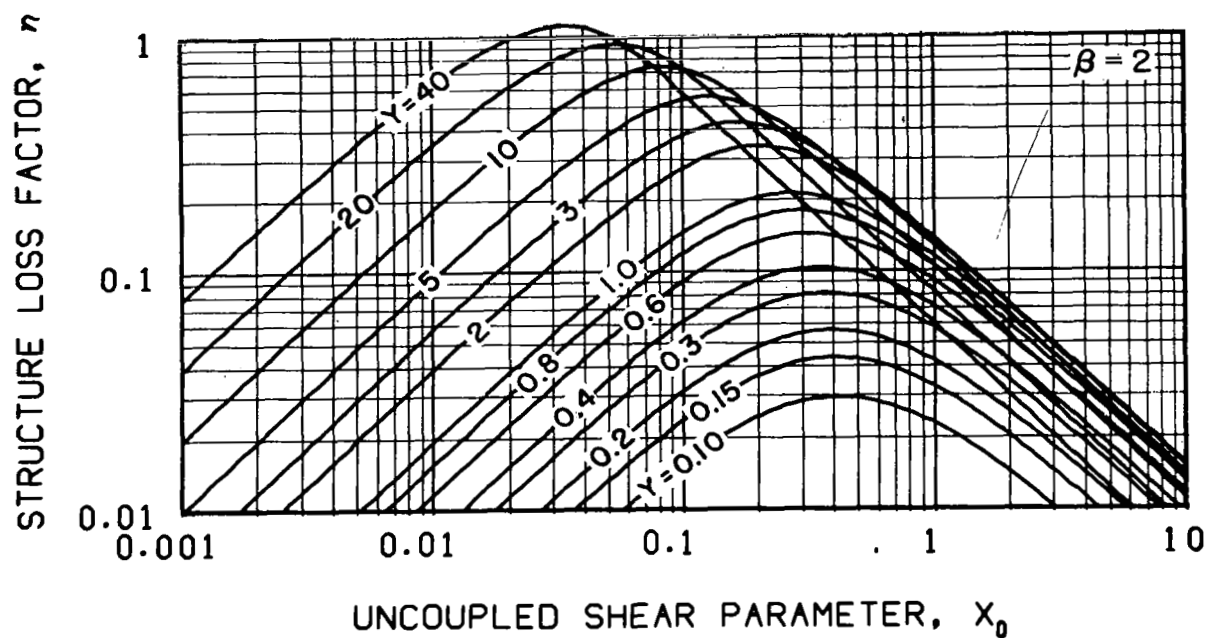
Figure 34. – Structure loss factor and frequency ratio of two- and three-elastic-element structural composites with the viscoelastic material loss factor $\beta = 2$

131
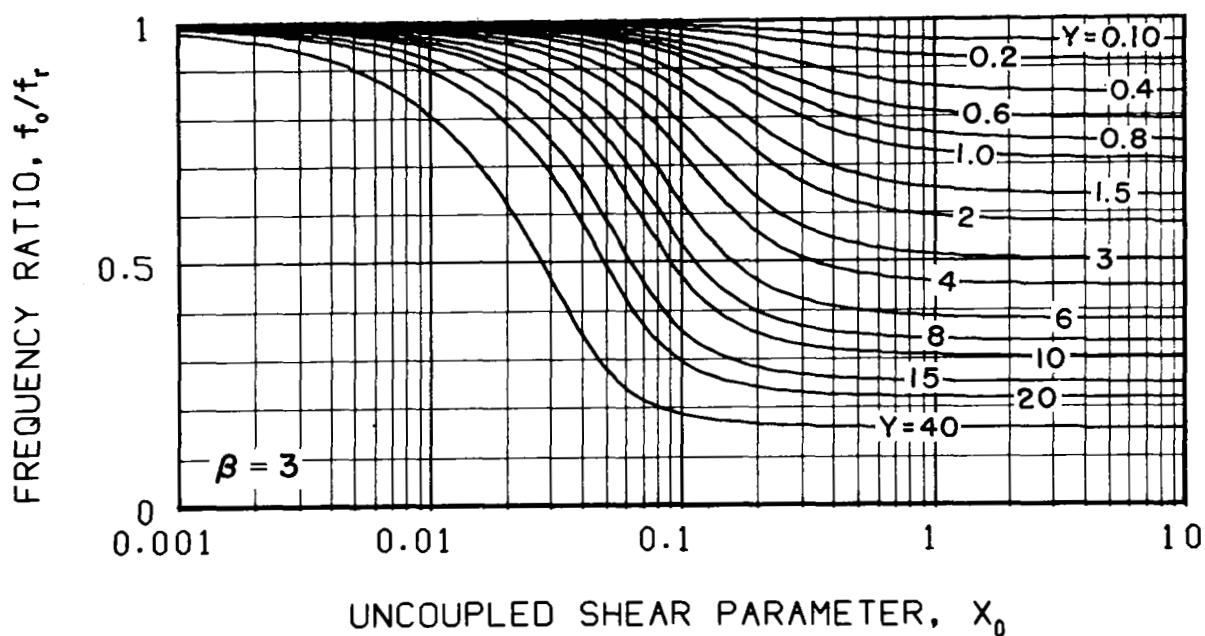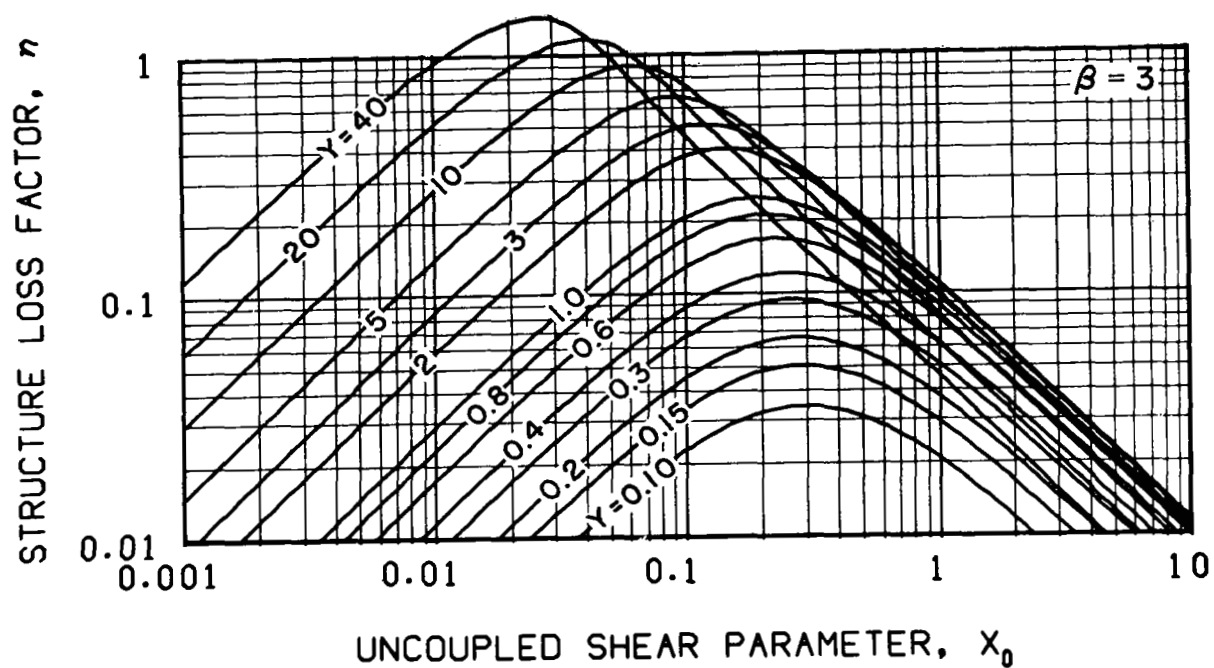
Figure 35. – Structure loss factor and frequency ratio of two- and three-elastic-element structural composites with the viscoelastic material loss factor $\beta = 3$
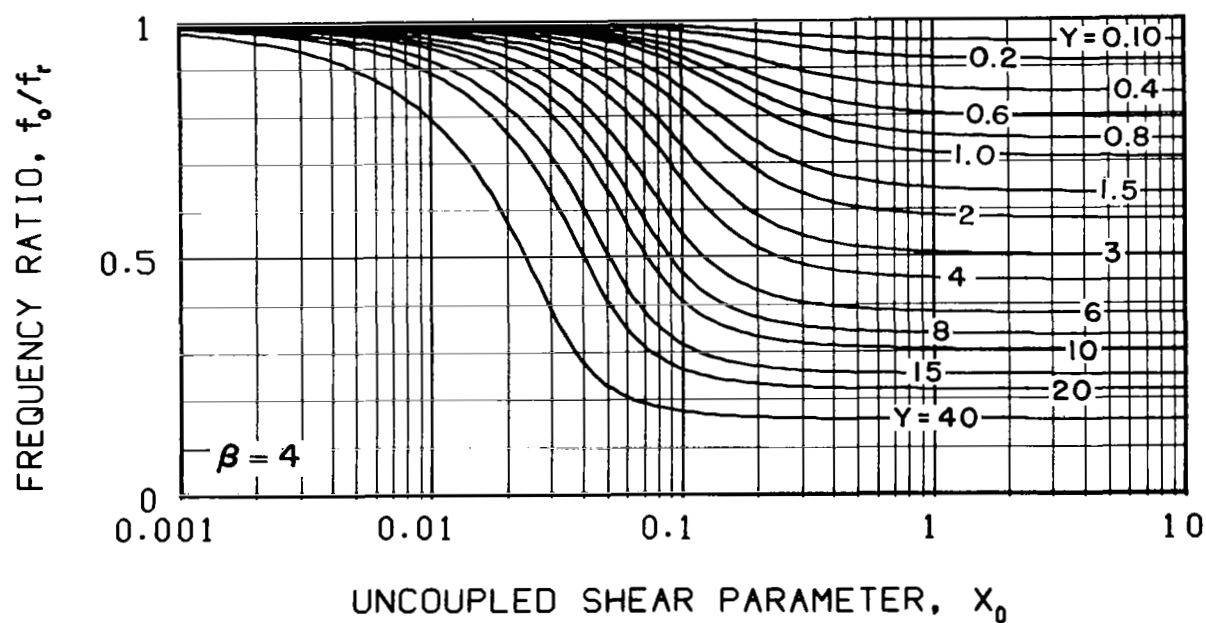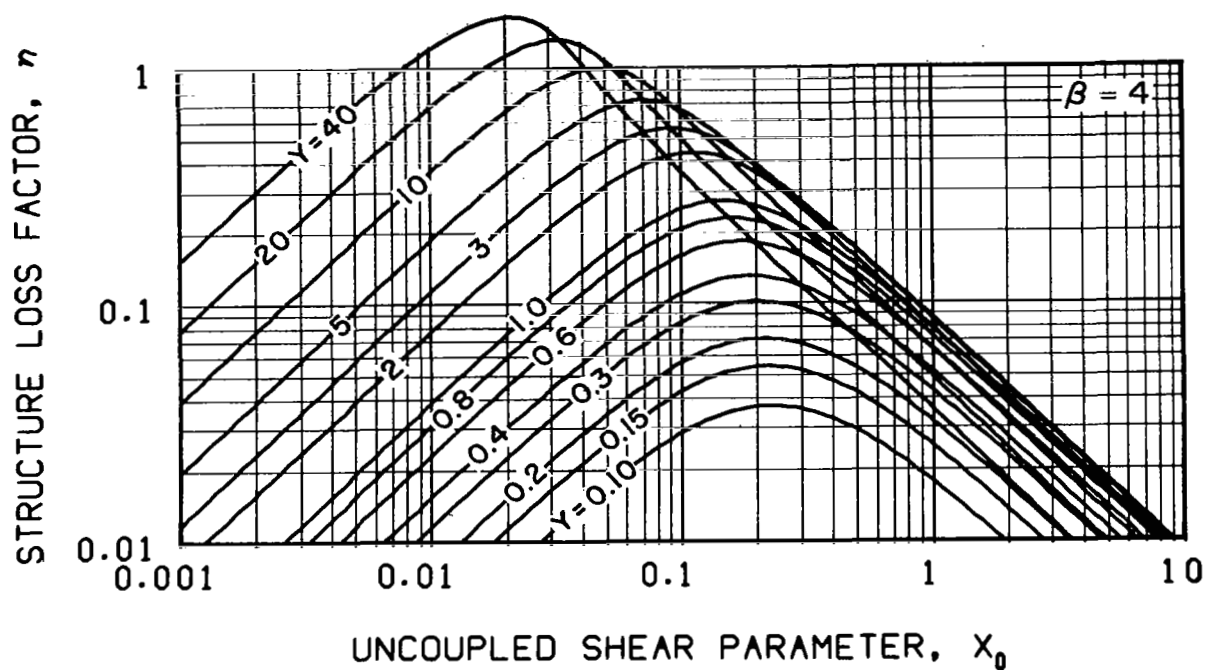
Figure 36. – Structure loss factor and frequency ratio of two- and three-elastic-element structural composites with the viscoelastic material loss factor $\beta = 4$

133
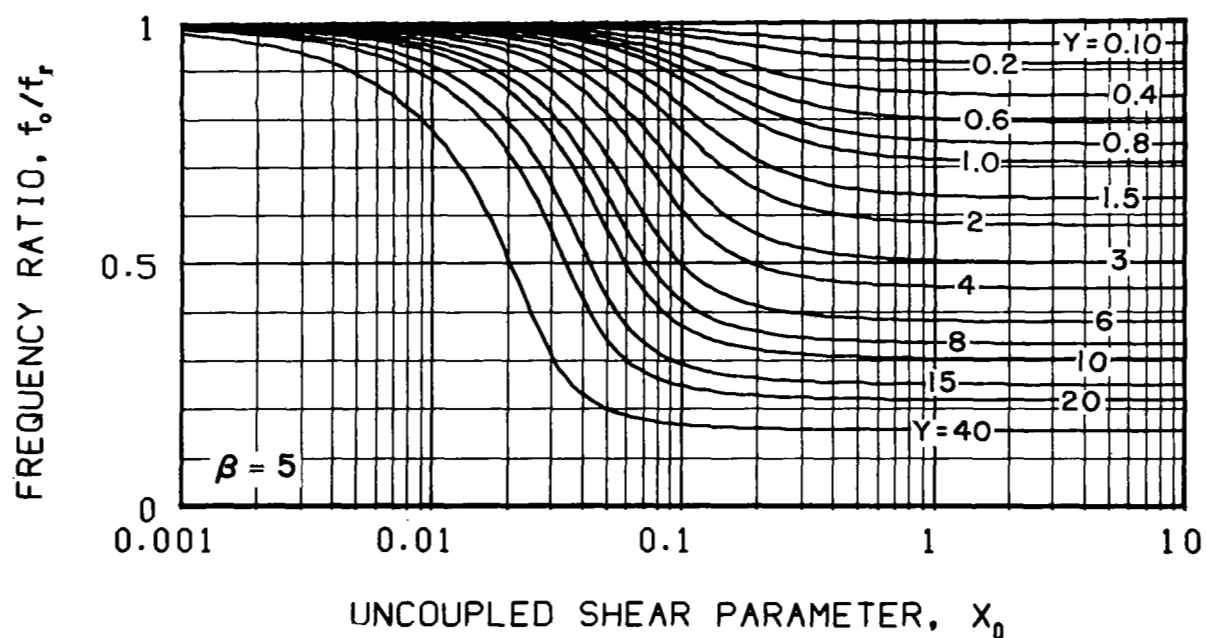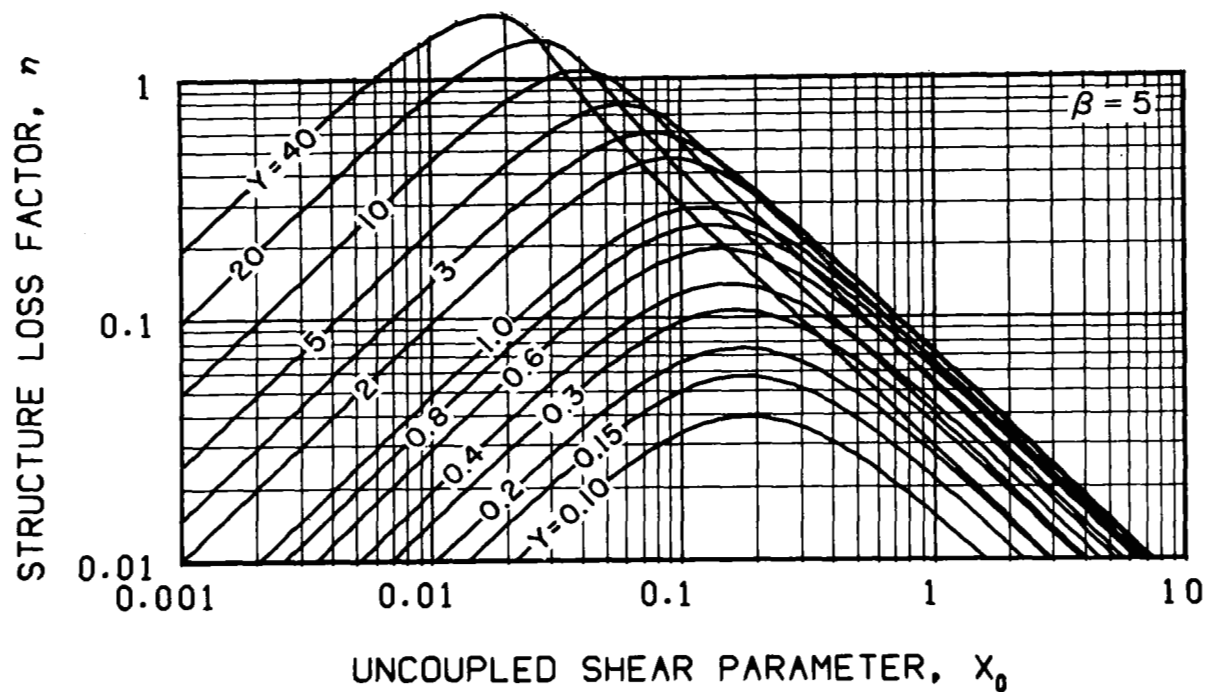
Figure 37. – Structure loss factor and frequency ratio of two- and
three-elastic-element structural composites with the
viscoelastic material loss factor $\beta = 5$

134
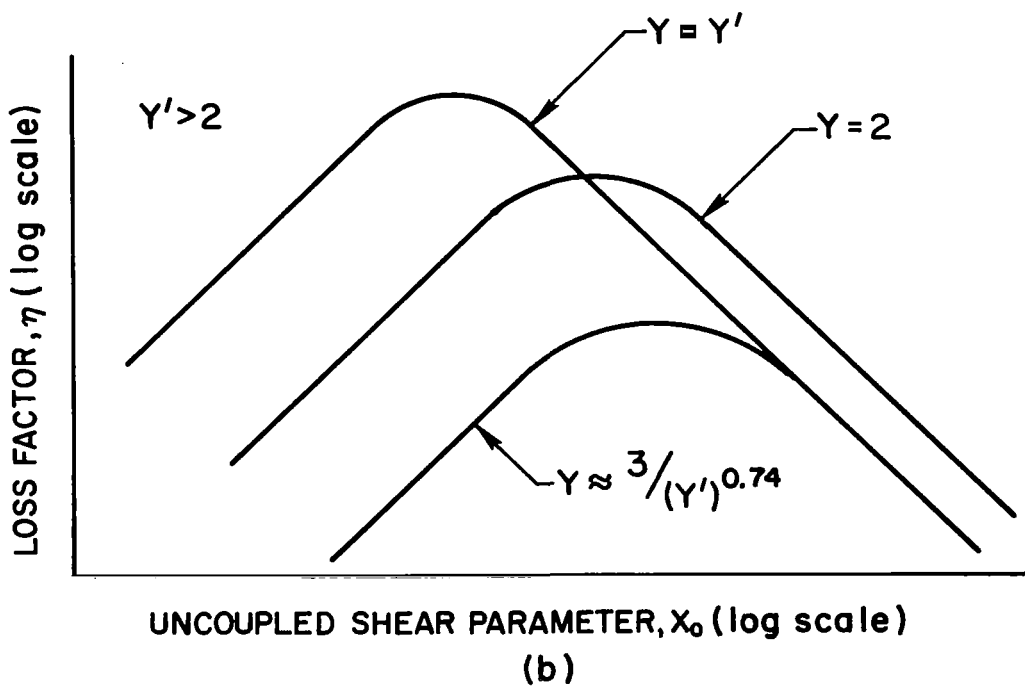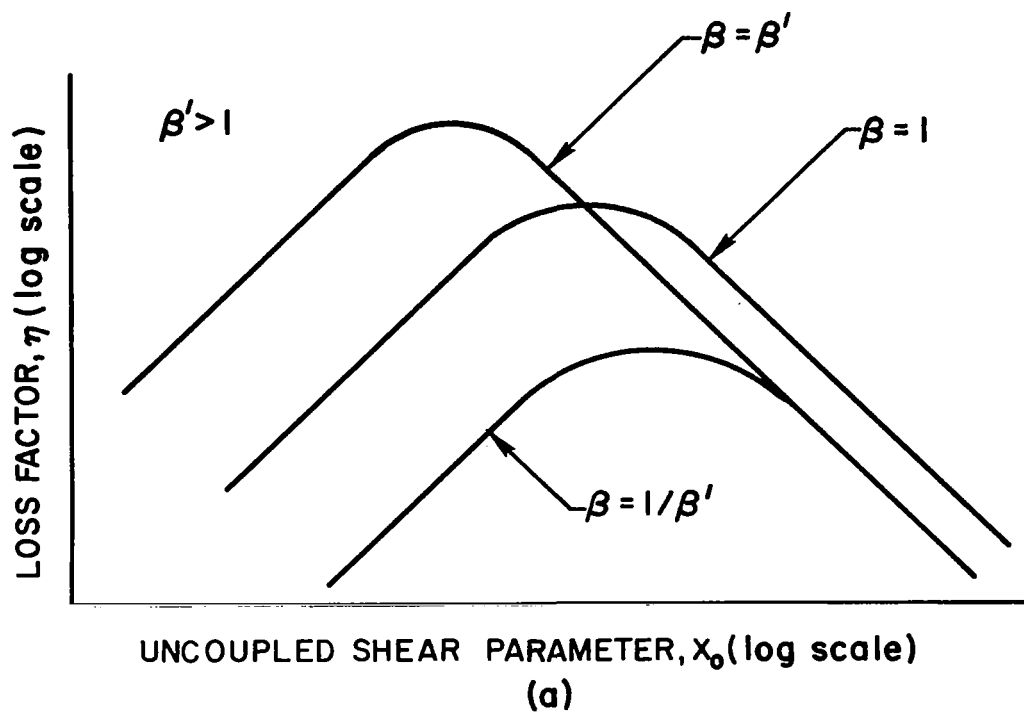
Figure 38. – Characteristics of the structure loss factor curves of (a) Figures 9 through 19 and (b) Figures 20 through 37

$$\eta_{max} = \frac{\beta Y}{Y + 2 + 2\sqrt{(Y+1)(1+\beta^2)}}$$
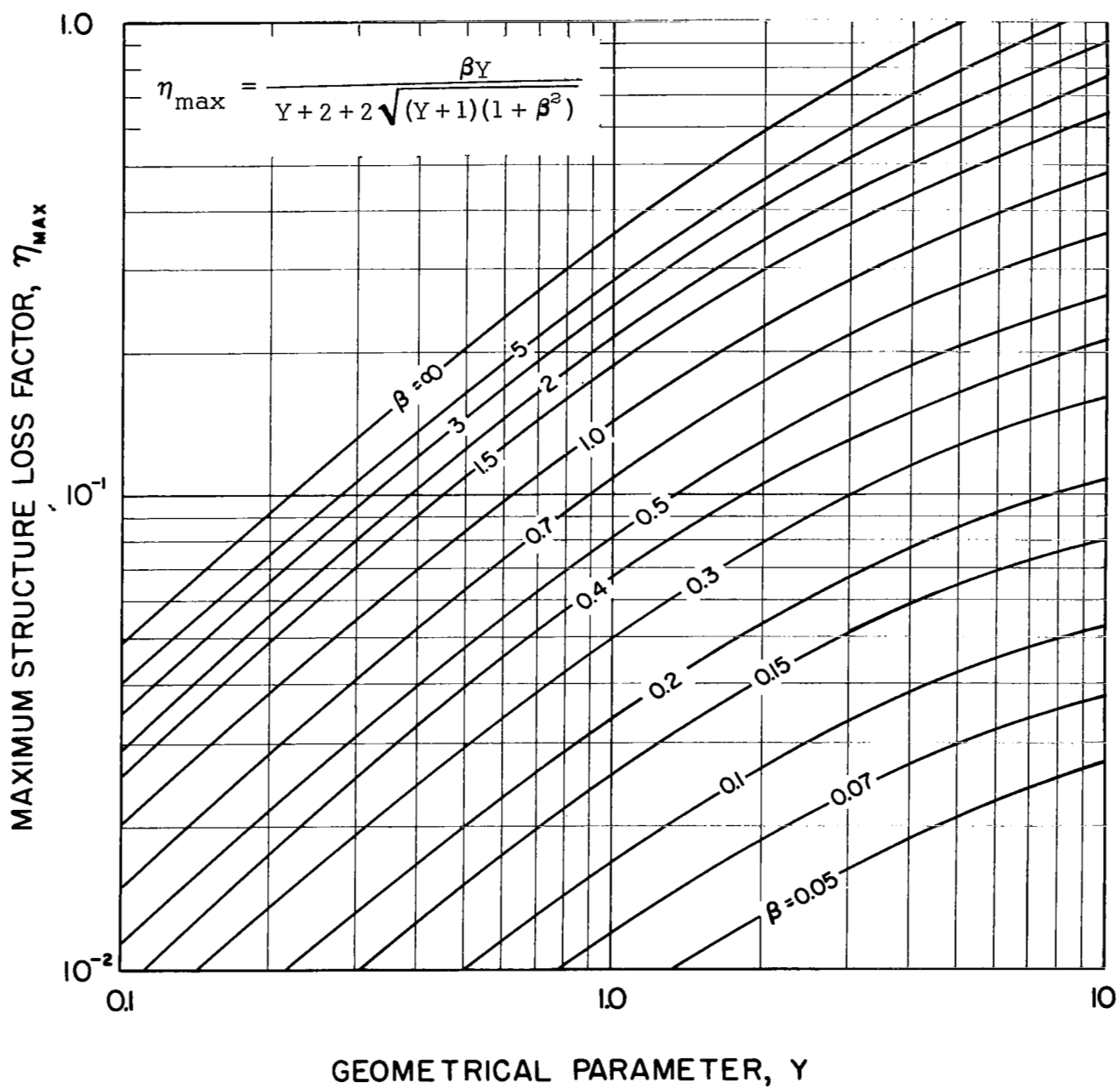
Figure 39. – Maximum structure loss factor of two- and three-elastic-element structural composites

136

OPTIMUM UNCOUPLED SHEAR PARAMETER, $(X_o)_{op}$

$$(X_o)_{op} = \sqrt{\dfrac{2\sqrt{(Y+1)(1+\beta^2)} + (Y+2)(1+\beta^2)}{2[(Y+1)(1+\beta^2)]^2 + (Y+2)\sqrt{[(Y+1)(1+\beta^2)]^3}}}$$

1.0

$\beta \leq 0.1$

0.4

0.7

1.0

0.5

1.5

2

3

$\beta = 5$

0

0.1   1.0   10

GEOMETRICAL PARAMETER, Y
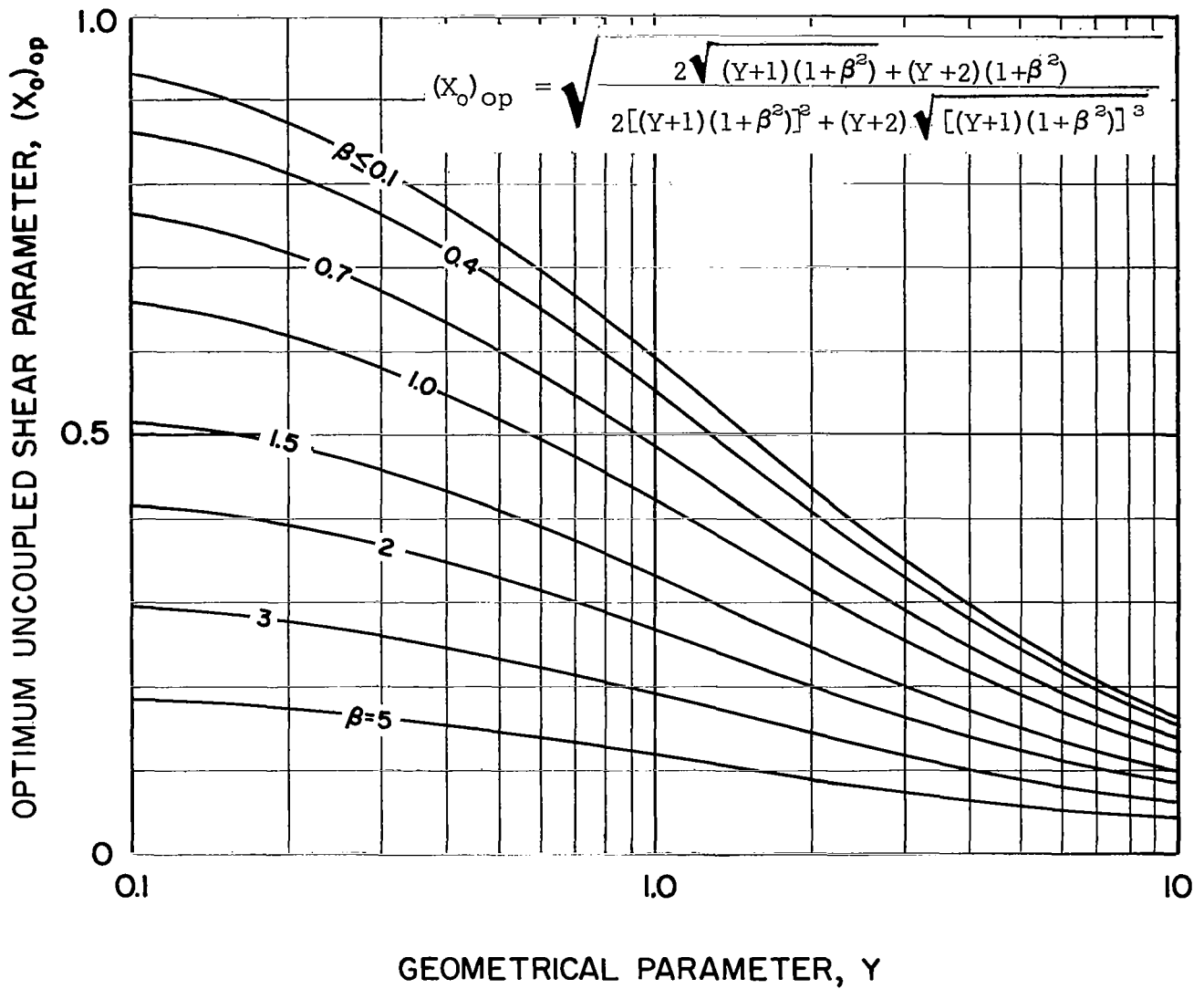
Figure 40. – Optimum uncoupled shear parameter of two- and three-
elastic-element structural composites

137
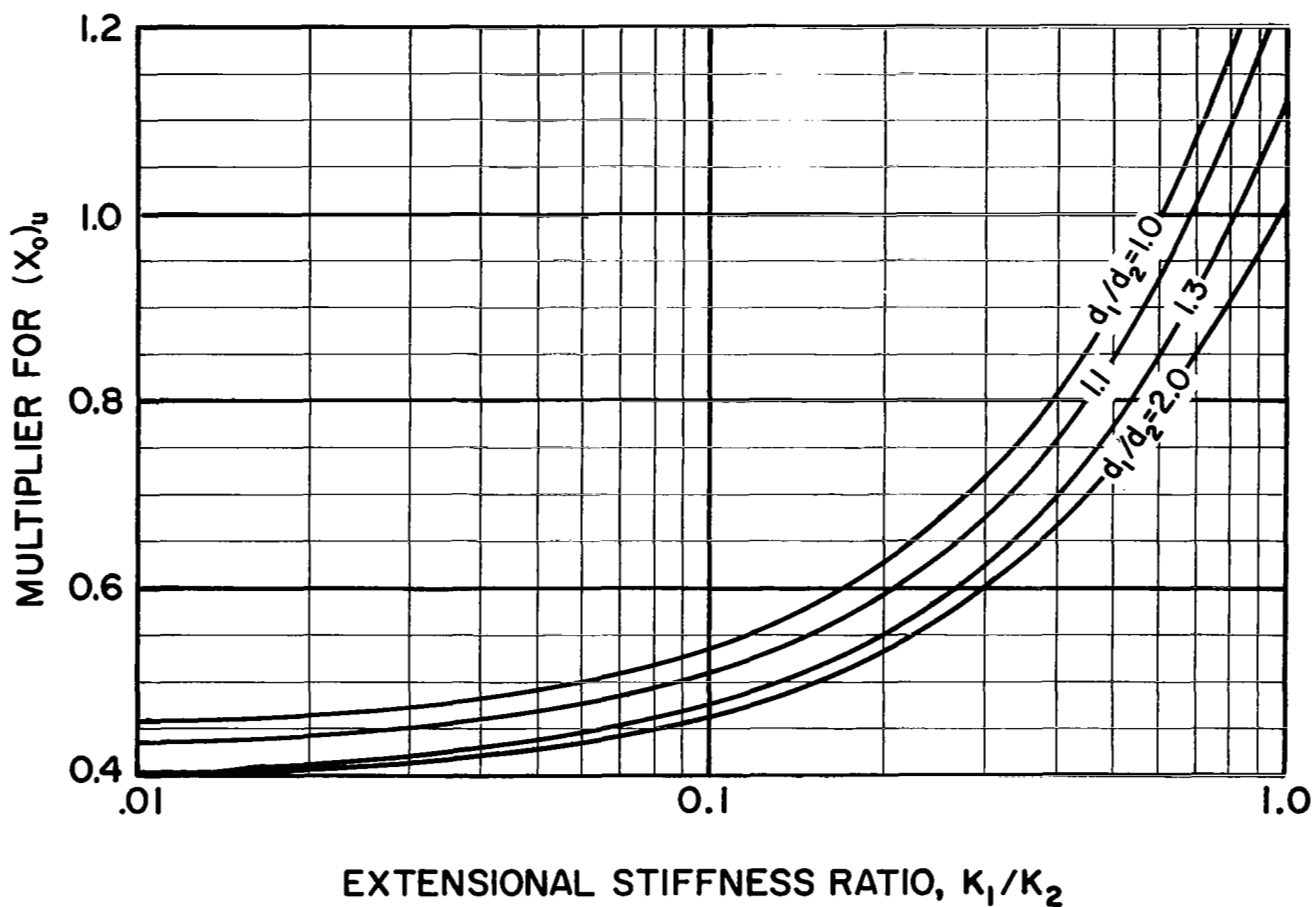
Figure 41. - Correction to the uncoupled shear parameter of unsymmetrical three-elastic-element composite structures to obtain approximate structure loss factors and frequency ratios from Figures 9 through 37
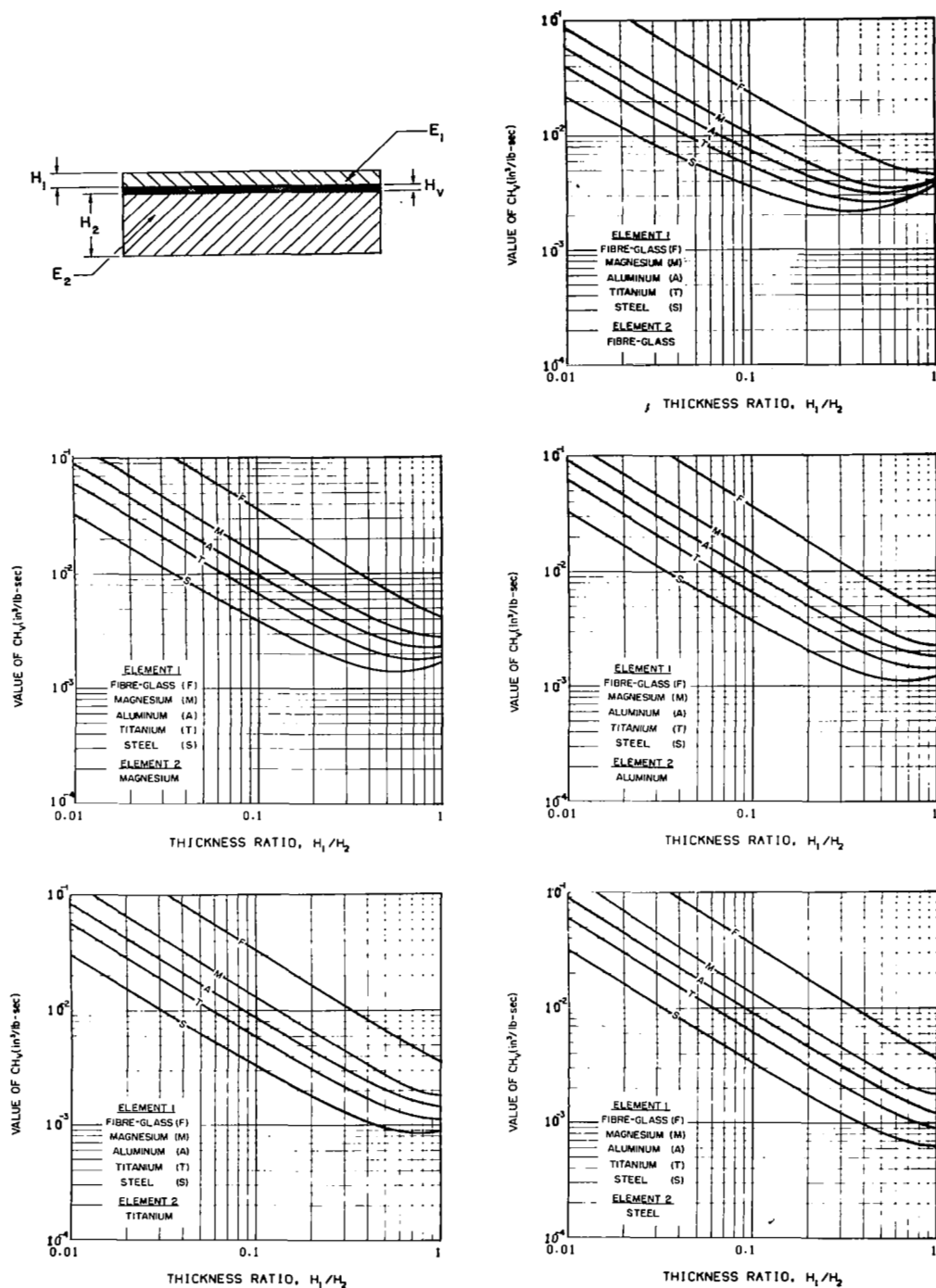
Figure 42. – Value of the shear parameter coefficient C times the viscoelastic layer thickness H_V for various two-elastic-laminate plates
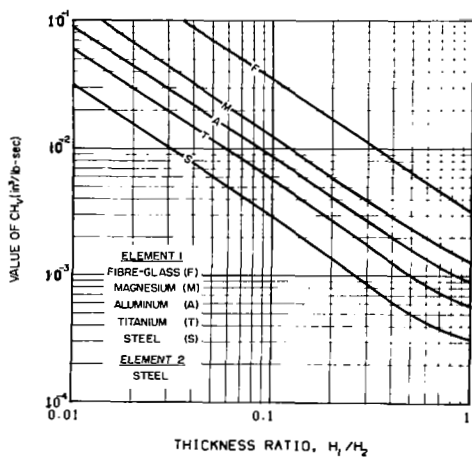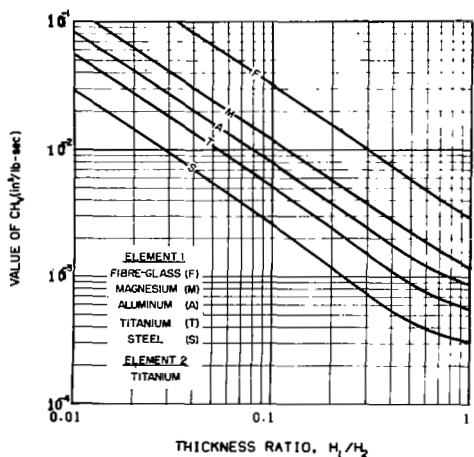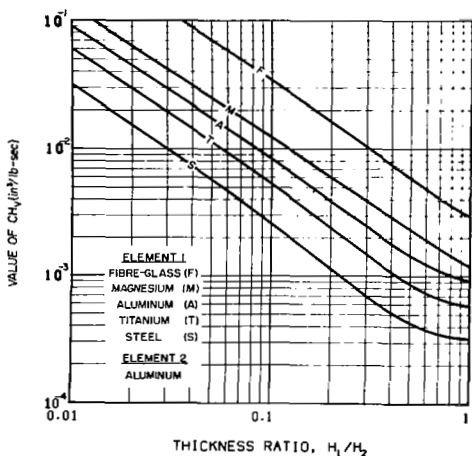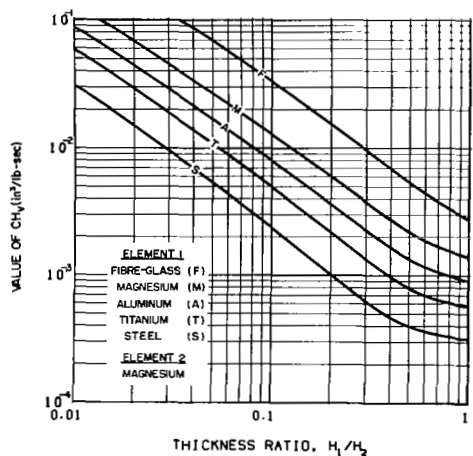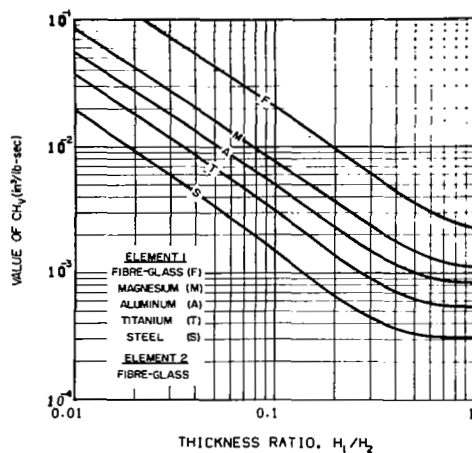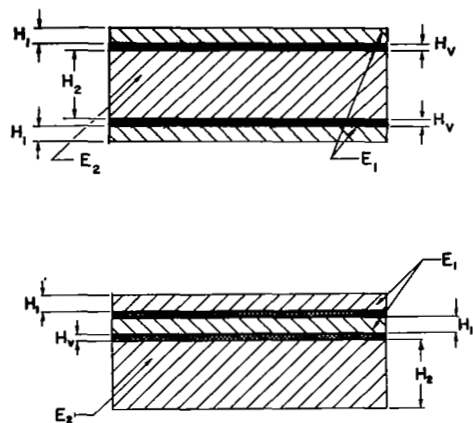
Figure 43. – Value of the shear parameter coefficient C times the viscoelastic layer thickness H_V for various three-elastic-laminate plates
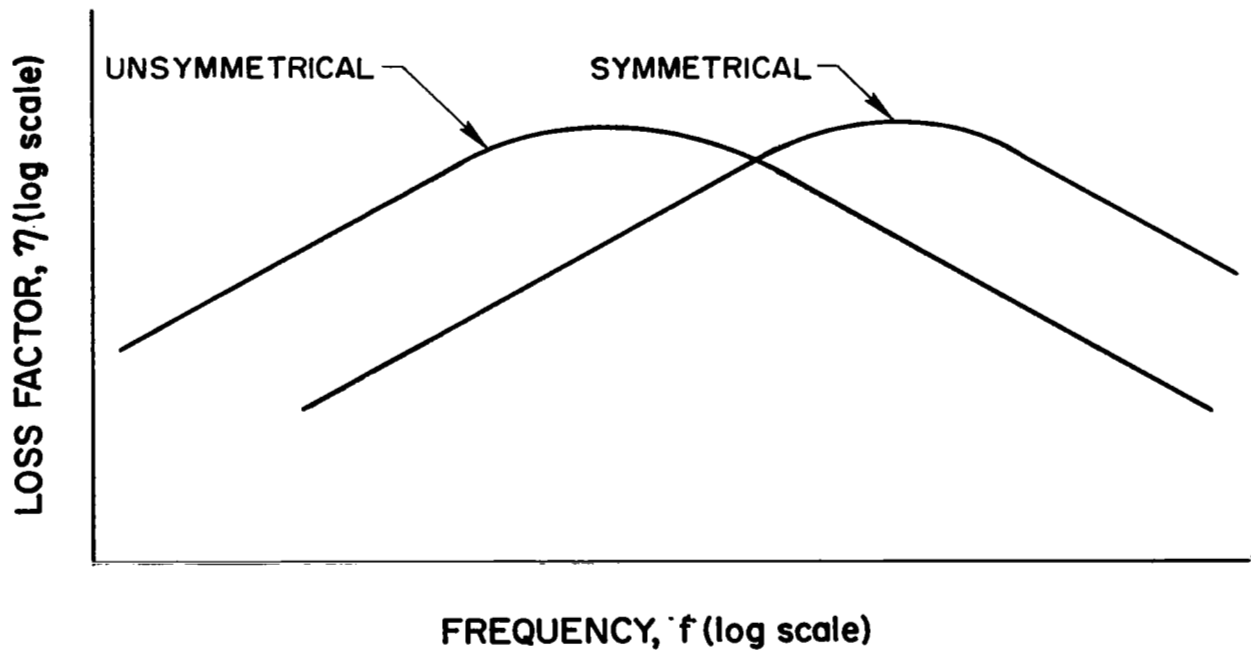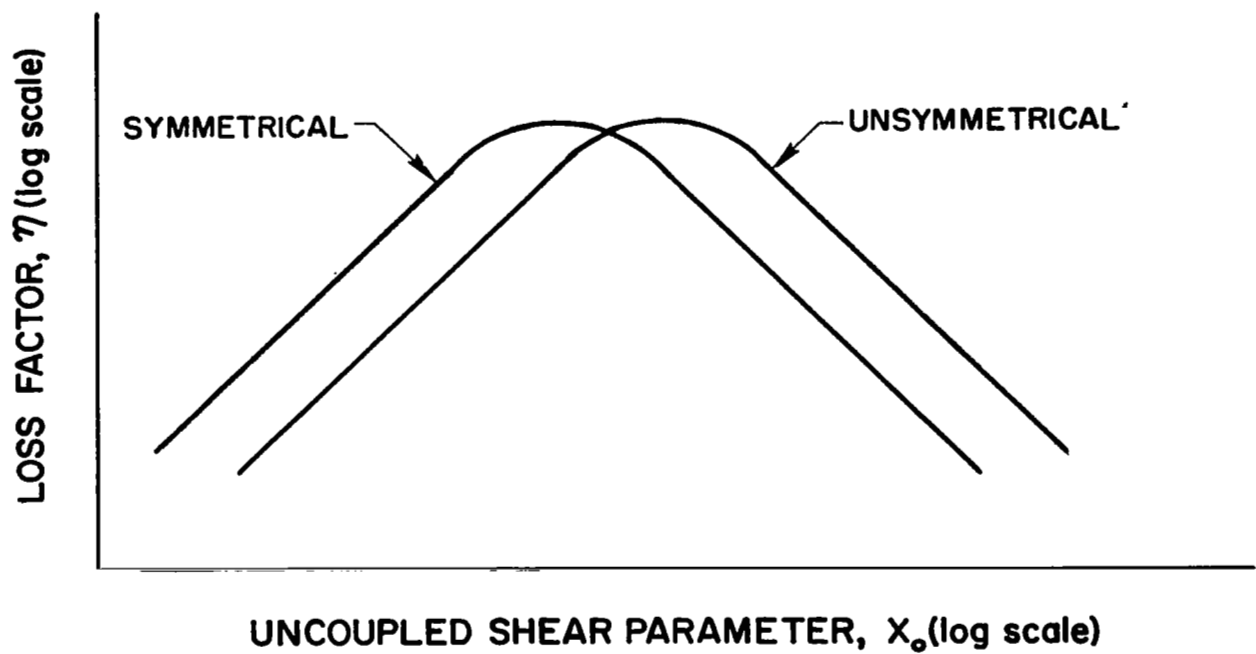
Figure 44. – Comparison of the structure loss factor curves for the symmetrical and unsymmetrical three-elastic-element structural composites

141
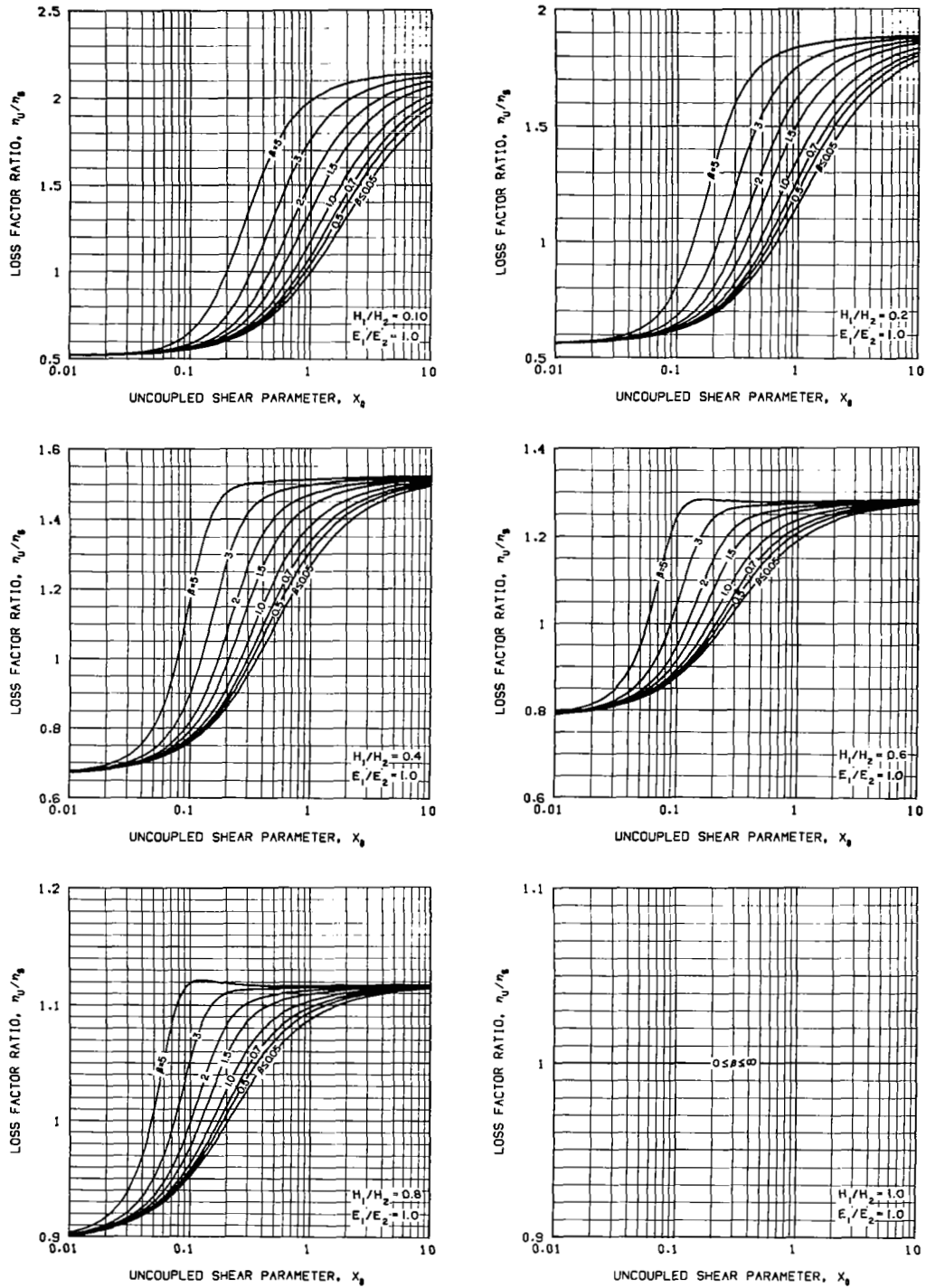
Figure 45. – Ratio of the structure loss factors of unsymmetrical and symmetrical three-elastic-laminate plates with the elastic modulus ratio $E_1/E_2 = 1.0$ and the viscoelastic damping layer thickness $H_v = 0$
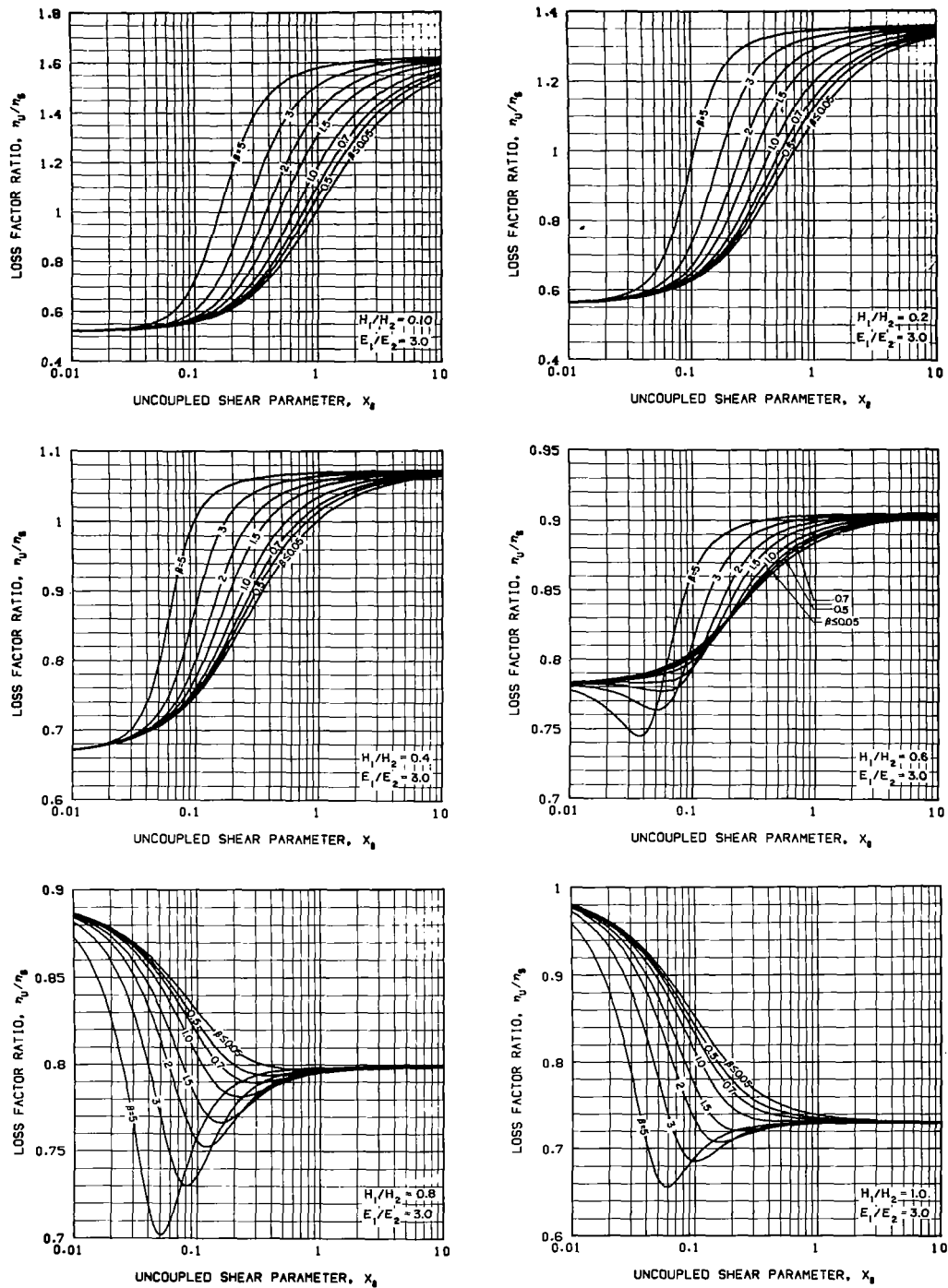
Figure 46. – Ratio of the structure loss factors of unsymmetrical and symmetrical three-elastic-laminate plates with the elastic modulus ratio $E_1/E_2 = 3$ and the viscoelastic damping layer thickness $H_v = 0$

143
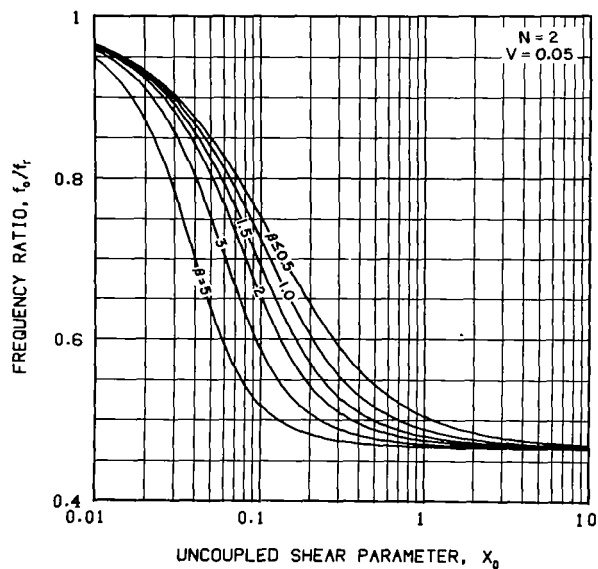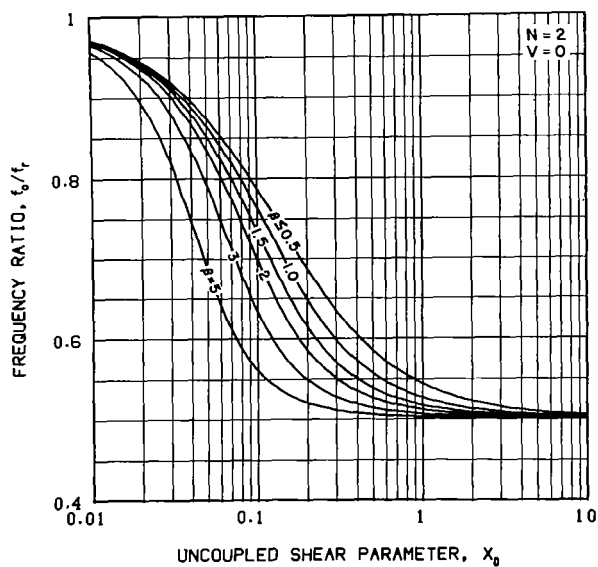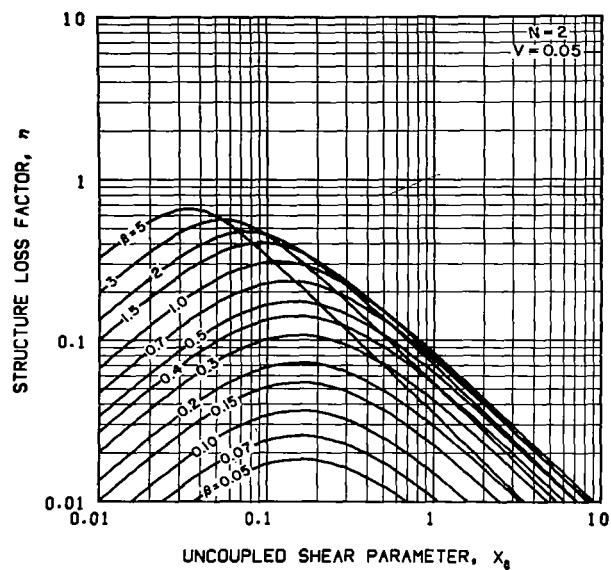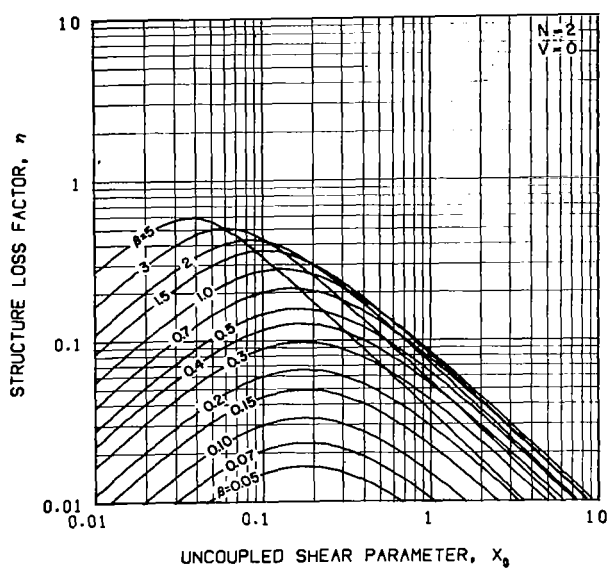
Figure 47. – Structure loss factor and frequency ratio of N identical-elastic-laminate structures with N = 2 and viscoelastic thickness parameter V = 0 and 0.05

144
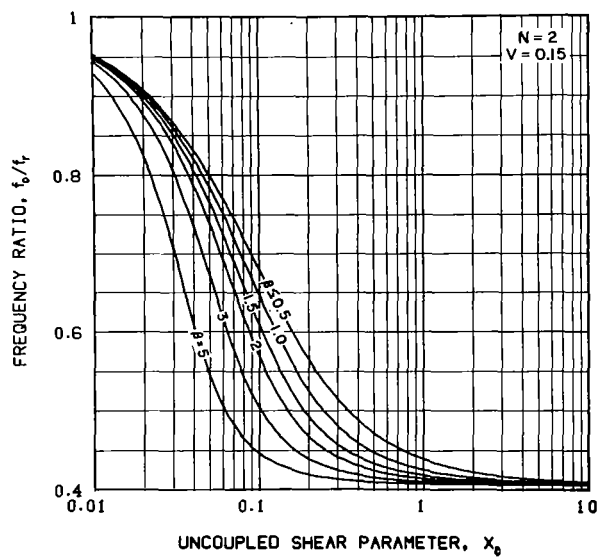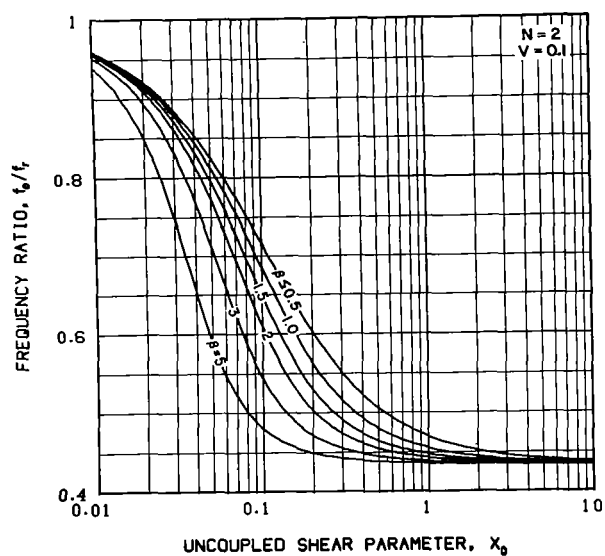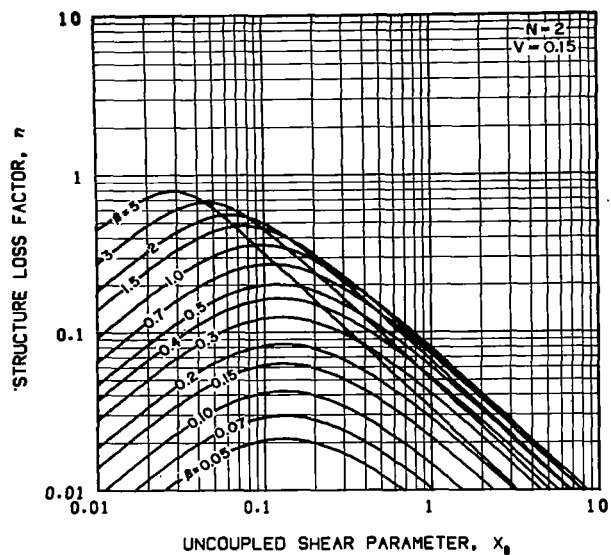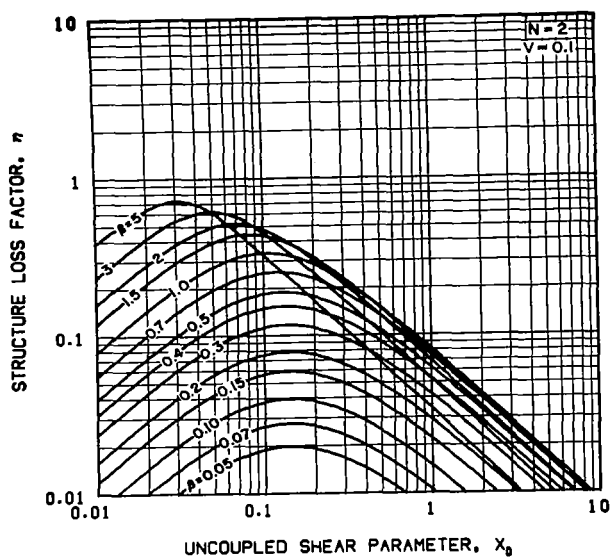
Figure 48. – Structure loss factor and frequency ratio of N identical-elastic-laminate structures with N = 2 and viscoelastic thickness parameter V = 0.1 and 0.15

145
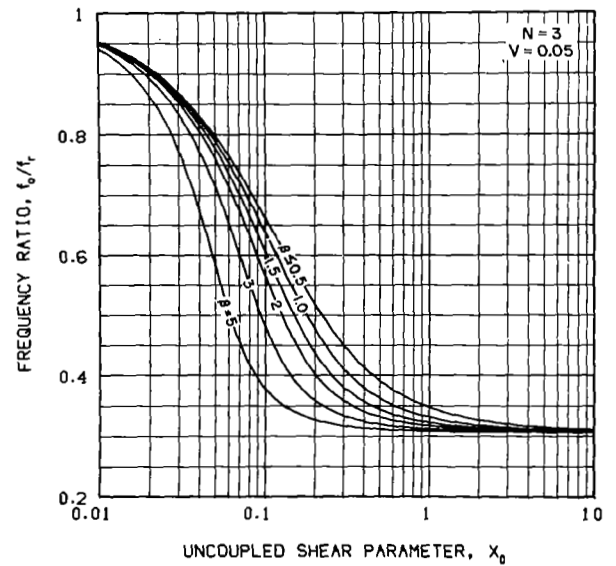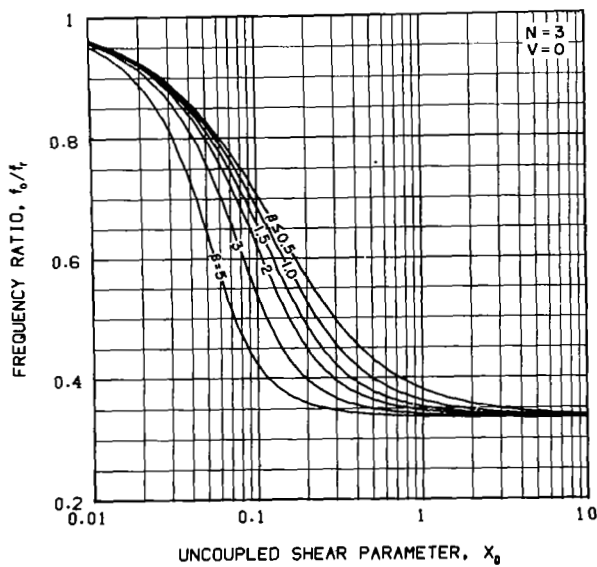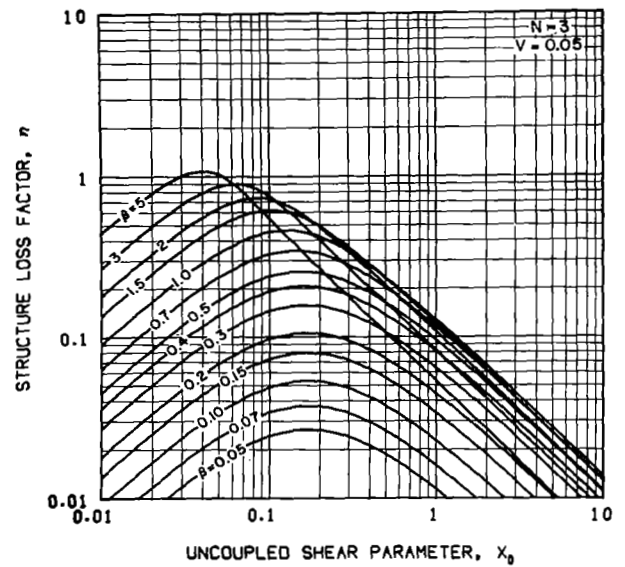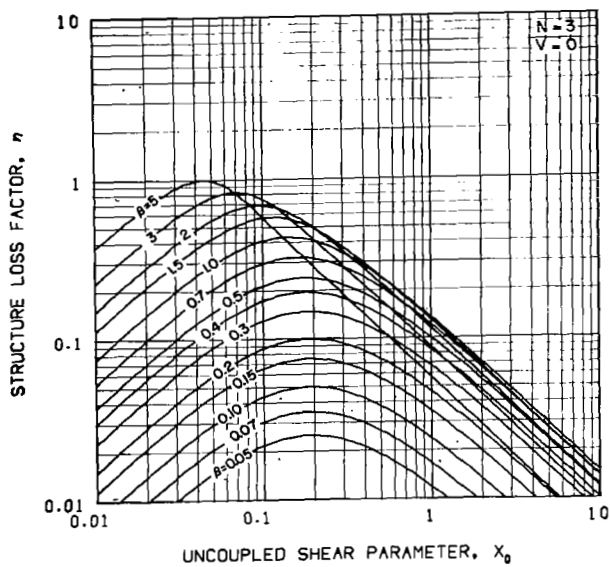
Figure 49. - Structure loss factor and frequency ratio of N identical-elastic-laminate structures with N = 3 and viscoelastic thickness parameter V = 0 and 0.05

146
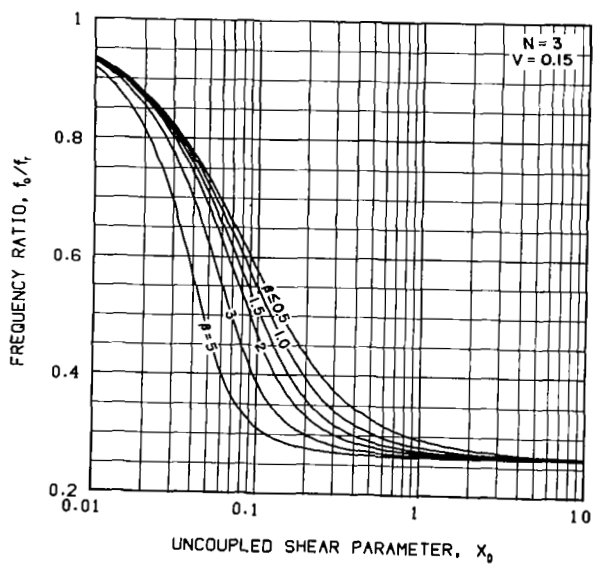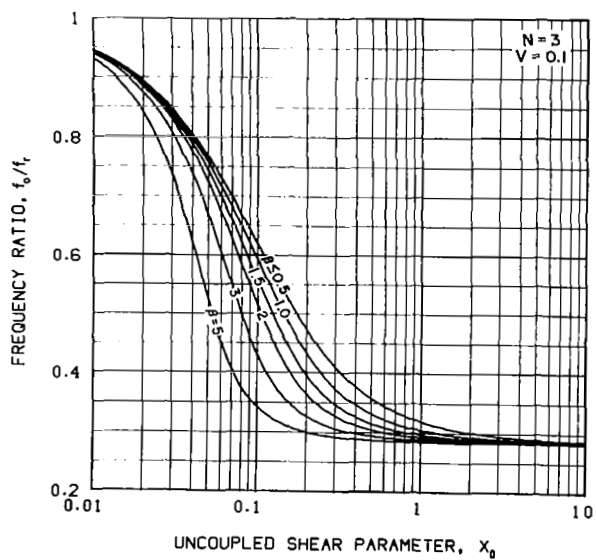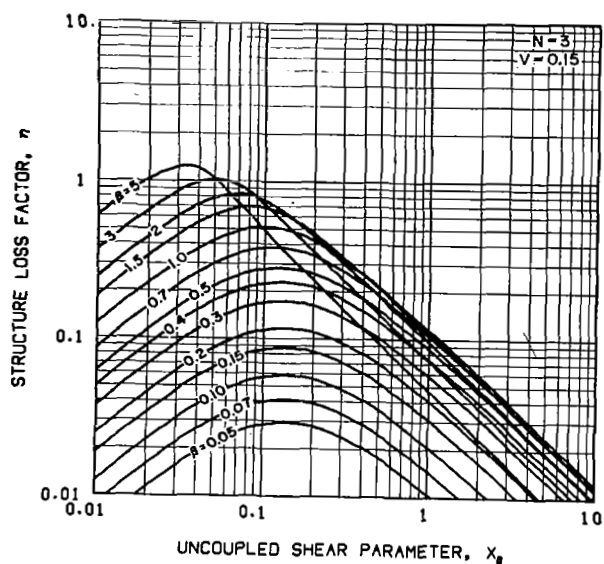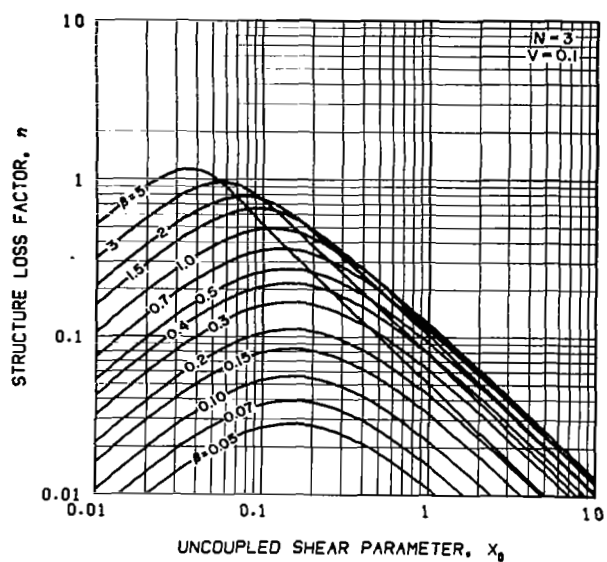
Figure 50. – Structure loss factor and frequency ratio of N identical-elastic-laminate structures with N = 3 and viscoelastic thickness parameter V = 0.1 and 0.15

147
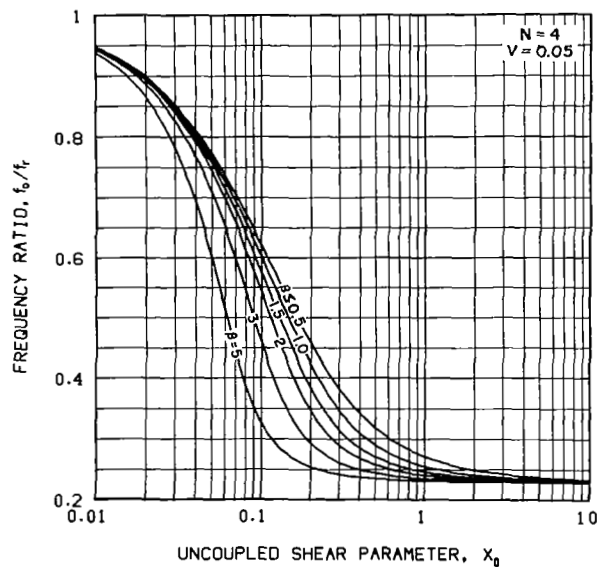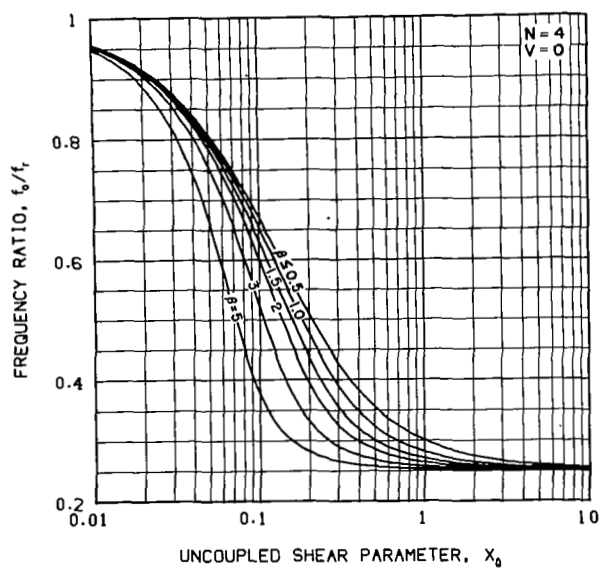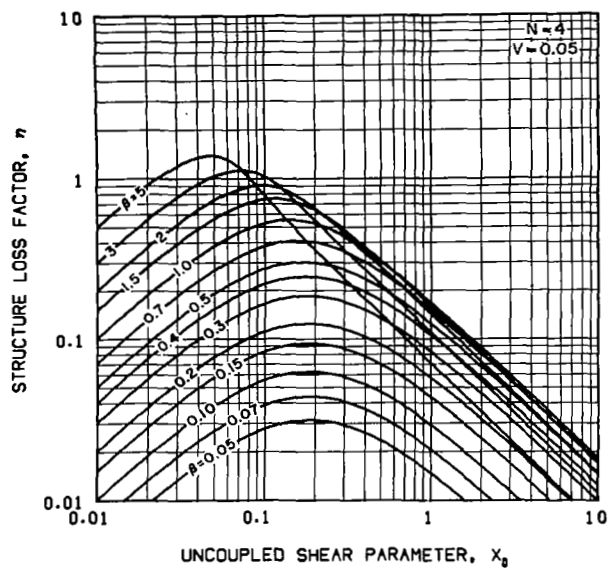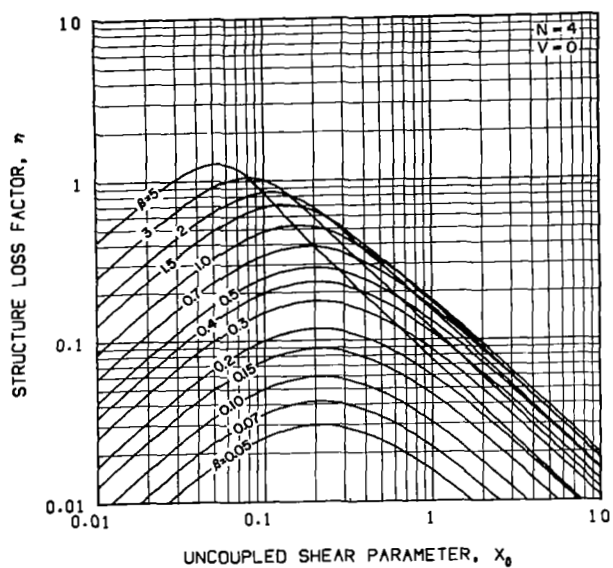
Figure 51. – Structure loss factor and frequency ratio of N identical-elastic-laminate structures with N = 4 and viscoelastic thickness parameter V = 0 and 0.05
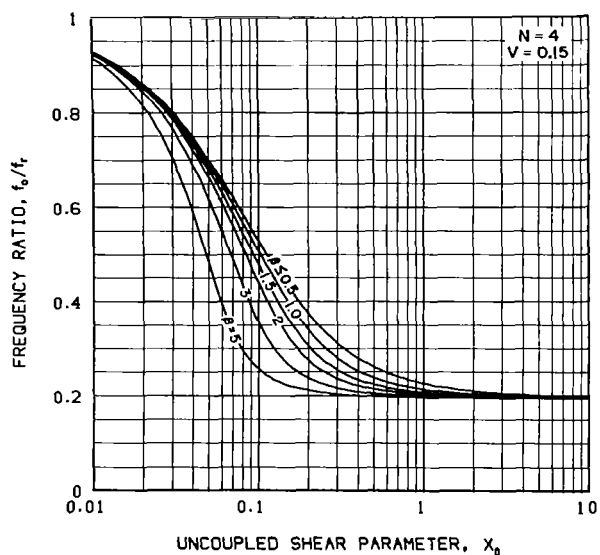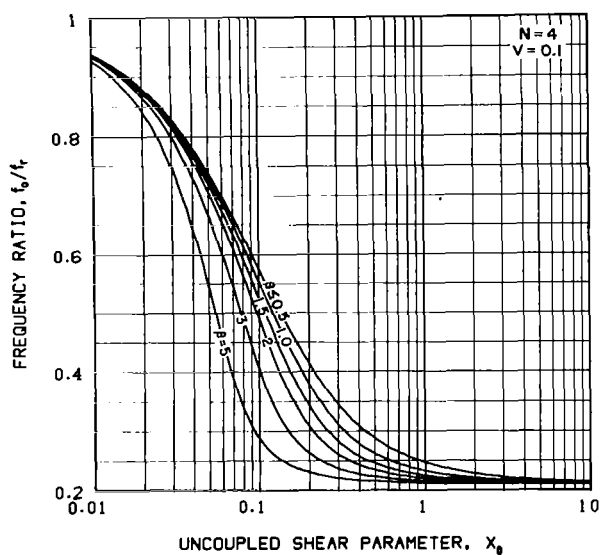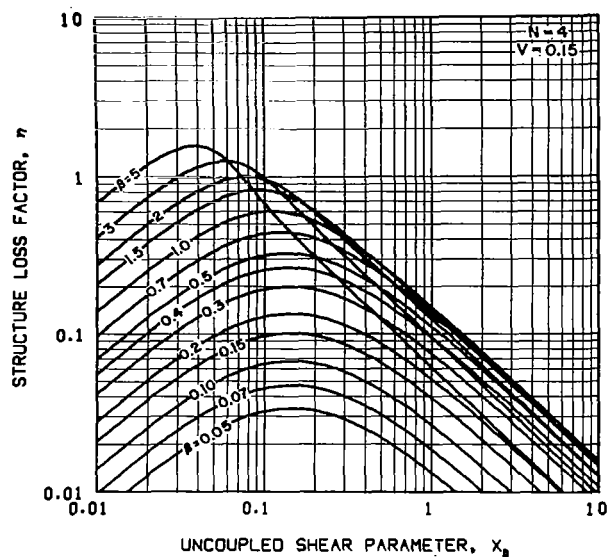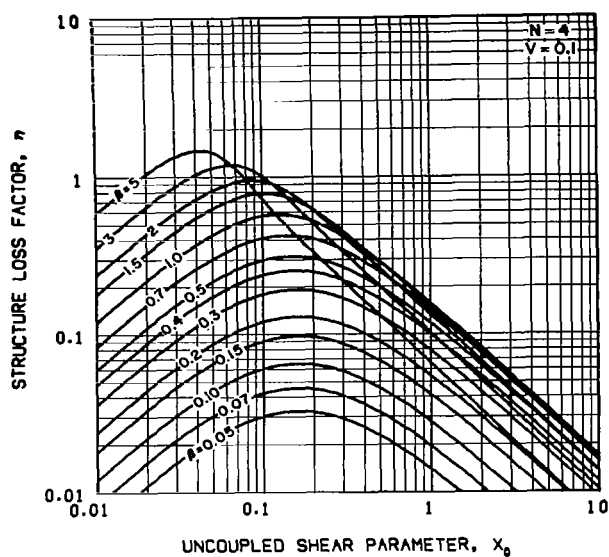
Figure 52. – Structure loss factor and frequency ratio of N identical-elastic-laminate structures with N = 4 and viscoelastic thickness parameter V = 0.1 and 0.15
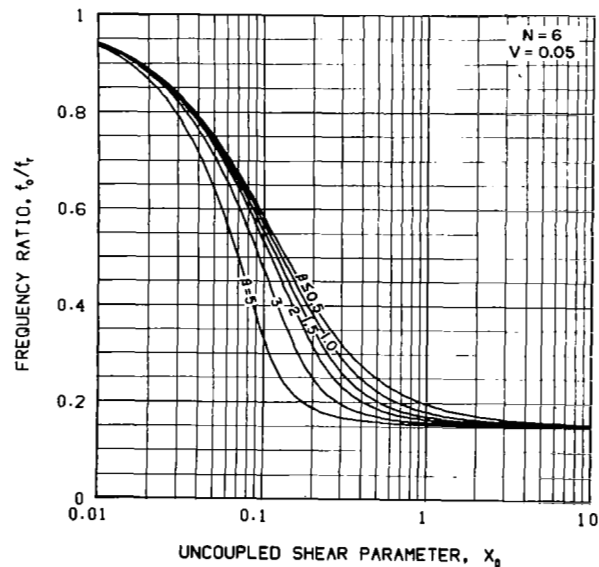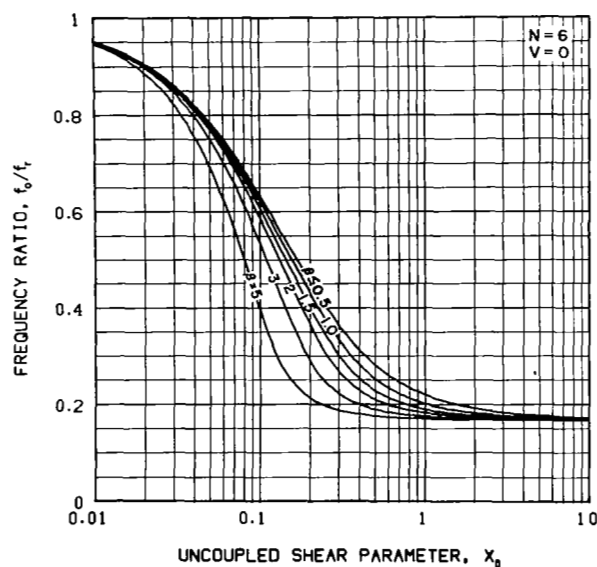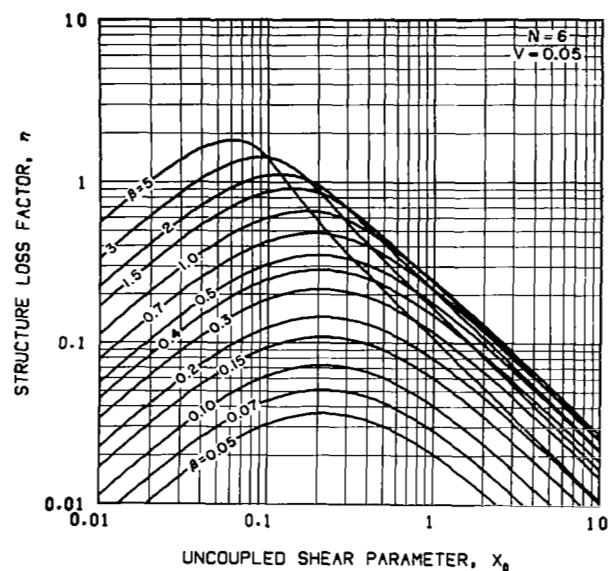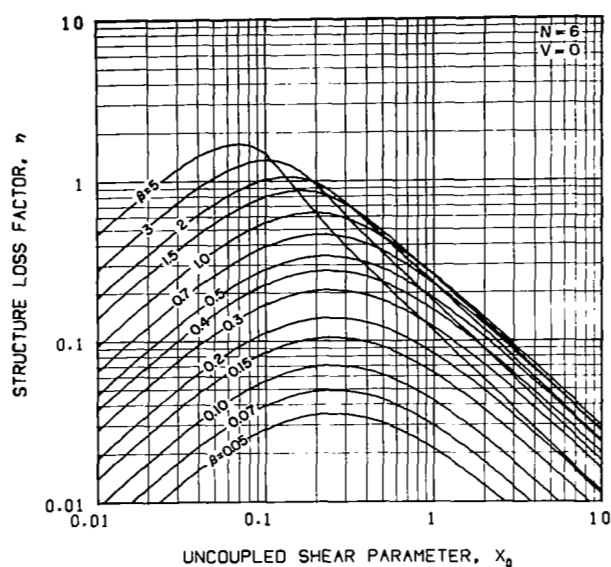
Figure 53. – Structure loss factor and frequency ratio of N identical-elastic-laminate structures with N = 6 and viscoelastic thickness parameter V = 0 and 0.05

150
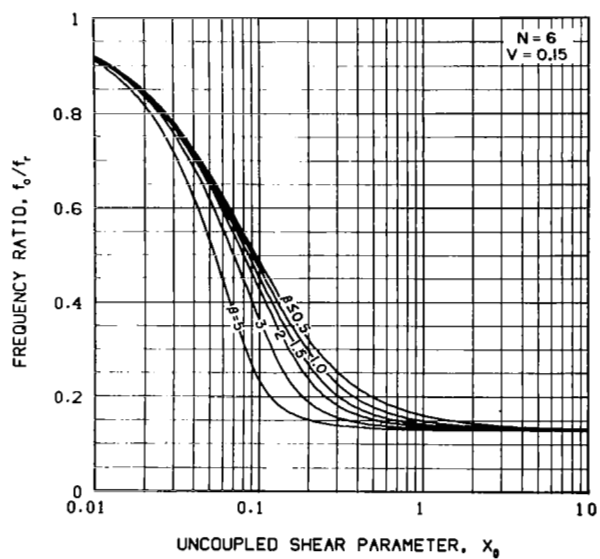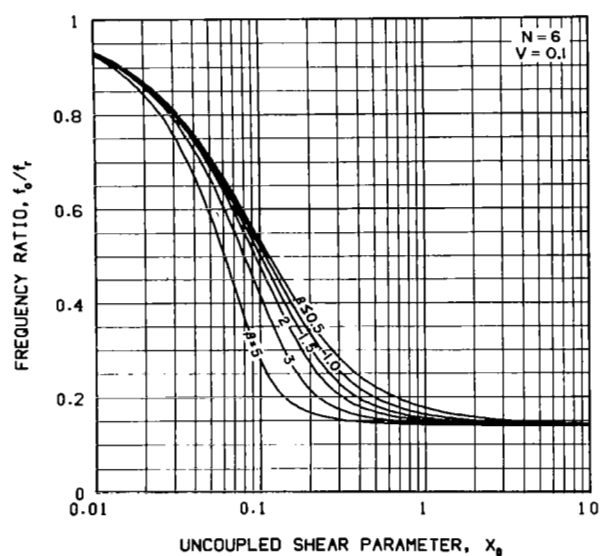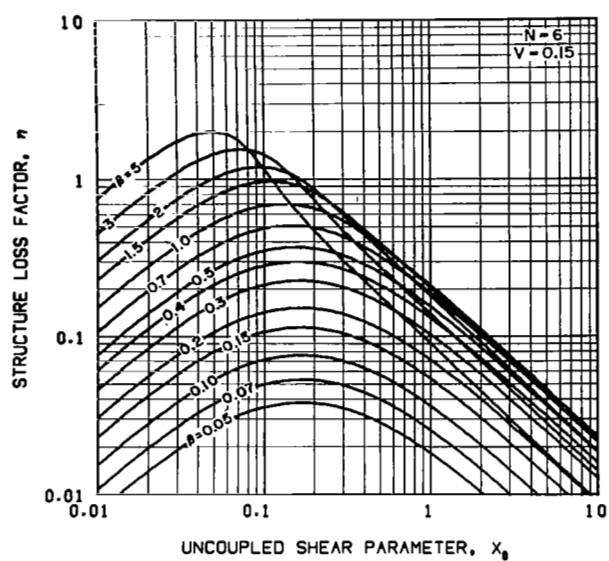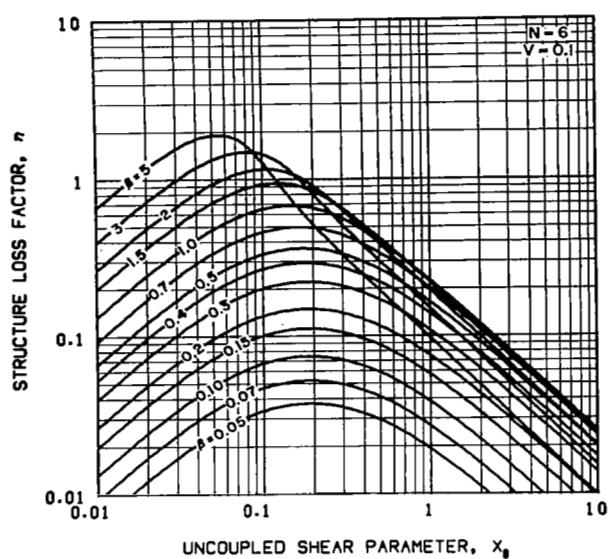
Figure 54. – Structure loss factor and frequency ratio of N identical-elastic-laminate structures with N = 6 and viscoelastic thickness parameter V = 0.1 and 0.15

151
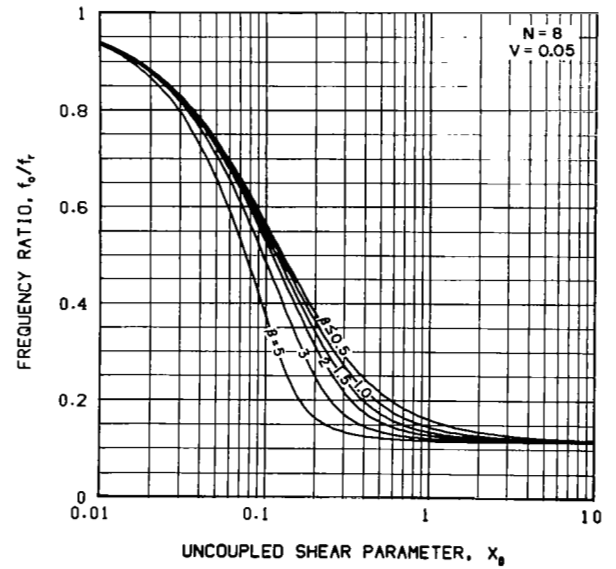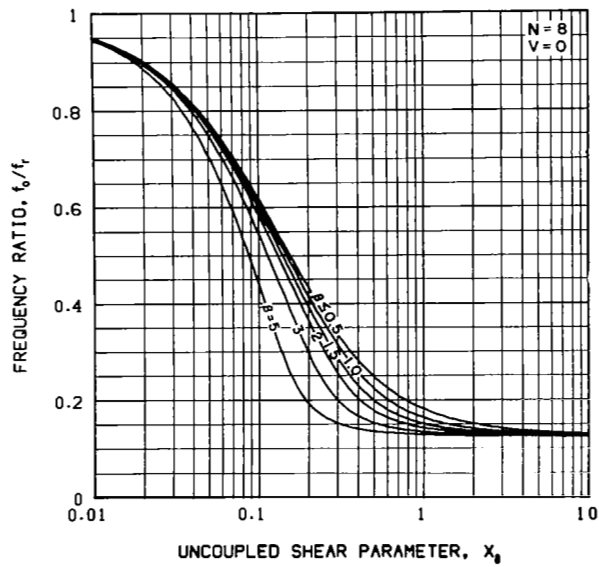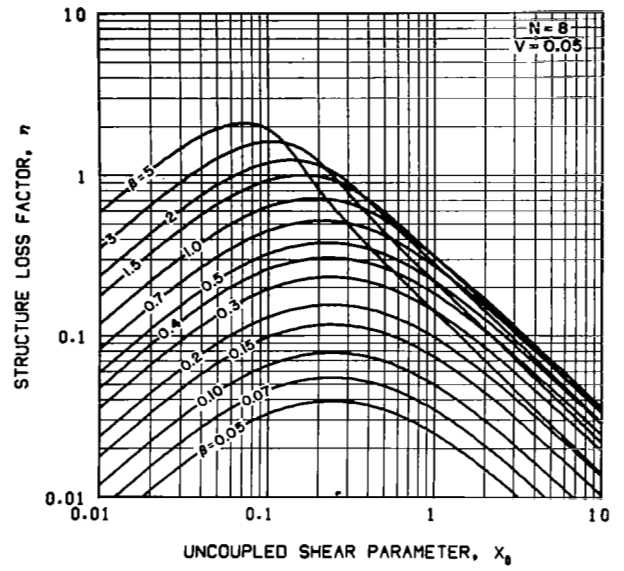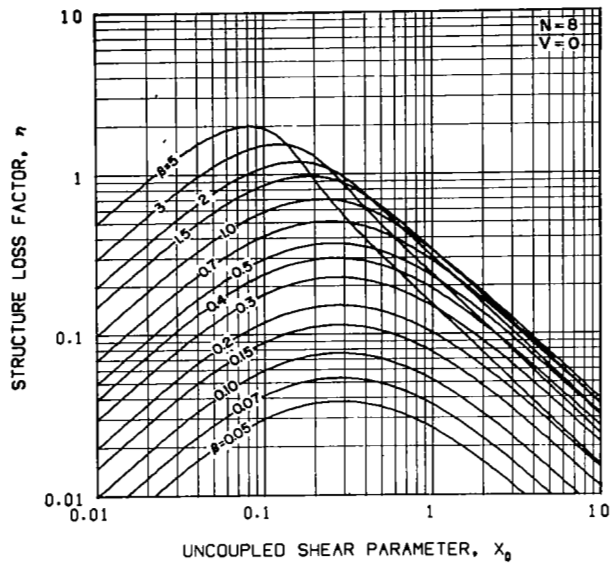
Figure 55. — Structure loss factor and frequency ratio of N identical-elastic-laminate structures with N = 8 and viscoelastic thickness parameter V = 0 and 0.05
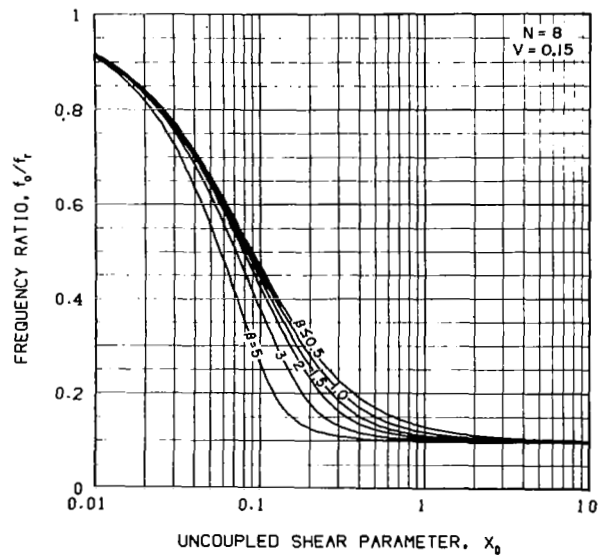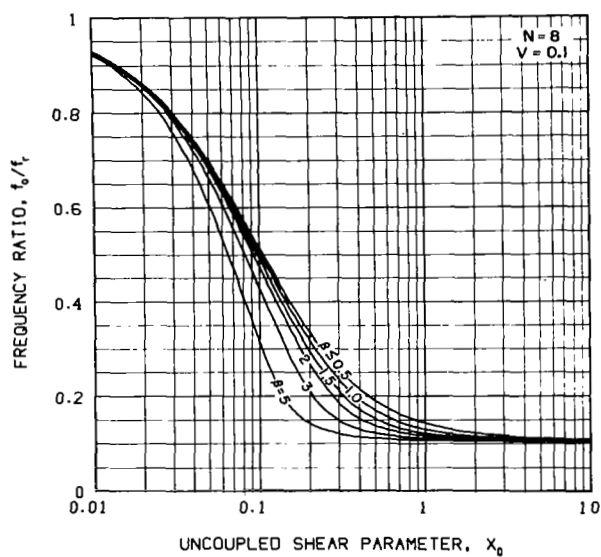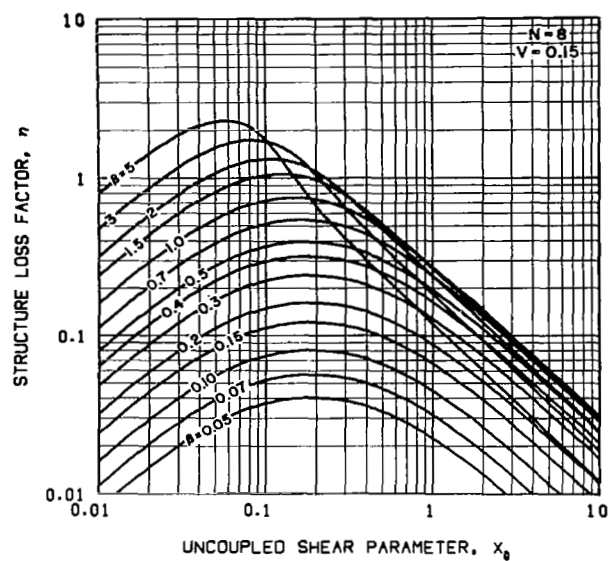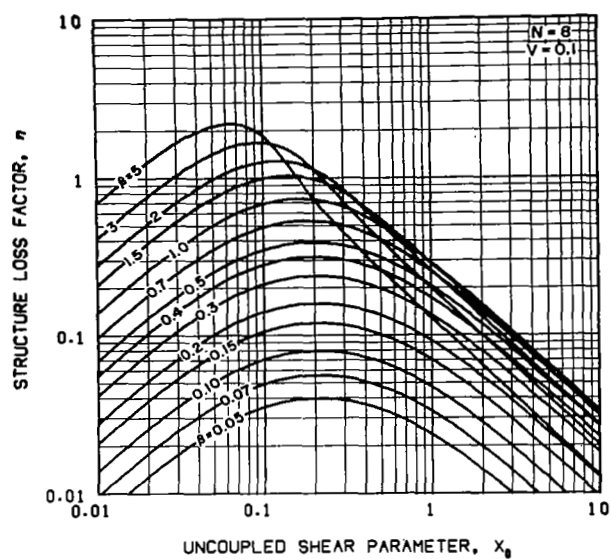
Figure 56. – Structure loss factor and frequency ratio of N identical-elastic-laminate structures with N = 8 and viscoelastic thickness parameter V = 0.1 and 0.15

153
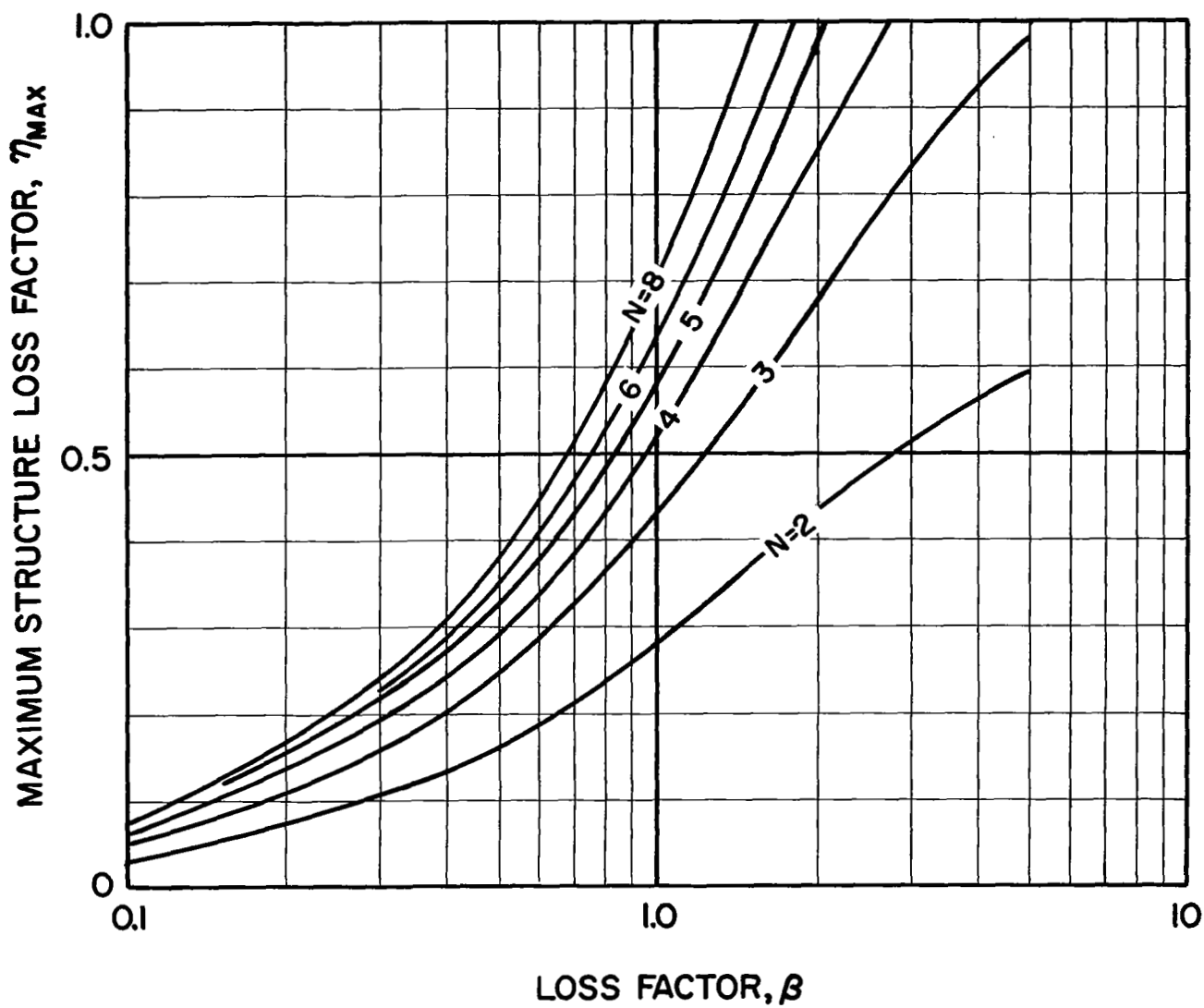
Figure 57. – Maximum structure loss factor for N identical-elastic-laminate structures with N = 2, 3, 4, 5, 6, and 8 and $H_v = 0$

154
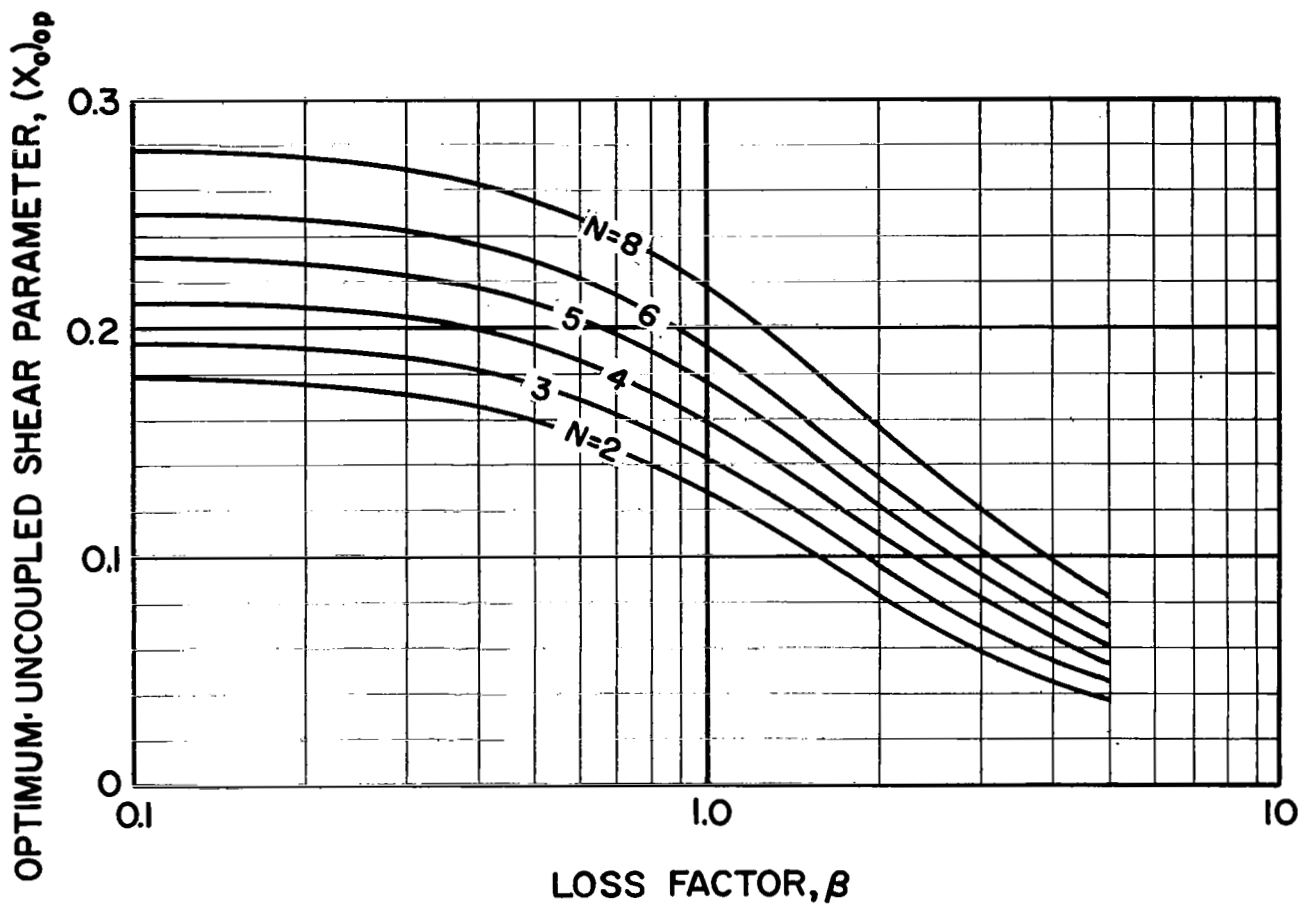
Figure 58. – Optimum uncoupled shear parameter for N identical-
elastic-laminate structures with N = 2, 3, 4, 5, 6, and 8
and $H_V = 0$
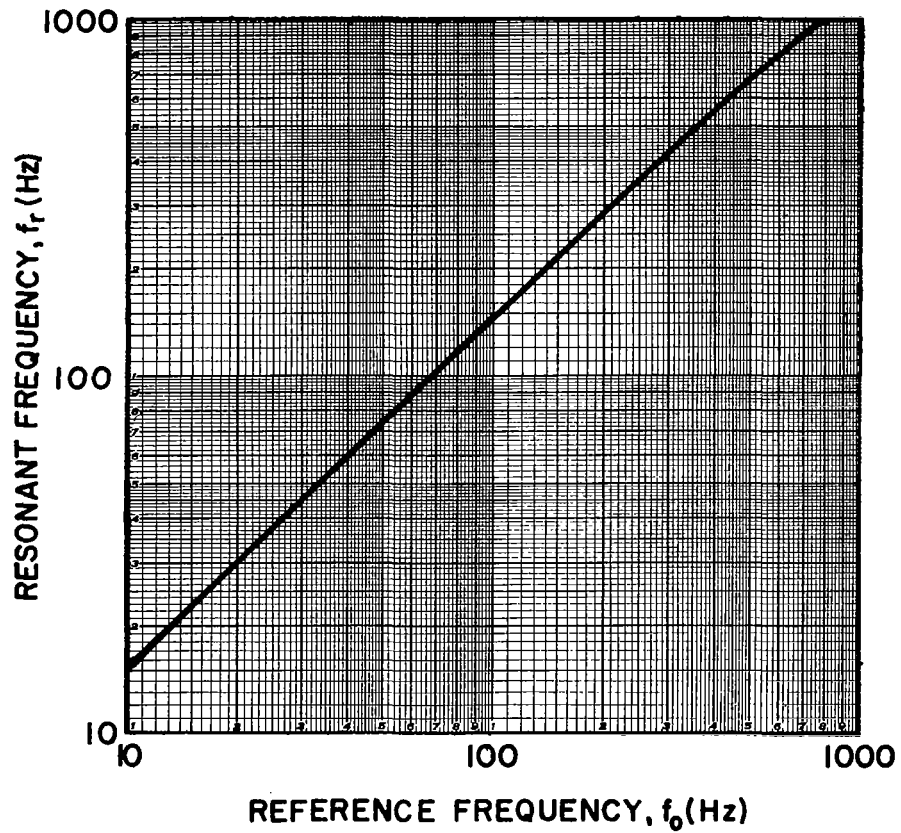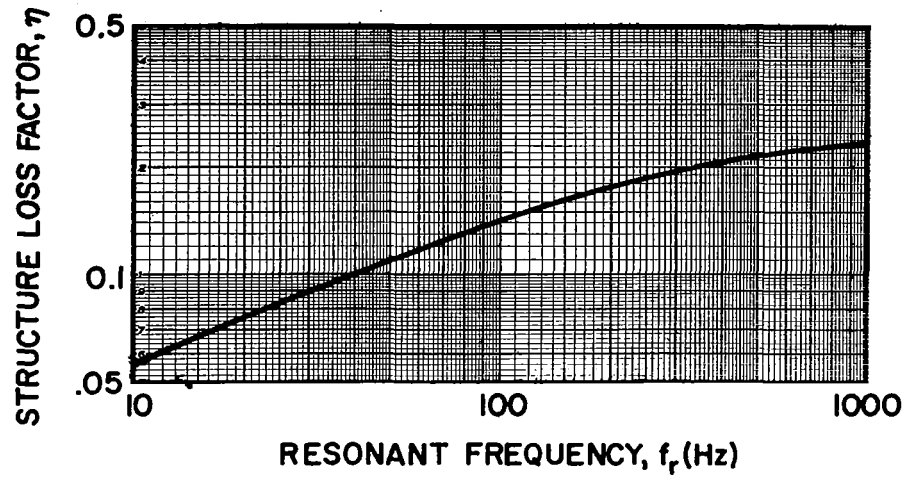
Figure 59. – Structure loss factor and resonant frequency for the beam
considered in the design example

156
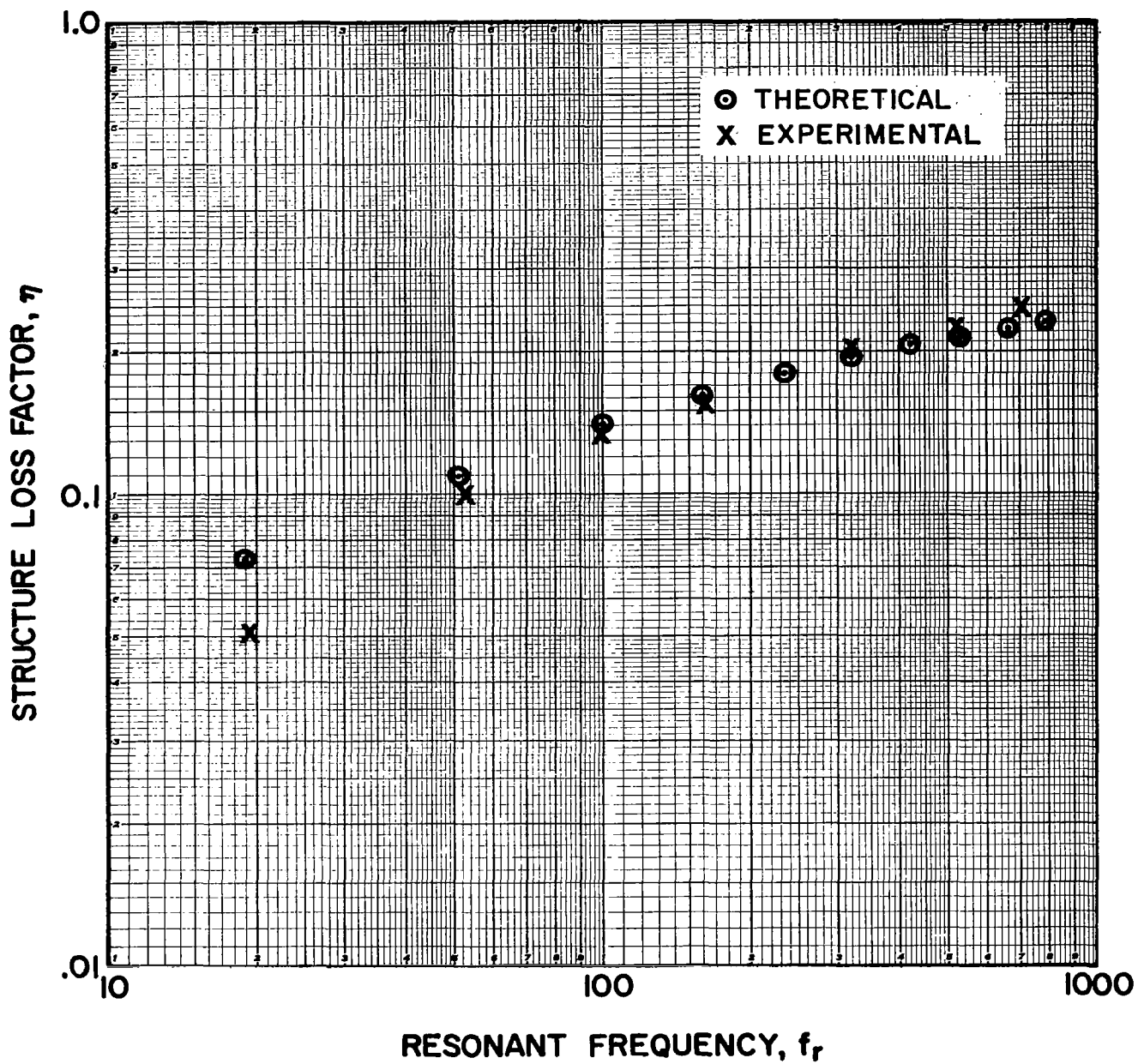
Figure 60. – Comparison of the experimental and theoretical structure loss factors and resonant frequencies for the beam considered in the design example
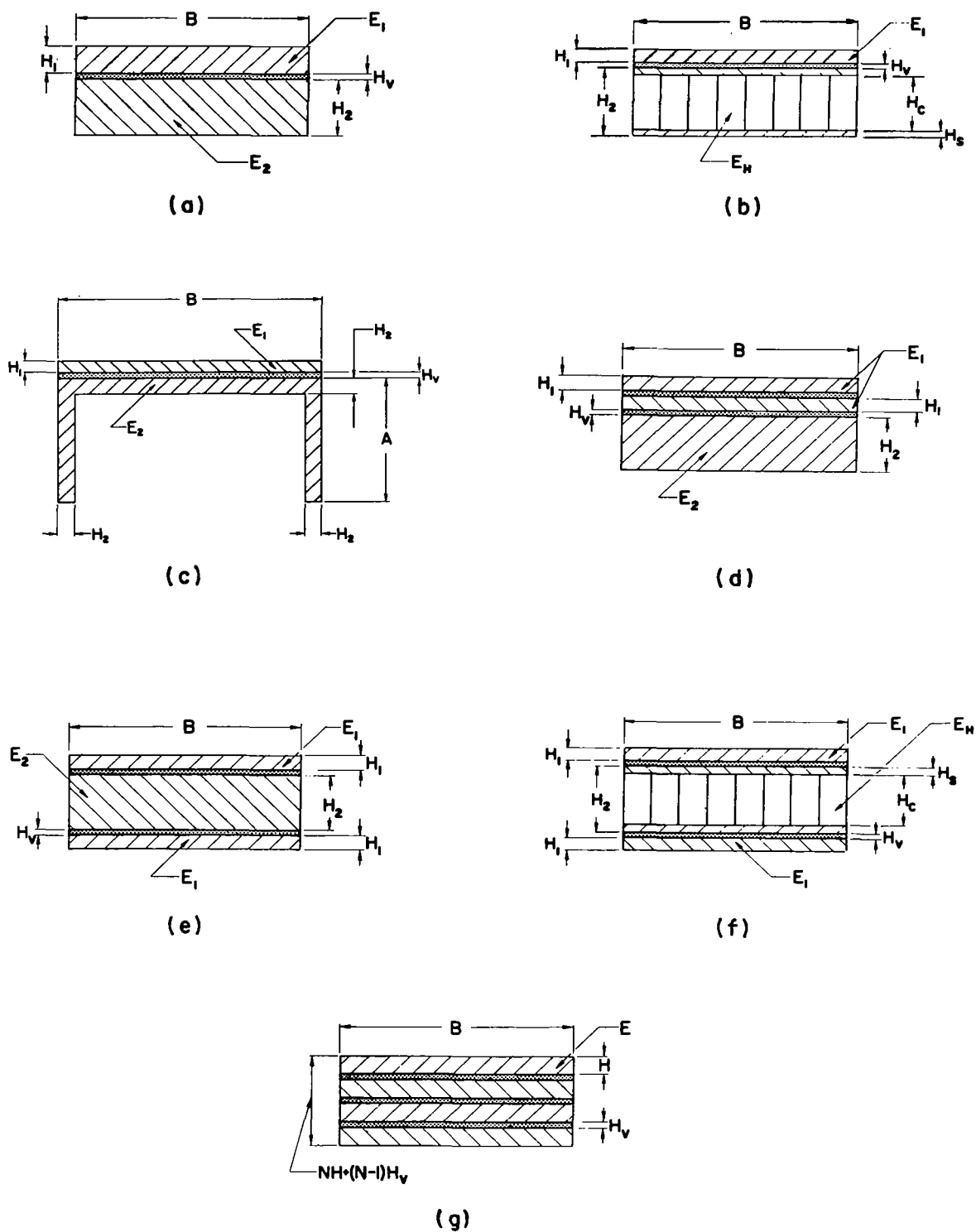
Figure 61. - Cross-sections of structural composites having viscoelastic layers parallel to the neutral axis of bending fabricated for experimental evaluation of structure loss factors and resonant frequencies.

158
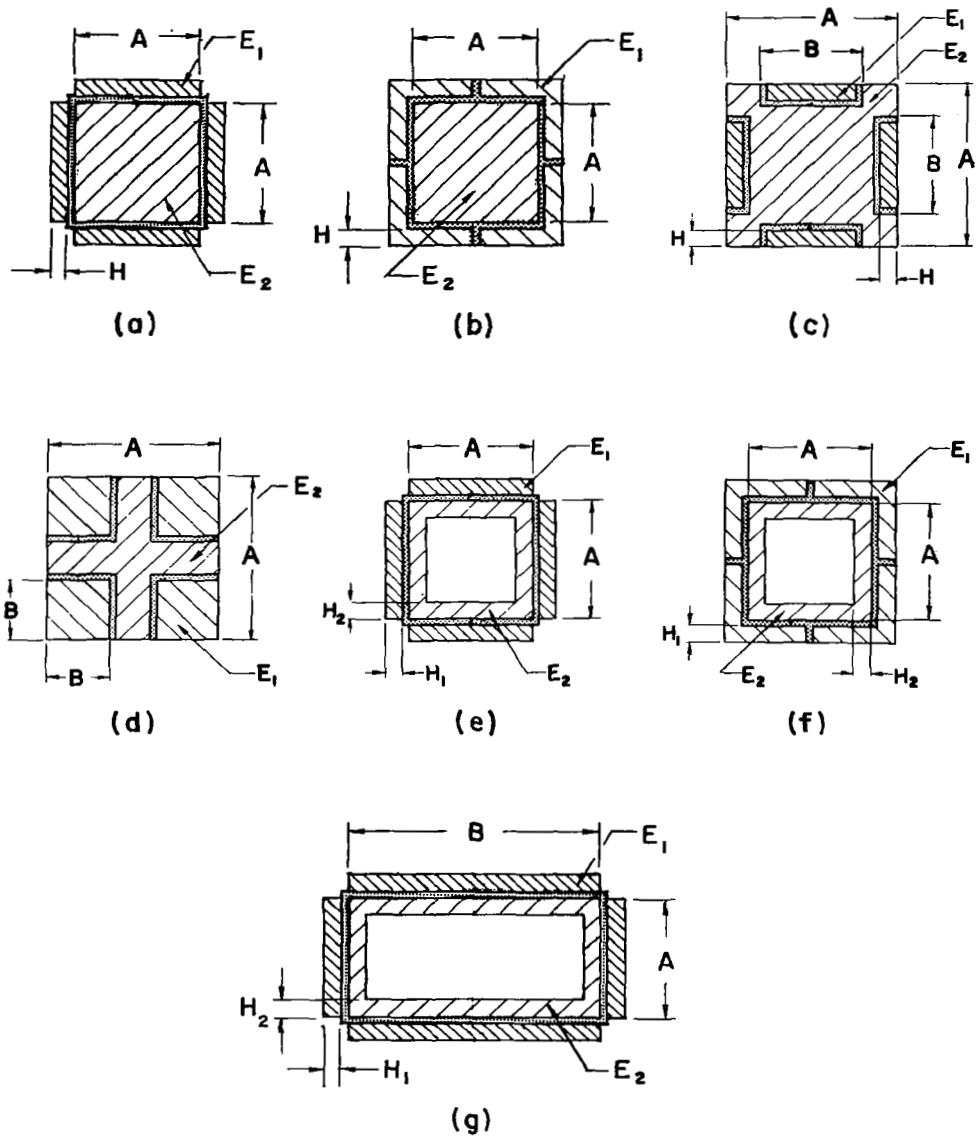
Figure 62. - Cross-sections of bar and tube designs fabricated for experimental evaluation of structure loss factors and resonant frequencies
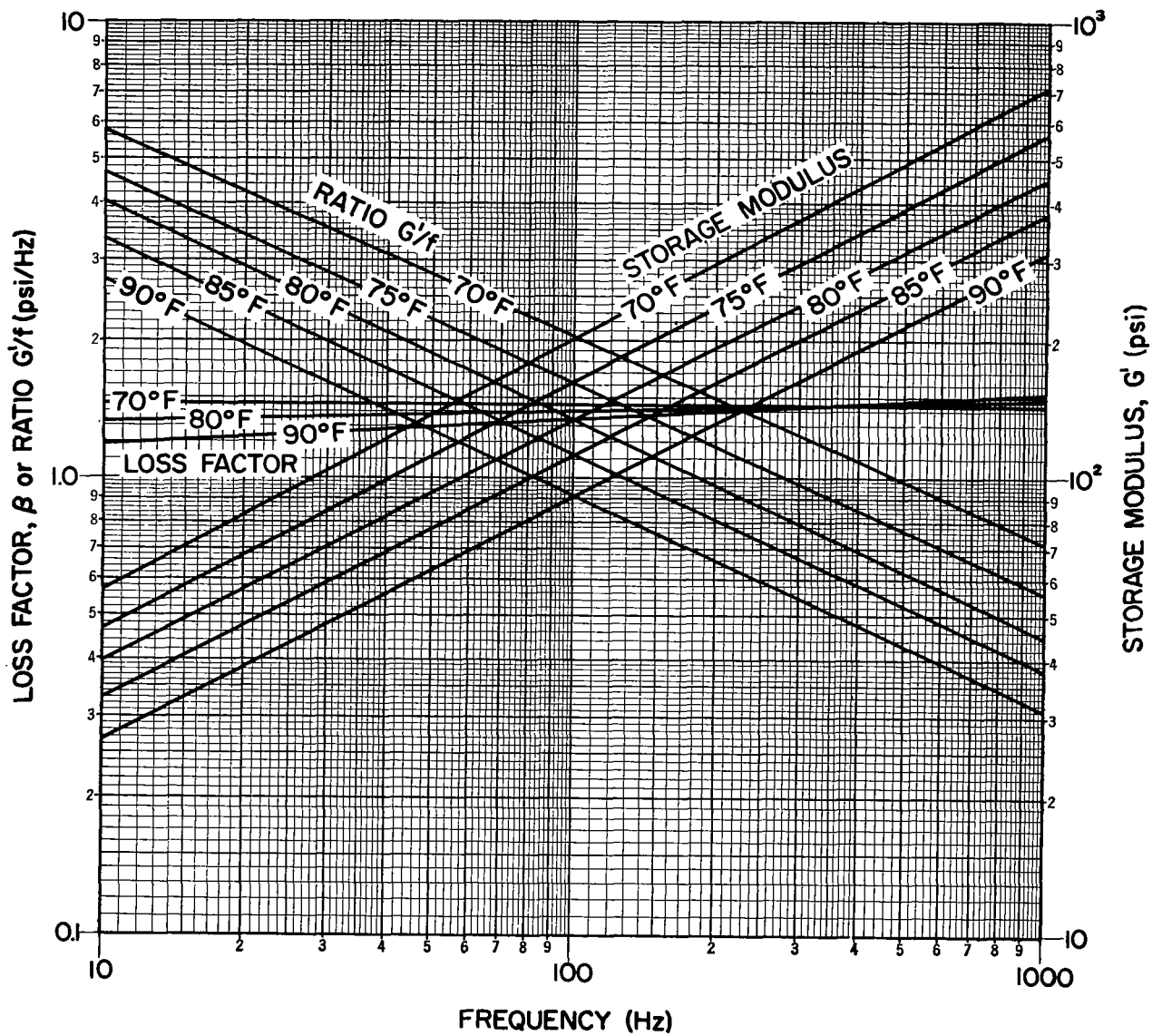
Figure 63. – Dynamic elastic characteristics of the viscoelastic material (3M No. 466 adhesive transfer tape) used in the structural composite beams fabricated for experimental evaluation

160
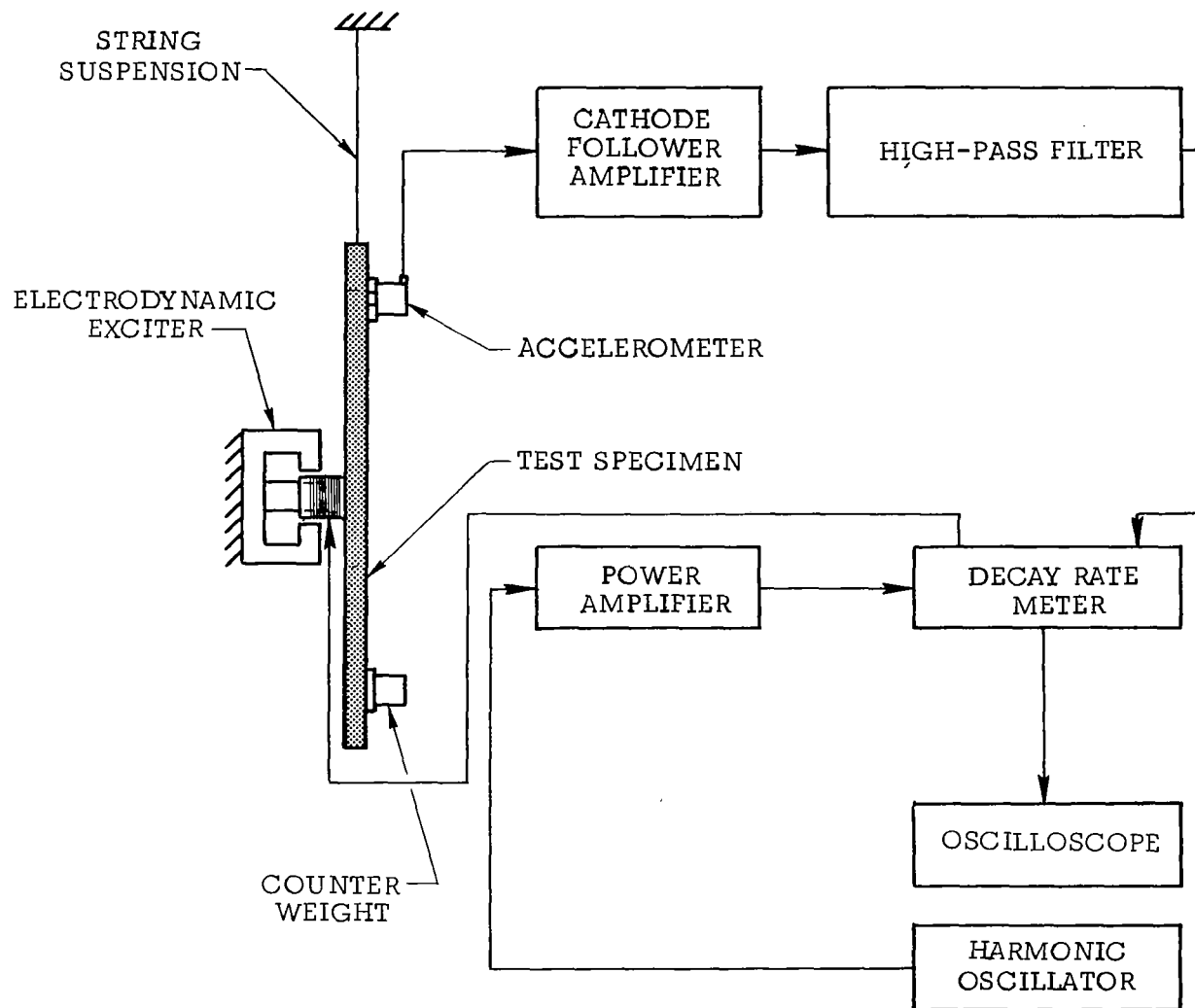
Figure 64. – Experimental system for measuring the loss factors and resonant frequencies of composite structural beam specimens

161
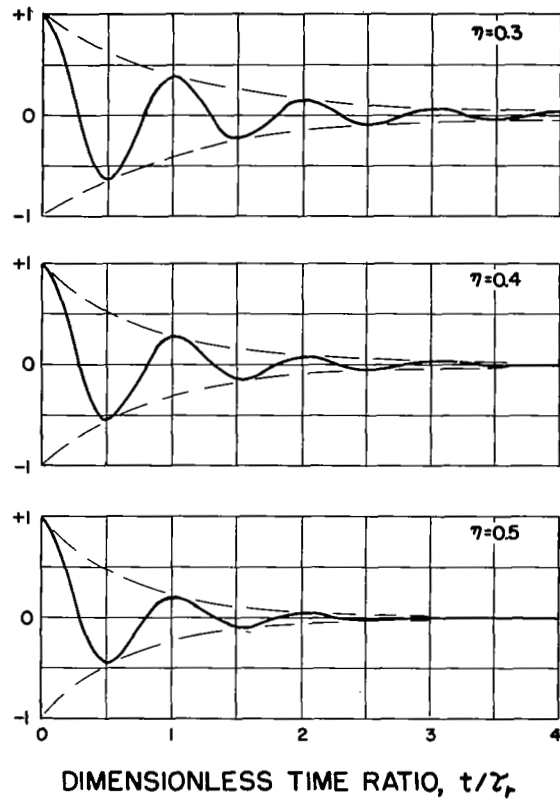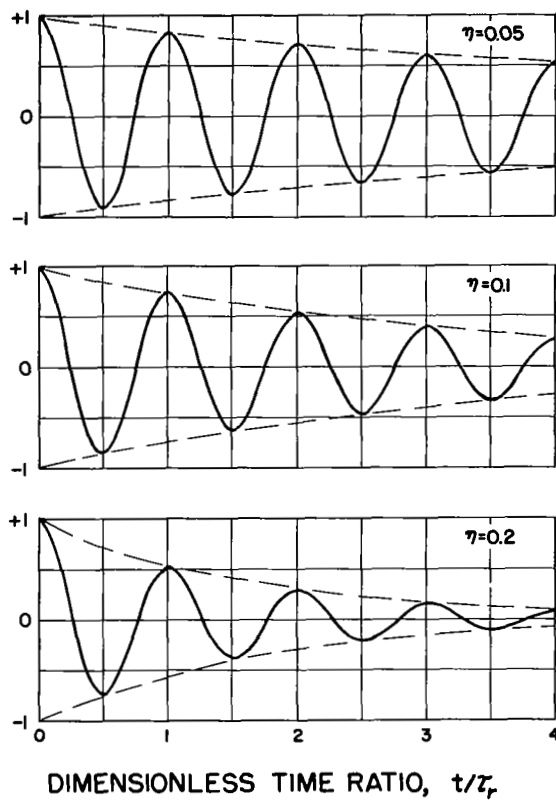
Figure 65. – Exponentially decaying sinusoidal vibration, with a natural period τ_r, for various values of loss factor η

162
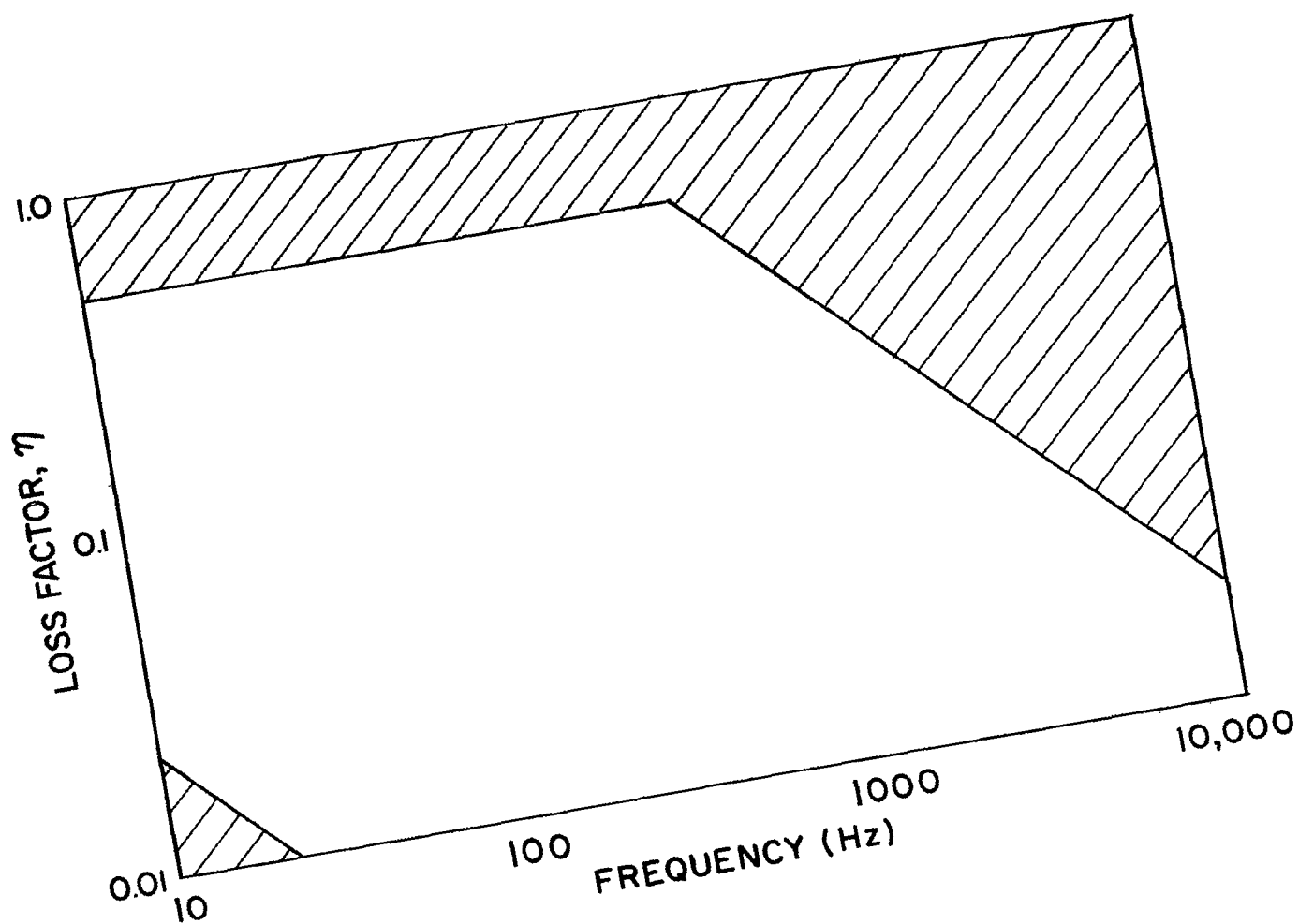
Figure 66. – Graph of loss factor versus frequency where the cross–hatched area indicates the region for which the experimental system is incapable of measuring loss factors
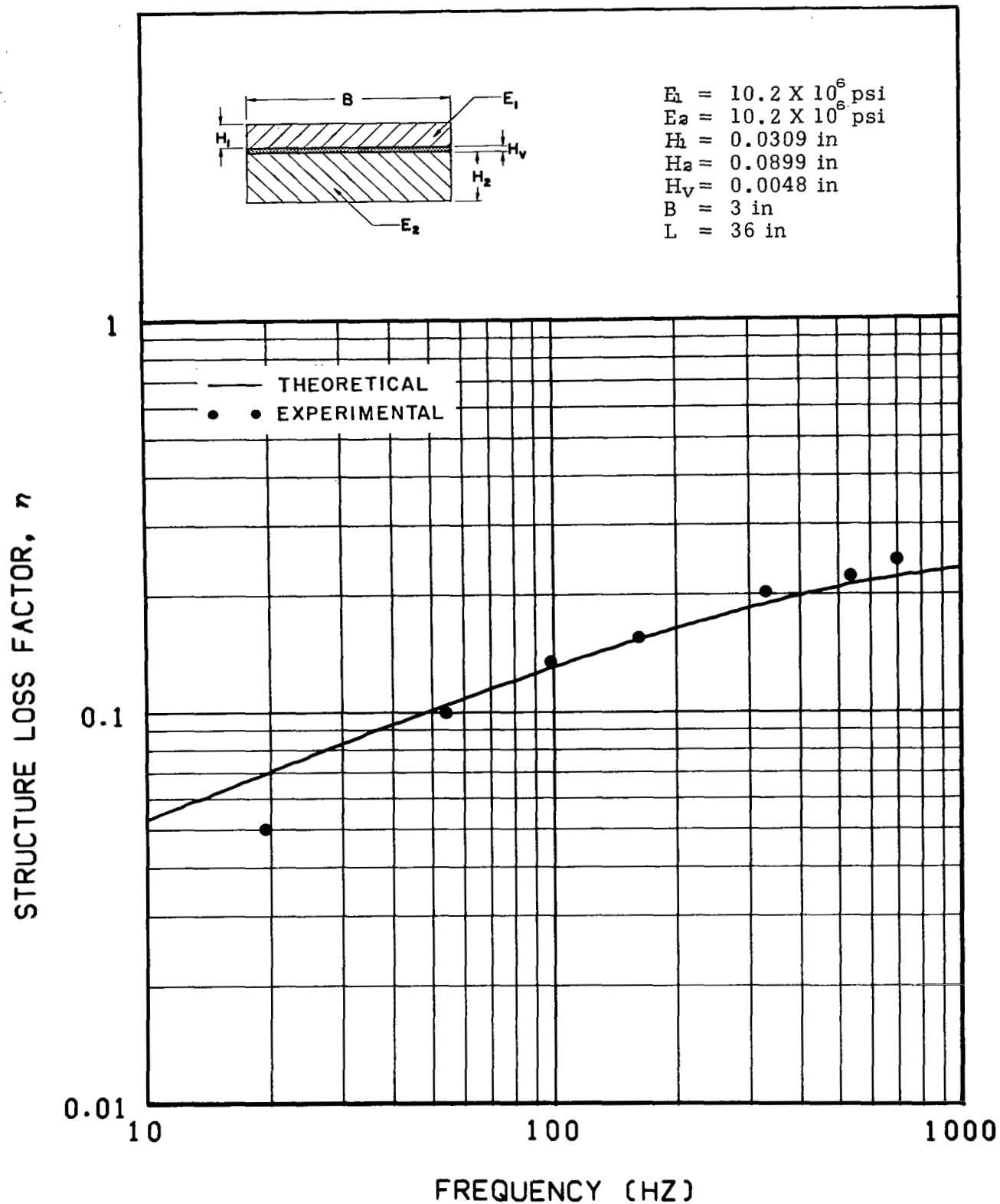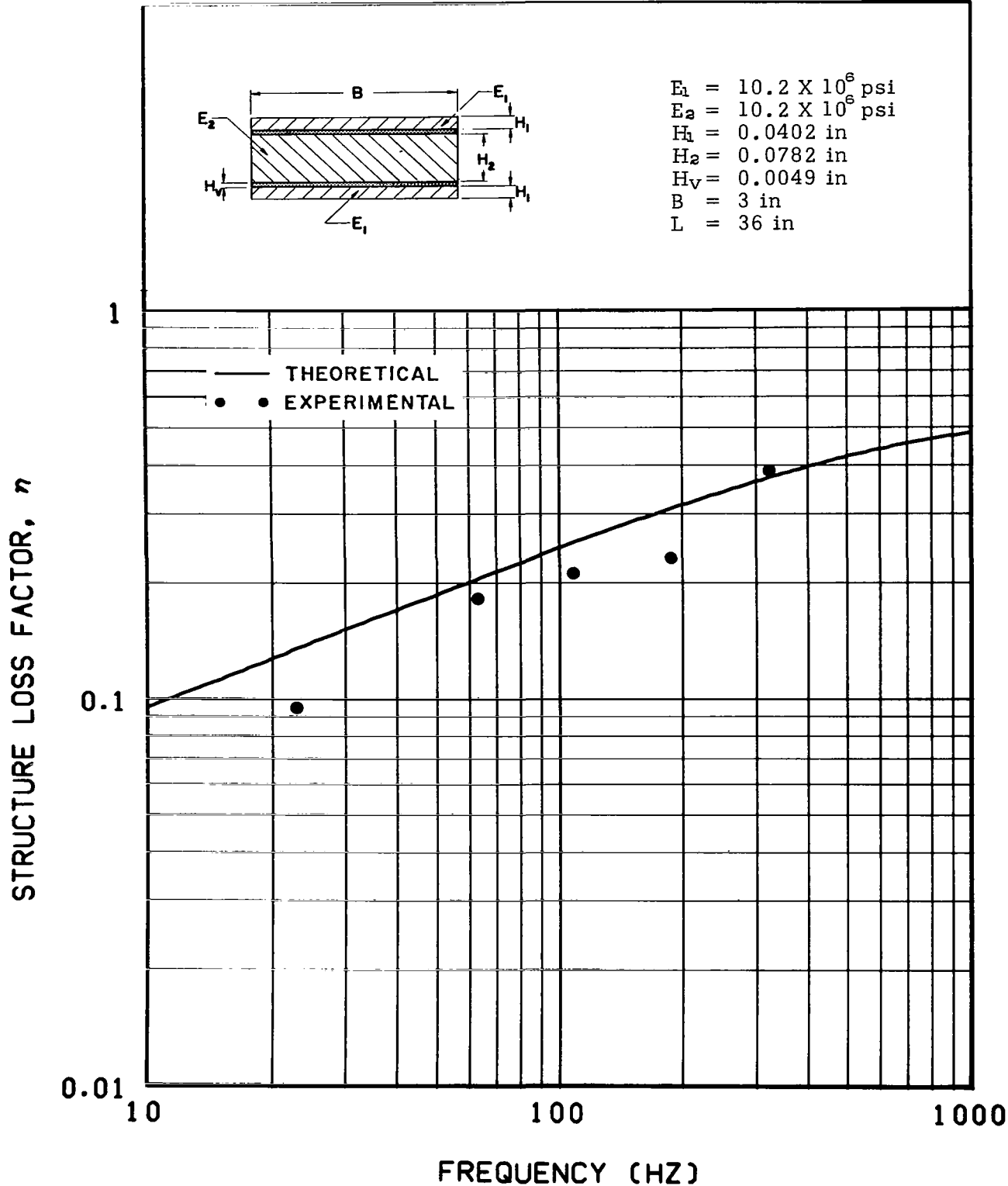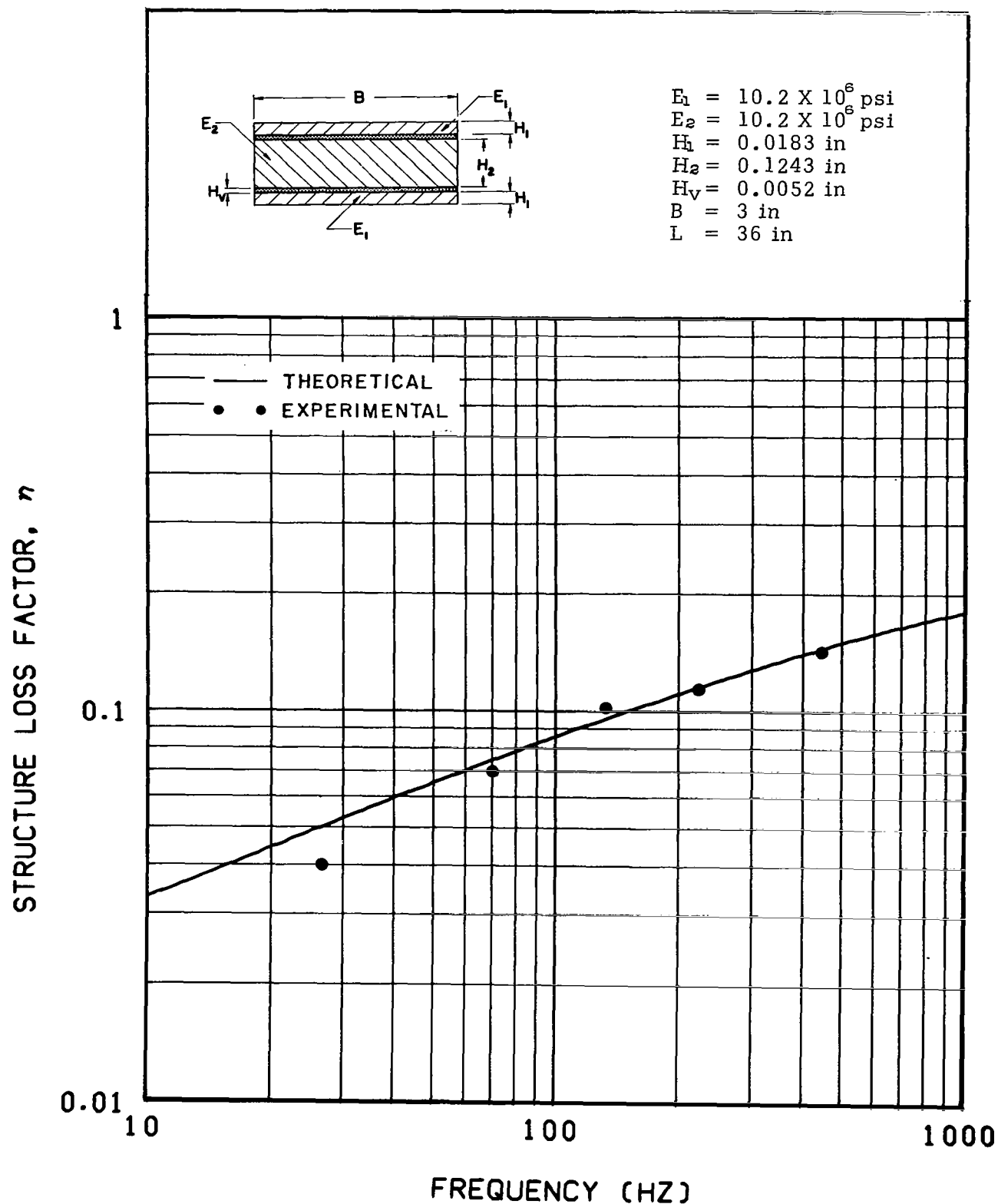
Figure 67. – Theoretically predicted and experimentally determined values of structure loss factor of a two-elastic-element free-free beam having a geometrical parameter $Y = 1.55$ and a shear parameter coefficient $C = 0.647$
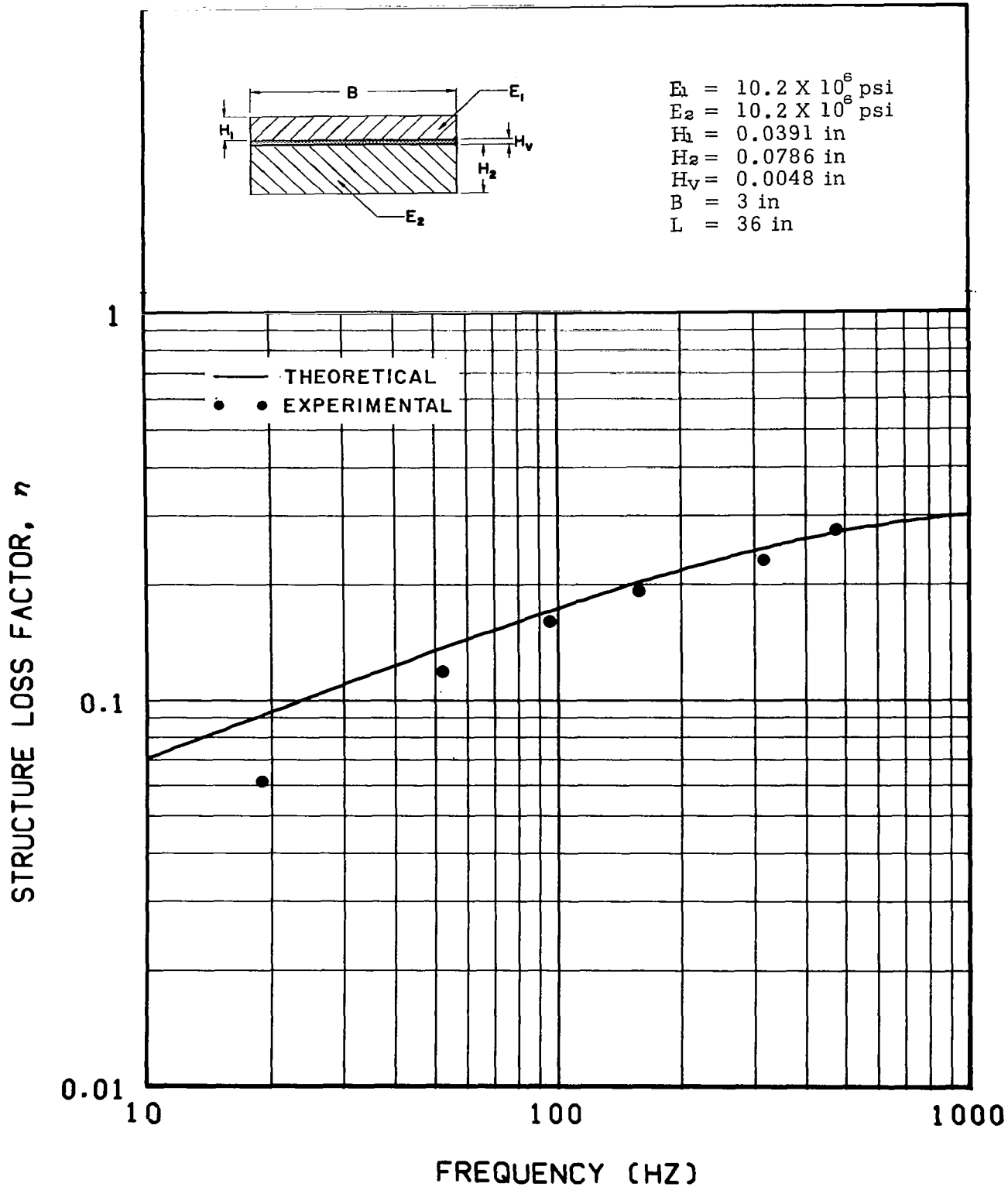
Figure 68. – Theoretically predicted and experimentally determined values of structure loss factor of a two-elastic-element free-free beam having a geometrical parameter $Y = 2.33$ and a shear parameter coefficient $C = 0.491$

165
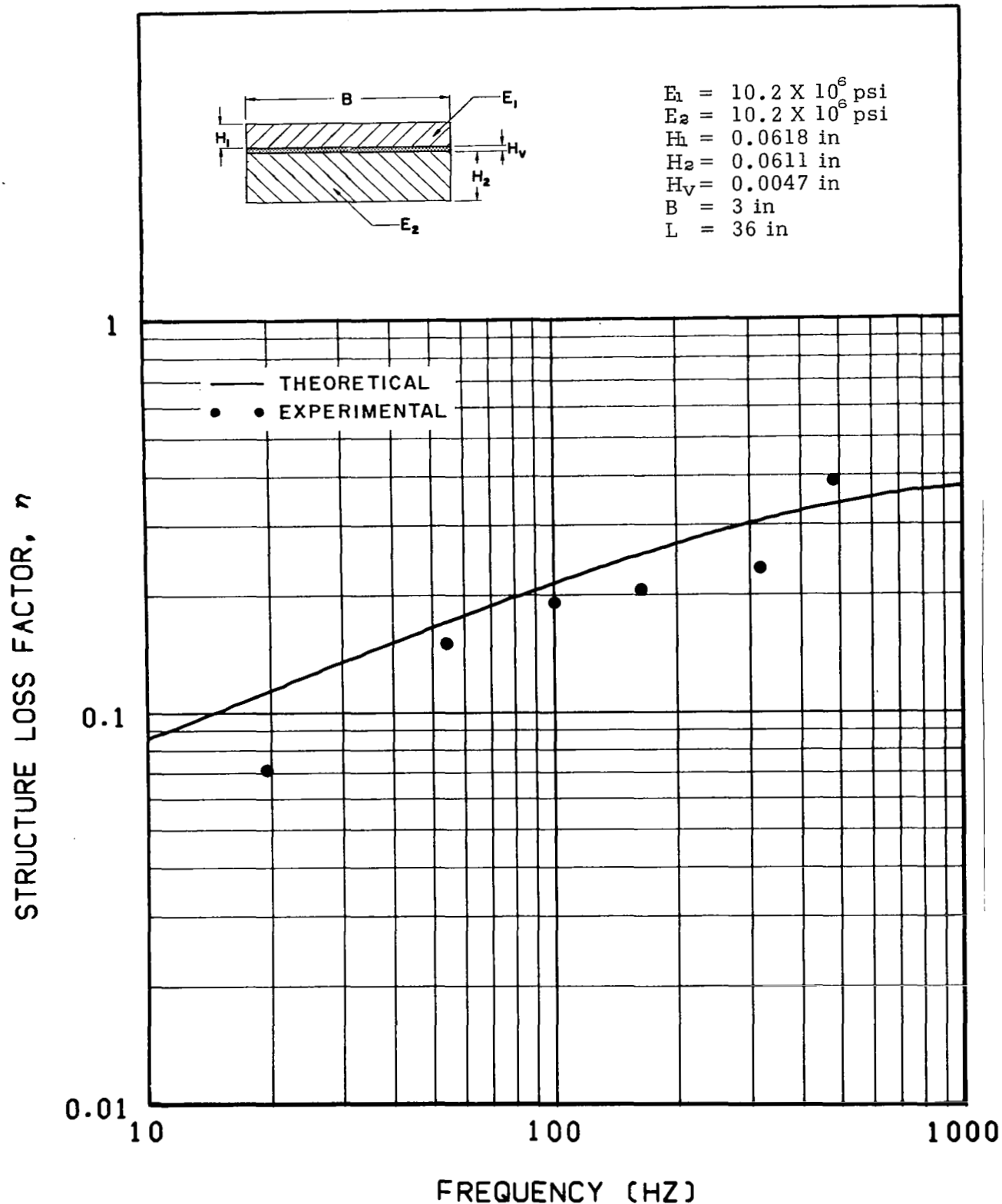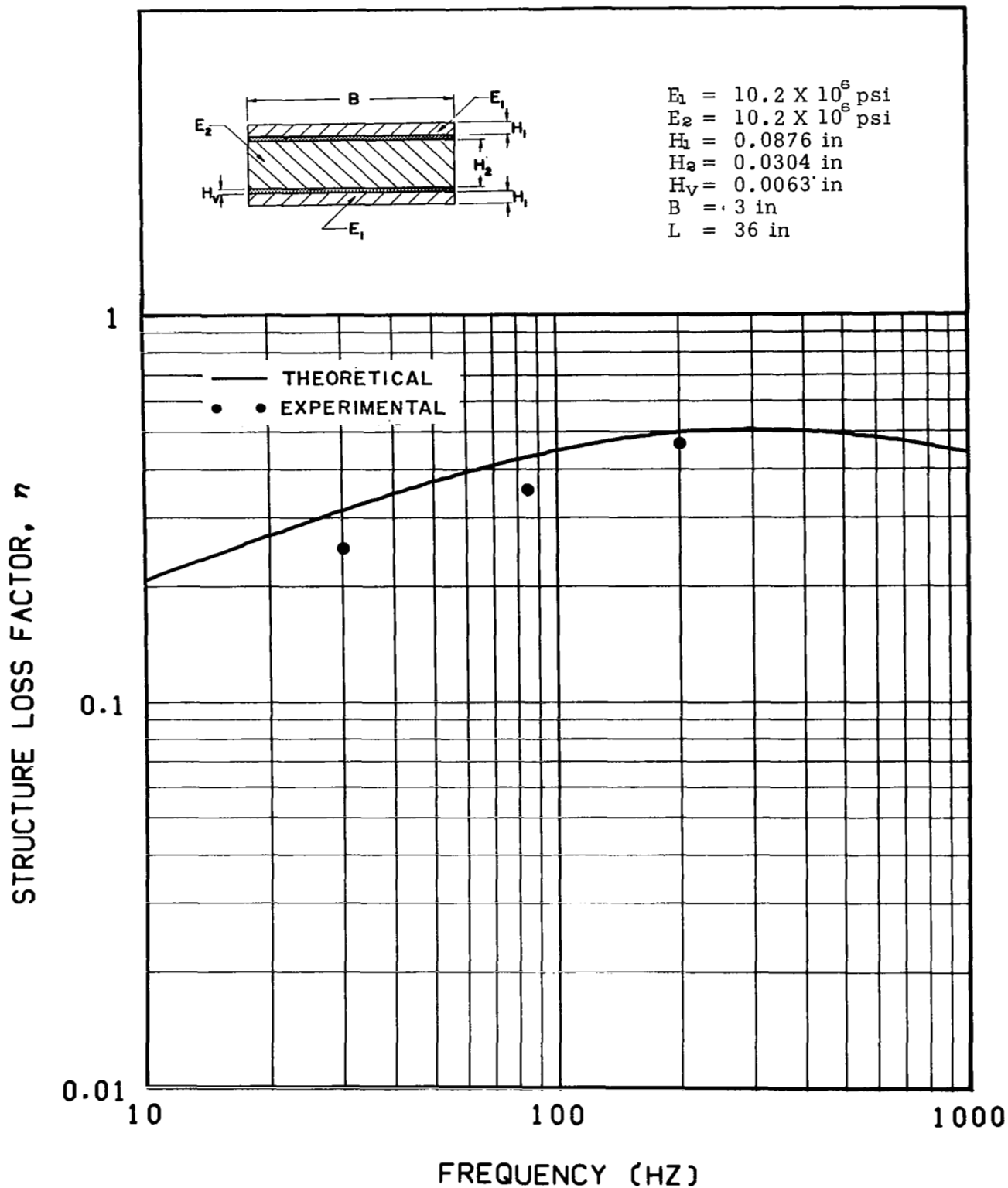
Figure 69. – Theoretically predicted and experimentally determined values of structure loss factor of a two-elastic-element free-free beam having a geometrical parameter $Y = 3.48$ and a shear parameter coefficient $C = 0.387$

166
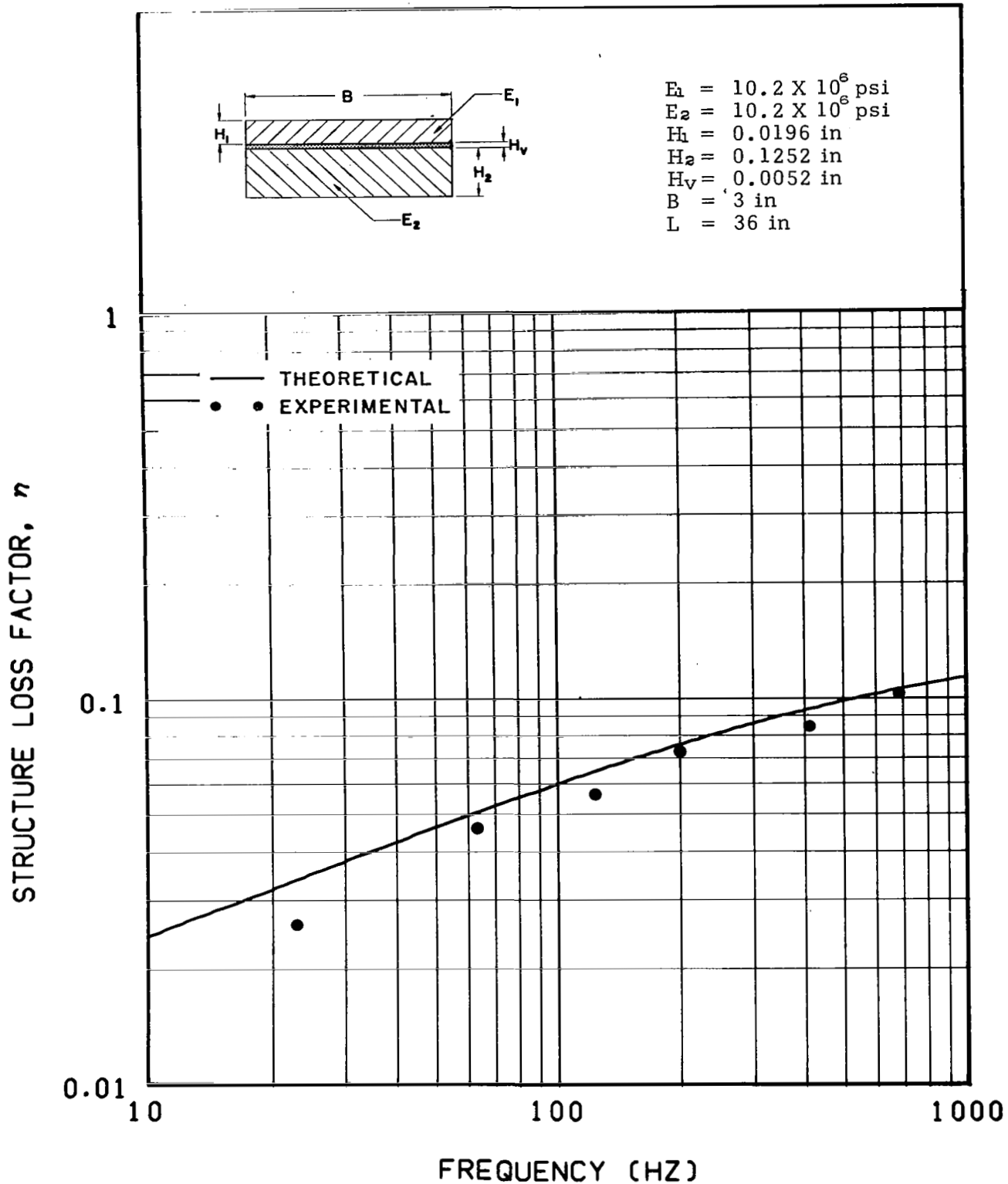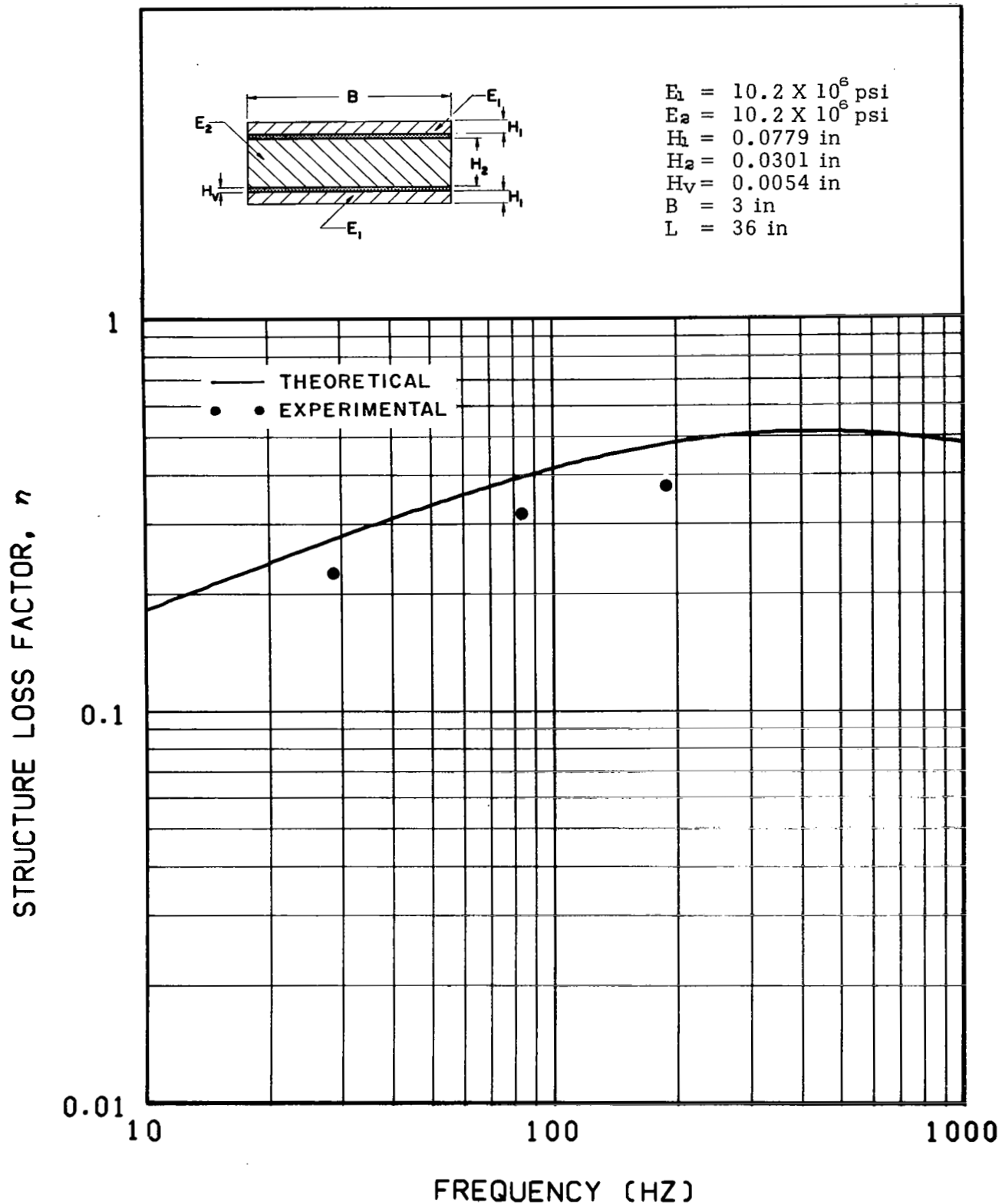
Figure 70. – Theoretically predicted and experimentally determined values
of structure loss factor of a two-elastic-element free-free
beam having a geometrical parameter $Y = 0.622$ and a shear
parameter coefficient $C = 1.21$

167
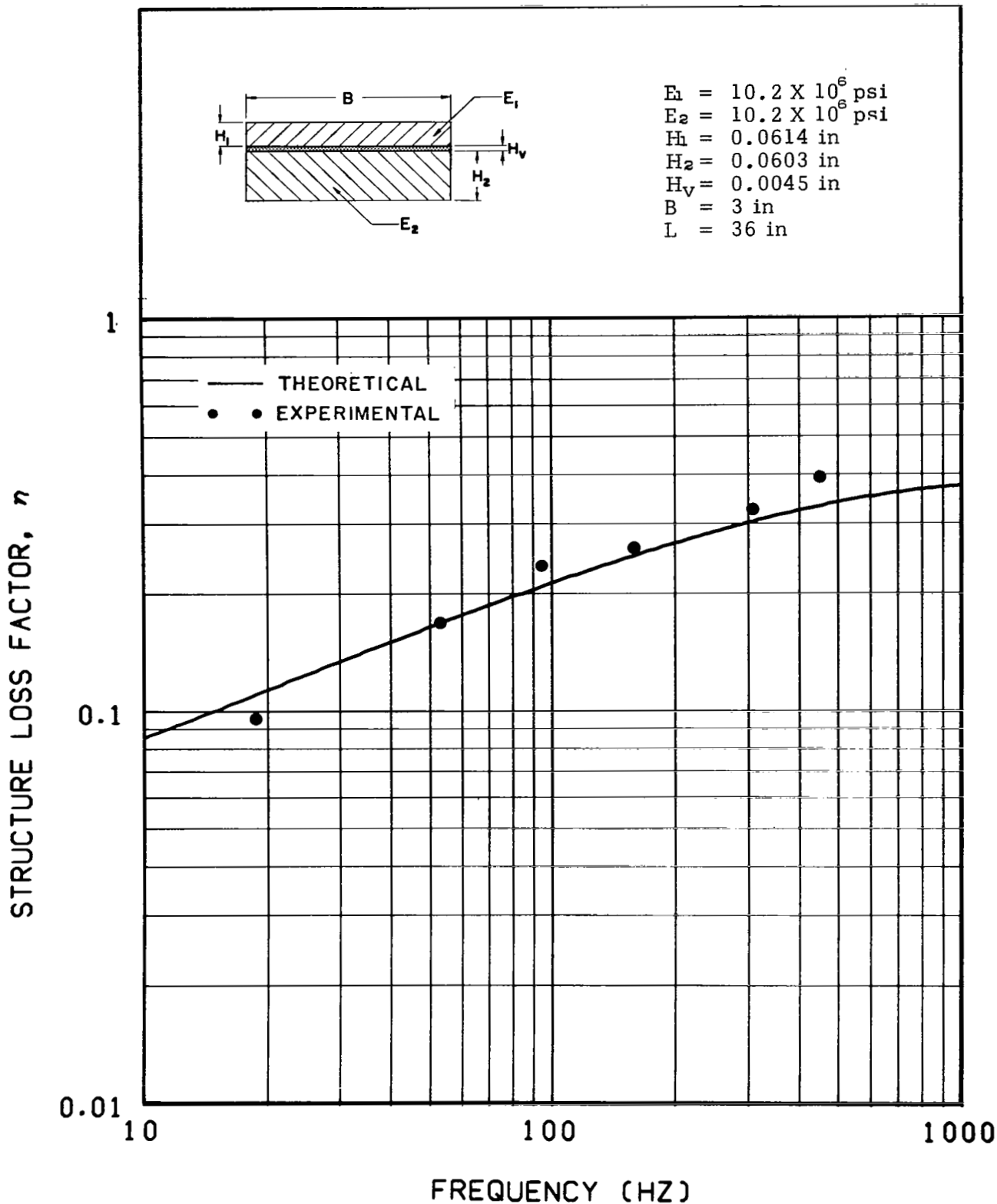
Figure 71. – Theoretically predicted and experimentally determined values
of structure loss factor of a two-elastic-element free-free
beam having a geometrical parameter Y = 3.46 and a shear
parameter coefficient C = 0.403

168
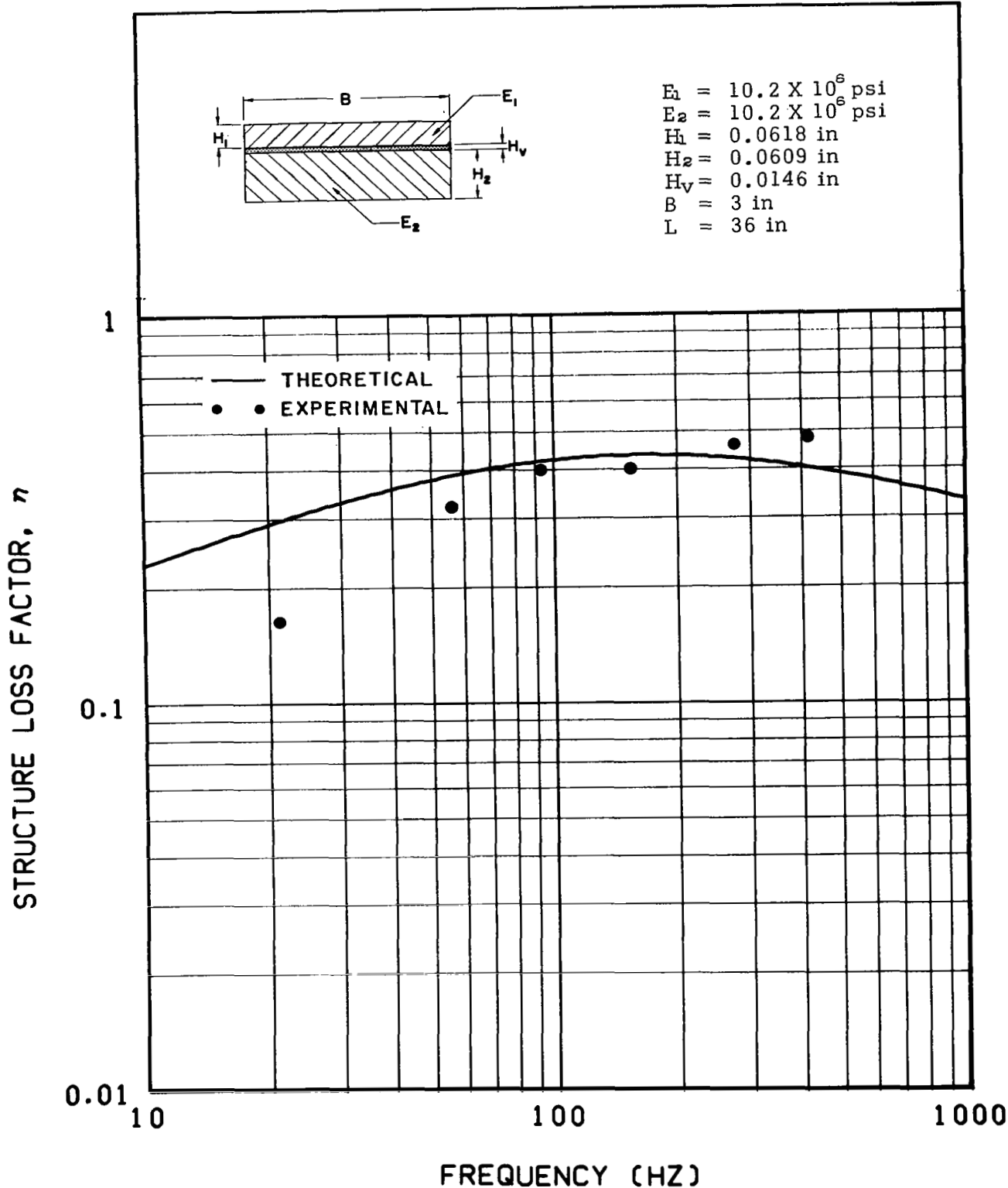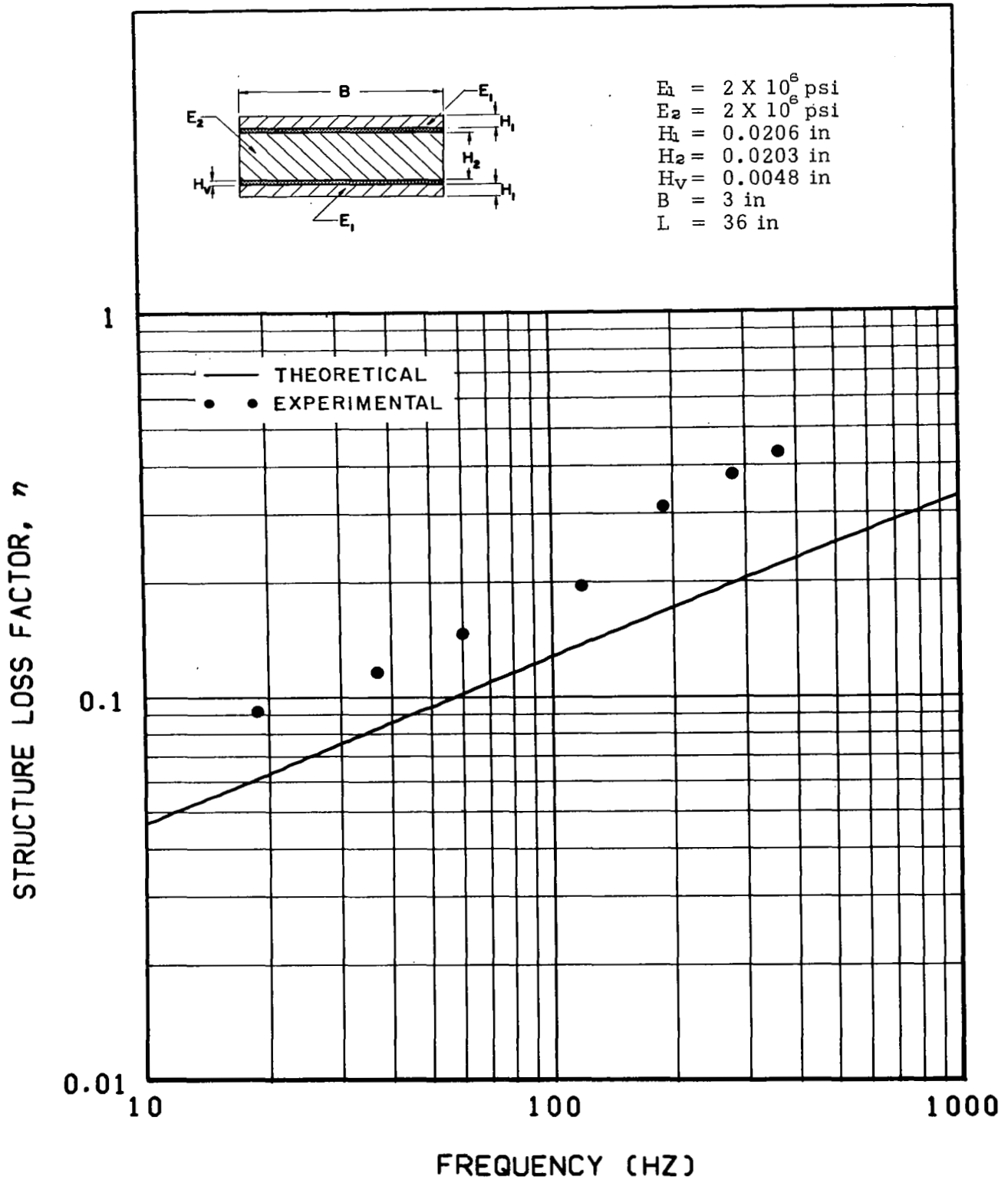
Figure 72. – Theoretically predicted and experimentally determined values of structure loss factor of a two-elastic-element free-free beam having a geometrical parameter $Y = 4.60$ and a shear parameter coefficient $C = 0.123$

169
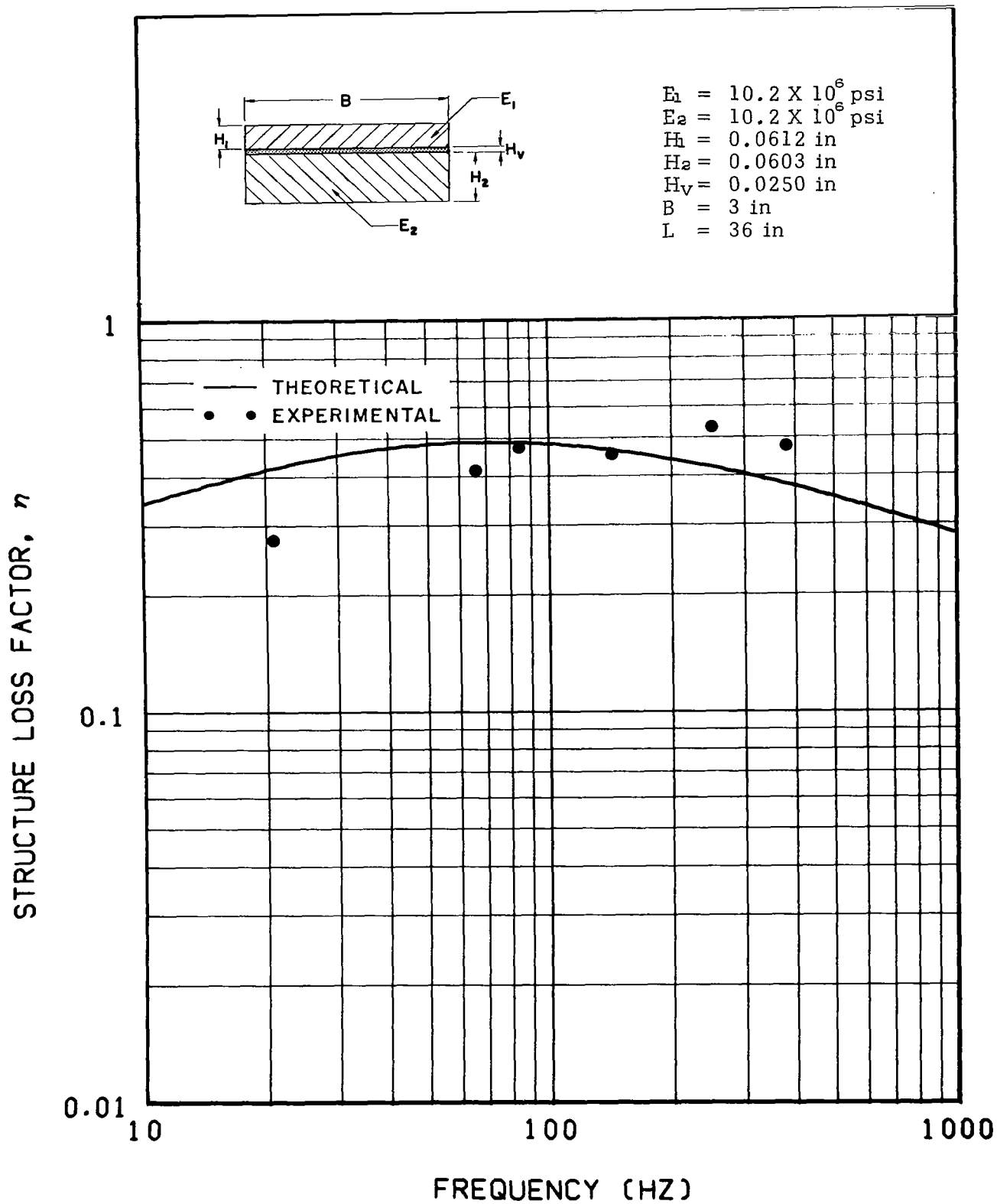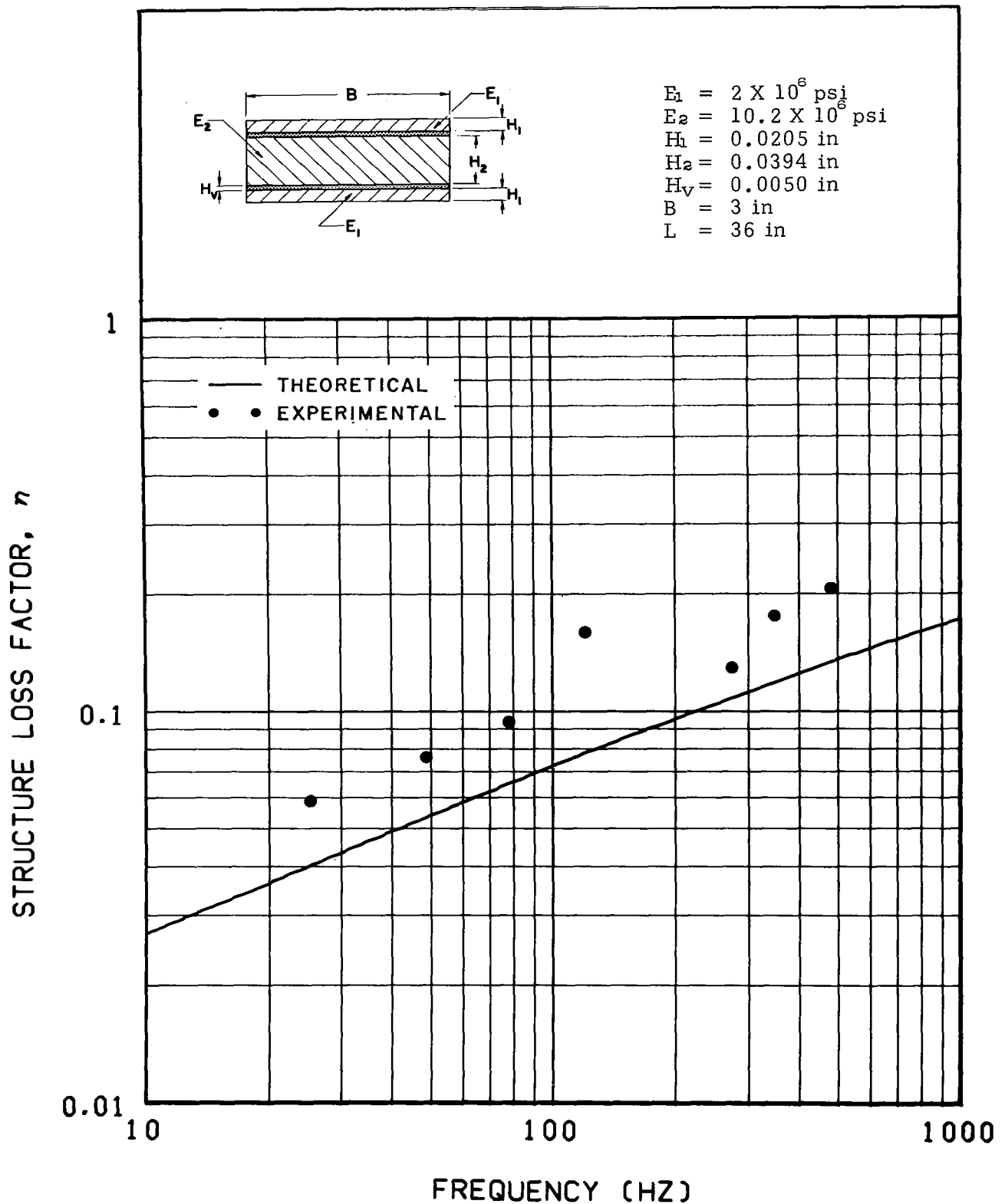
Figure 73. – Theoretically predicted and experimentally determined values of structure loss factor of a two-elastic-element free-free beam having a geometrical parameter Y = 5.98 and a shear parameter coefficient C = 0.071
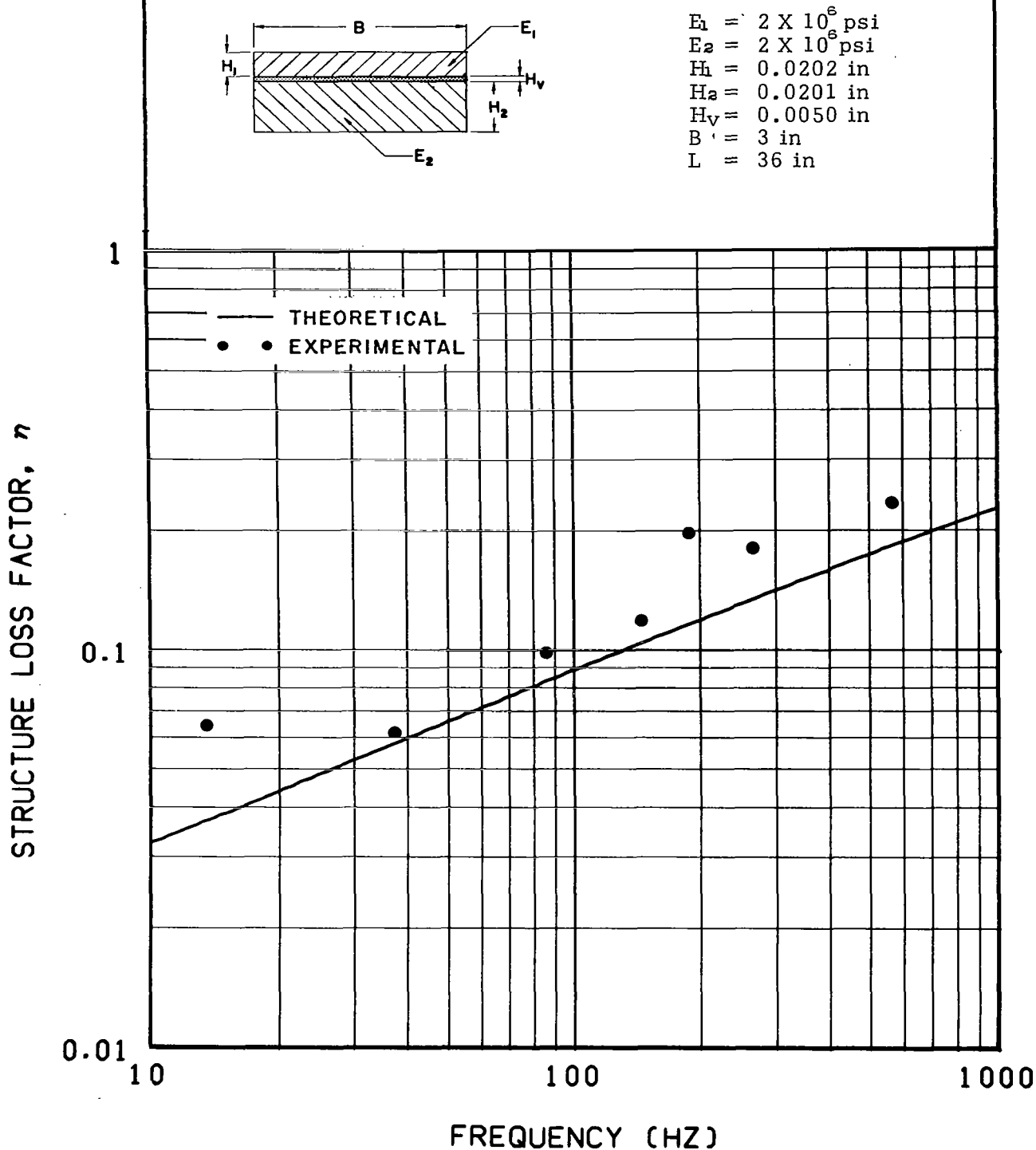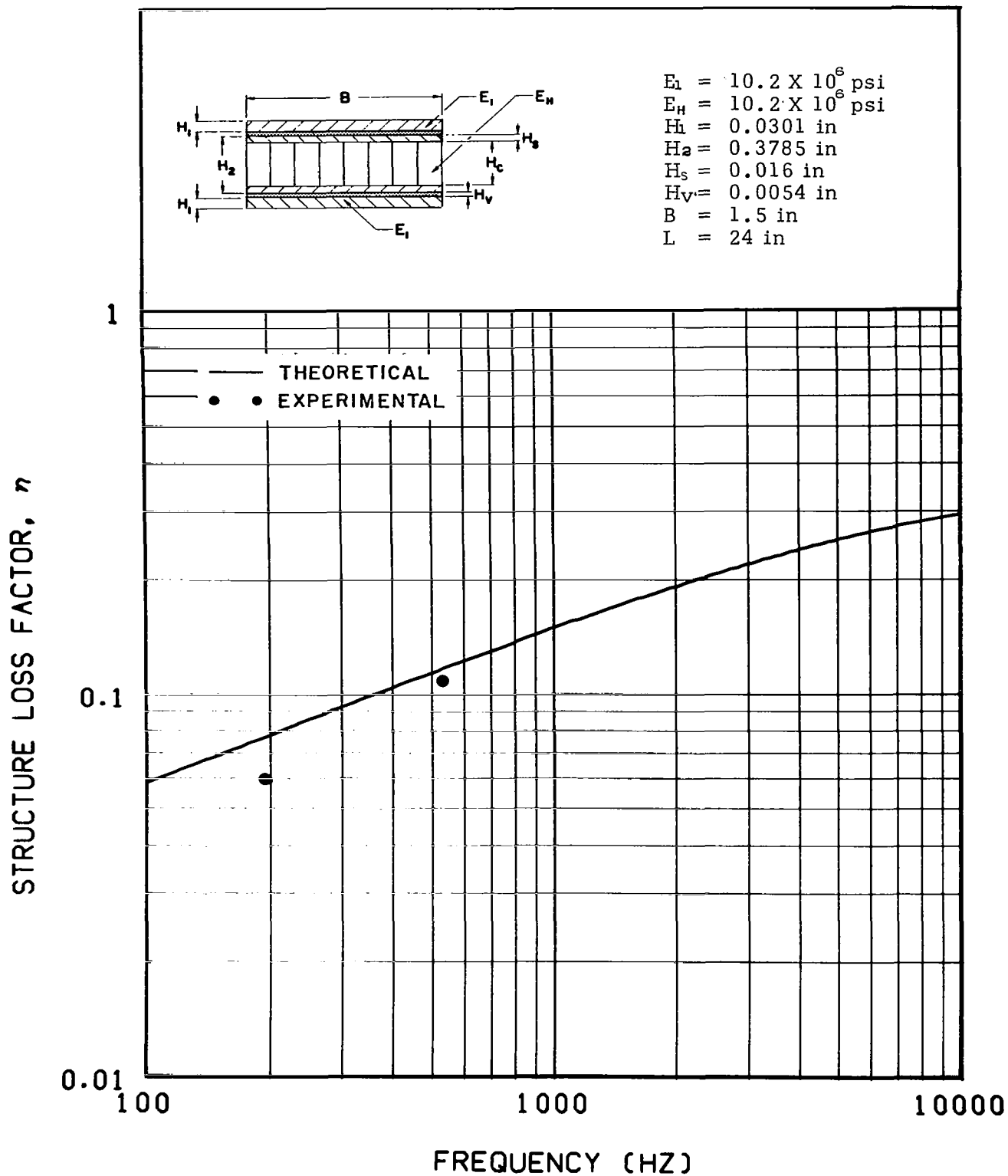
Figure 74. – Theoretically predicted and experimentally determined values of structure loss factor of a two-elastic-element free-free beam having a geometrical parameter Y = 4.67 and a shear parameter coefficient C = 1.01

171
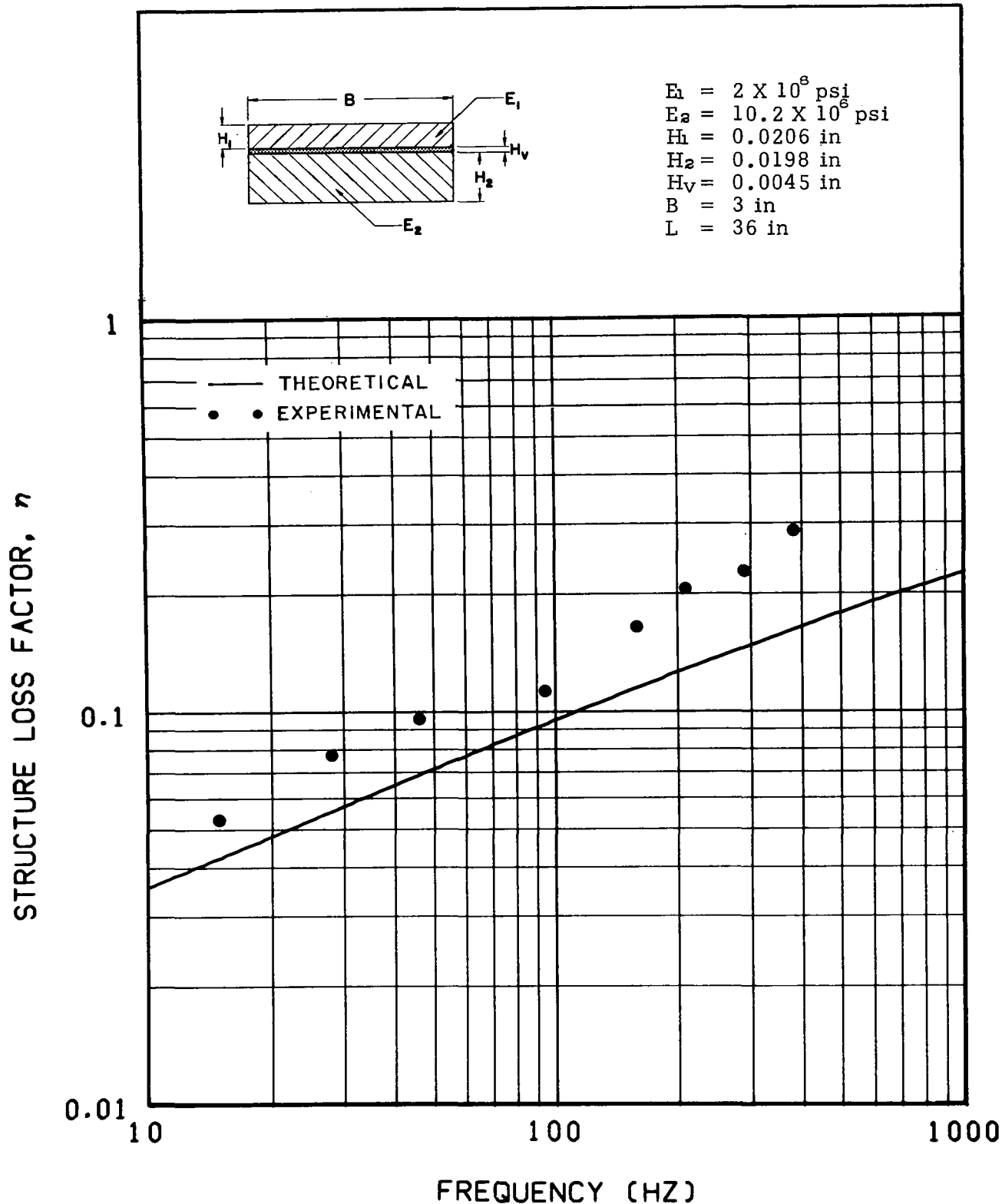
Figure 75. – Theoretically predicted and experimentally determined values
of structure loss factor of a two-elastic-element free-free
beam having a geometrical parameter Y = 2.59 and a shear
parameter coefficient C = 1.04
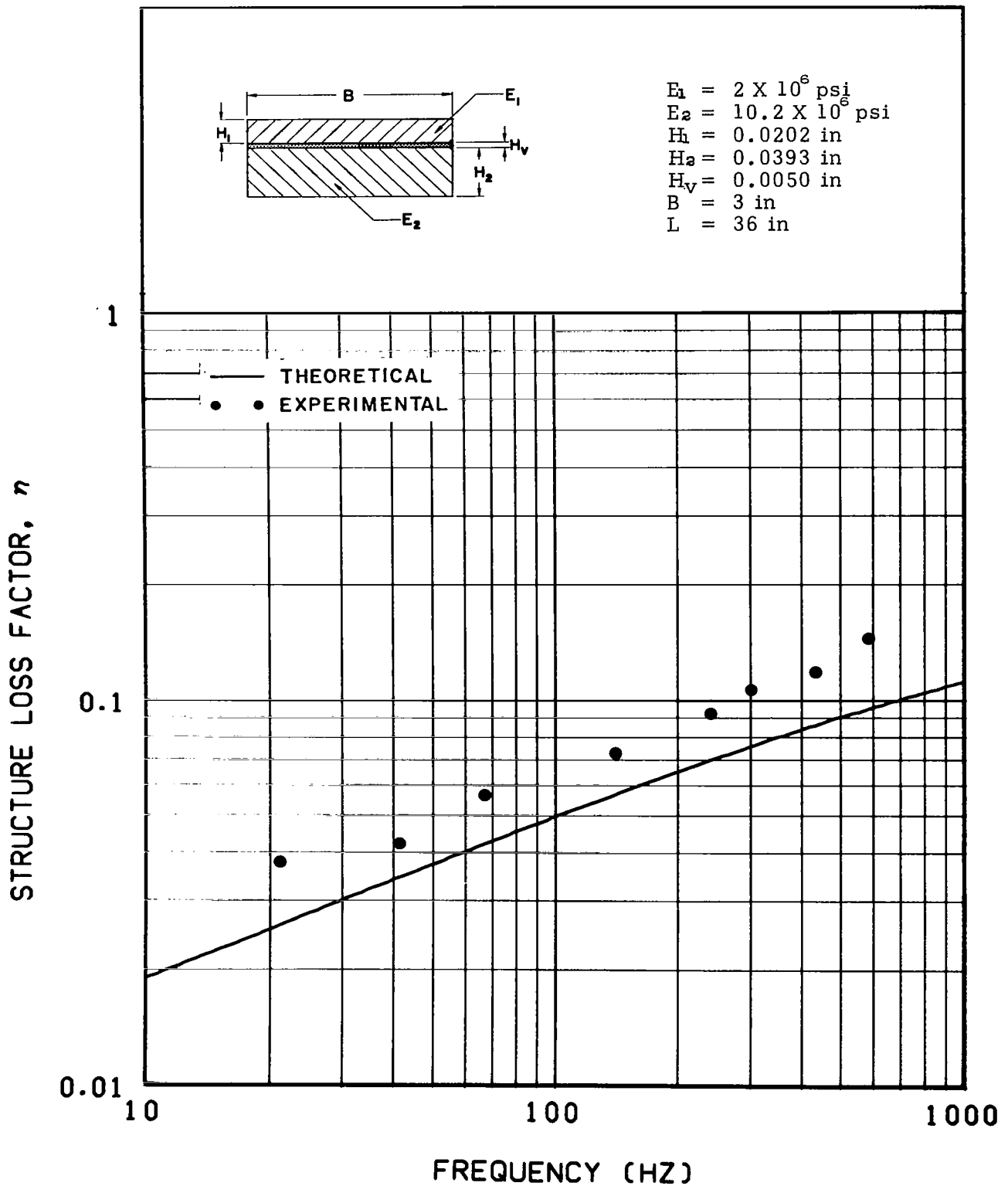
Figure 76. – Theoretically predicted and experimentally determined values of structure loss factor of a two-elastic-element free-free beam having a geometrical parameter Y = 0.837 and a shear parameter coefficient C = 1.72
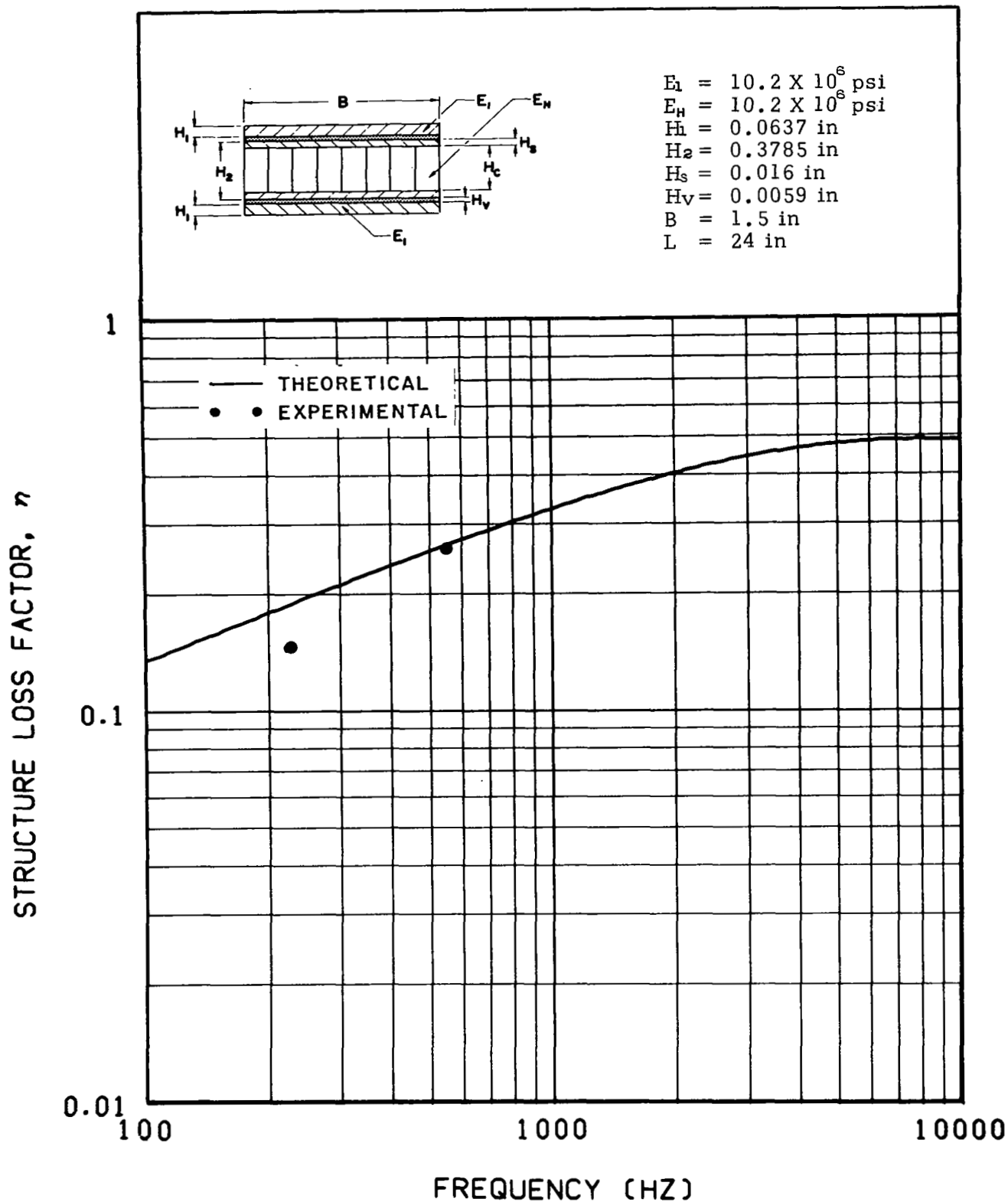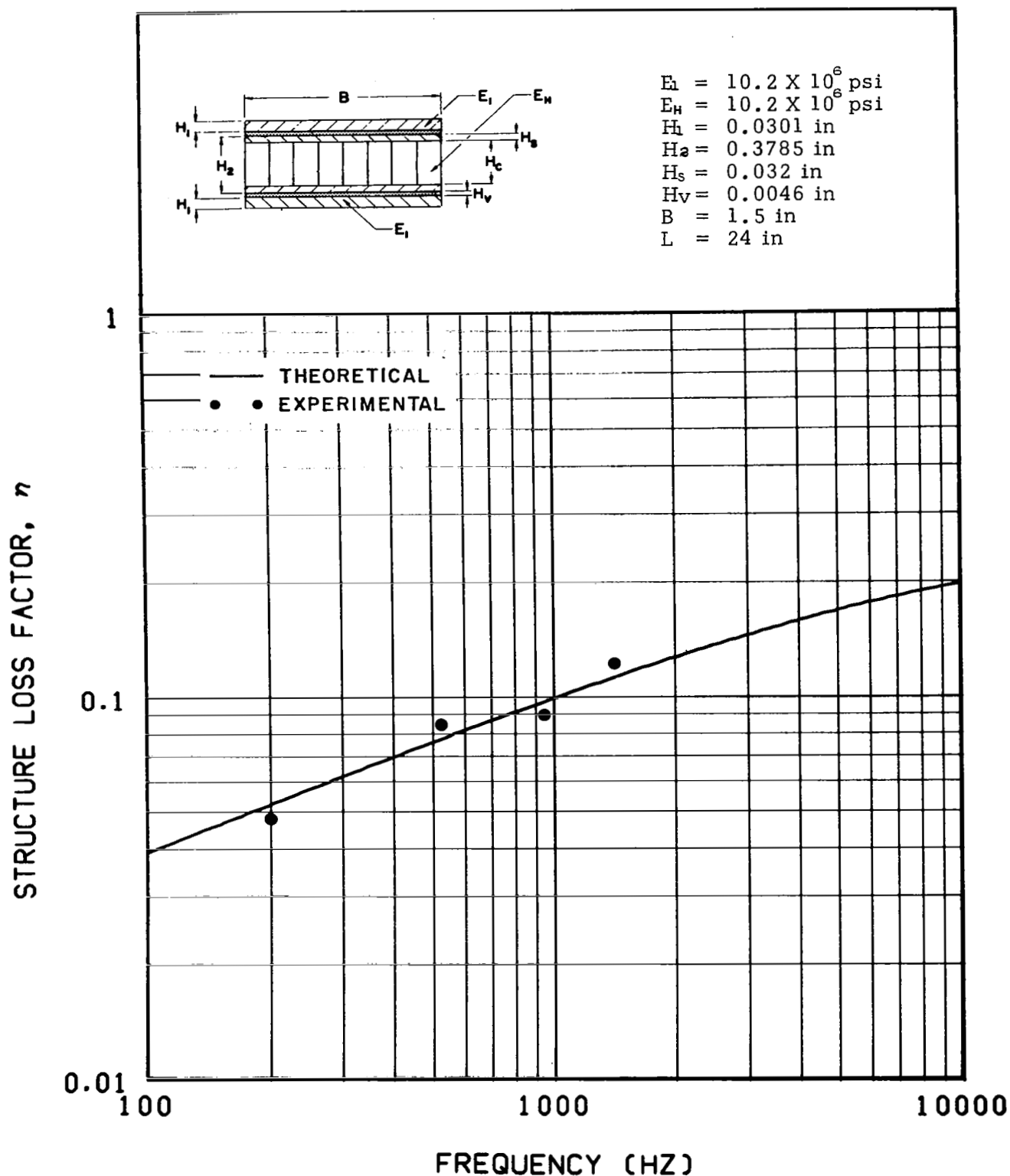
173
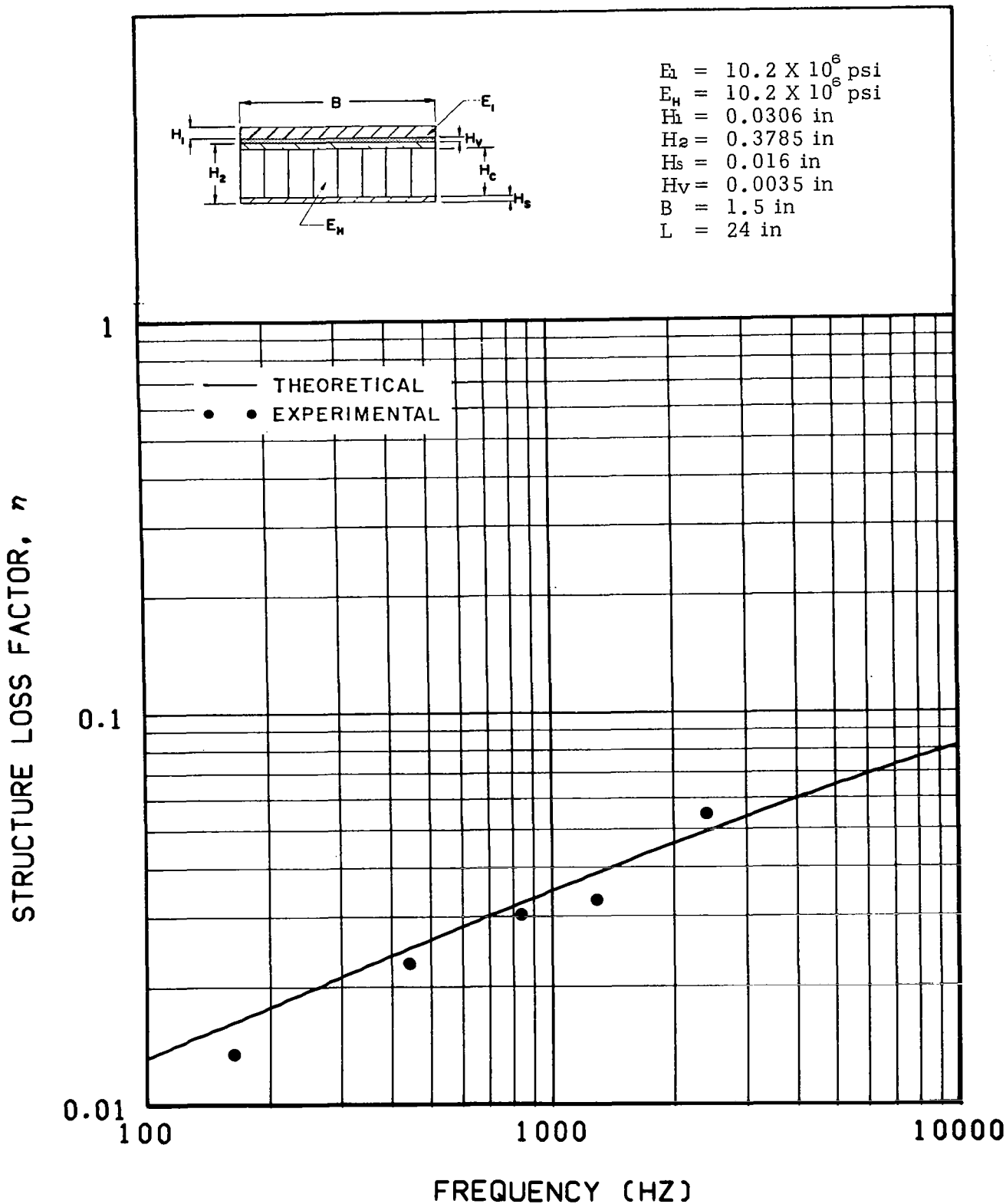
Figure 77. – Theoretically predicted and experimentally determined values of structure loss factor of a two-elastic-element free-free beam having a geometrical parameter Y = 0.642 and a shear parameter coefficient C = 6.21

174
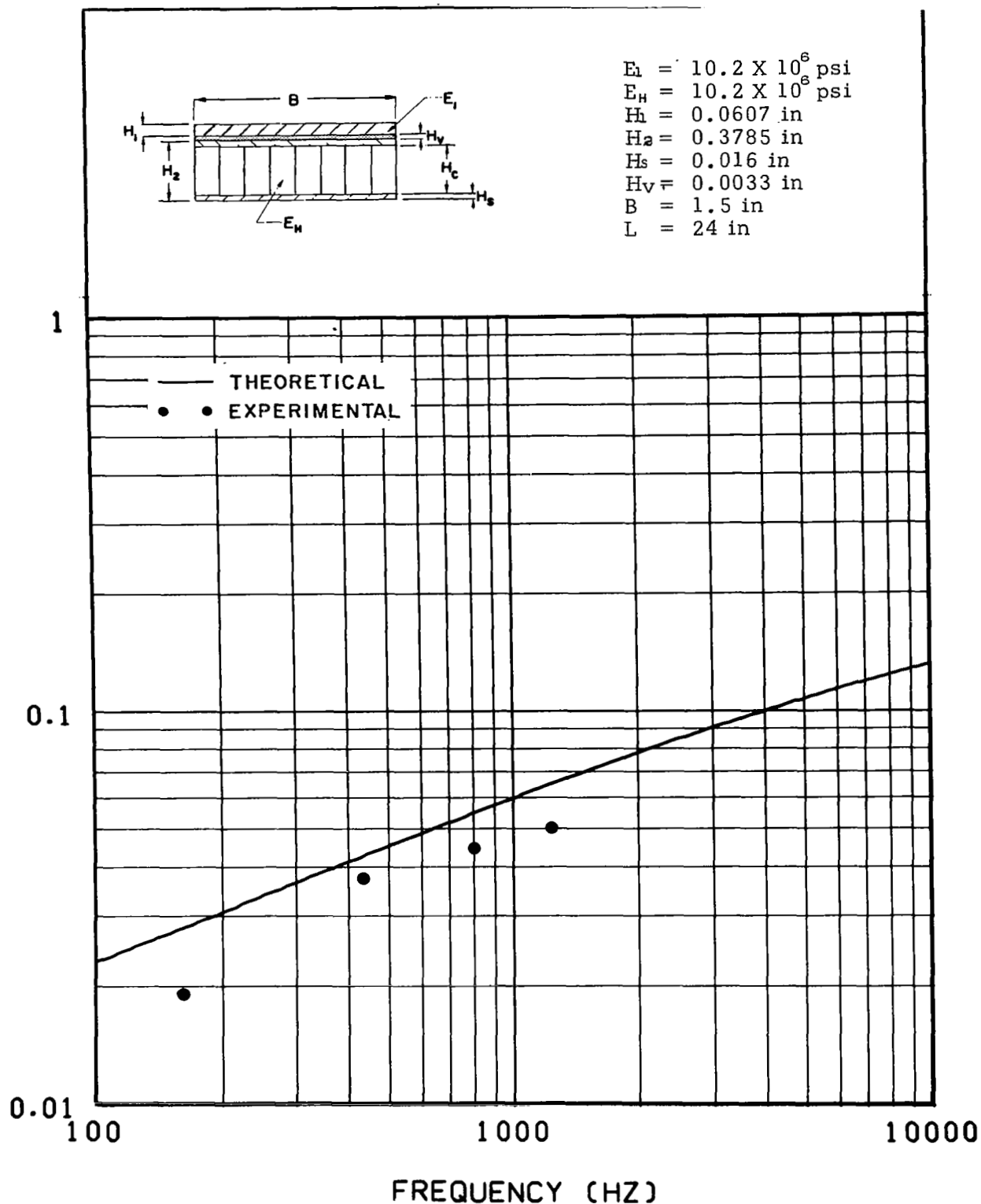
Figure 78. – Theoretically predicted and experimentally determined values of structure loss factor of a two-elastic-element free-free beam having a geometrical parameter Y = 0.972 and a shear parameter coefficient C = 4.22
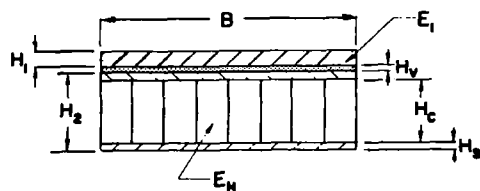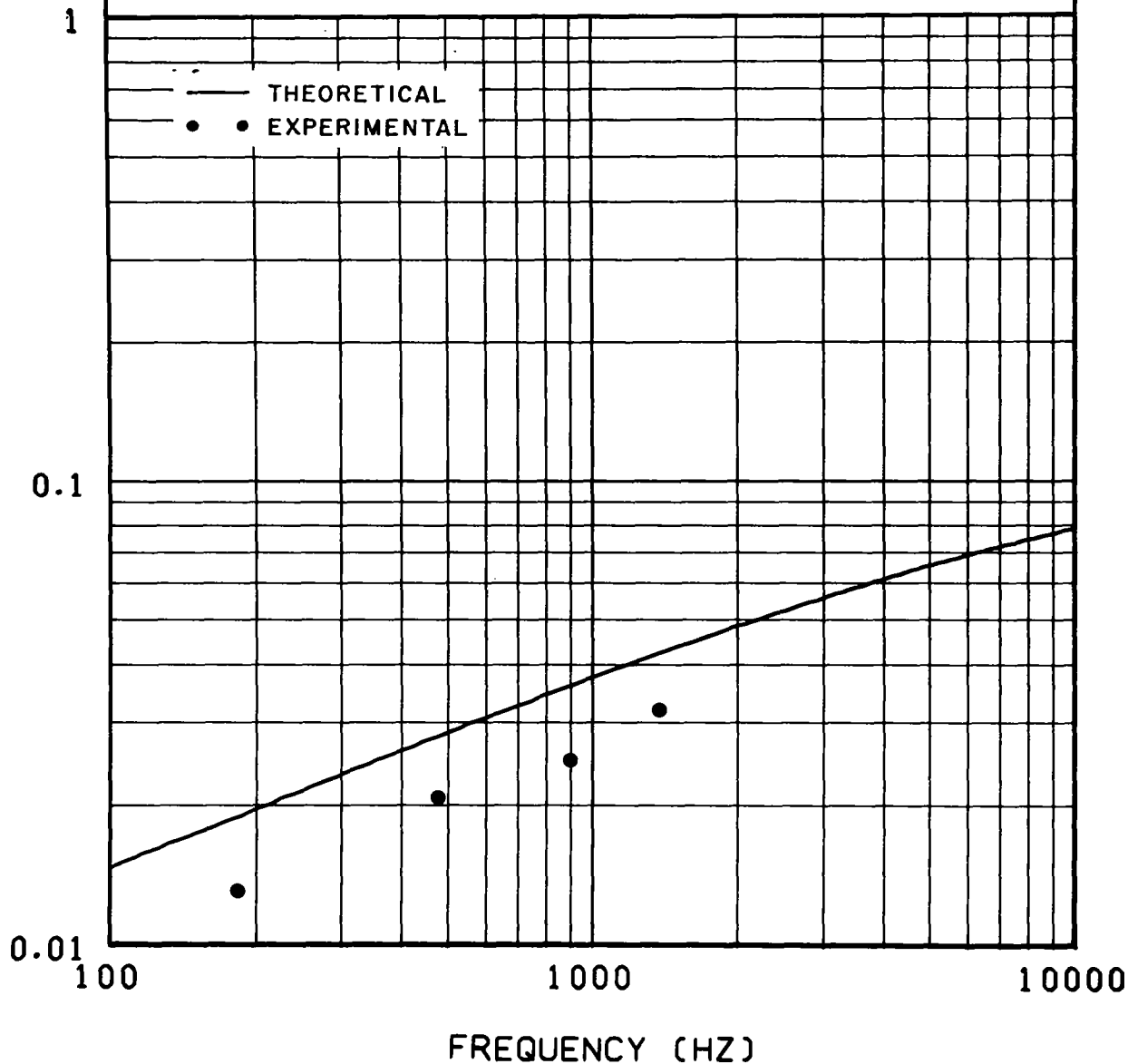
175
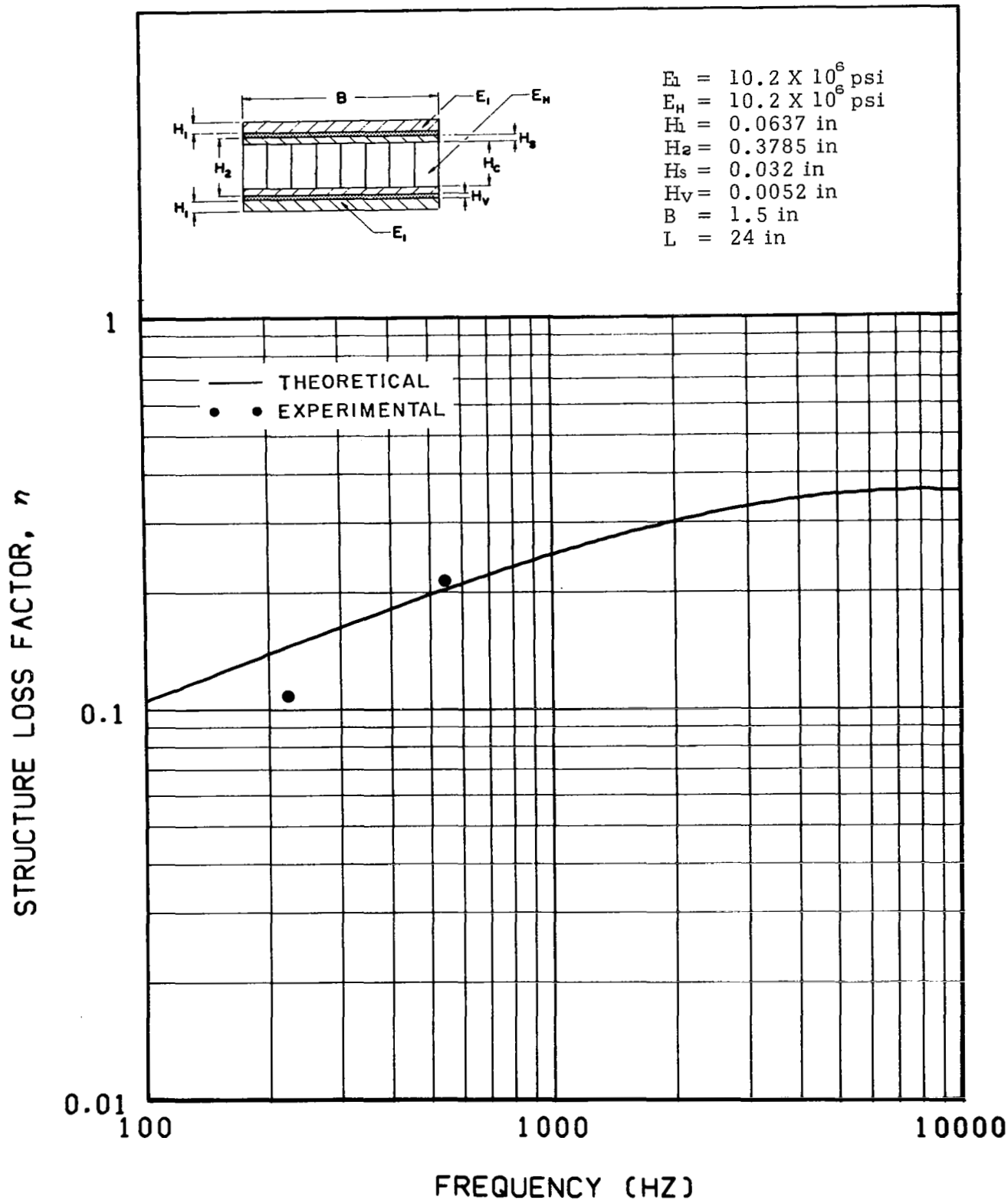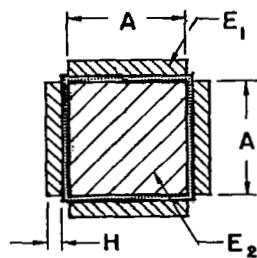
Figure 79. – Theoretically predicted and experimentally determined values of structure loss factor of a two-elastic-element free-free beam having a geometrical parameter Y = 0.466 and a shear parameter coefficient C = 4.89
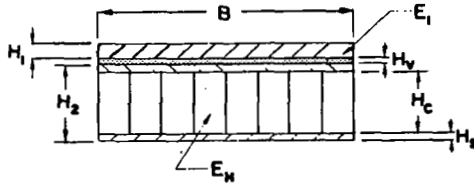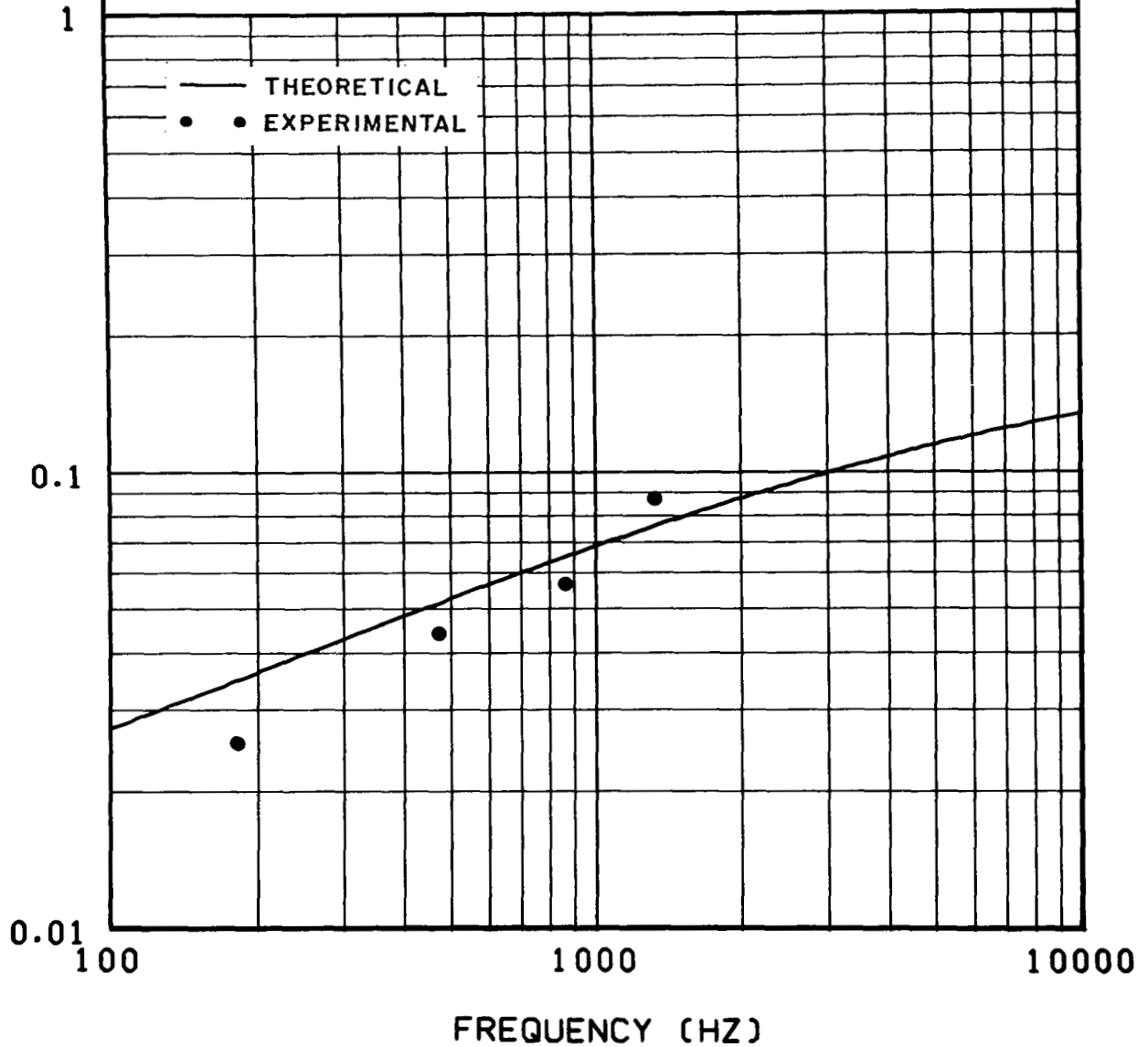
176
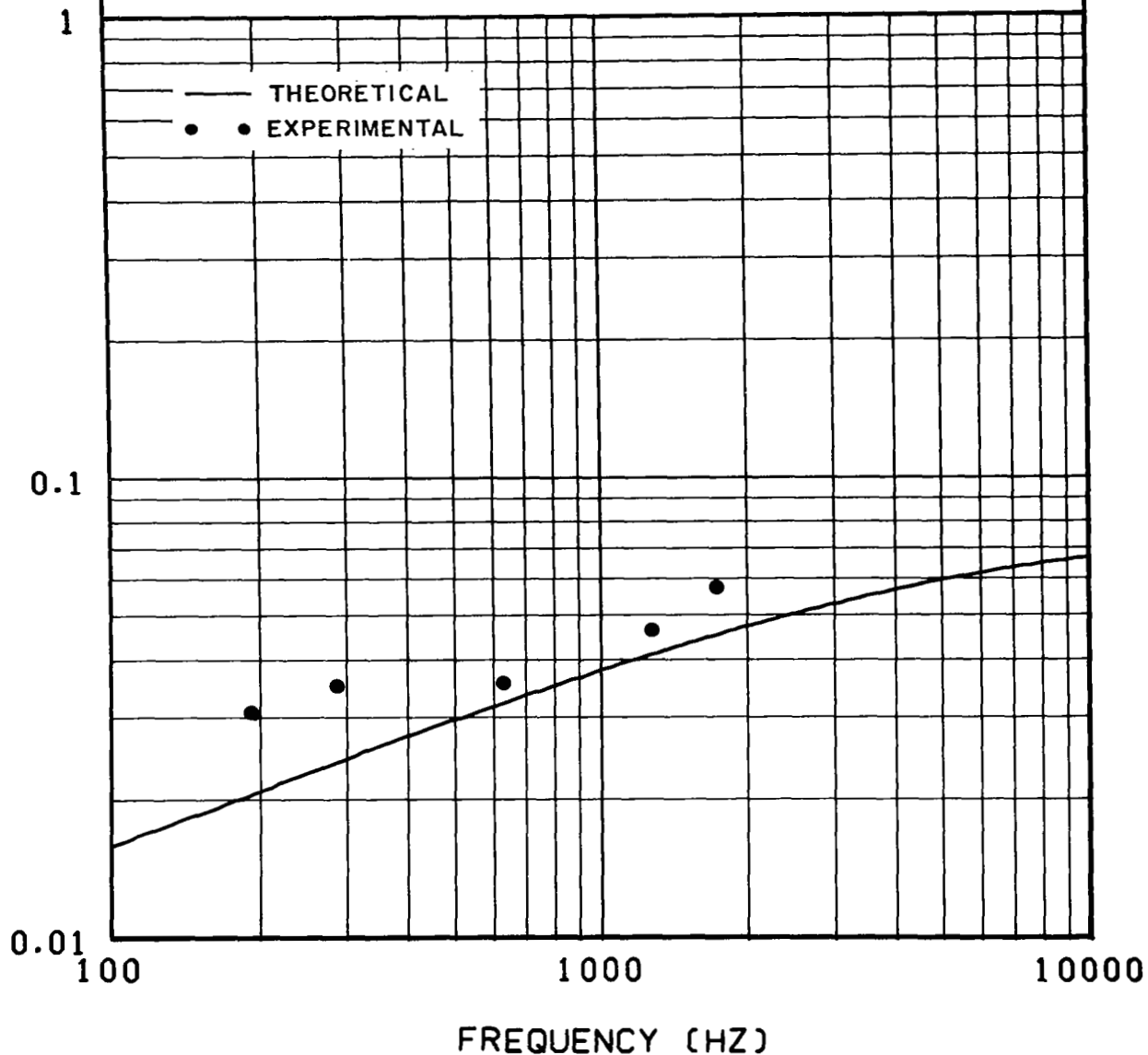
Figure 80. – Theoretically predicted and experimentally determined values of structure loss factor of a two-elastic-element free-free beam having a geometrical parameter Y = 0.795 and a shear parameter coefficient C = 3.27

177
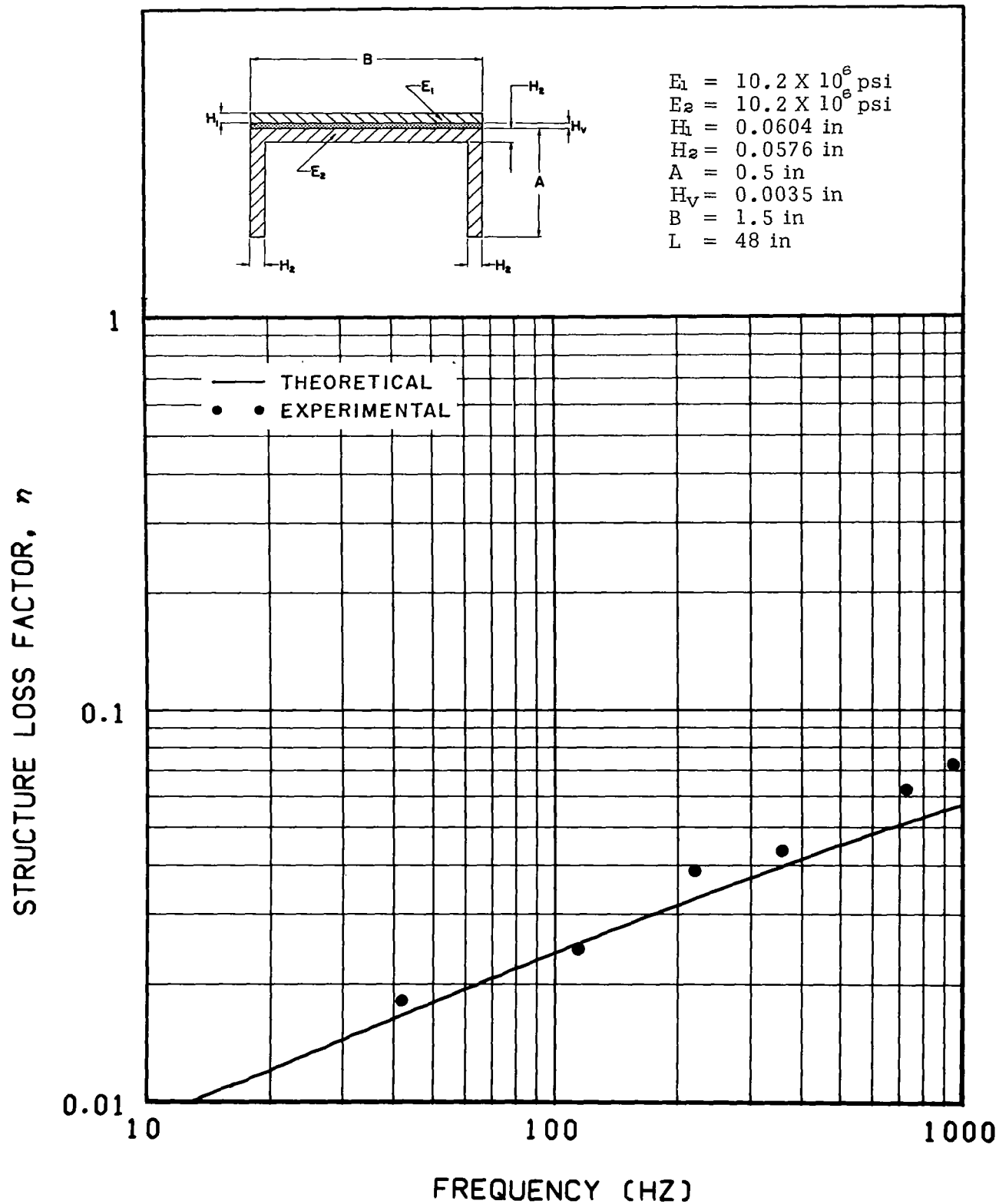
Figure 81. – Theoretically predicted and experimentally determined values of structure loss factor of a two-elastic-element free-free beam having a geometrical parameter $Y = 0.464$ and a shear parameter coefficient $C = 2.75$
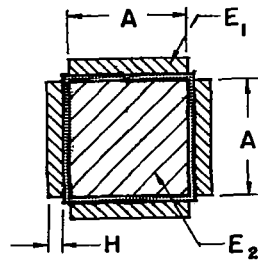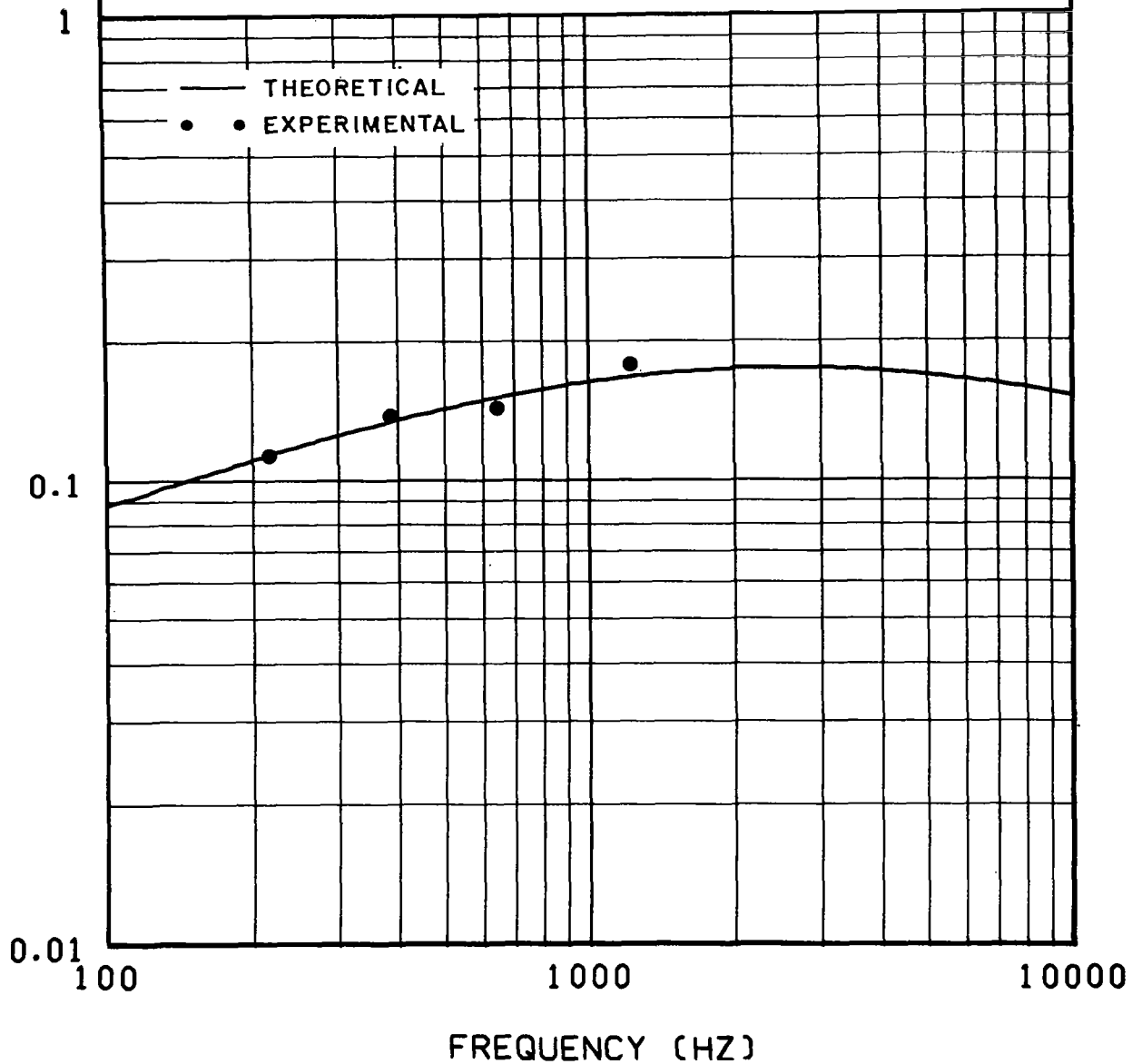
178
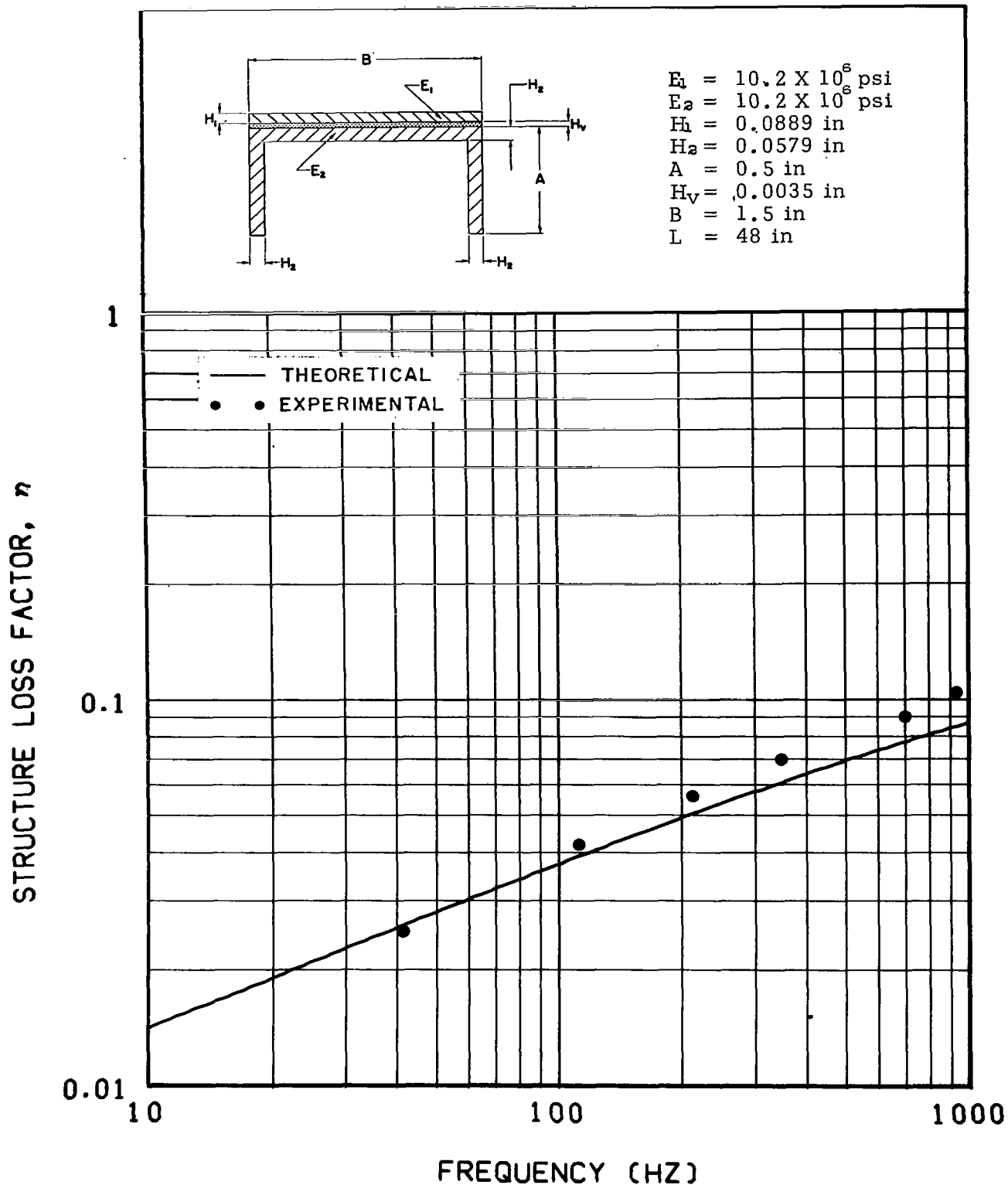
Figure 82. — Theoretically predicted and experimentally determined values of structure loss factor of a two-elastic-element free-free beam having a geometrical parameter Y = 0.672 and a shear parameter coefficient C = 2.06
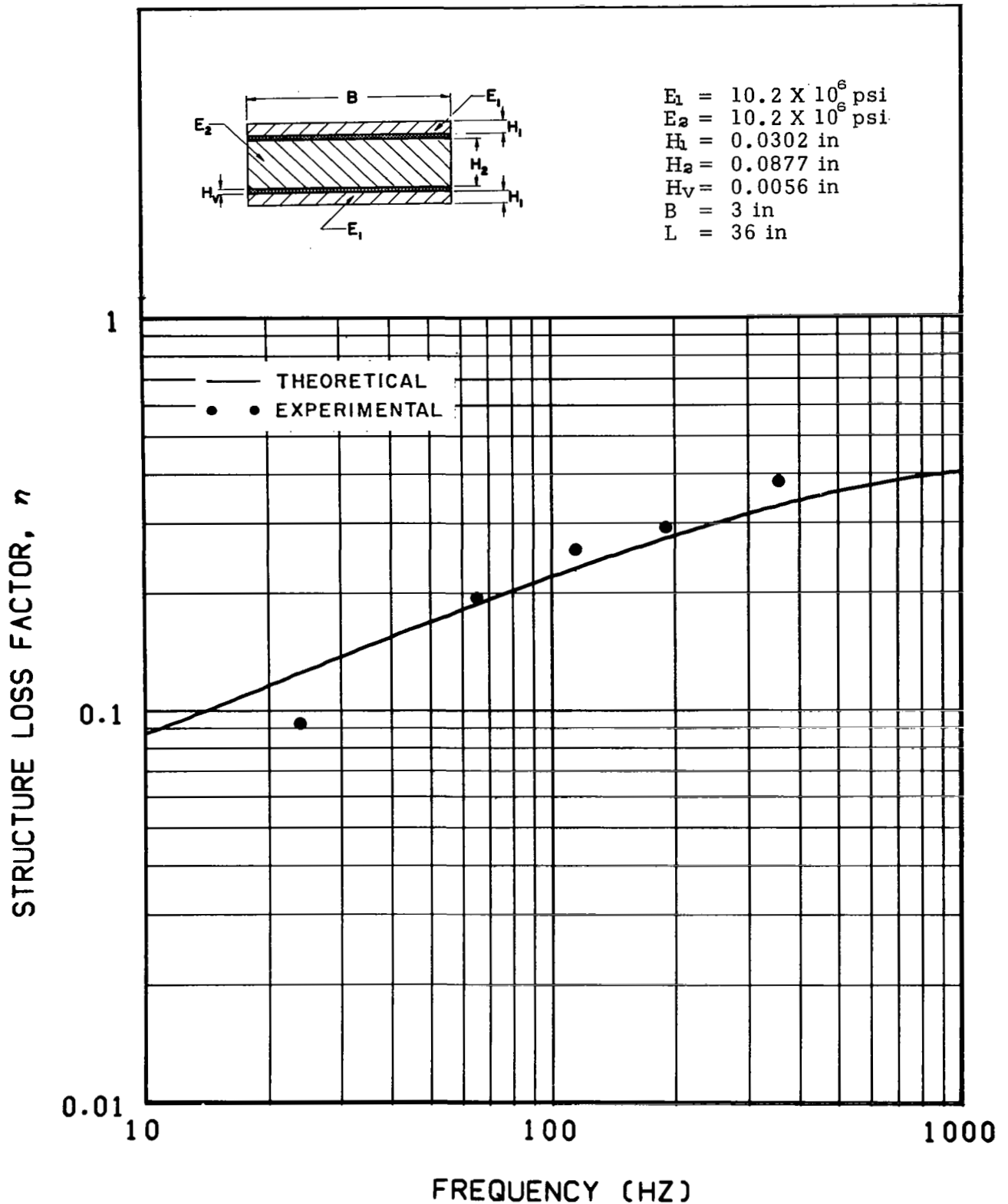
Figure 83. – Theoretically predicted and experimentally determined values of structure loss factor of a symmetrical three-elastic-element free-free beam having a geometrical parameter $Y = 4.14$ and a shear parameter coefficient $C = 0.372$

180

Figure 84. – Theoretically predicted and experimentally determined values of structure loss factor of a symmetrical three-elastic-element free-free beam having a geometrical parameter Y = 6.51 and a shear parameter coefficient C = 0.305
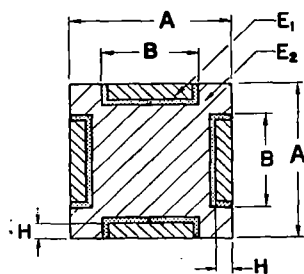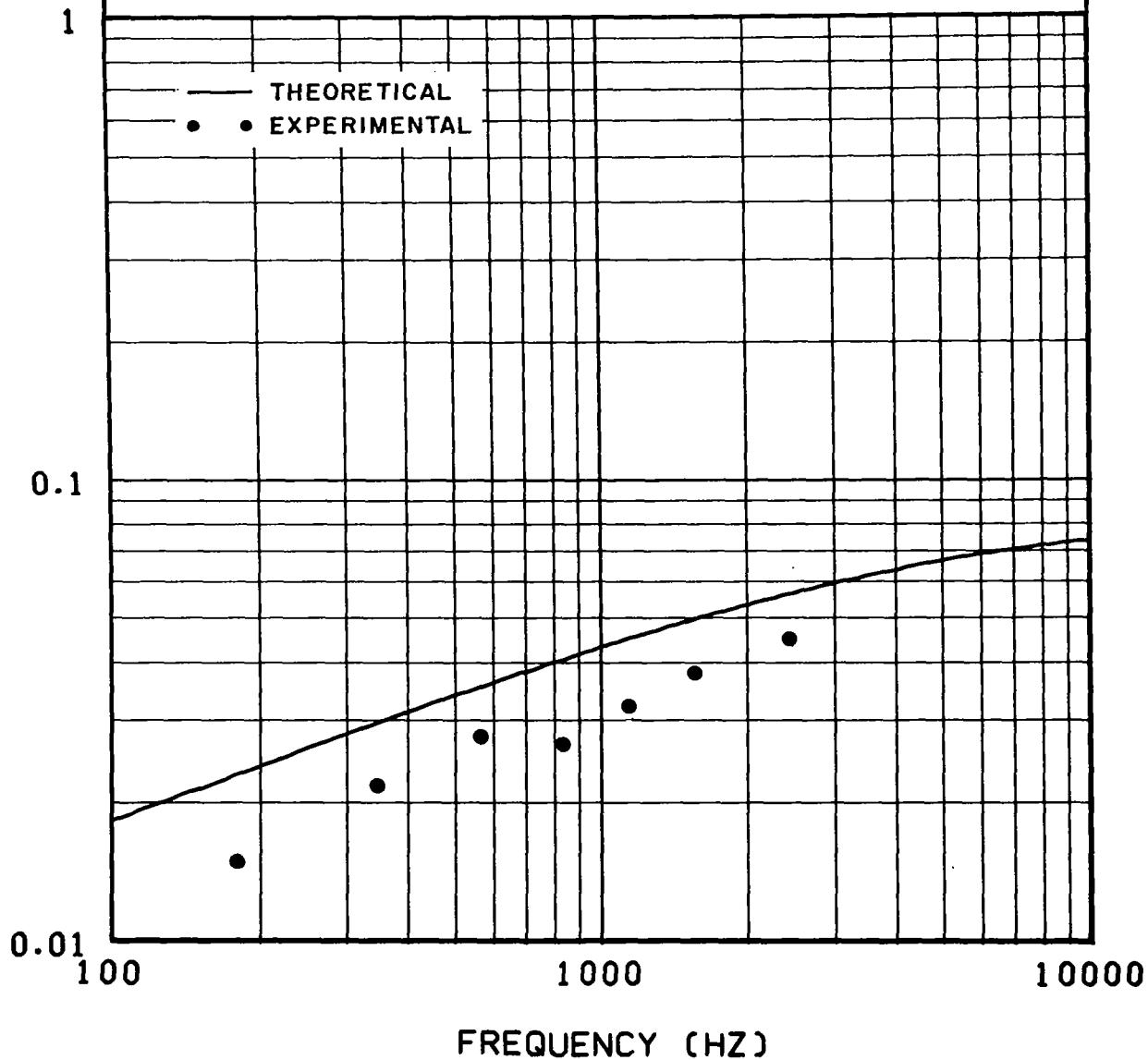
Figure 85. – Theoretically predicted and experimentally determined values of
structure loss factor of a symmetrical three-elastic-element
free-free beam having a geometrical parameter Y = 1.33 and
a shear parameter coefficient C = 1.04

Figure 86. – Theoretically predicted and experimentally determined values of structure loss factor of a symmetrical three-elastic-element free-free beam having a geometrical parameter $Y = 6.52$ and a shear parameter coefficient $C = 0.135$

183

Figure 87. – Theoretically predicted and experimentally determined values of structure loss factor of a symmetrical three-elastic-element free-free beam having a geometrical parameter Y = 6.78 and a shear parameter coefficient C = 0.155

184

Figure 88. – Theoretically predicted and experimentally determined values of structure loss factor of a symmetrical three-elastic-element free-free beam having a geometrical parameter Y = 12.2 and a shear parameter coefficient C = 0.519
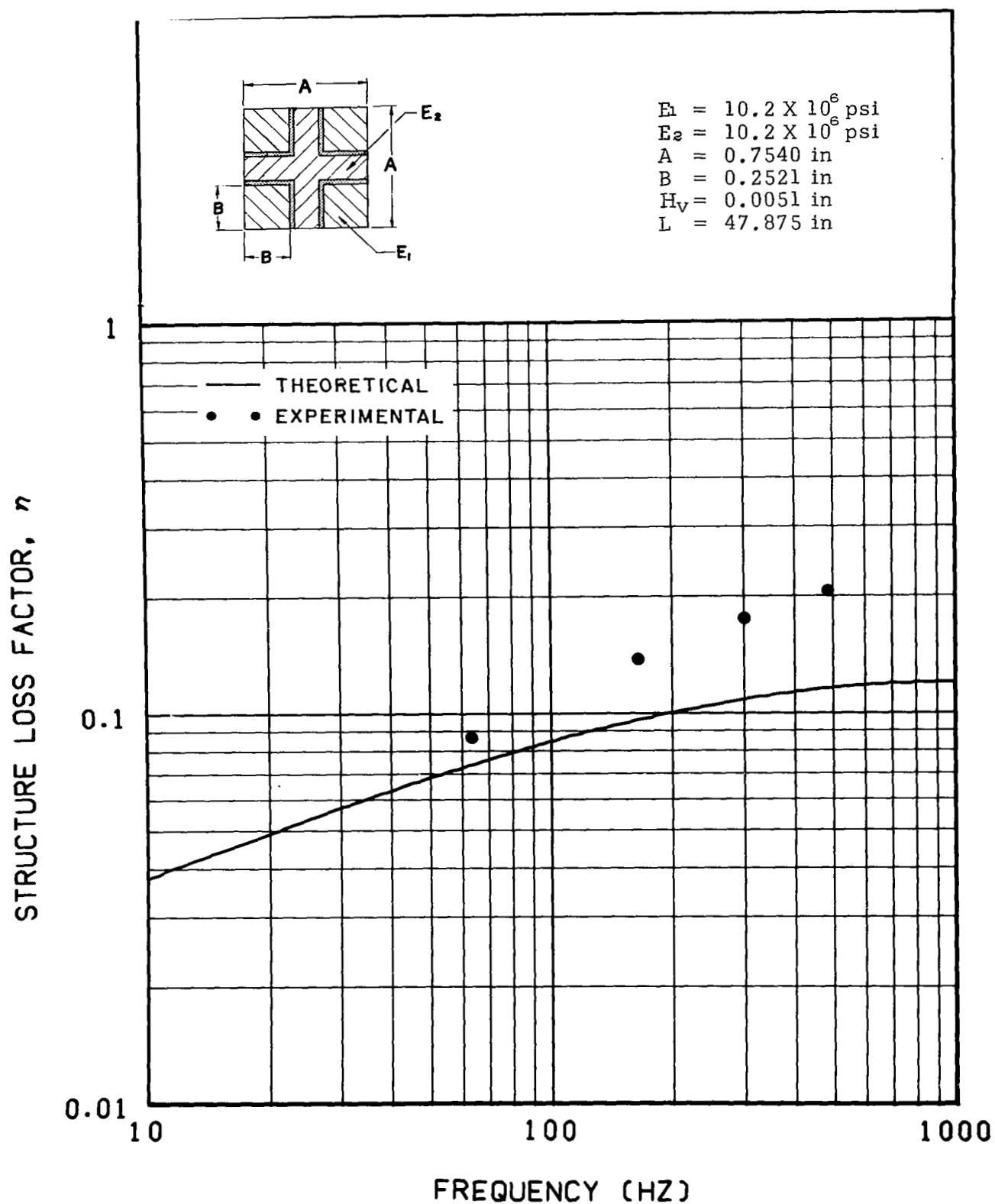
185

Figure 89. – Theoretically predicted and experimentally determined values of
structure loss factor of a symmetrical three-elastic-element
free-free beam having a geometrical parameter Y = 1.82 and
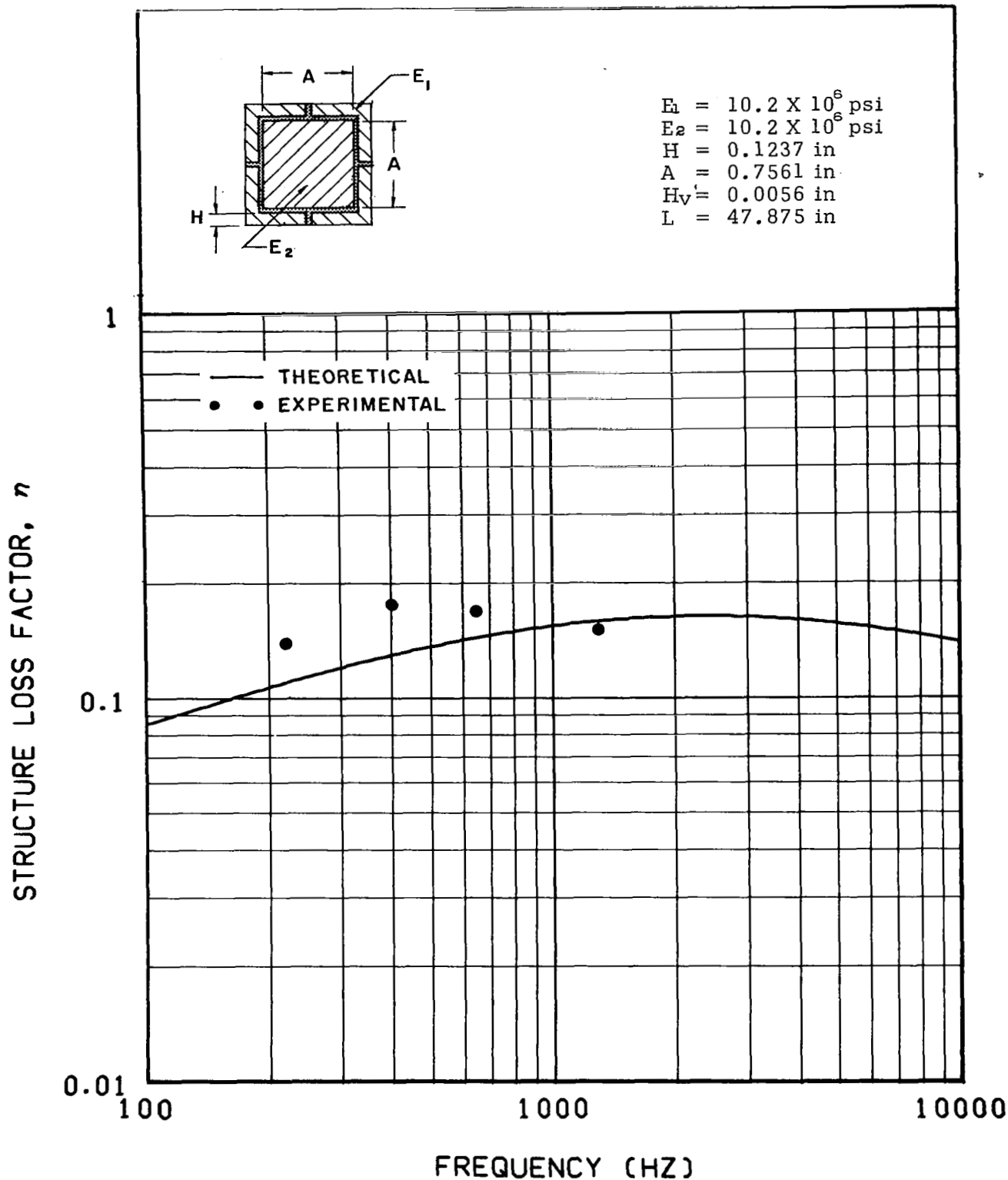a shear parameter coefficient C = 1.39

Figure 90. — Theoretically predicted and experimentally determined values of structure loss factor of a symmetrical three-elastic-element free-free beam having a geometrical parameter $Y = 2.51$ and a shear parameter coefficient $C = 1.77$
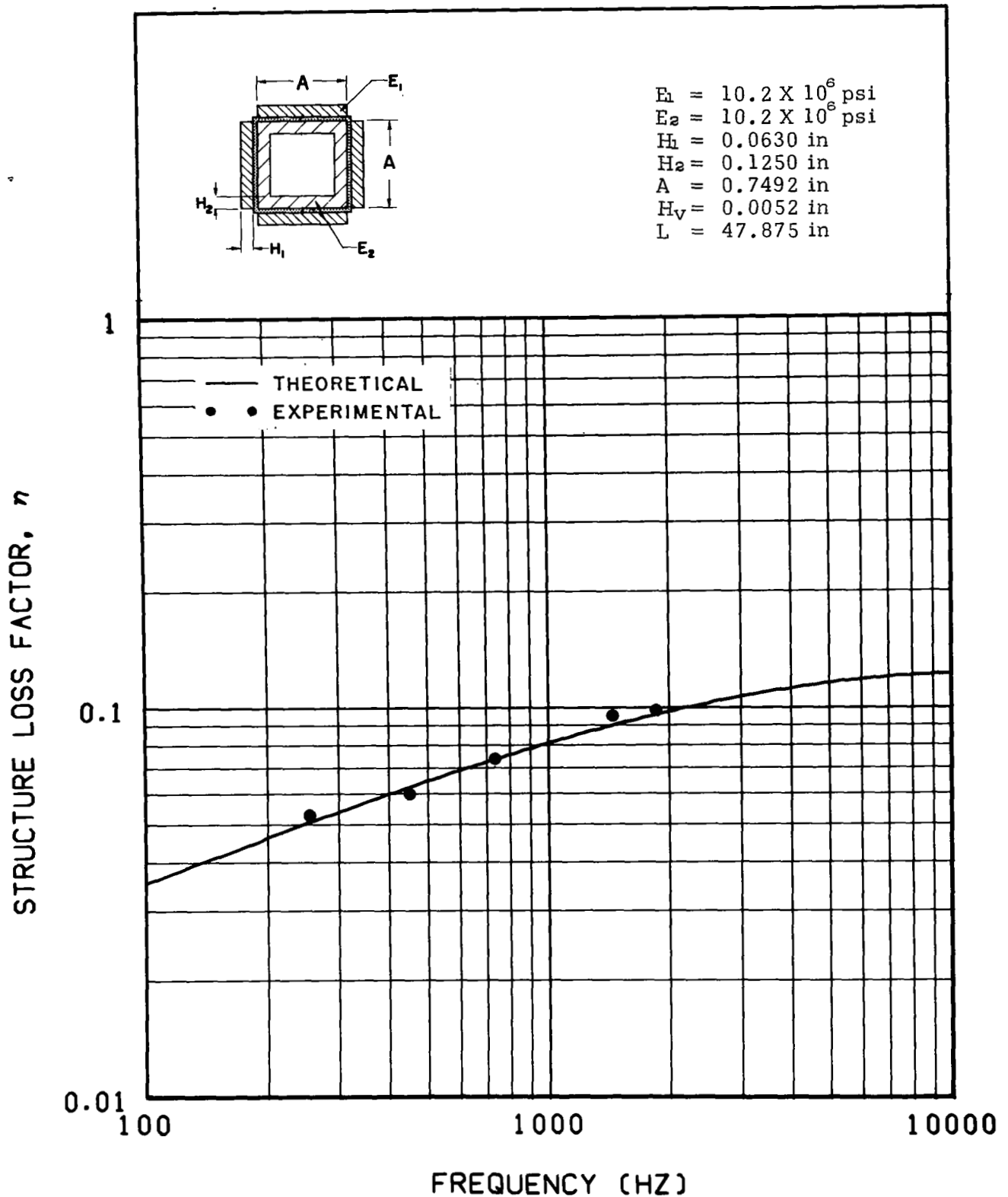
Figure 91. – Theoretically predicted and experimentally determined values of structure loss factor of a symmetrical three-elastic-element free-free beam having a geometrical parameter Y = 5.99 and a shear parameter coefficient C = 0.635

188

Figure 92. – Theoretically predicted and experimentally determined values of structure loss factor of a symmetrical three-elastic-element free-free beam having a geometrical parameter $Y = 1.37$ and a shear parameter coefficient $C = 2.51$
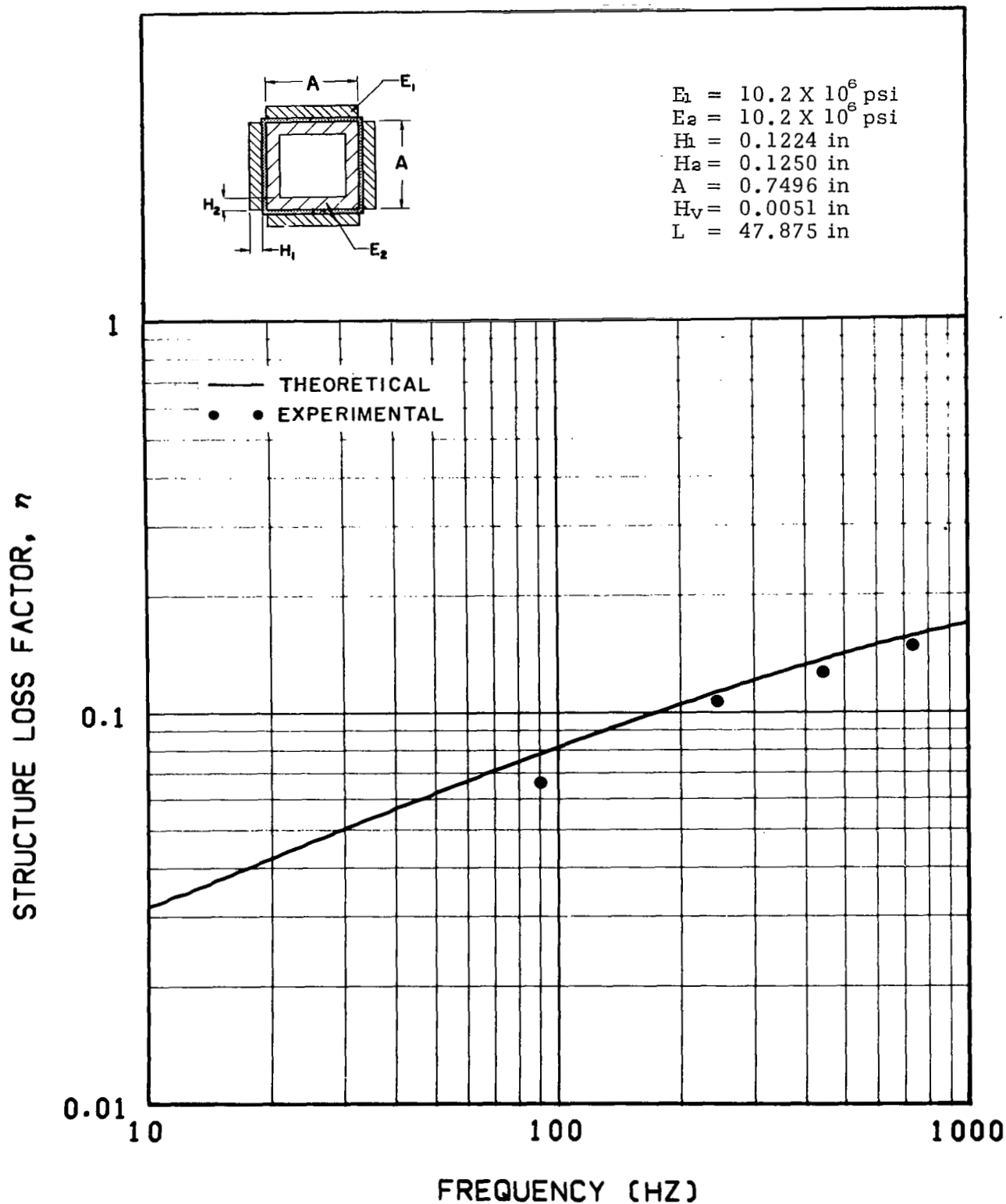
189

Figure 93. – Theoretically predicted and experimentally determined values of
structure loss factor of a symmetrical three-elastic-element
free-free beam having a geometrical parameter Y = 3.32 and
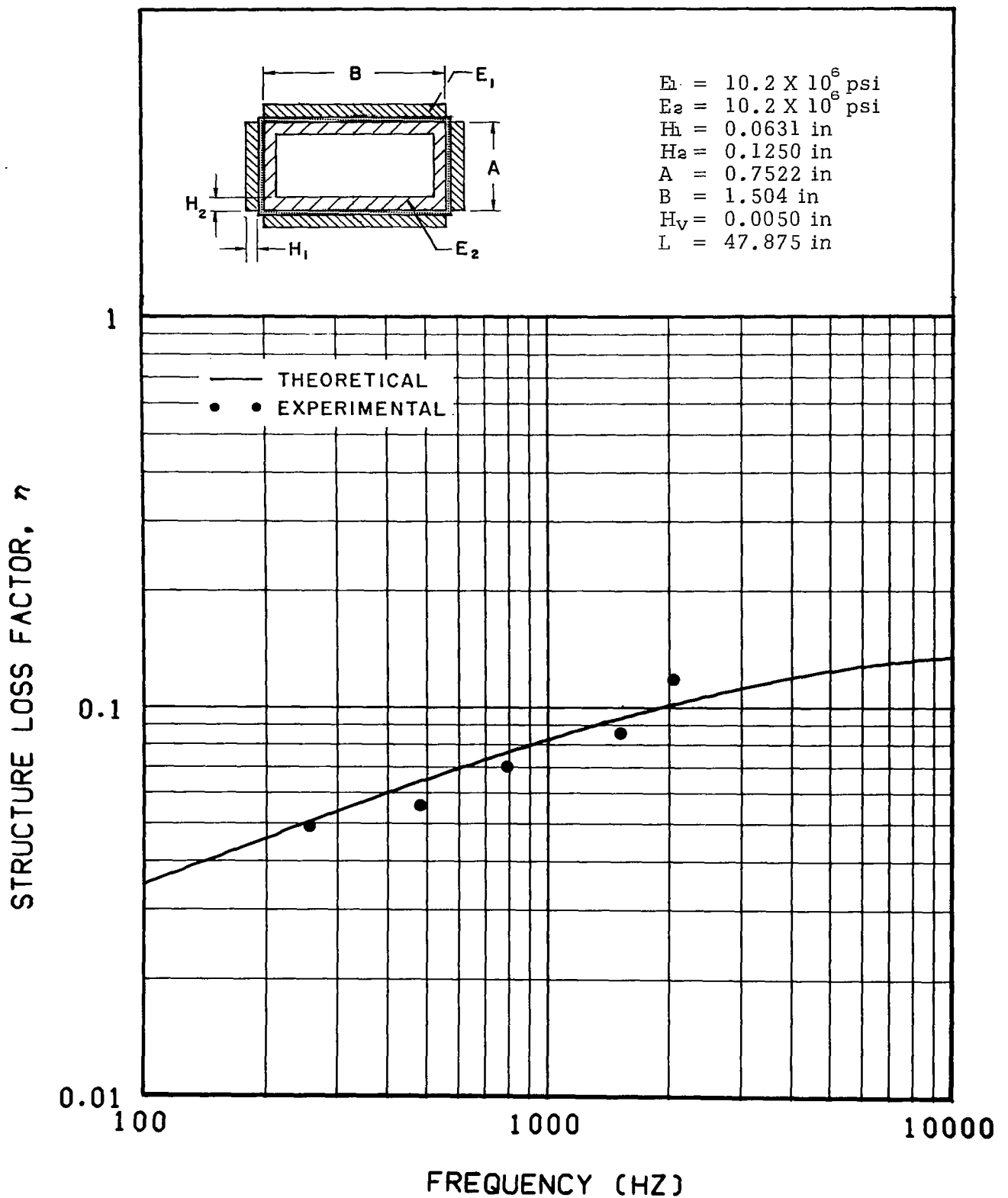a shear parameter coefficient C = 0.893

Figure 94. — Theoretically predicted and experimentally determined values of
structure loss factor of a symmetrical three-elastic-element
free-free beam having a geometrical parameter $Y = 0.316$ and
a shear parameter coefficient $C = 3.50$

Figure 95. – Theoretically predicted and experimentally determined values of structure loss factor of a symmetrical three-elastic-element free-free beam having a geometrical parameter Y = 0.974 and a shear parameter coefficient C = 0.930
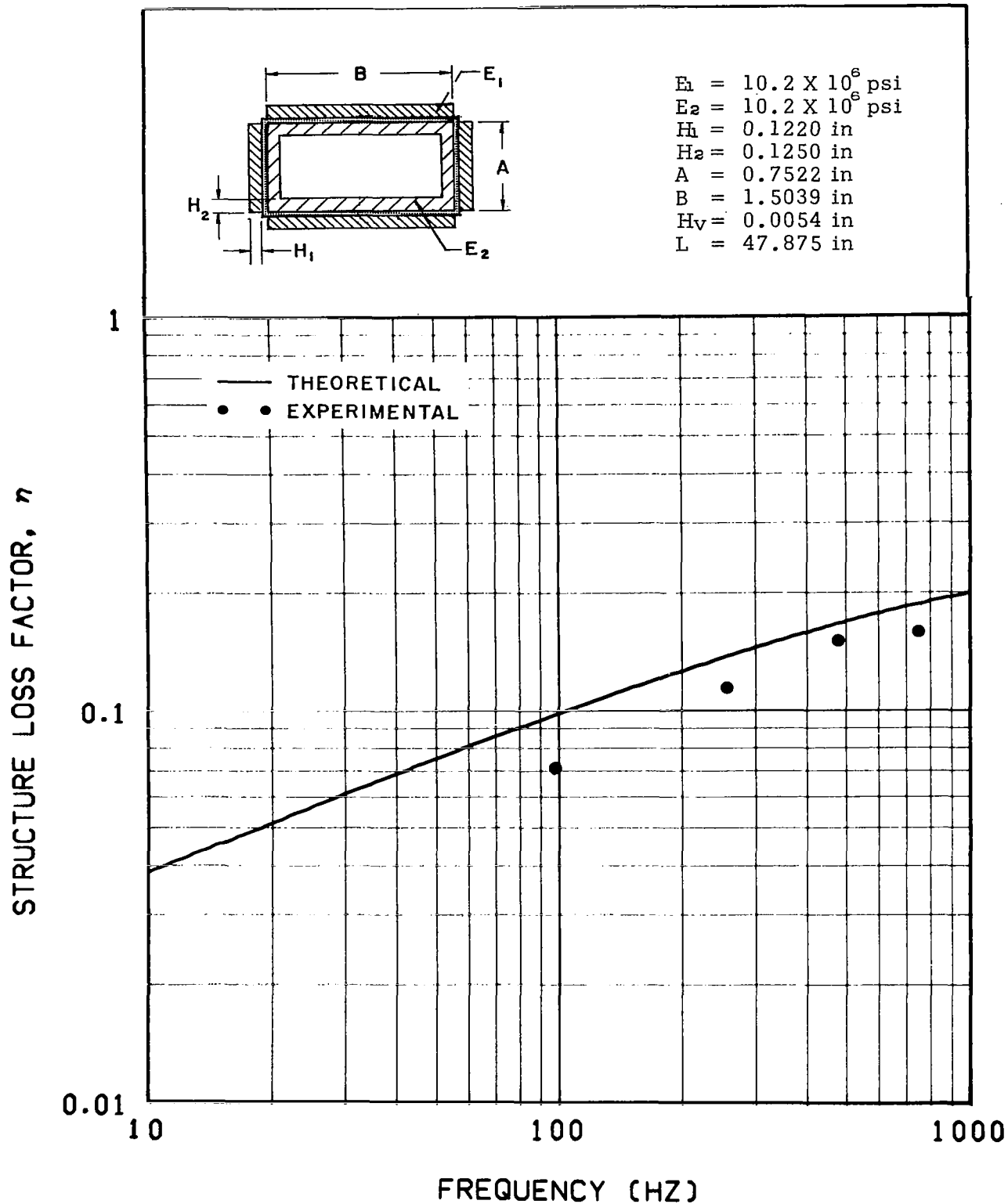
Figure 96. — Theoretically predicted and experimentally determined values of structure loss factor of a symmetrical three-elastic-element free-free beam having a geometrical parameter $Y = 0.347$ and a shear parameter coefficient $C = 3.10$
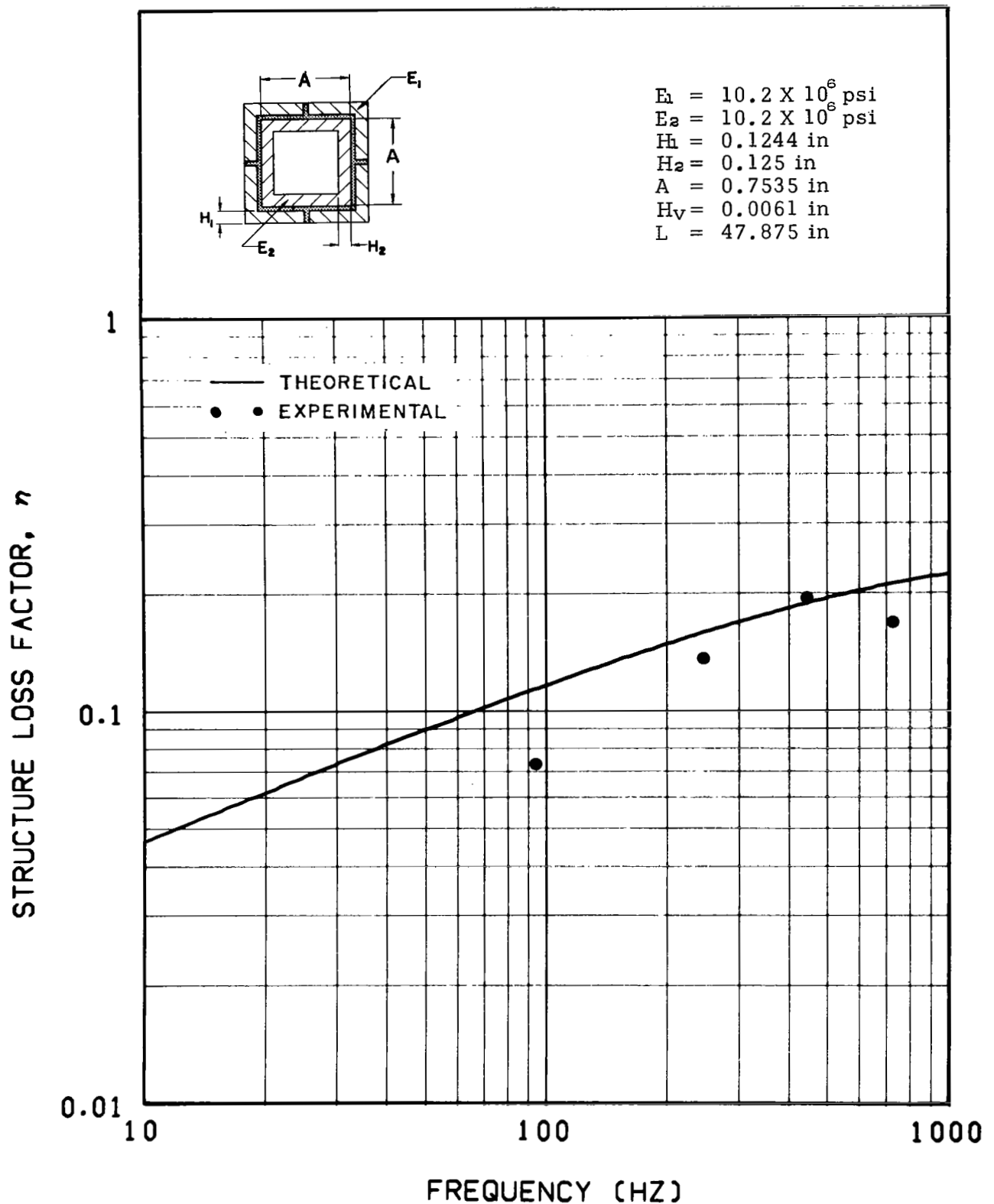
193

Figure 97. – Theoretically predicted and experimentally determined values of
structure loss factor of a symmetrical three-elastic-element
free-free beam having a geometrical parameter Y = 0.594 and
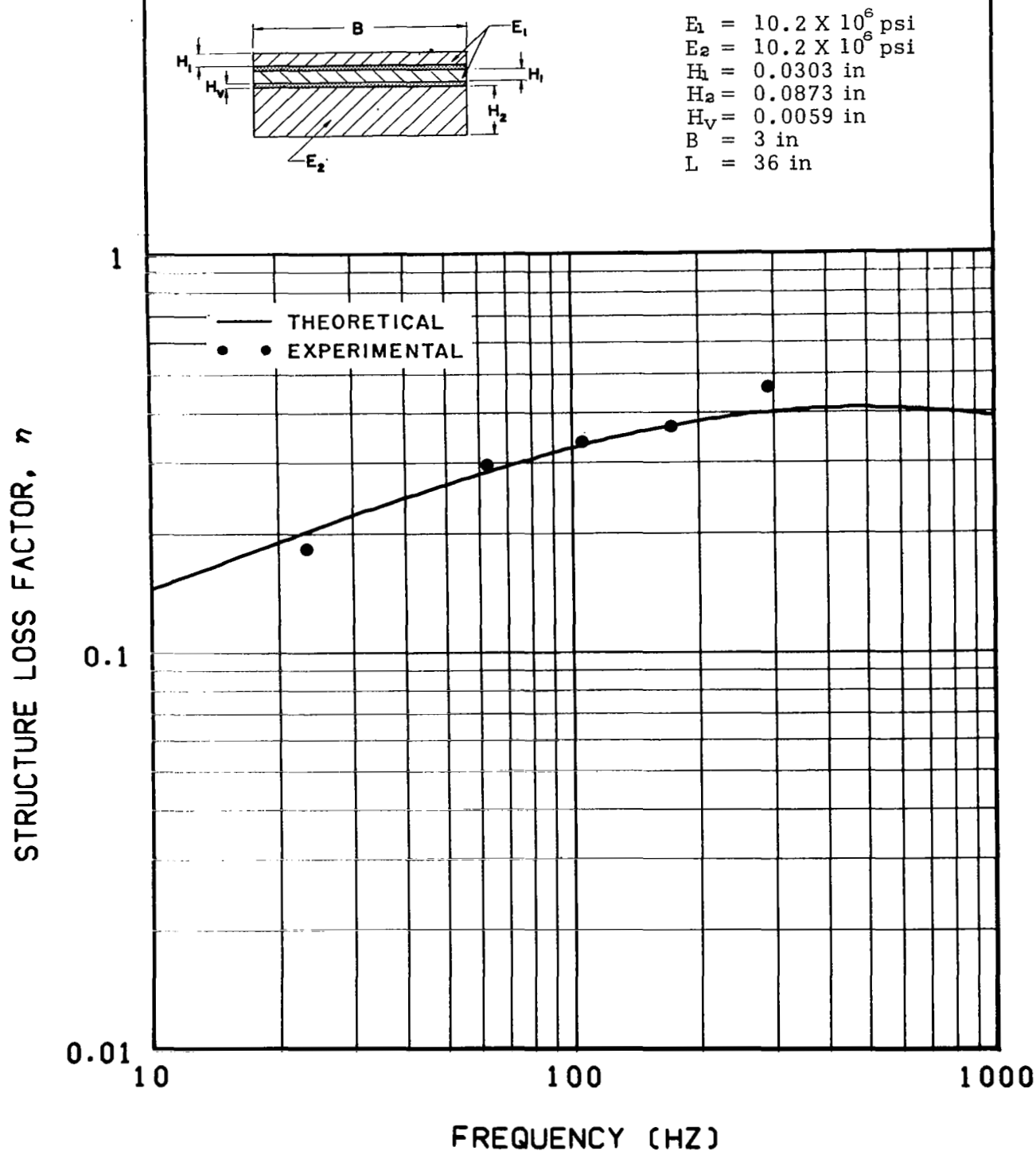a shear parameter coefficient C = 0.671

194

Figure 98. – Theoretically predicted and experimentally determined values of structure loss factor of a symmetrical three-elastic-element free-free beam having a geometrical parameter Y = 0.889 and a shear parameter coefficient C = 0.925

Figure 99. – Theoretically predicted and experimentally determined values of structure loss factor of a symmetrical three-elastic-element free-free beam having a geometrical parameter Y = 0.610 and a shear parameter coefficient C = 2.18
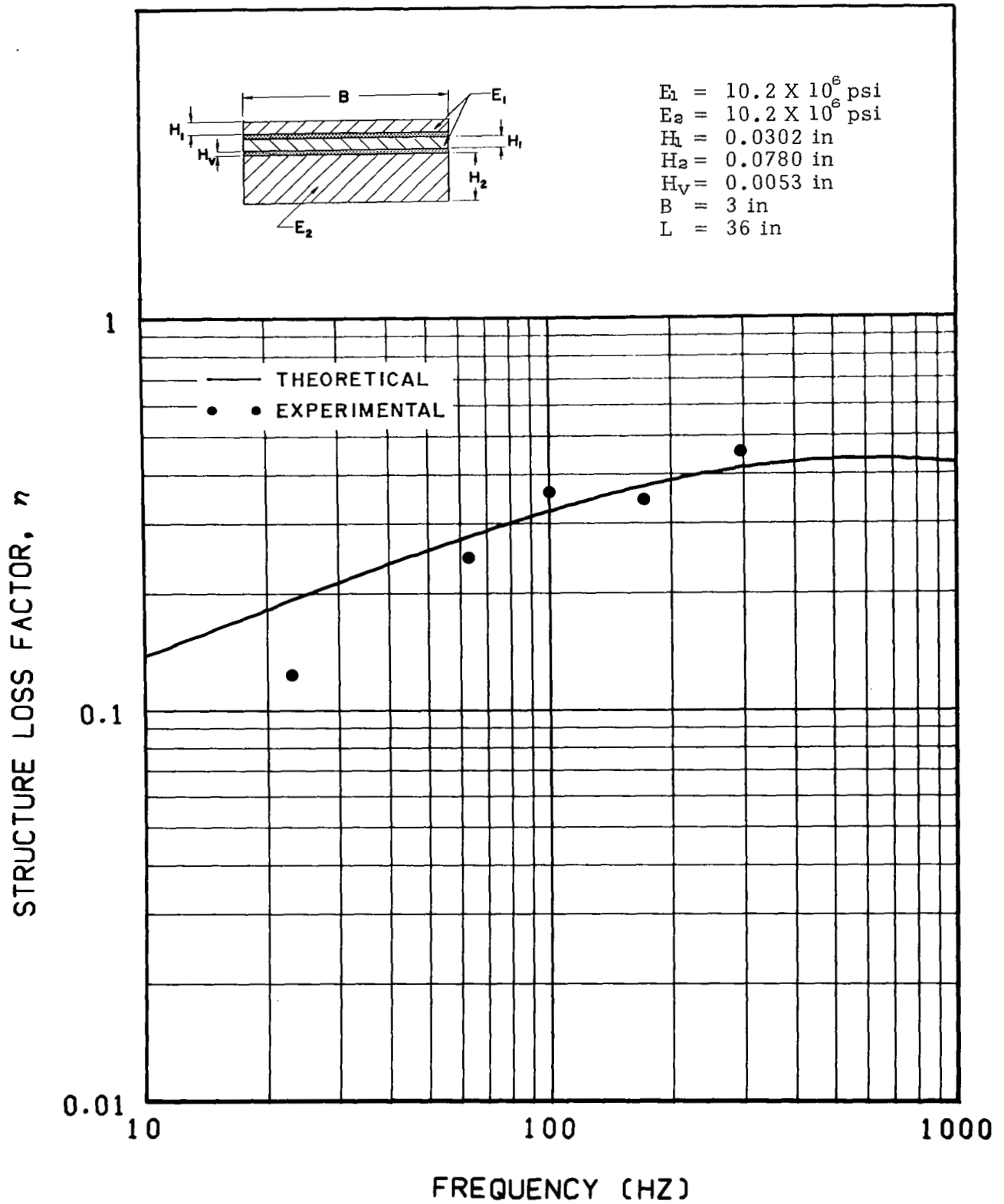
Figure 100. – Theoretically predicted and experimentally determined values of structure loss factor of a symmetrical three-elastic-element free-free beam having a geometrical parameter Y = 1.17 and a shear parameter coefficient C = 1.06
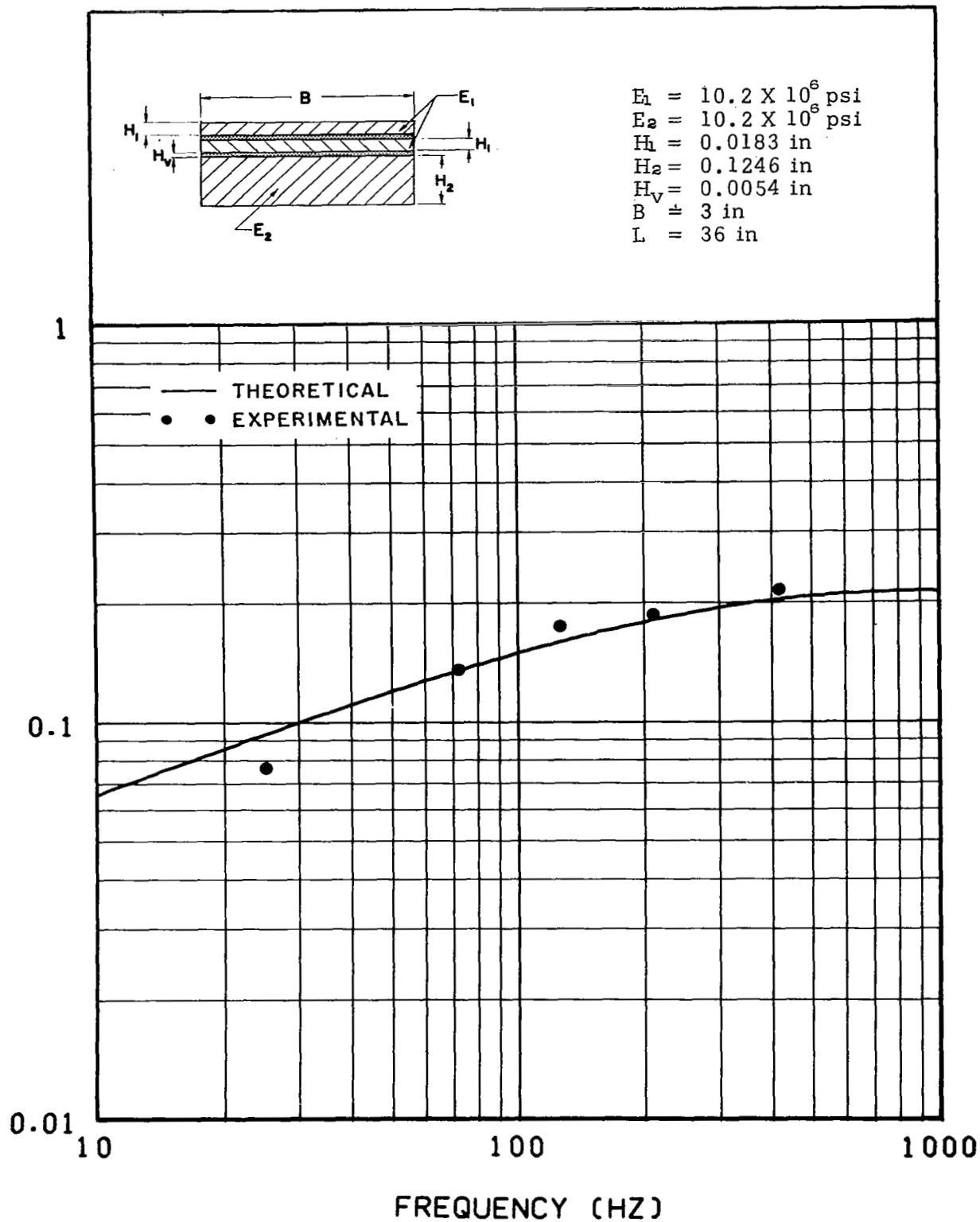
197

Figure 101. — Theoretically predicted and experimentally determined values of structure loss factor of a symmetrical three-elastic-element free-free beam having a geometrical parameter $Y = 0.705$ and a shear parameter coefficient $C = 2.38$

198

Figure 102. – Theoretically predicted and experimentally determined values of structure loss factor of a symmetrical three-elastic-element free-free beam having a geometrical parameter Y = 1.42 and a shear parameter coefficient C = 0.965
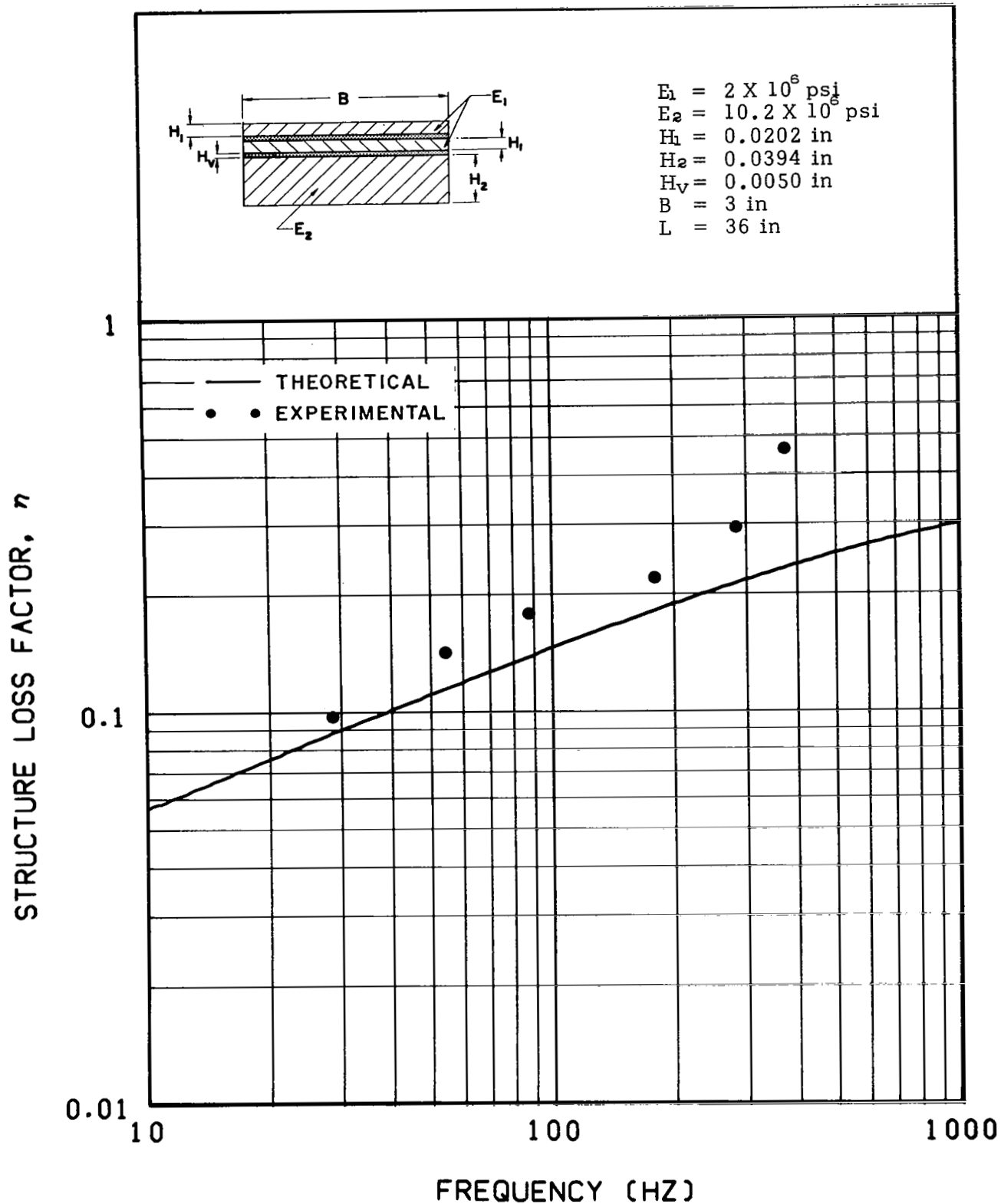
Figure 103. – Theoretically predicted and experimentally determined values of structure loss factor of a symmetrical three-elastic-element free-free beam having a geometrical parameter Y = 1.56 and a shear parameter coefficient C = 0.748

Figure 104. – Theoretically predicted and experimentally determined values of structure loss factor of an unsymmetrical three-elastic-element free-free beam having a geometrical parameter $Y = 4.06$ and a shear parameter coefficient $C = 0.353$
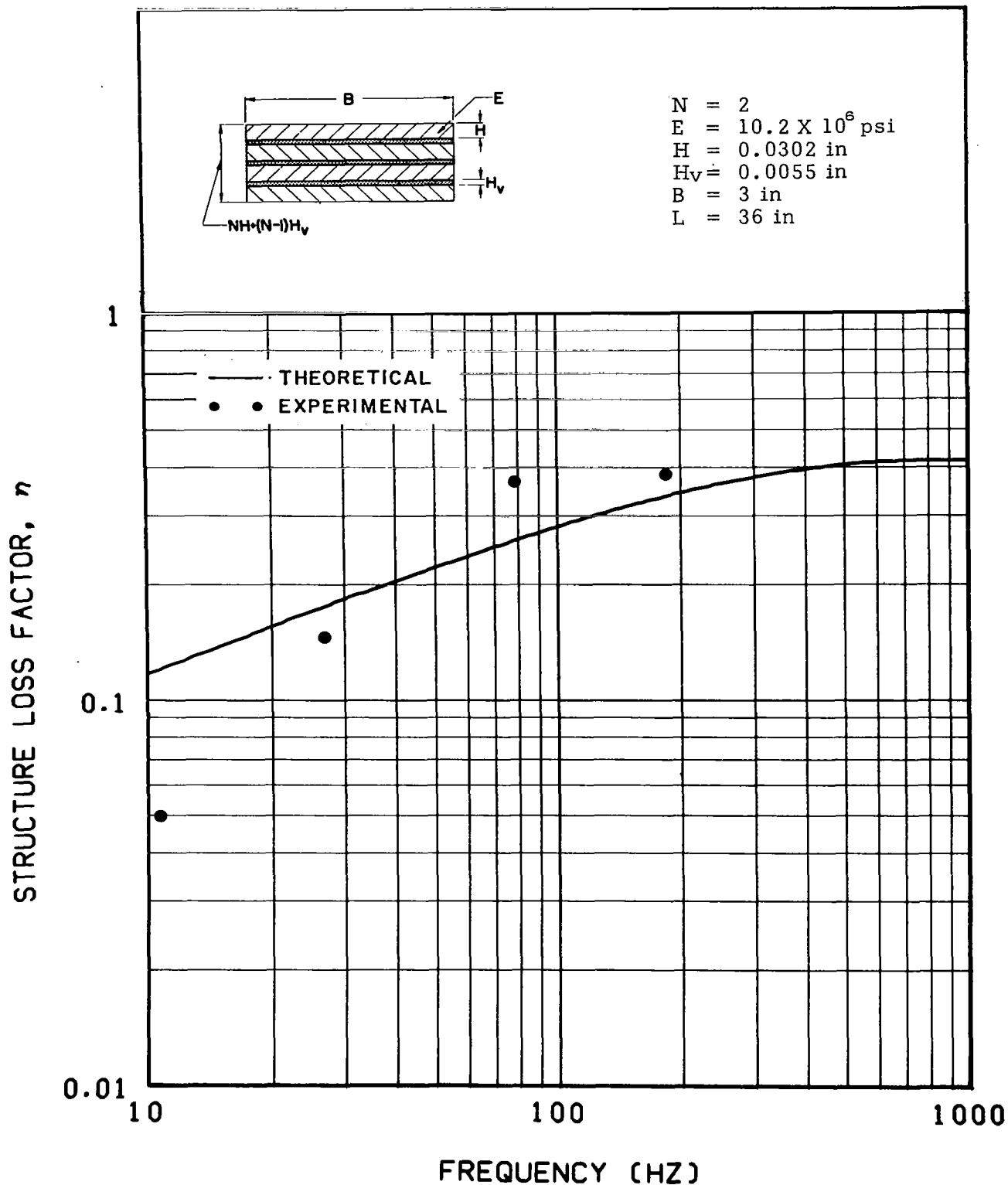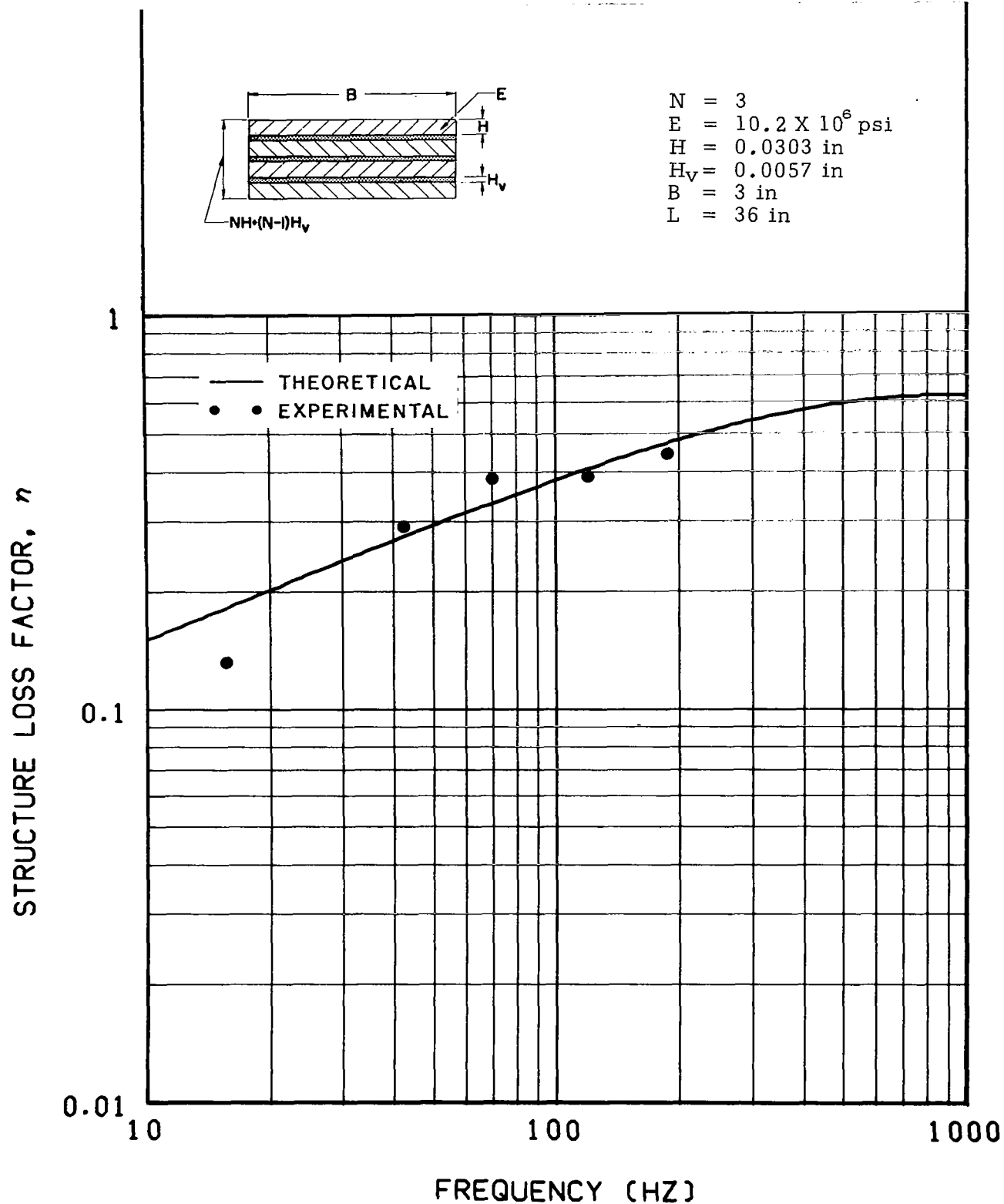
Figure 105. – Theoretically predicted and experimentally determined values of structure loss factor of an unsymmetrical three-elastic-element free-free beam having a geometrical parameter Y = 4.63 and a shear parameter coefficient C = 0.352

Figure 106. – Theoretically predicted and experimentally determined values of structure loss factor of an unsymmetrical three-elastic-element free-free beam having a geometrical parameter $Y = 1.29$ and a shear parameter coefficient $C = 1.01$

203

Figure 107. – Theoretically predicted and experimentally determined values of structure loss factor of an unsymmetrical three-elastic-element free-free beam having a geometrical parameter $Y = 2.68$ and a shear parameter coefficient $C = 1.41$
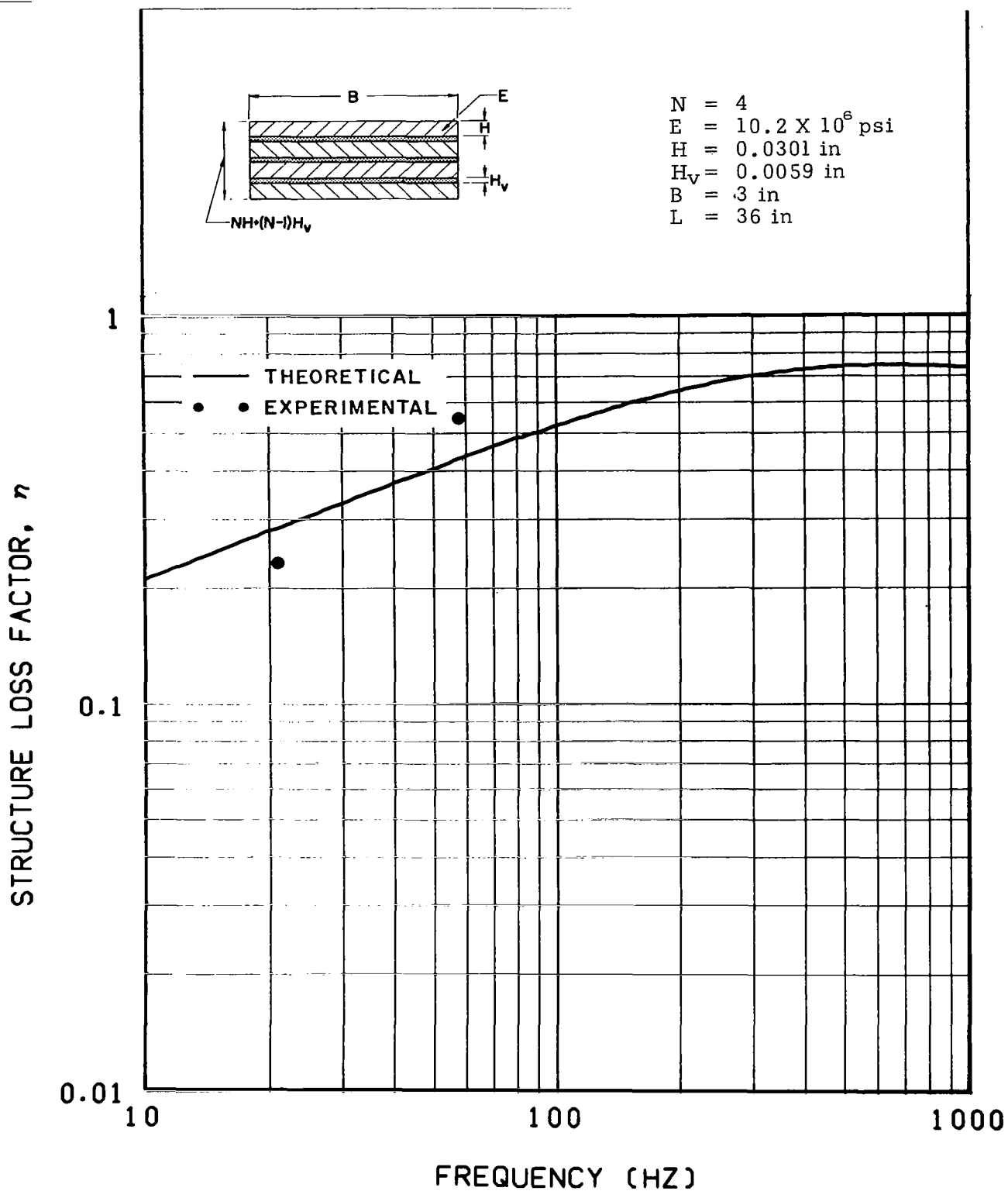
204

Figure 108. – Theoretically predicted and experimentally determined values of structure loss factor of an N identical-elastic-laminate free-free beam having the number of laminates N = 2, the viscoelastic thickness parameter V = 0.091, and the shear parameter coefficient C = 0.162

Figure 109. – Theoretically predicted and experimentally determined values of structure loss factor of an N identical-elastic-laminate free-free beam having the number of laminates N = 3, the viscoelastic thickness parameter V = 0.094, and the shear parameter coefficient C = 0.157

Figure 110. – Theoretically predicted and experimentally determined values of structure loss factor of an N identical-elastic-laminate free-free beam having the number of laminates N = 4, the viscoelastic thickness parameter V = 0.098, and the shear parameter coefficient C = 0.152
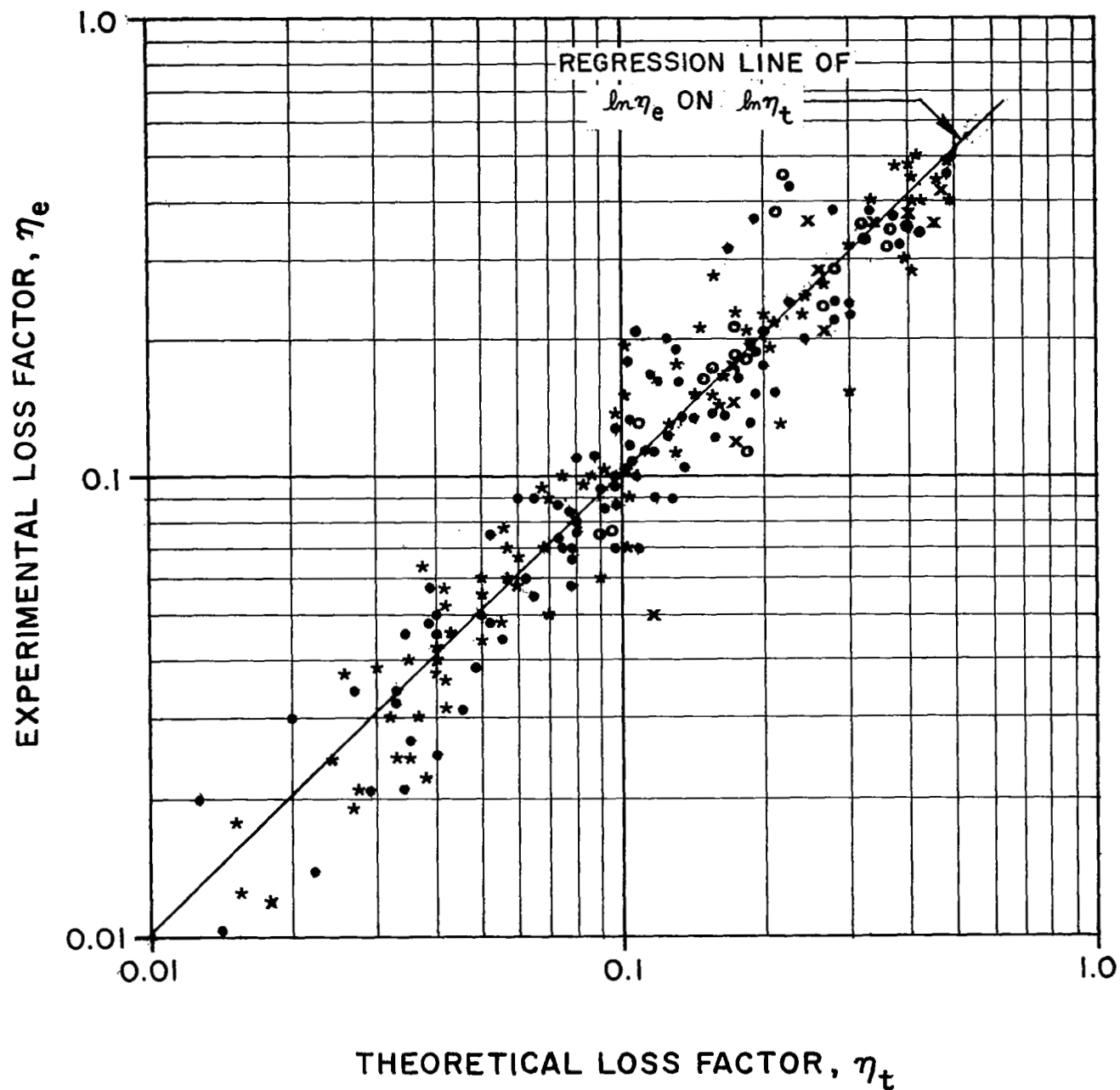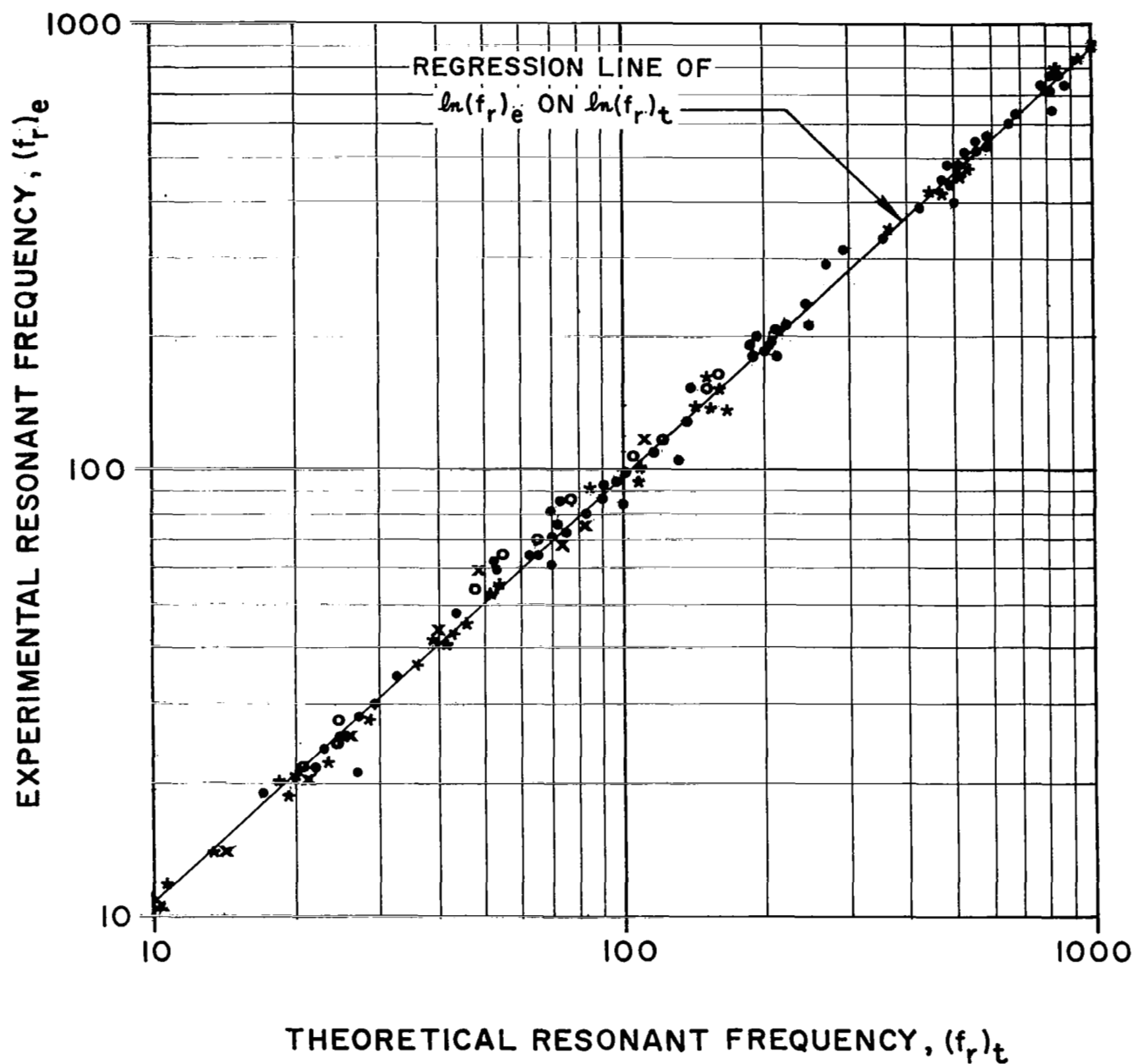
Figure 111. - Comparison of the experimental and theoretical values of loss factor for the composite structural beam specimens, where (∗) refers to two-elastic-element structures, (•) refers to symmetrical three-elastic-element structures, (o) refers to unsymmetrical three-elastic-element structures, and (x) refers to N identical-elastic-laminate structures
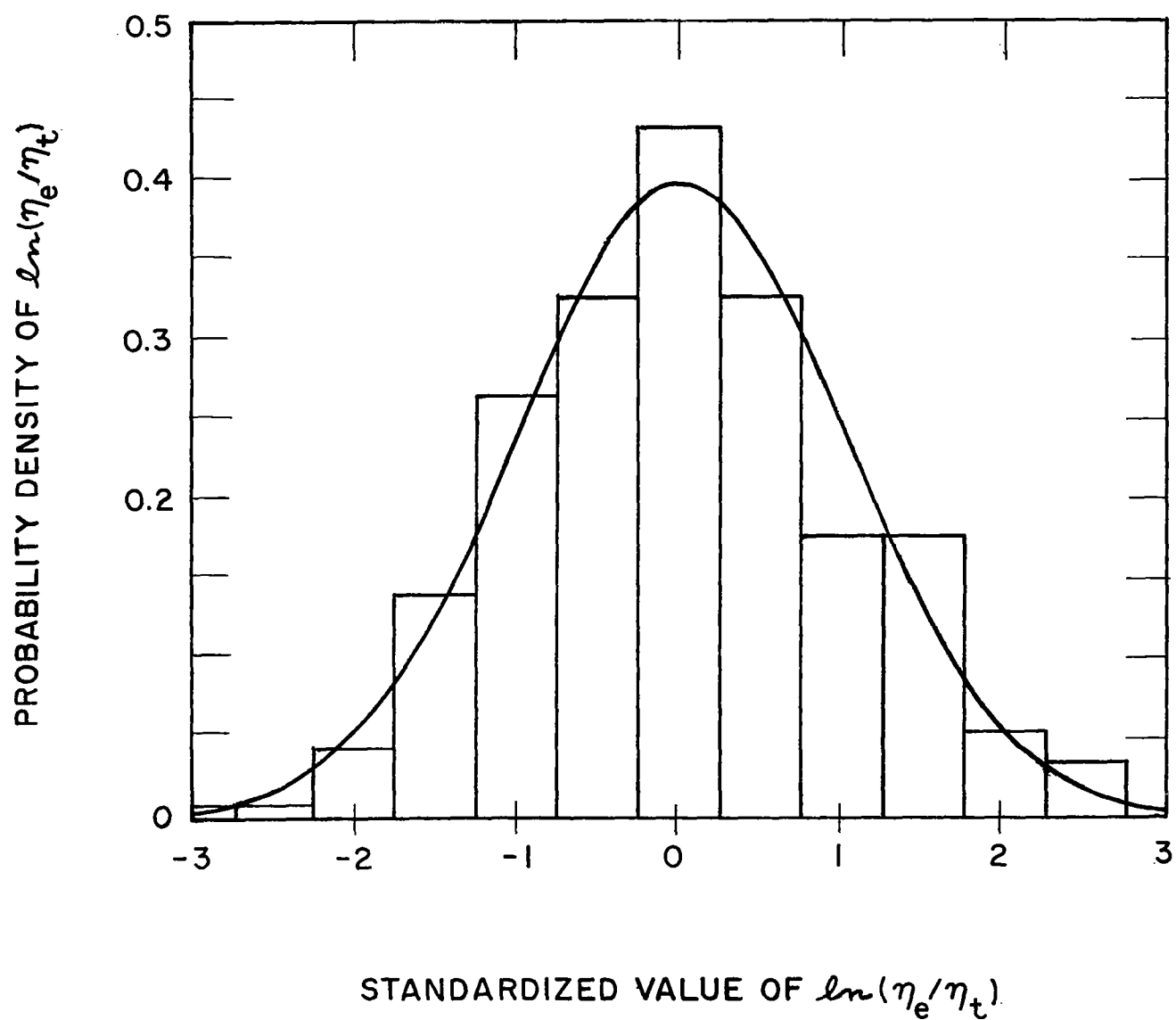
Figure 112. - Comparison of the experimental and theoretical values of resonant frequency for the composite structural beam specimens, where (*) refers to two-elastic-element structures, (•) refers to symmetrical three-elastic-element structures, (o) refers to unsymmetrical three-elastic-element structures, and (**x**) refers to N identical-elastic-laminate structures

Figure 113. — Comparison of the standardized probability density of $\ln(\eta_e/\eta_t)$, shown as vertical bars, with that of a normal distribution, shown as the continuous curve
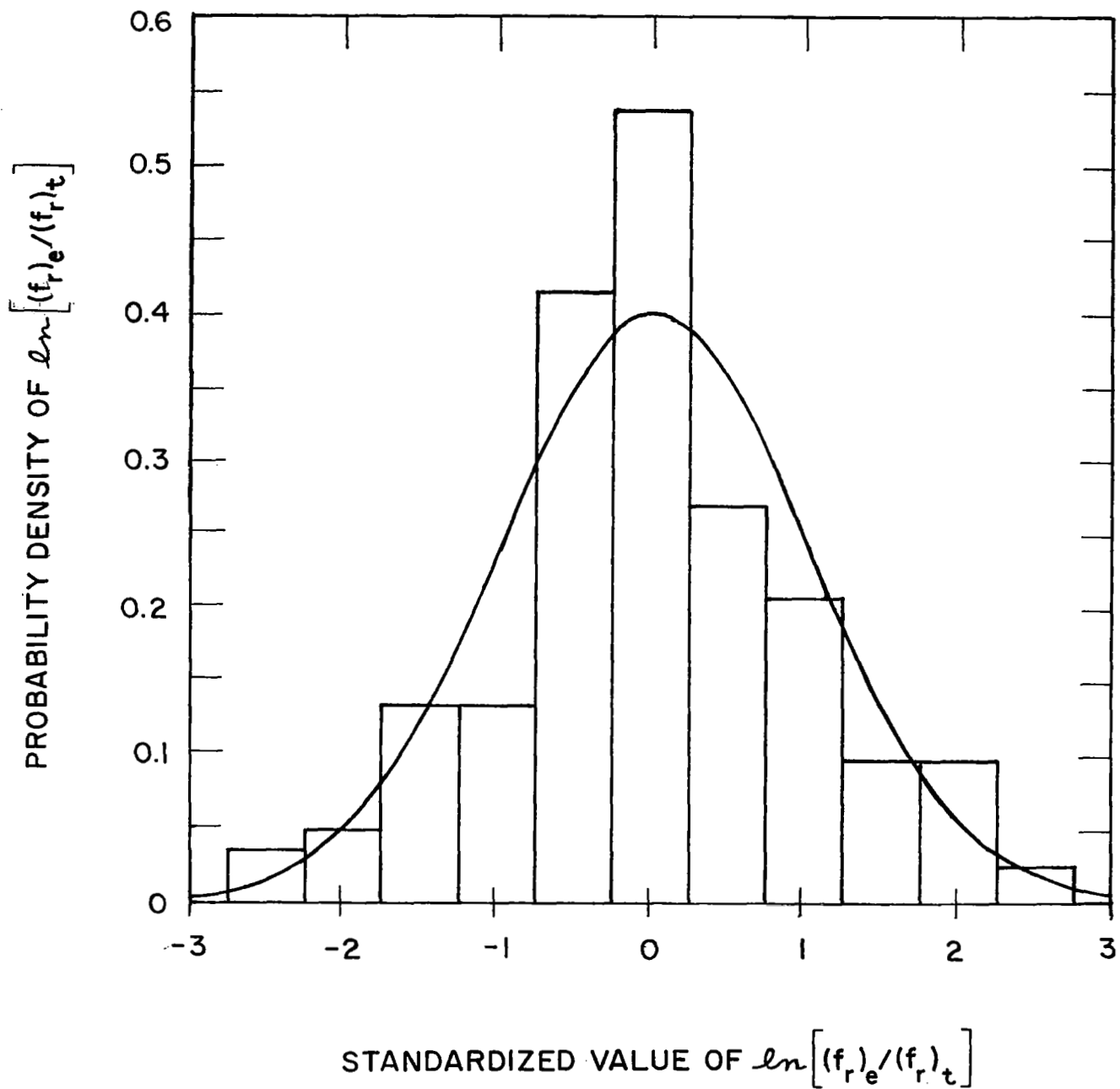
Figure 114. – Comparison of the standardized probability density of $\ln\left[(f_r)_e/(f_r)_t\right]$, shown as vertical bars, with that of a normal distribution, shown as the continuous curve
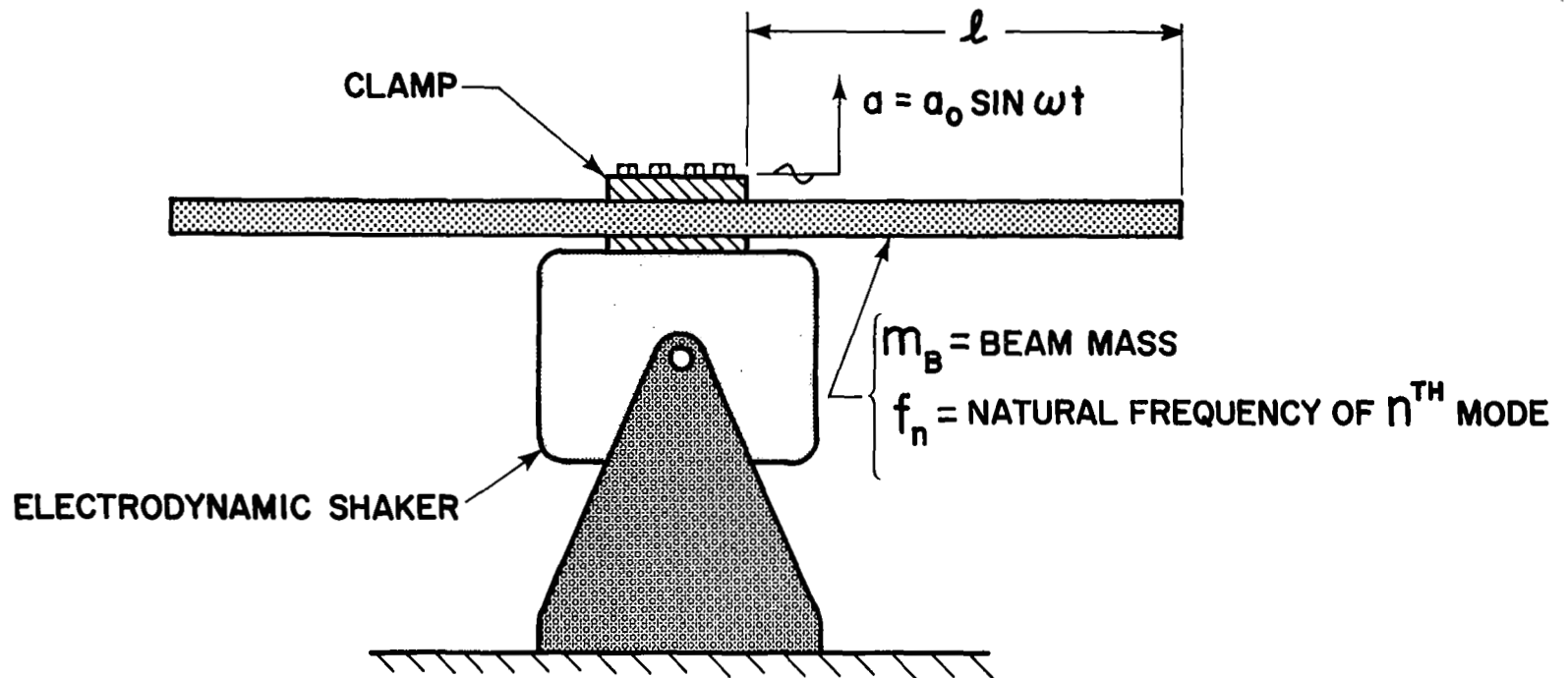
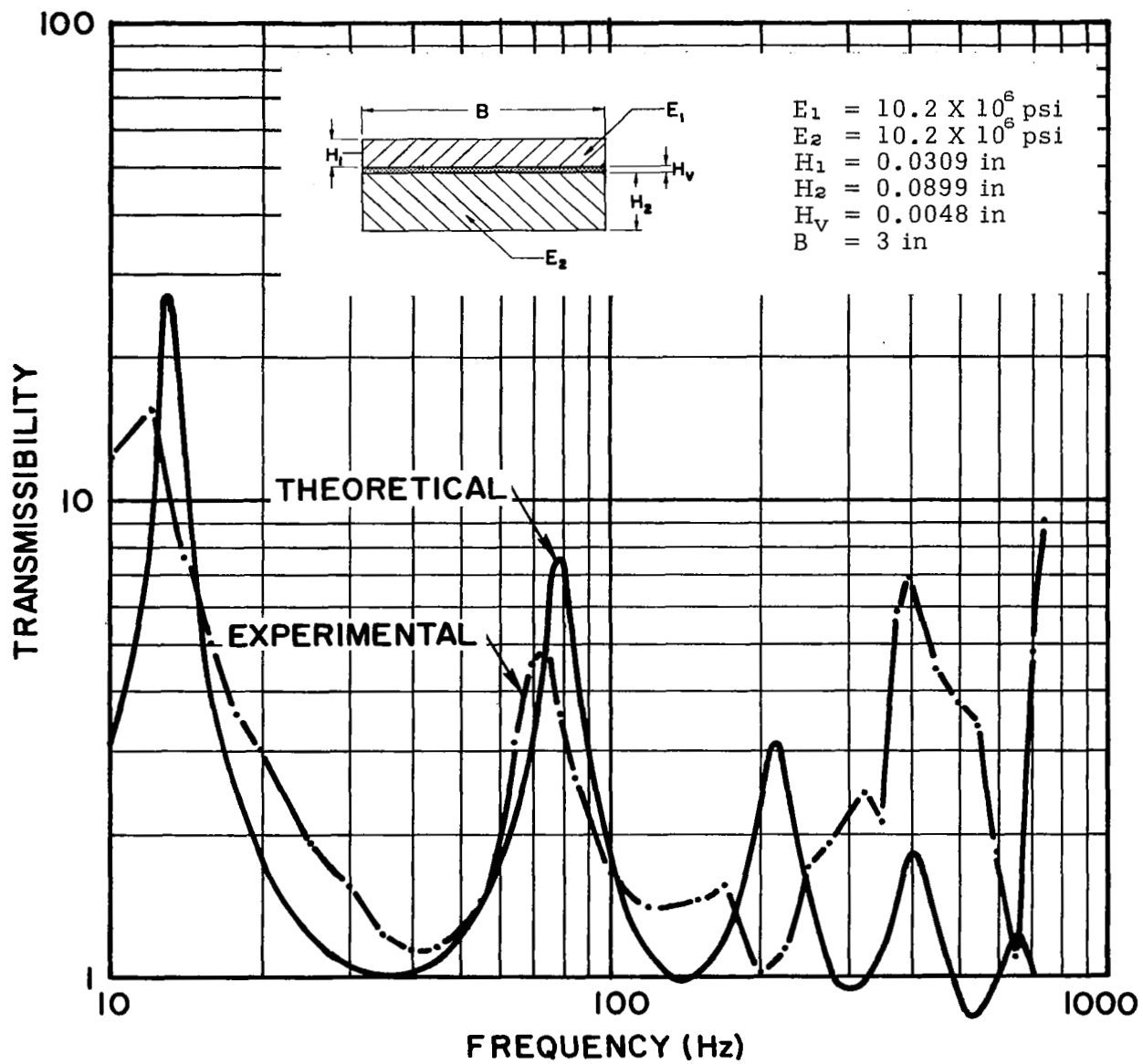Figure 115. – Schematic diagram of a cantilever beam test configuration for steady-state vibration excitation

Figure 116. – Comparison of theoretical and experimental transmissibility curves of a two-elastic-element structural composite damp-free beam
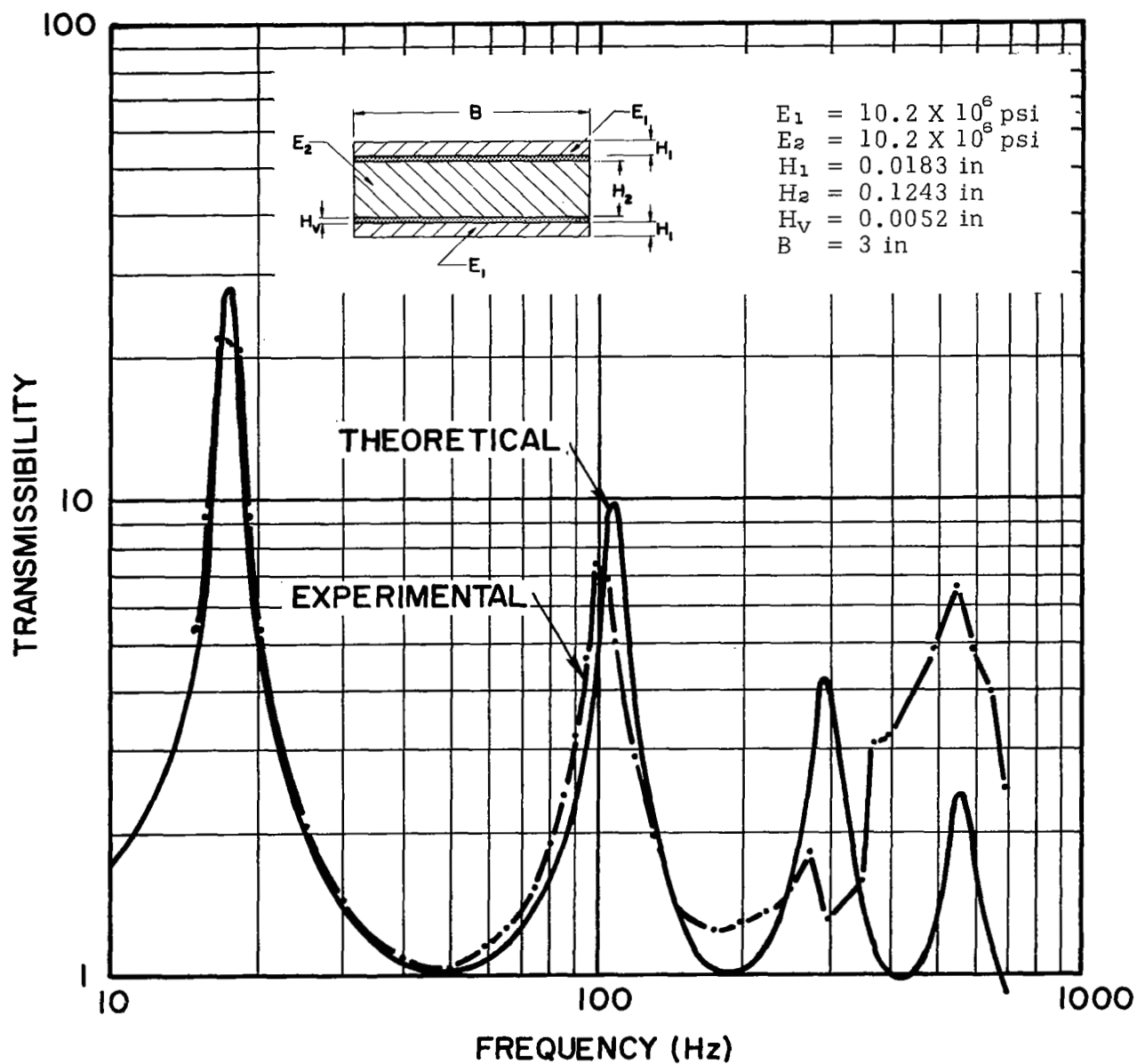
Figure 117. – Comparison of theoretical and experimental transmissibility
curves of a symmetrical three-elastic-element clamp-free
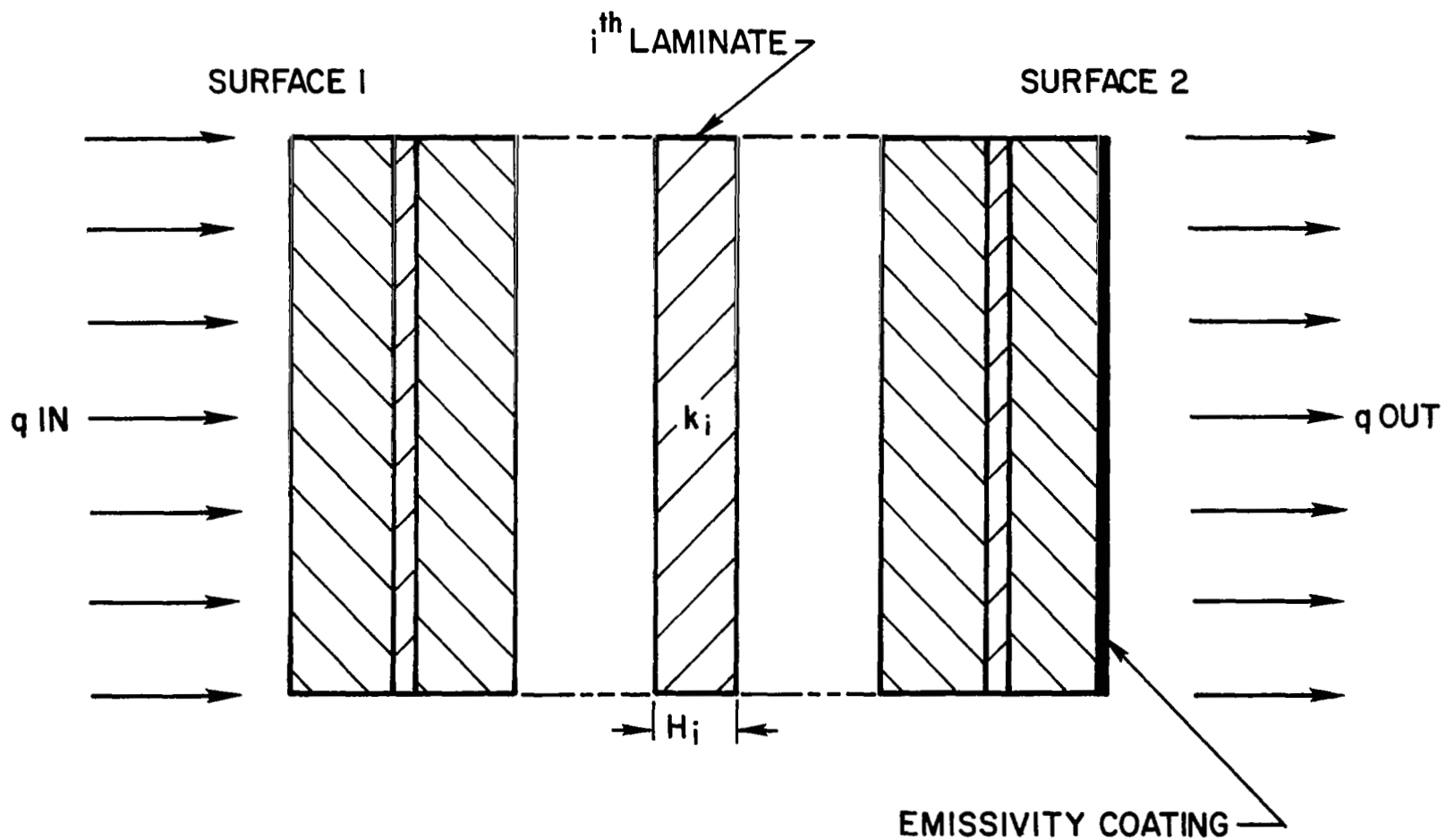structural composite beam

214

Figure 118. - Schematic diagram of a laminated plate considered in the thermal conductivity study